Columbia/Snake River Temperature Modeling
Preliminary Results

Bill Perkins, Marshall Richmond, Greg Guensch
Pacific Northwest National Laboratory

May 31, 2001

Contents

1 1977 Conditions Scenario **2**

2 77H/94M Scenario **16**

3 77H/94M/DWR10 Scenario **16**

4 77H/94M/DWR1 Scenario **16**

5 Scenario Temperature Comparisons **22**

6 Scenario Discharge Comparisons **116**

Appendix **124**

A Estimation of Clearwater Main Stem Temperature **124**

B Meterological Data **127**

C MASS1 Model Schematics **134**

1 1977 Conditions Scenario

The simulation period was limited to April 1, 1977 to October 31, 1977. The heat exchange component of MASS1 was recalibrated for this period and the conditions listed below. Simulated temperatures were compared to observed at several locations. Table 1 summarizes the comparison for the period. Several figures follow showing graphical comparisons.

This simulation was performed using the following conditions:

- Observed 1977 flows for model boundaries:
  - Columbia River at Grand Coulee (hourly),
  - Snake River at Anatone (daily),
  - North Fork Clearwater River at Dworshak (hourly), and
  - Clearwater River at Orofino (daily)
- Observed 1977 flows at all gaged tributaries;
- Constant project forebay stages (normal pool elevation);
- Observed 1977 daily water temperatures at Grand Coulee;
- Observed 1977 daily water temperatures at Anatone;
- Dworshak and Orofino temperatures set to that observed at Spalding;
- Water temperatures at tributaries were set to observed 1977 daily values when available, long term monthly averages when observed data not available;
- Gas levels were assumed to be 100% saturated in the Grand Coulee and Dworshak forebays, and at all tributaries;
- At all projects, spill was assumed to occur only if the powerhouse capacity was exceeded[1]; and
- Meteorology data was used from the following stations (see Figures 130 and 131):
  - Pranghorn Airport, Wenatchee,
  - Hanford Meteorological Station, and
  - Portland International Airport.

[1]The application of this rule resulted in zero spill at all projects for the entire season.

Table 1: Statistical comparison of simulated and observed temperatures from April through September (RMS and AME units are degrees Celsius)

	N	R^2	Bias	RMS	AME
LMN Scroll Case	128	0.89	-0.36	1.52	1.17
LGS Scroll Case	124	0.89	-0.30	1.49	1.18
IHR Scroll Case	200	0.94	-0.17	1.31	1.02
RIS Scroll Case	212	0.98	-0.30	0.59	0.49
MCN Scroll Case	151	0.97	-0.94	1.26	1.06
BON Scroll Case	85	0.97	-1.25	1.56	1.35
Snake R. @ Burbank	210	0.95	-0.33	1.27	0.95
Columbia R. @ Vernita Bridge	214	0.98	-0.29	0.62	0.51
Columbia R. @ Richland	214	0.98	-0.57	0.82	0.68
Columbia R. @ Umatilla	201	0.98	-0.47	0.77	0.62
Columbia R. @ Warrendale	214	0.98	-0.37	1.26	0.95
Columbia R. @ Vancouver	191	0.97	-0.69	1.46	1.10
Columbia R. @ Kalama	214	0.98	-0.75	1.28	1.01

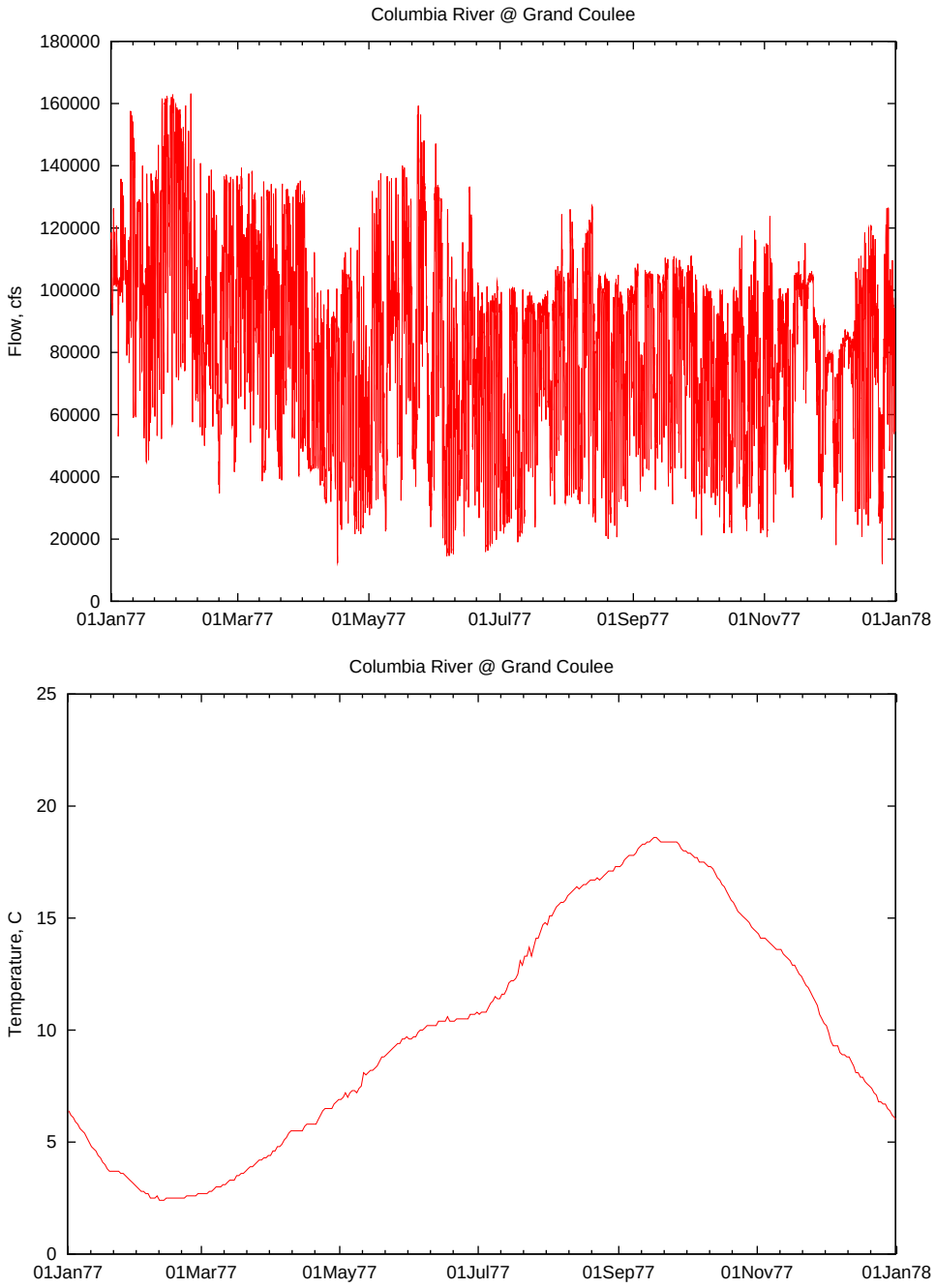

Figure 1: Flow and temperature boundary conditions at Grand Coulee dam.

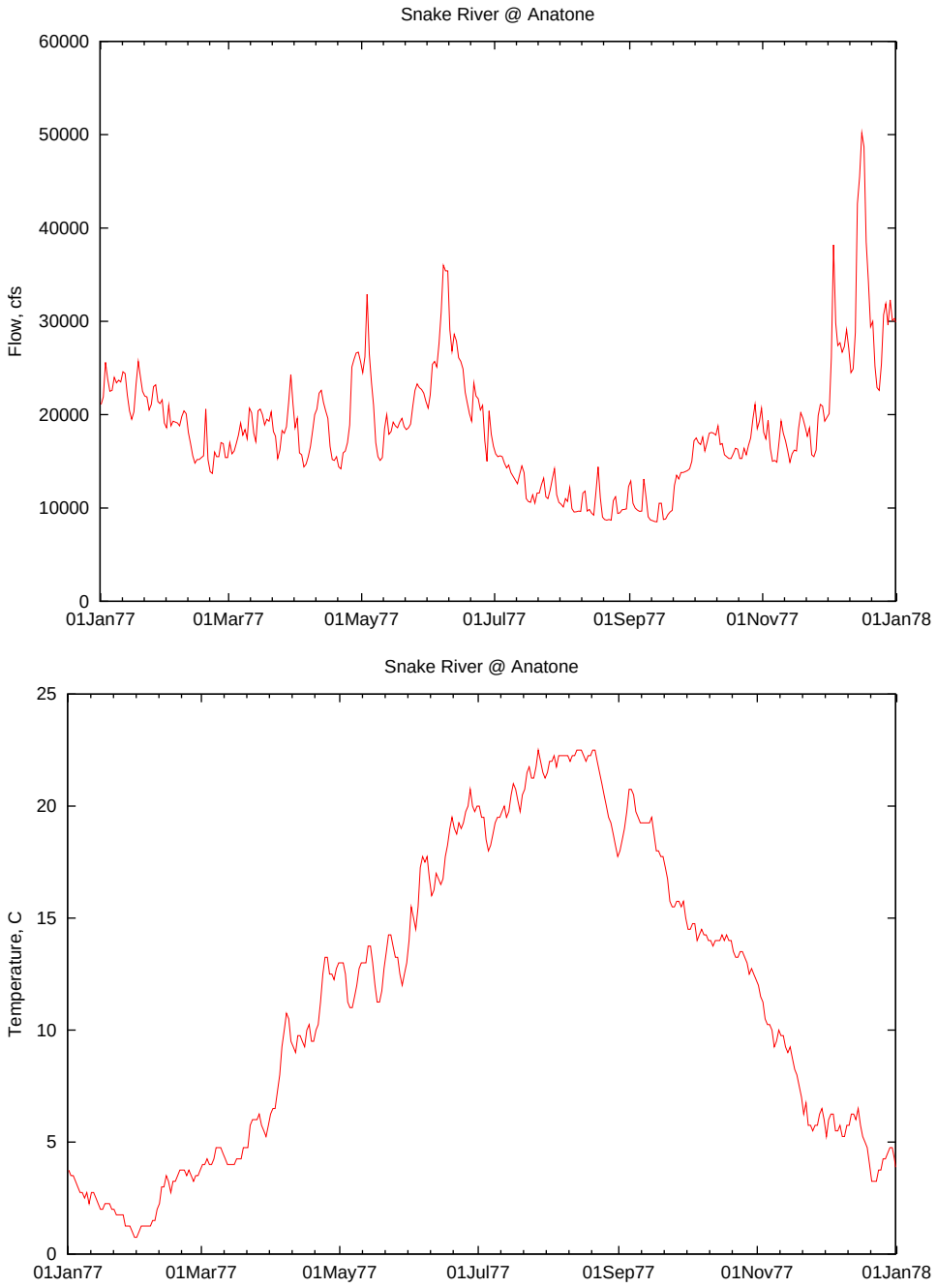

Figure 2: 1977 Snake River flow and temperature boundary conditions at Anatone.

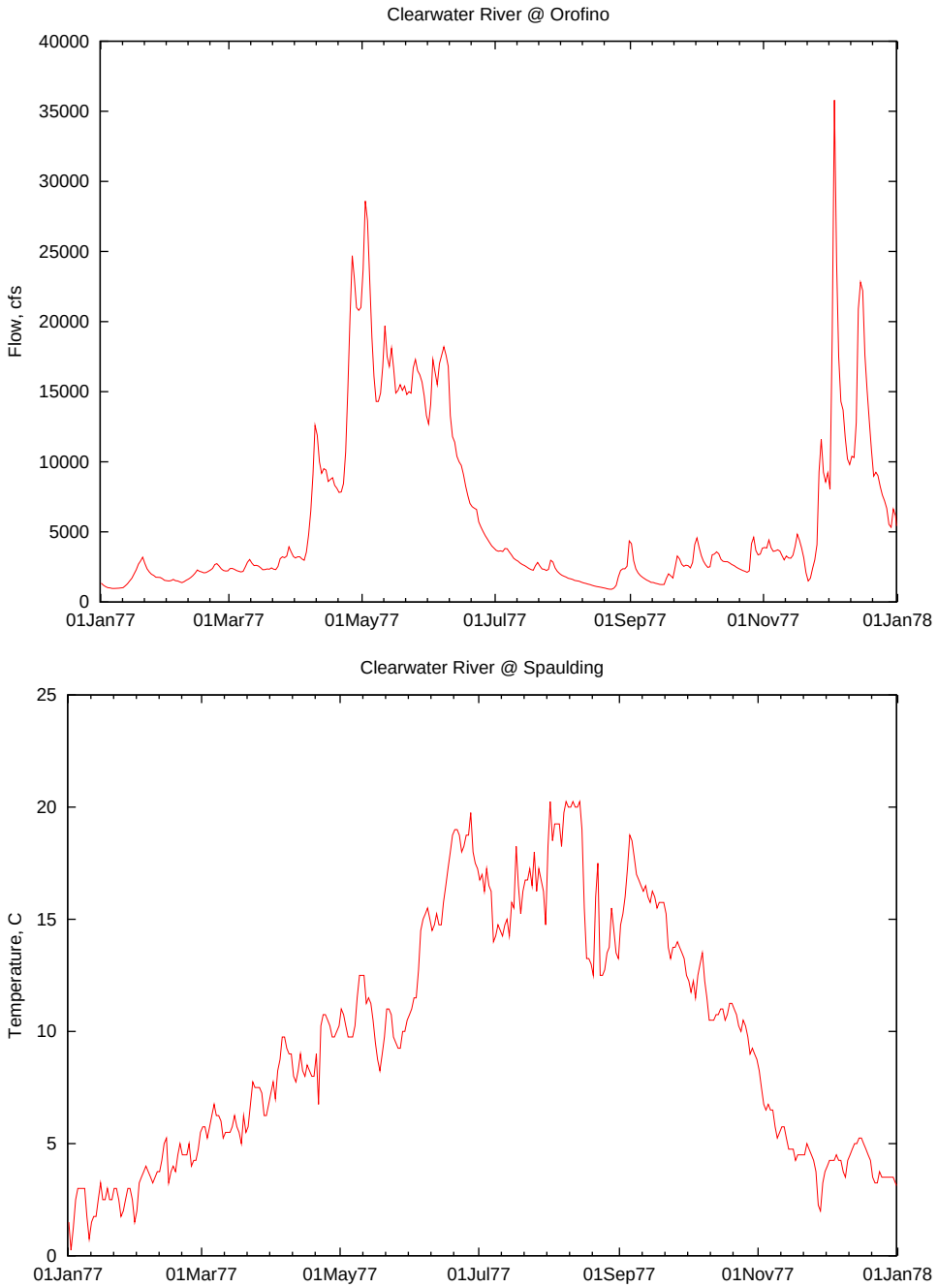

Figure 3: 1977 Clearwater River flow and temperature boundary conditions at Orofino. Temperature is taken from the Spaulding gage downstream.

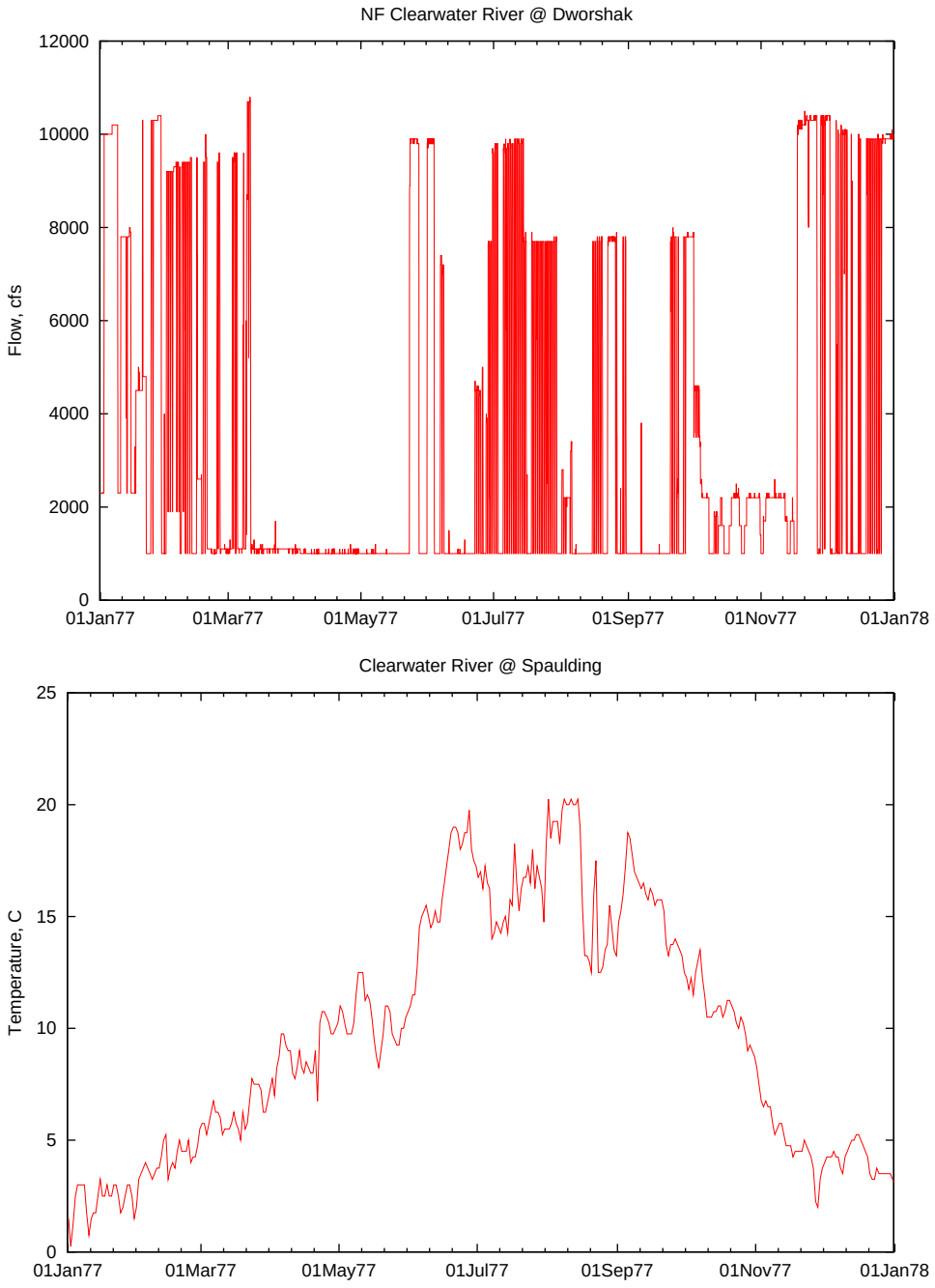

Figure 4: 1977 North Fork Clearwater River flow and temperature boundary conditions at Dworshak dam. Temperature is taken from the Spaulding gage downstream.

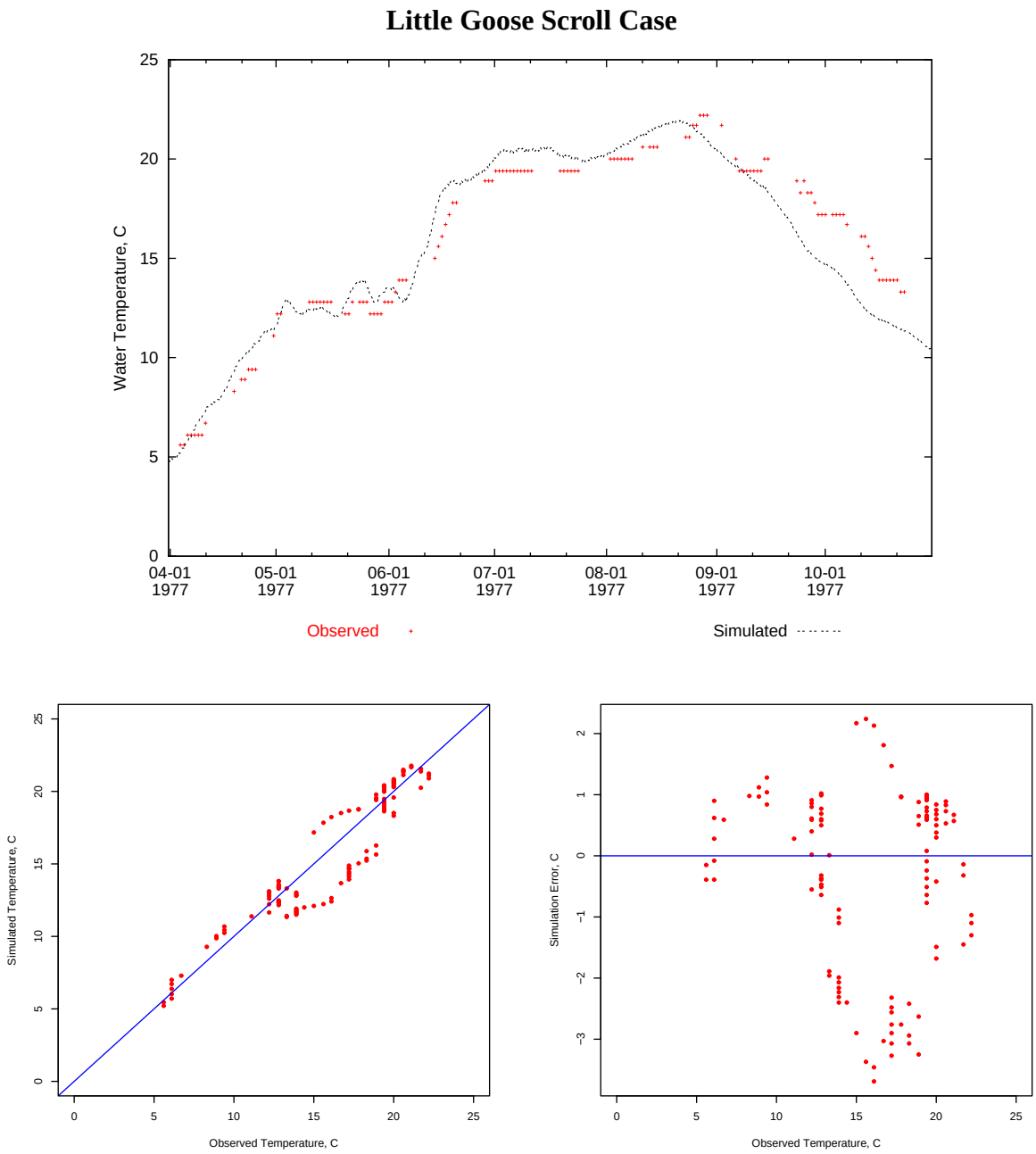

Figure 5: Comparison of simulated temperature and observed scroll case temperature (instantaneous) at Little Goose dam.

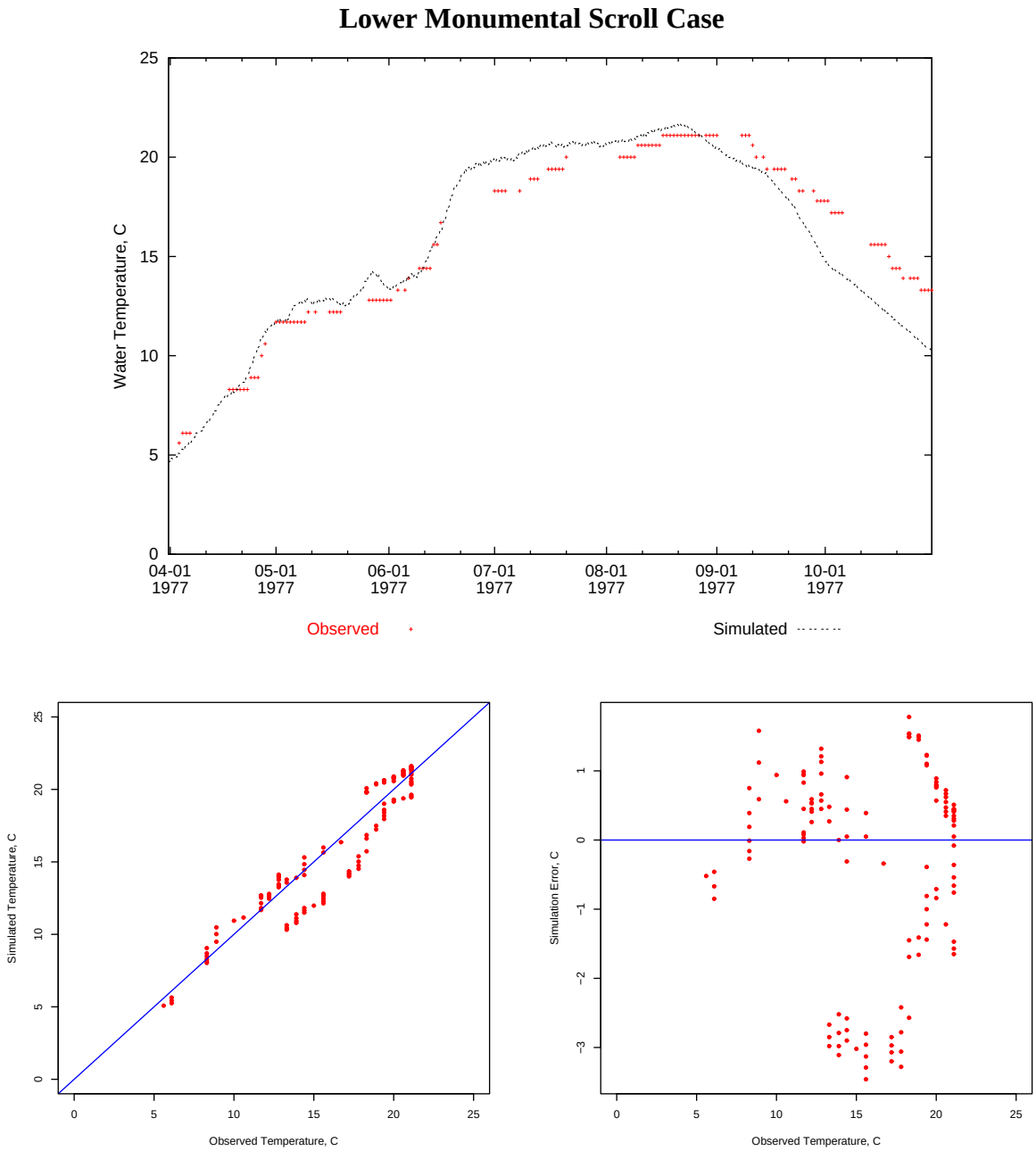

Figure 6: Comparison of simulated temperature and observed scroll case temperature (instantaneous) at Lower Monumental dam.

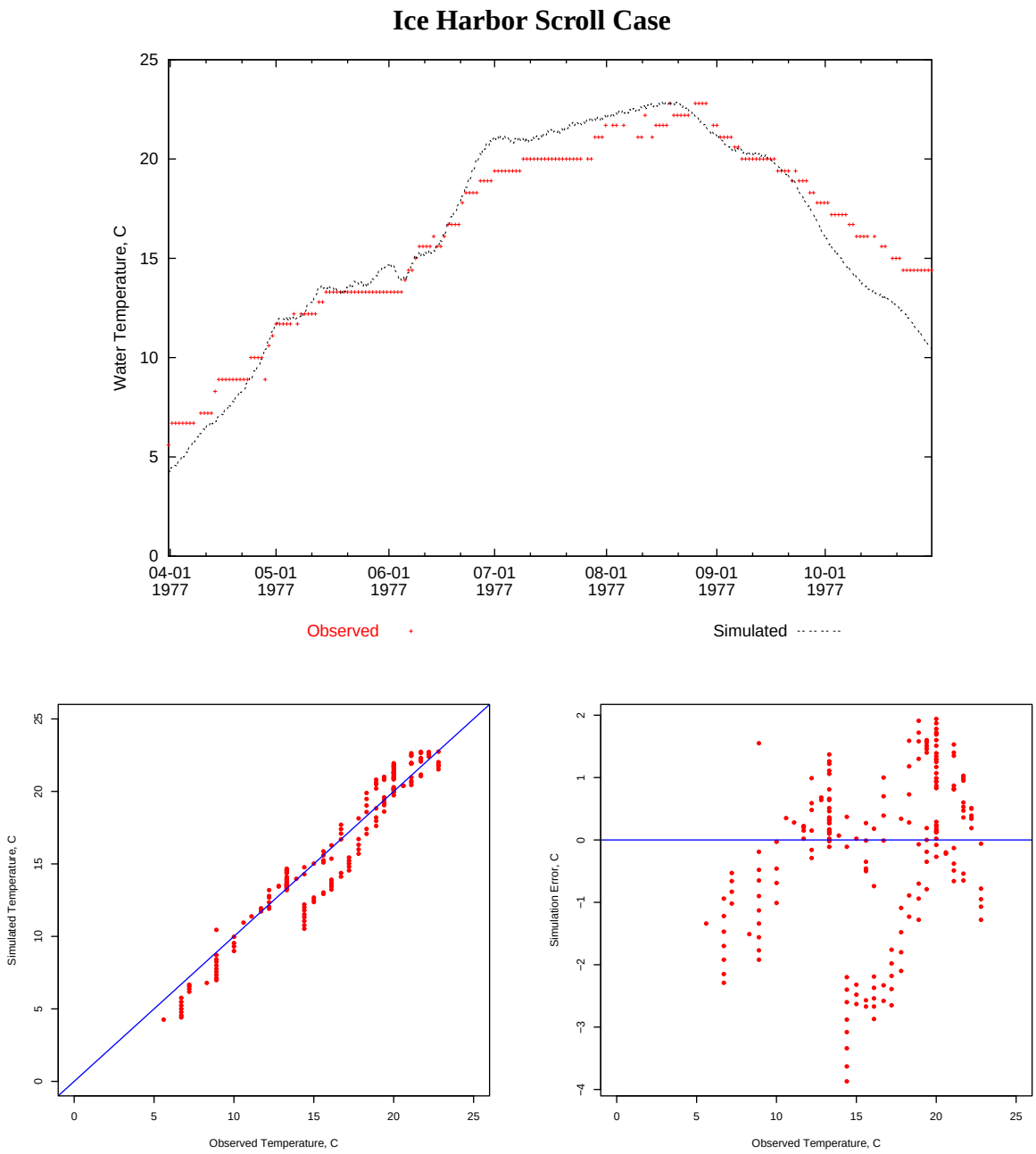

Figure 7: Comparison of simulated temperature and observed scroll case temperature (instantaneous) at Ice Harbor dam.

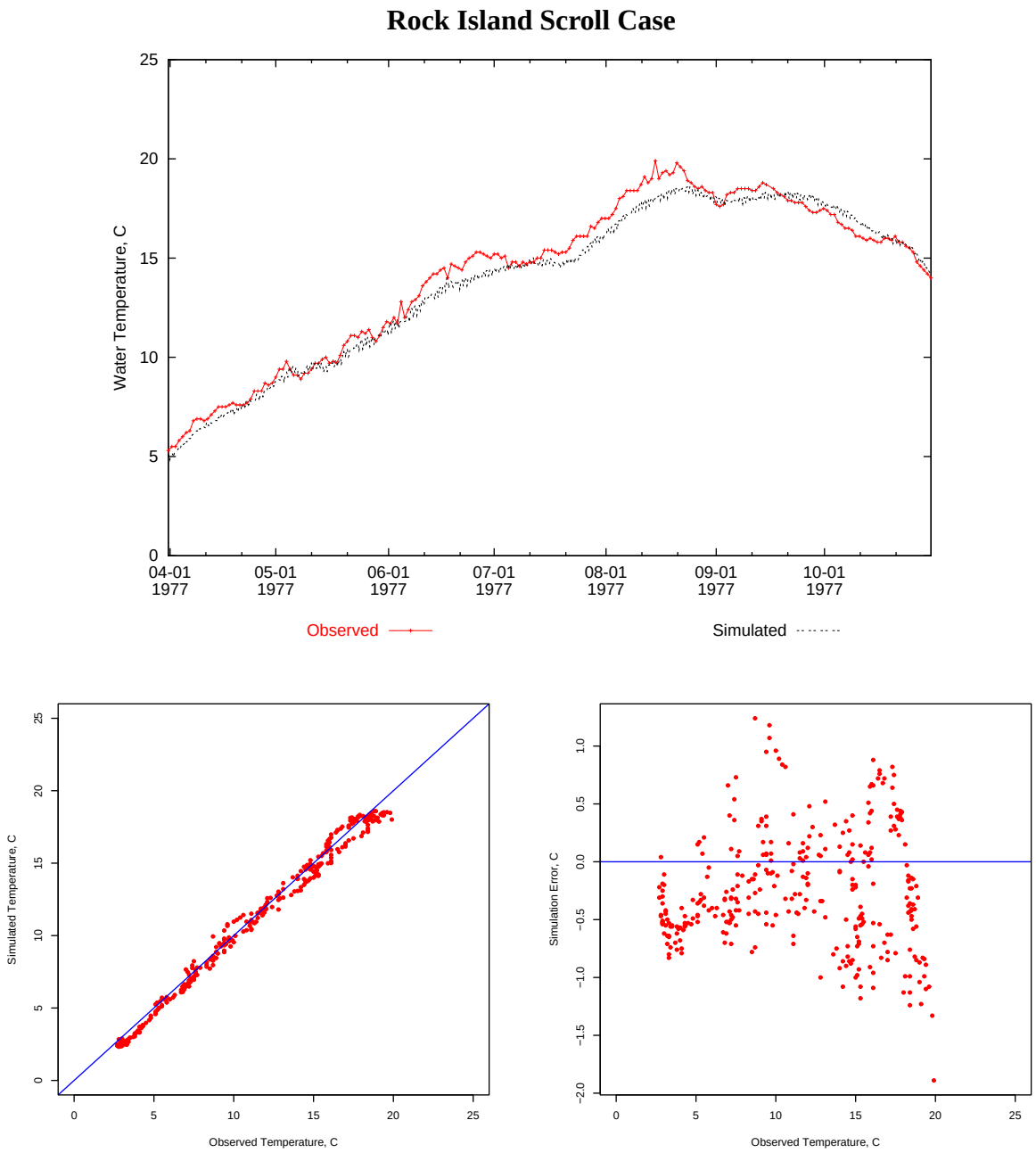

Figure 8: Comparison of simulated temperature and observed scroll case temperature (instantaneous) at Rock Island dam.

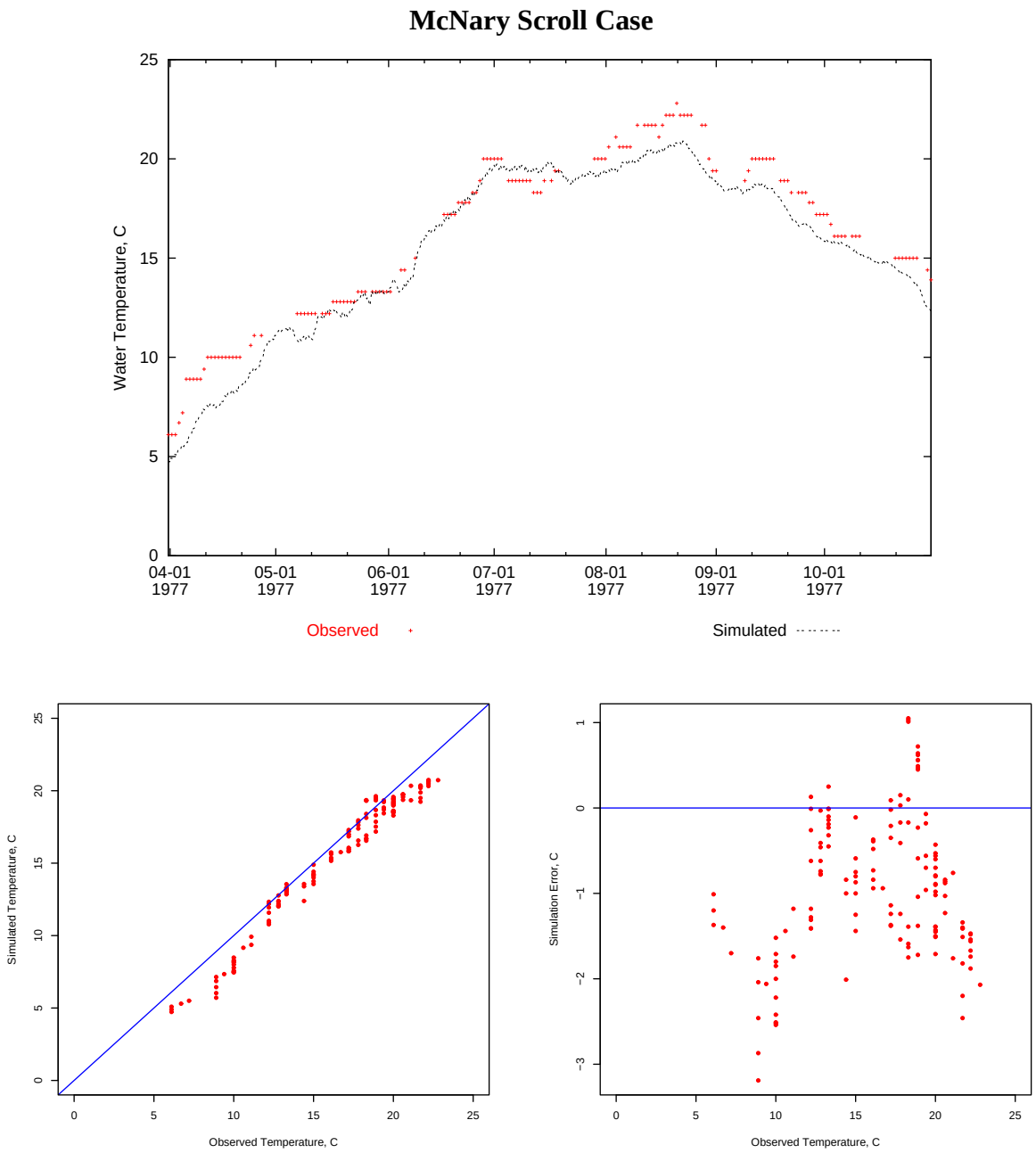

Figure 9: Comparison of simulated temperature and observed scroll case temperature (instantaneous) at McNary dam.

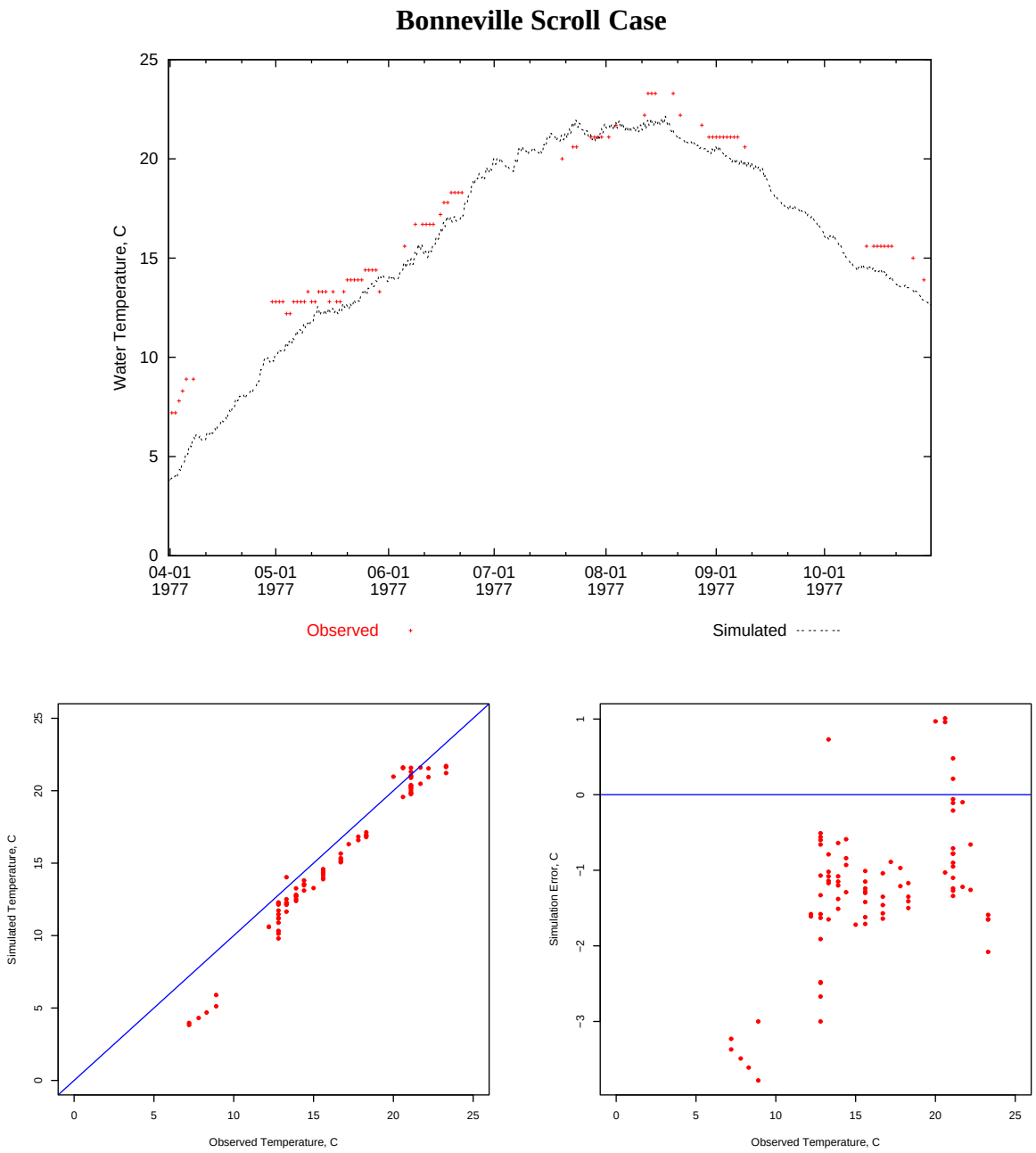

Figure 10: Comparison of simulated temperature observed scroll case temperature (instantaneous) at Bonneville dam.

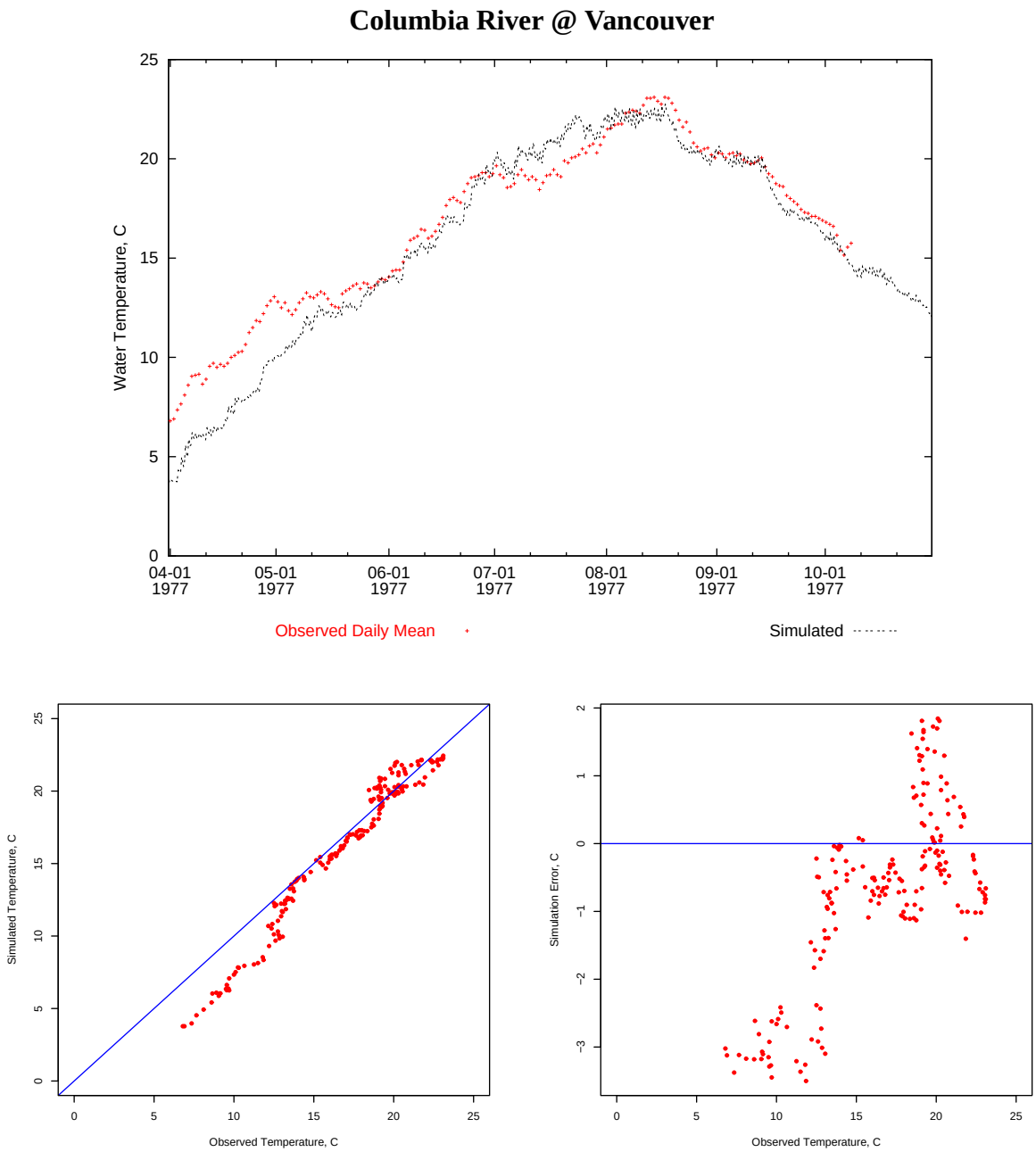

Figure 11: Comparison of simulated and observed daily mean Columbia River temperature at the USGS gage near Vancouver, Washington.

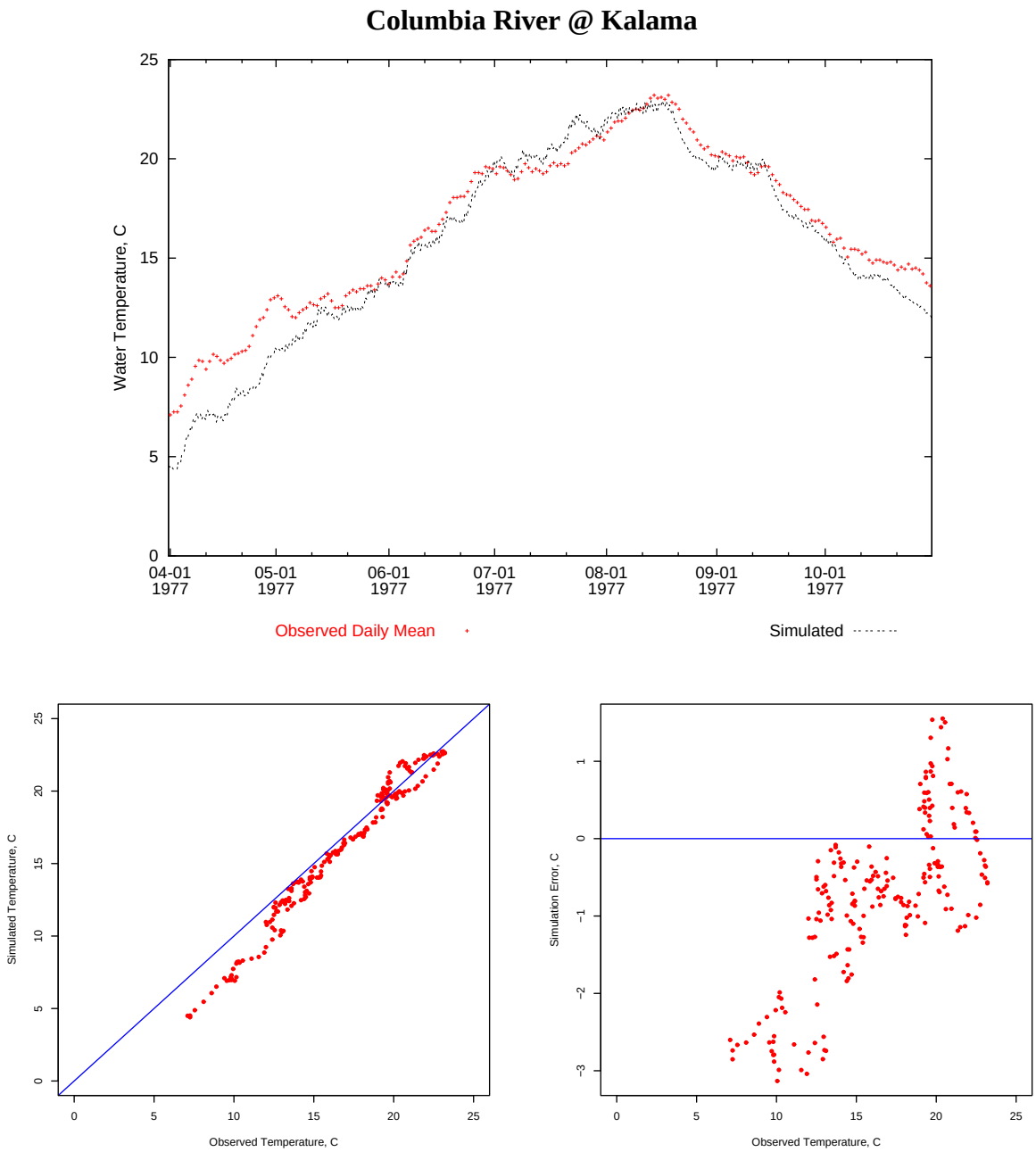

Figure 12: Comparison of simulated and observed daily mean Columbia River temperature at the USGS gage near Kalama, Washington.

2 77H/94M Scenario

This scenario is the same as the 1977 conditions scenario, except that 1994 weather, from the same stations (Wenatchee, Hanford, Portland), was used. This means that the same water temperatures were used at the boundaries (Grand Coulee and Clearwater and Snake Rivers).

3 77H/94M/DWR10 Scenario

Simulation of this scenario was the same as the 77H/94M Scenario, with the following modifications:

- Dworshak discharge was increased to 10.0 kcfs from July 1 to September 30, with 1977 flows for remainder of the season;
- Dworshak temperature during that period was assumed to be 8.89°C (48°F) July 1 to September 30, with temperatures the same as the 1994 Weather Scenario for the remainder of the season;
- Clearwater main stem temperature during the July 1 to September 30 were estimated using the method described in Appendix A; and
- Flow is augmented on the Columbia in order to maintain flows at Priest Rapids above 65 kcfs.

Figure 13 compares the Clearwater River boundary conditions used in the 77H/94M/DWR10 scenario to those used in the 77H/94M scenario. When the Priest Rapids discharge (in the 77H/94M scenario) dropped below 65 kcfs, the amount required to bring it to 65 kcfs was lagged 6 hours (the approximate wave travel time from Grand Coulee to Priest Rapids) and added to the original (1977) Grand Coulee discharge. Figure 14 compares the discharge used at Grand Coulee with the 77H/94M scenario, and also shows the result change in flow at Priest Rapids. In general, this augmentation had the desired effect – Priest Rapids minimum flows were raised, but minimum flows were closer to 60 kcfs than 65 kcfs. This is probably because the wave travel time between Grand Coulee was not precisely 6 hours. Any augmentation done in this fashion in going to be imprecise.

4 77H/94M/DWR1 Scenario

This senario differs from the base scenario (77H/94M, Section 2) in two ways: (1) discharge at Grand Coulee is manipulated in an attempt to meet minimum flow targets at Priest Rapids, and (2) Dworshak discharge and temperature is manipulated. Figures 15 and 16 show differences in boundary conditions, from the 77H/94M scenario, used at Dworshak Grand Coulee.

For this scenario, the observed, hourly 1977 flows at Grand Coulee were modified in an attempt to meet a target minimum flow at Priest Rapids. This target varied through the simulated season,

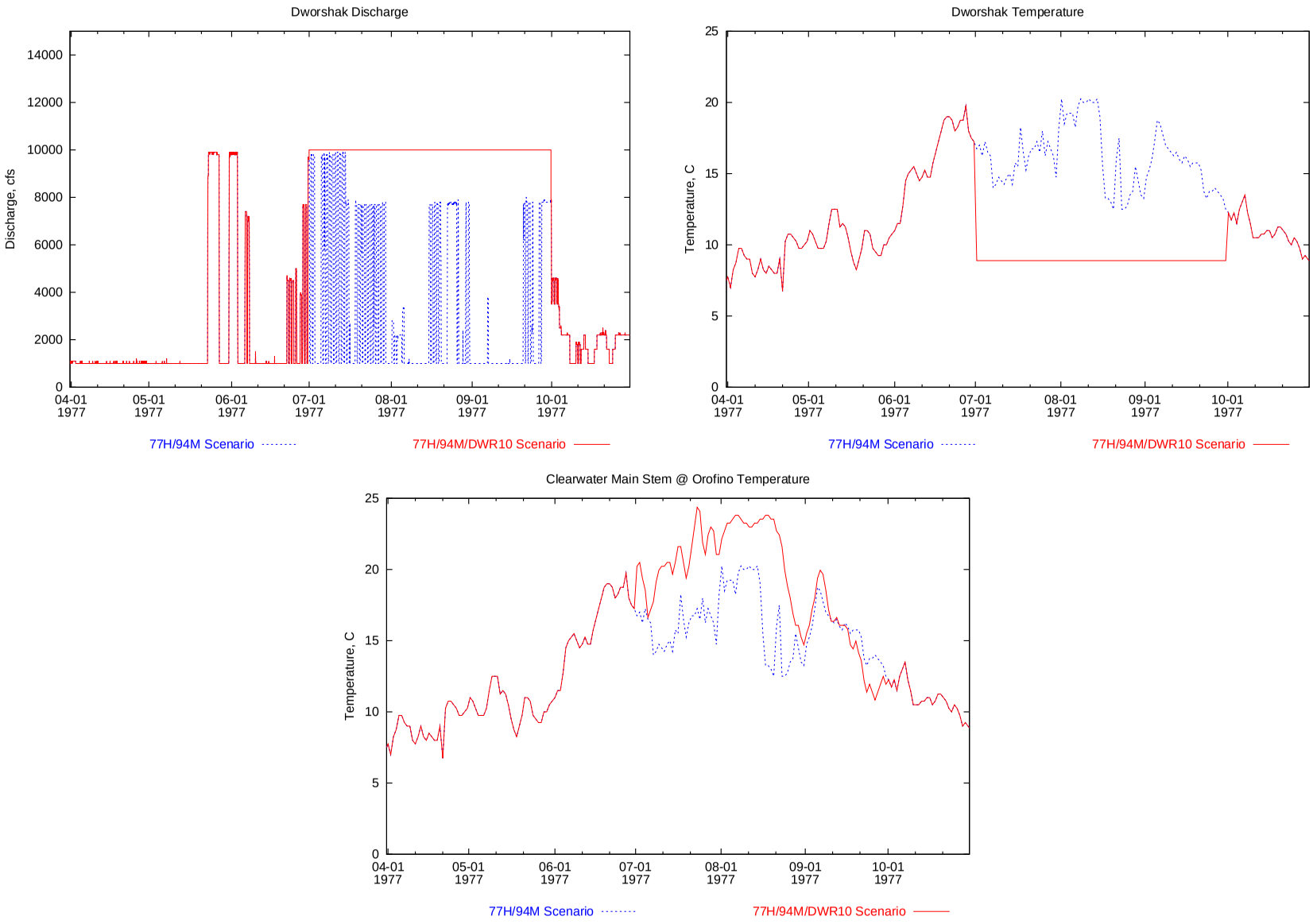

Figure 13: Altered Clearwater River boundary conditions for the 77H/94M/DWR10 scenario.

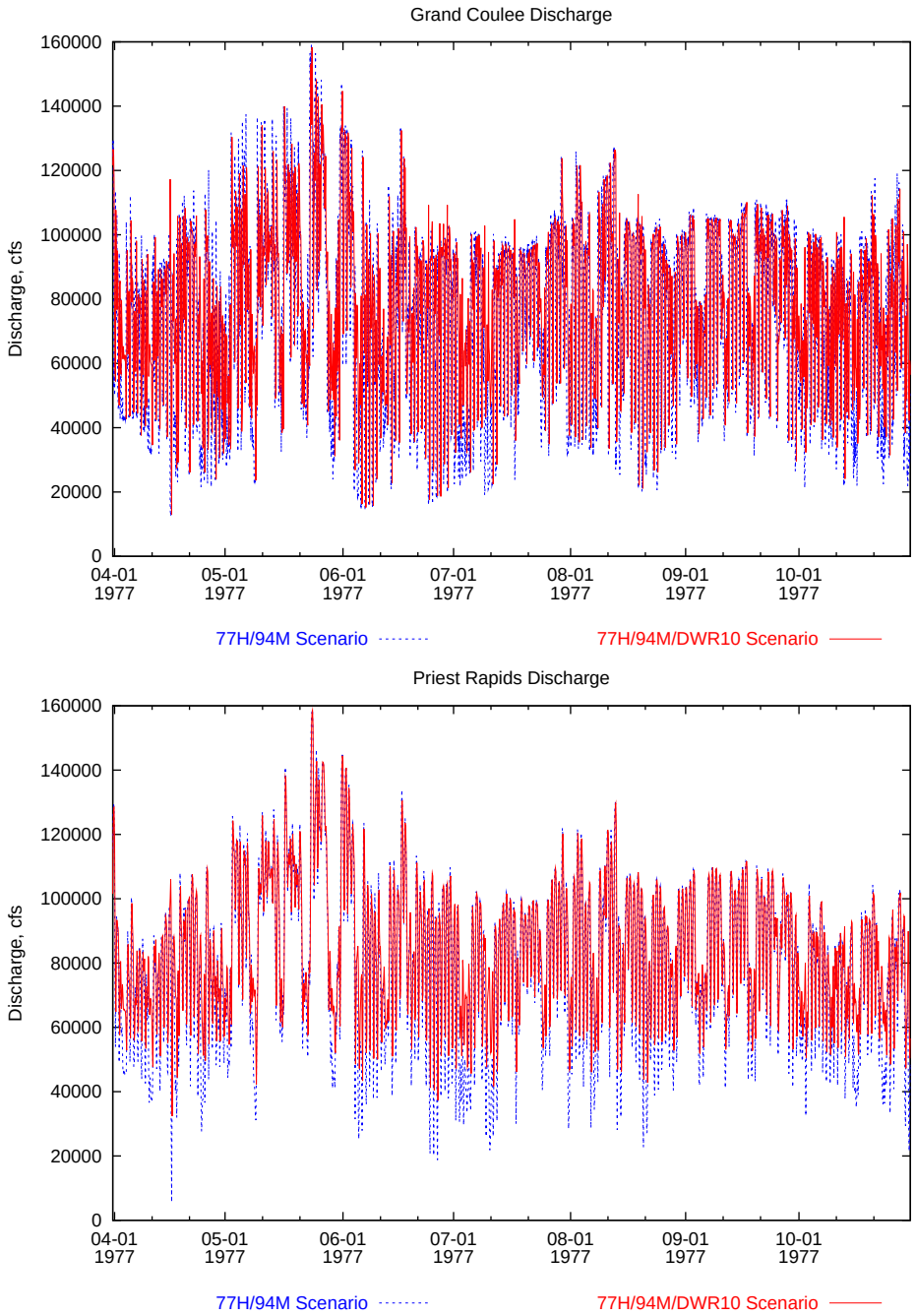

Figure 14: Altered flow boundary conditions at Grand Coulee and comparison of resulting flow at Priest Rapids.

as shown in Table 2. To produce the target minimum flow at PRD, the flow at Grand Coulee was not allowed to go below the Priest Rapids target minimum less 5 kcfs. This was a rough approximation to account for tributary inflow and discharge wave attenuation, but seemed to have the desired effect, as shown in Figure 16.

Table 2: Priest Rapids target minimum flows and Grand Coulee minimum flows used in the 77H/94M/DWR1 Scenario.

Start Date	**End Date**	**PRD Target Minimum Flow (kcfs)**	**GCL Minimum Flow (kcfs)**
01 Jan	07 May	65.0	60.0
08 May	08 May	60.0	55.0
09 May	09 May	55.0	50.0
10 May	10 May	50.0	45.0
11 May	11 May	45.0	40.0
12 May	31 Dec	36.0	31.0

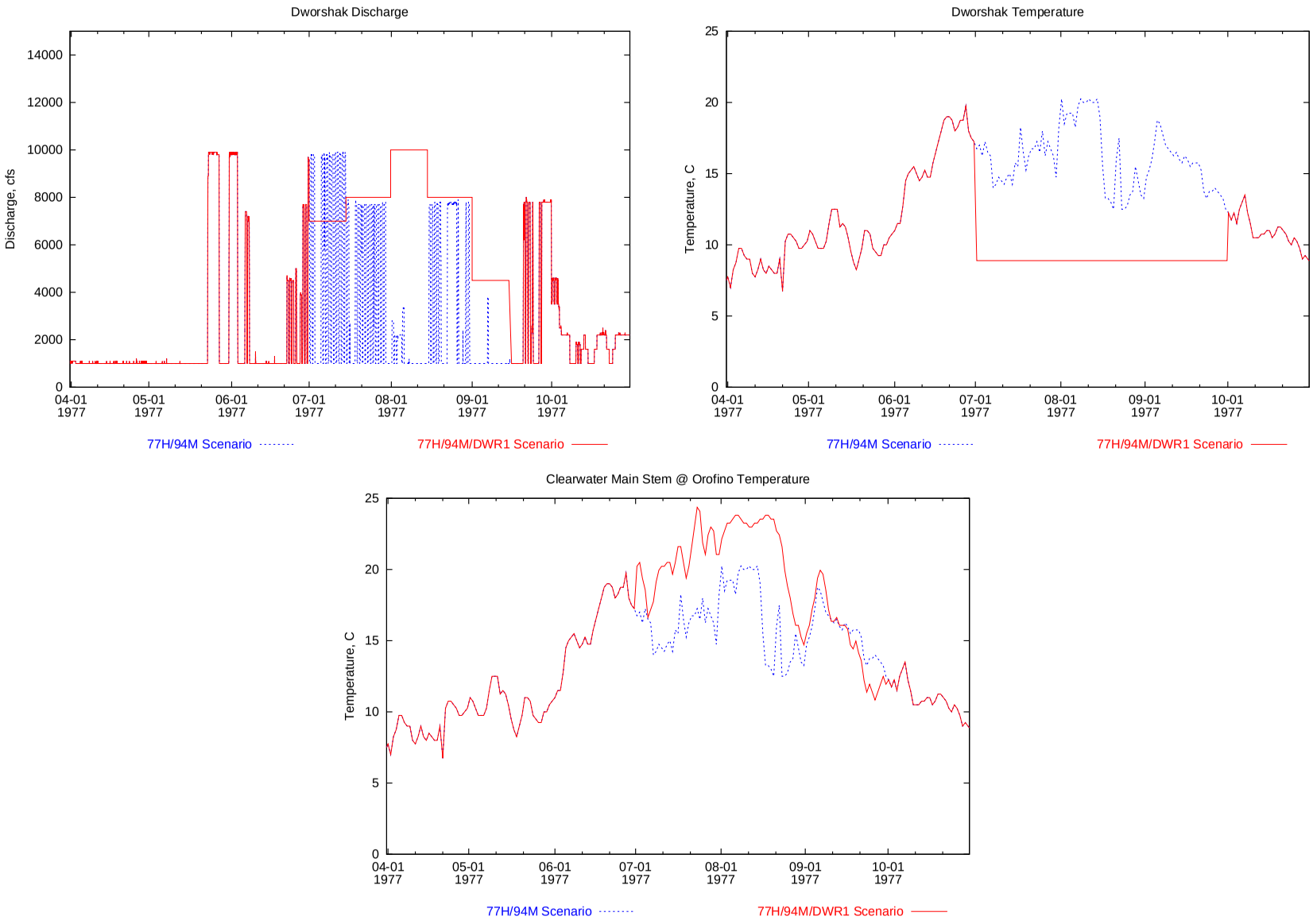

Figure 15: Altered Clearwater River boundary conditions for the 77H/94M/DWR1 scenario.

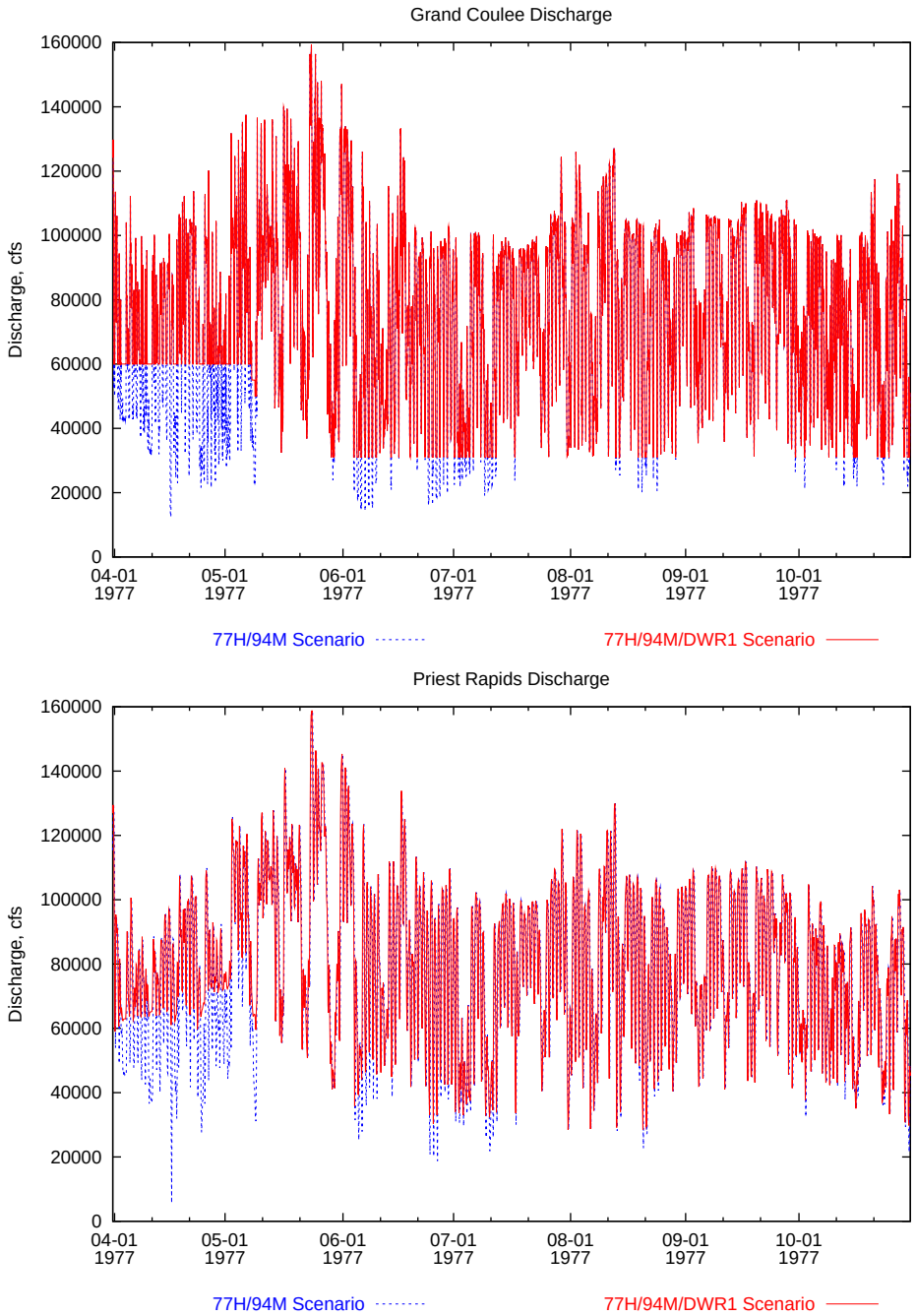

Figure 16: Altered flow boundary conditions at Grand Coulee and comparison of resulting flow at Priest Rapids in the 77H/94M/DWR1 scenario.

5 Scenario Temperature Comparisons

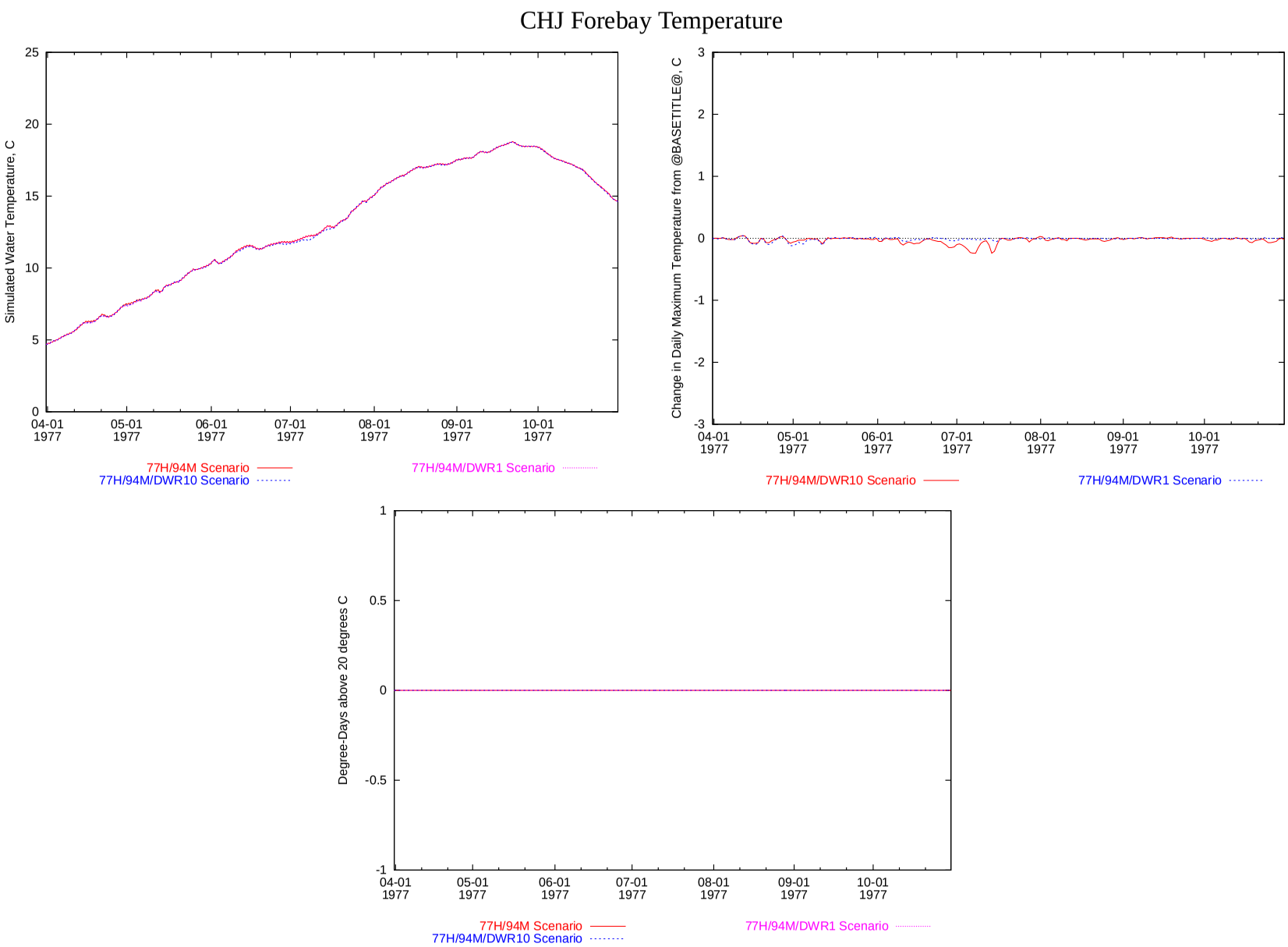

Figure 17: Time series comparison of simulated temperature at the CHJ Forebay.

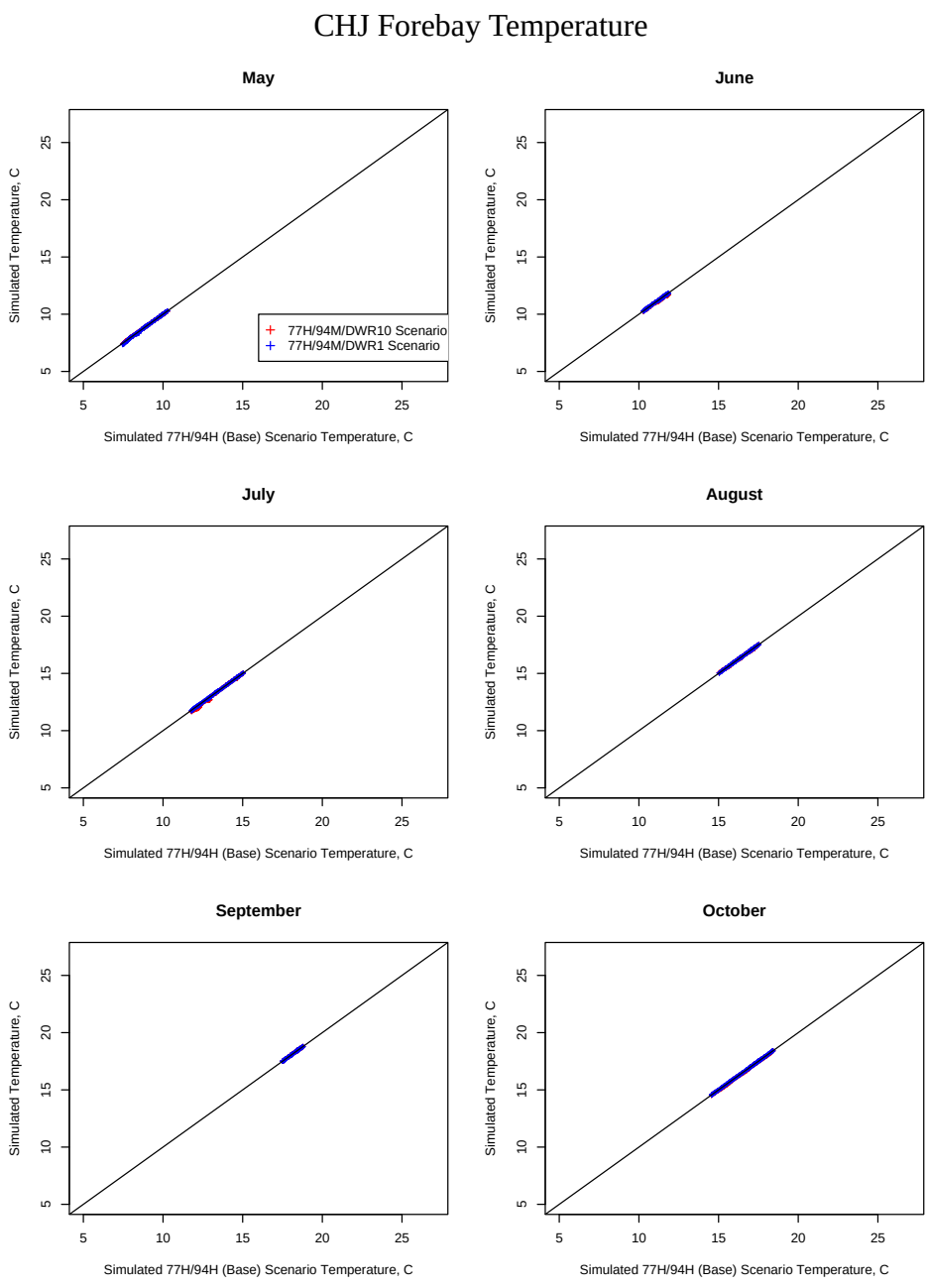

Figure 18: Scatter plot comparison, by month, of simulated temperature at the CHJ Forebay.

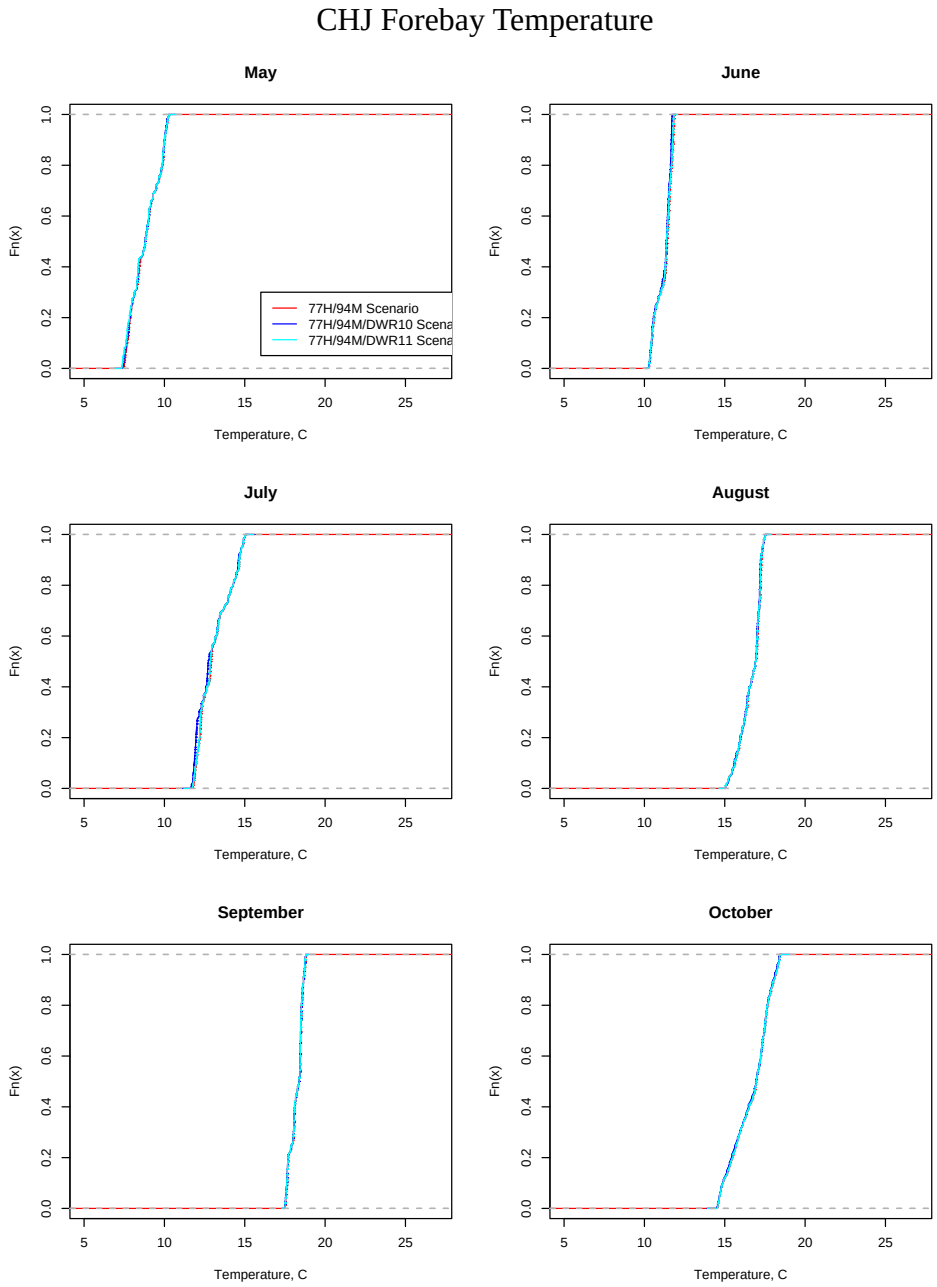

Figure 19: Cumulative frequency distribution (CFD) plot comparison, by month, of simulated temperature at the CHJ Forebay.

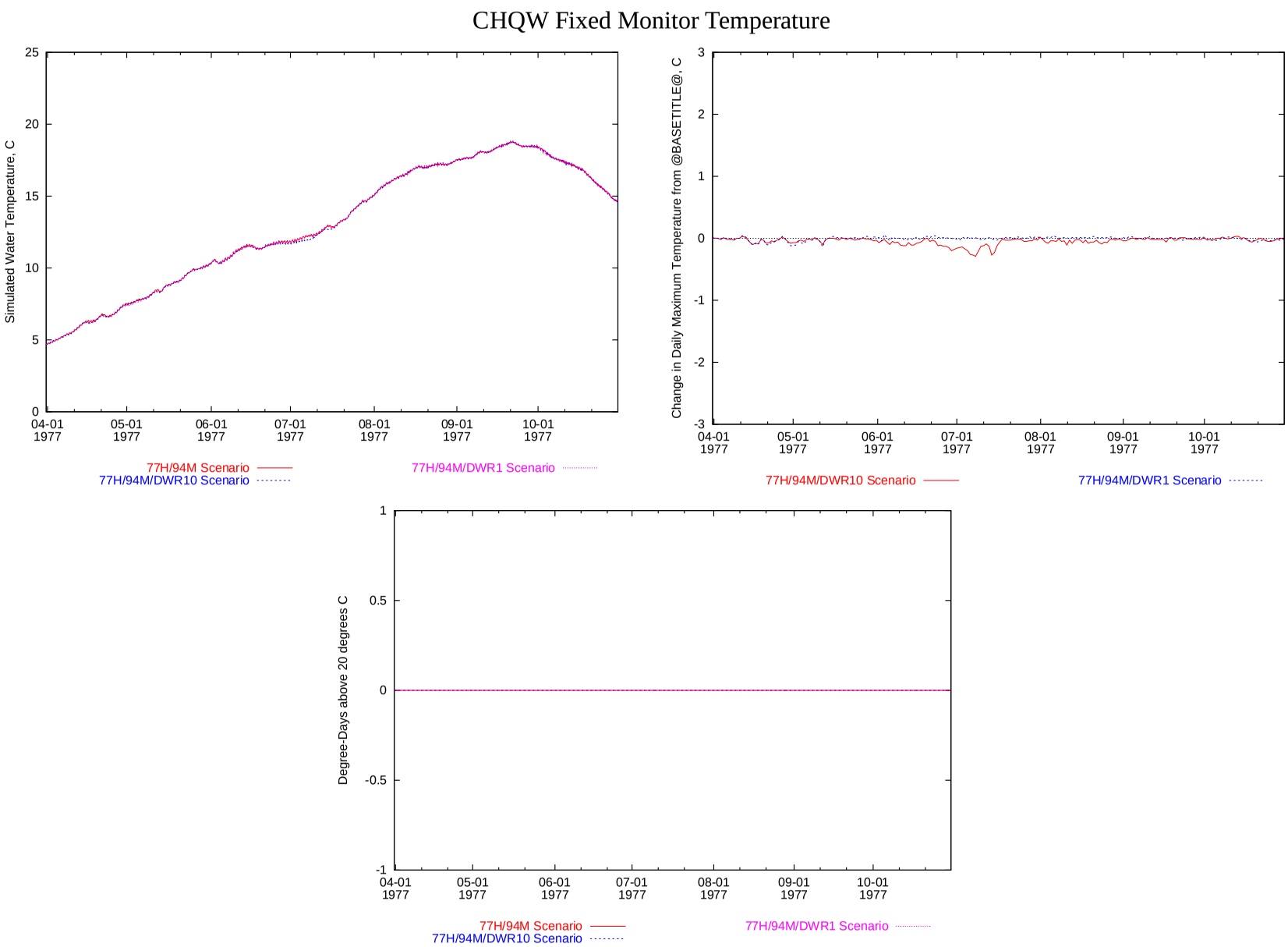

Figure 20: Time series comparison of simulated temperature at the CHQW Fixed Monitor.

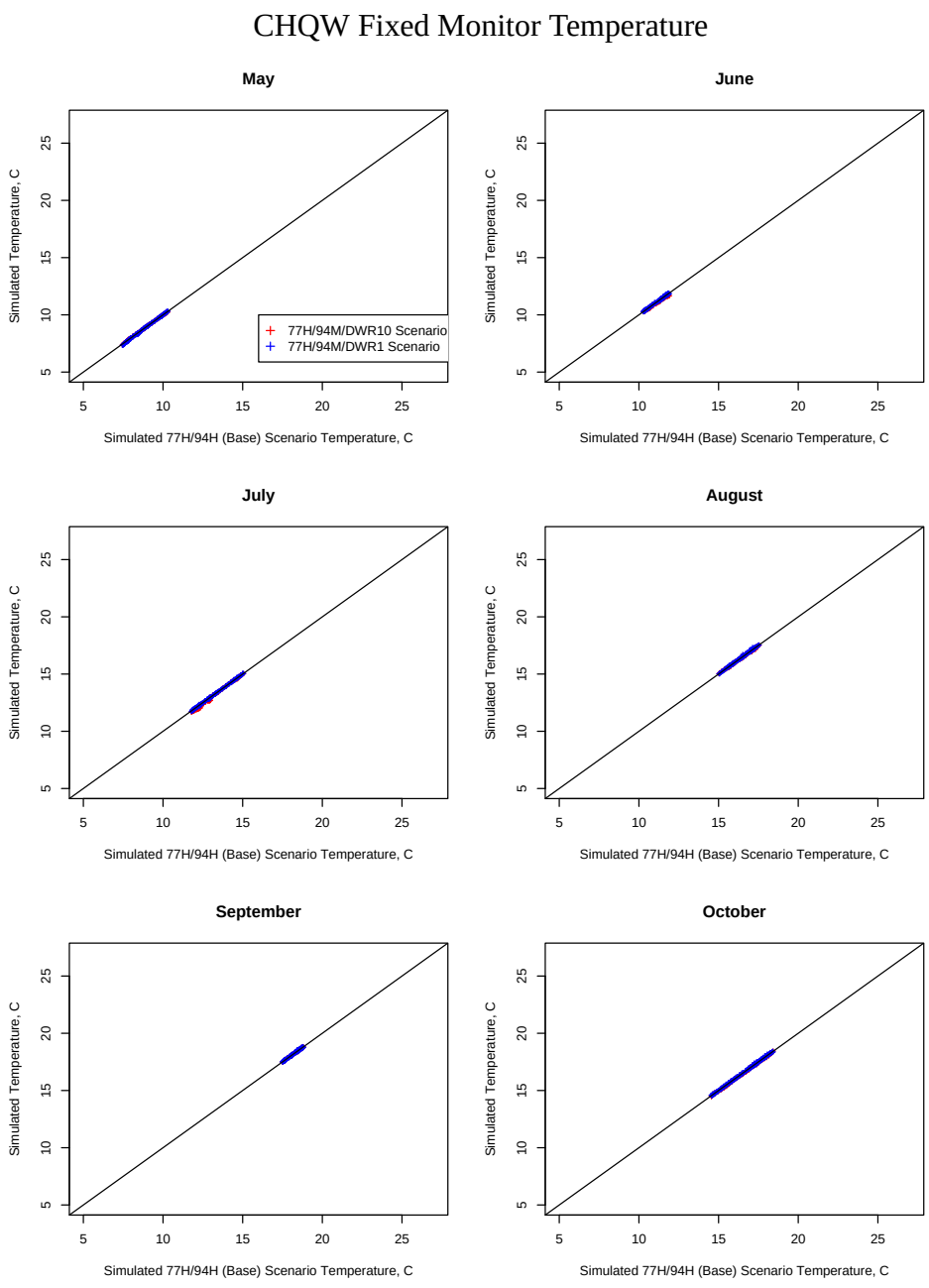

Figure 21: Scatter plot comparison, by month, of simulated temperature at the CHQW Fixed Monitor.

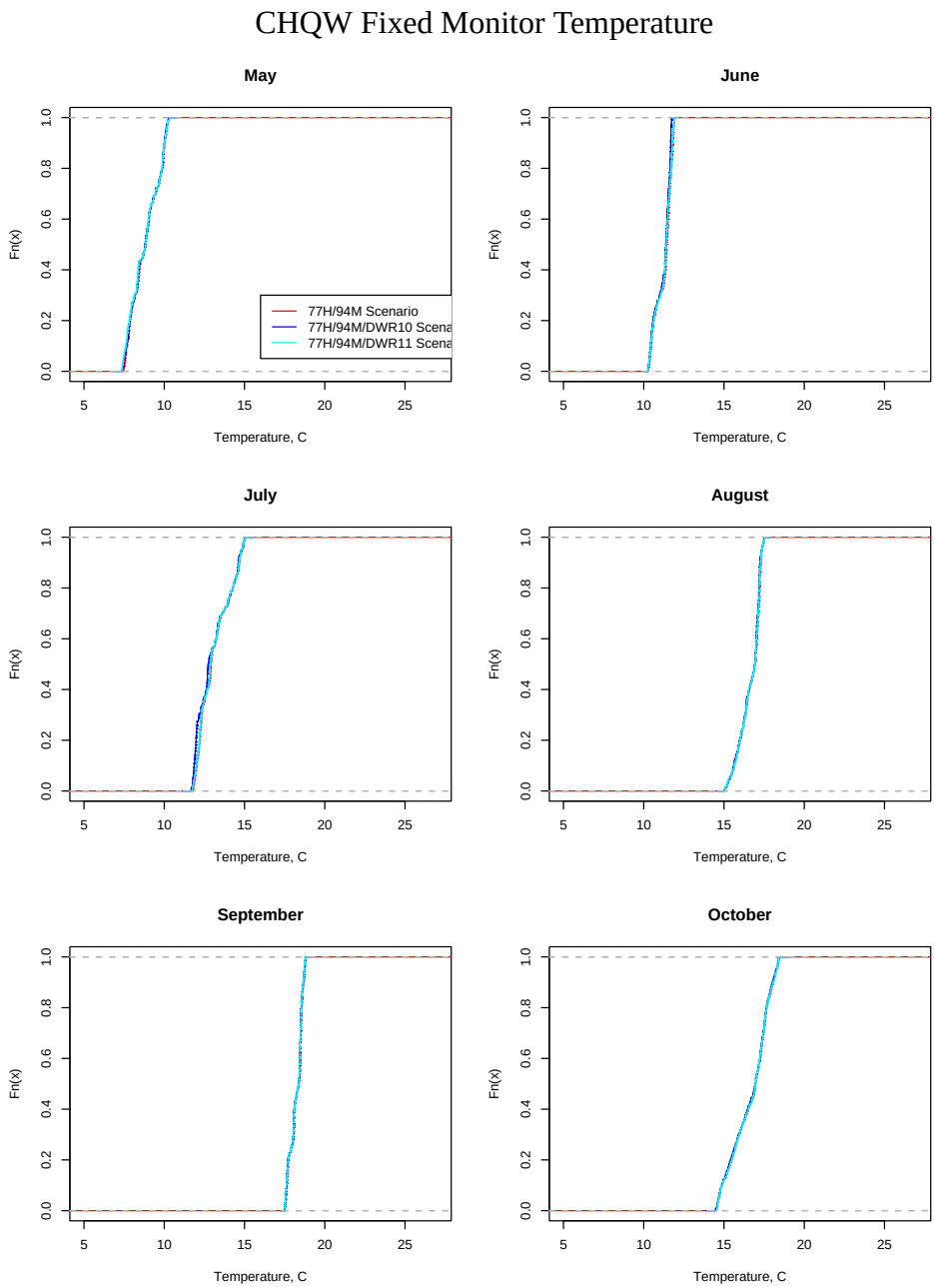

Figure 22: Cumulative frequency distribution (CFD) plot comparison, by month, of simulated temperature at the CHQW Fixed Monitor.

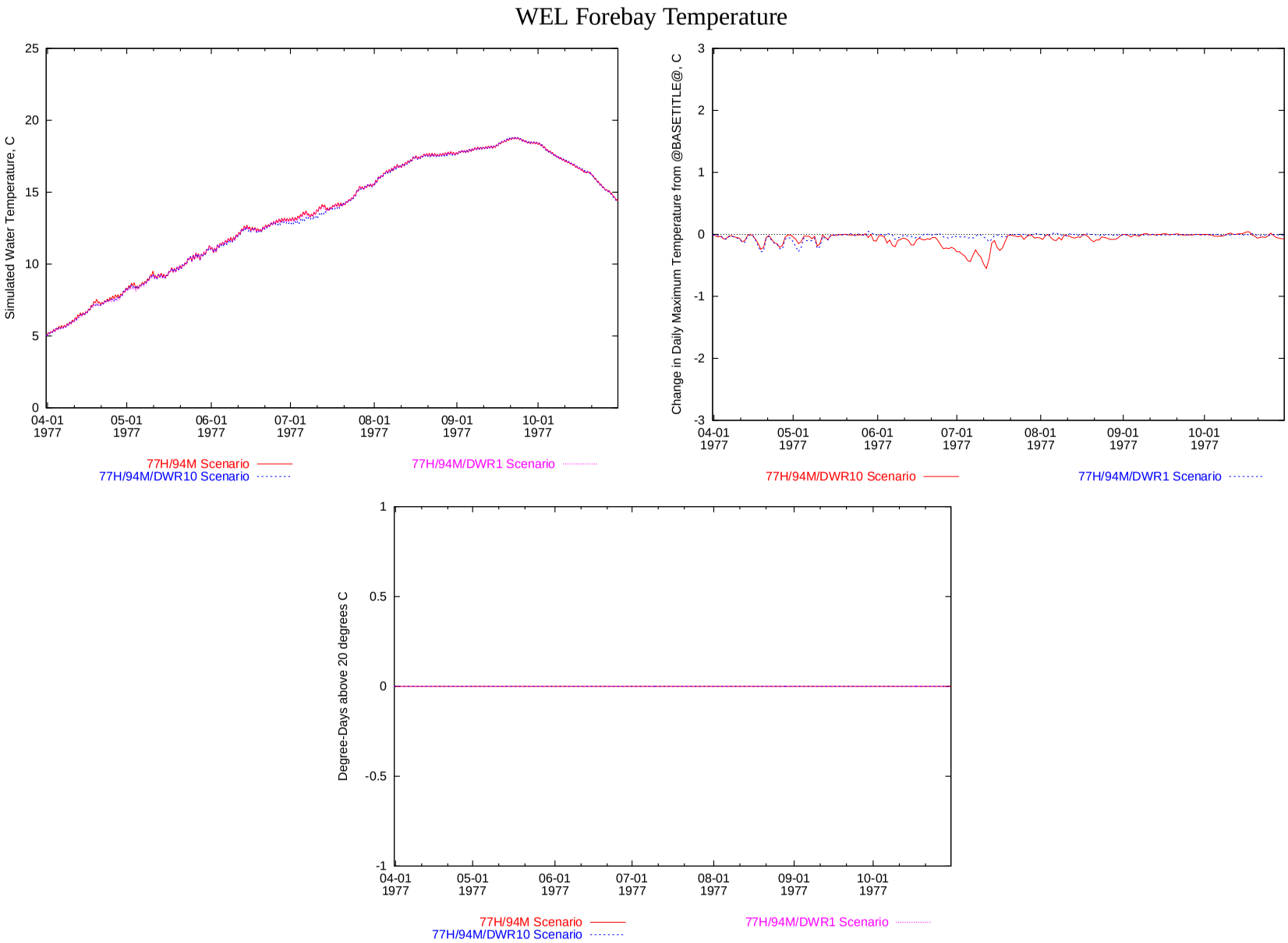

Figure 23: Time series comparison of simulated temperature at the WEL Forebay.

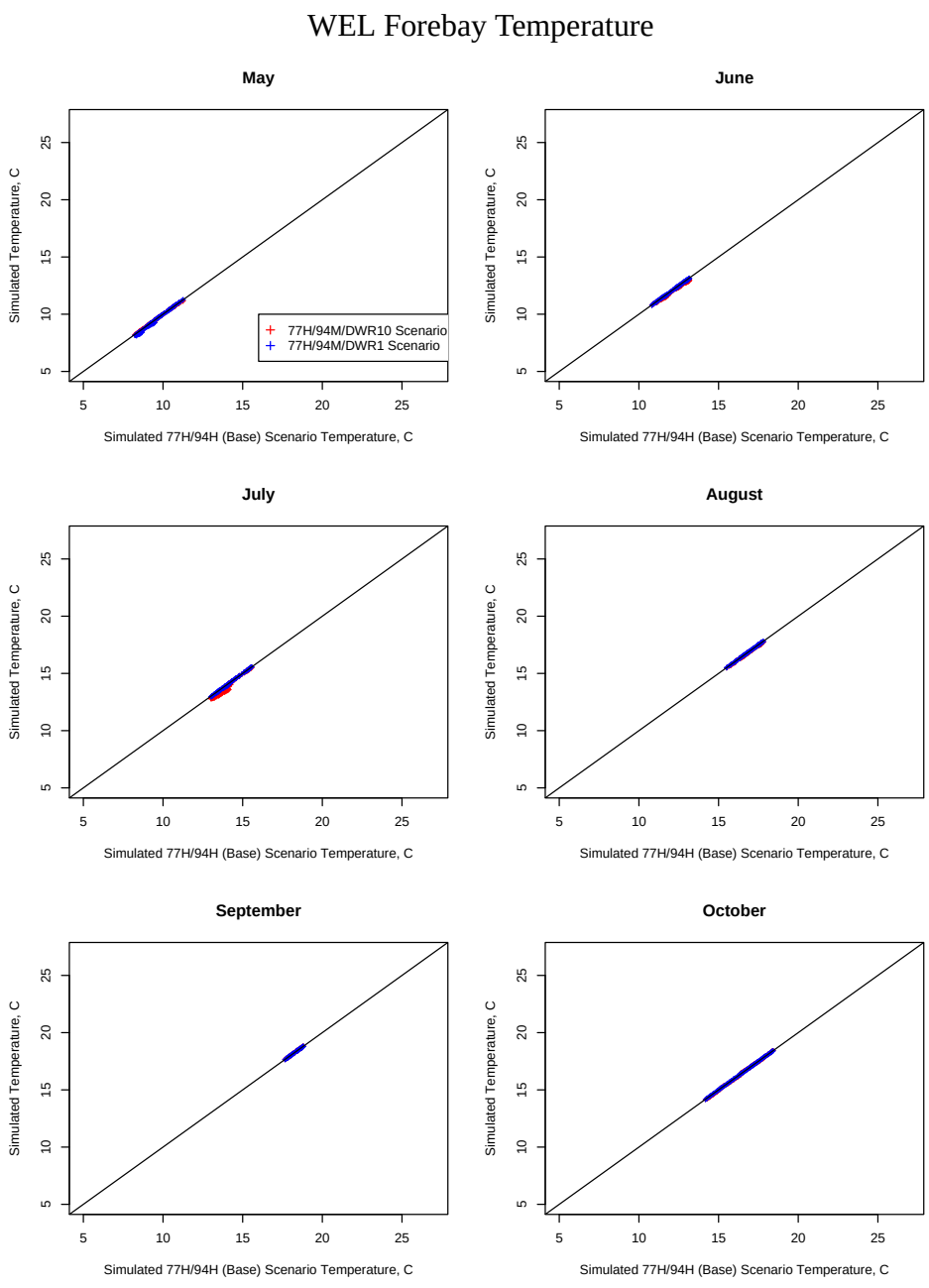

Figure 24: Scatter plot comparison, by month, of simulated temperature at the WEL Forebay.

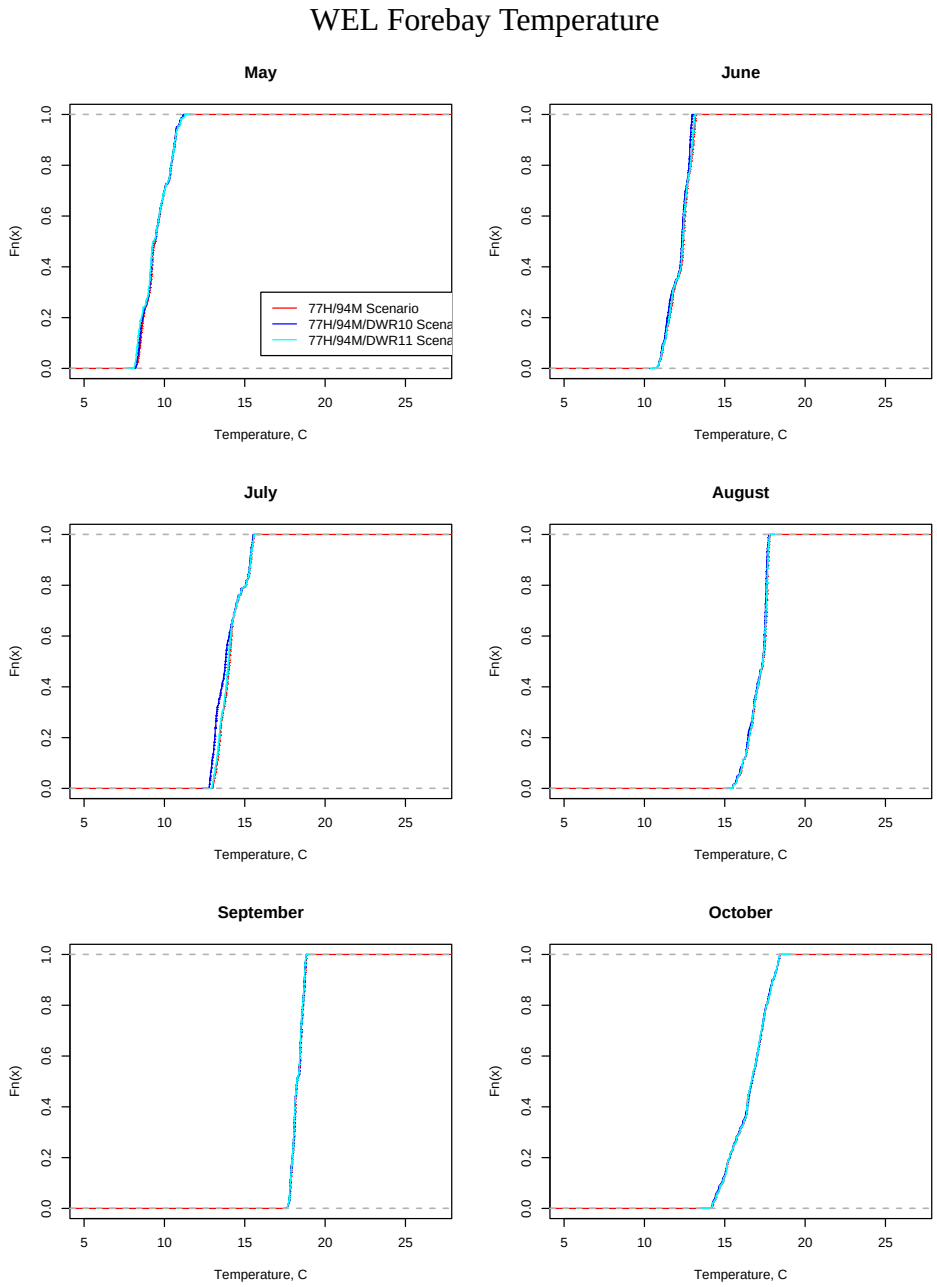

Figure 25: Cumulative frequency distribution (CFD) plot comparison, by month, of simulated temperature at the WEL Forebay.

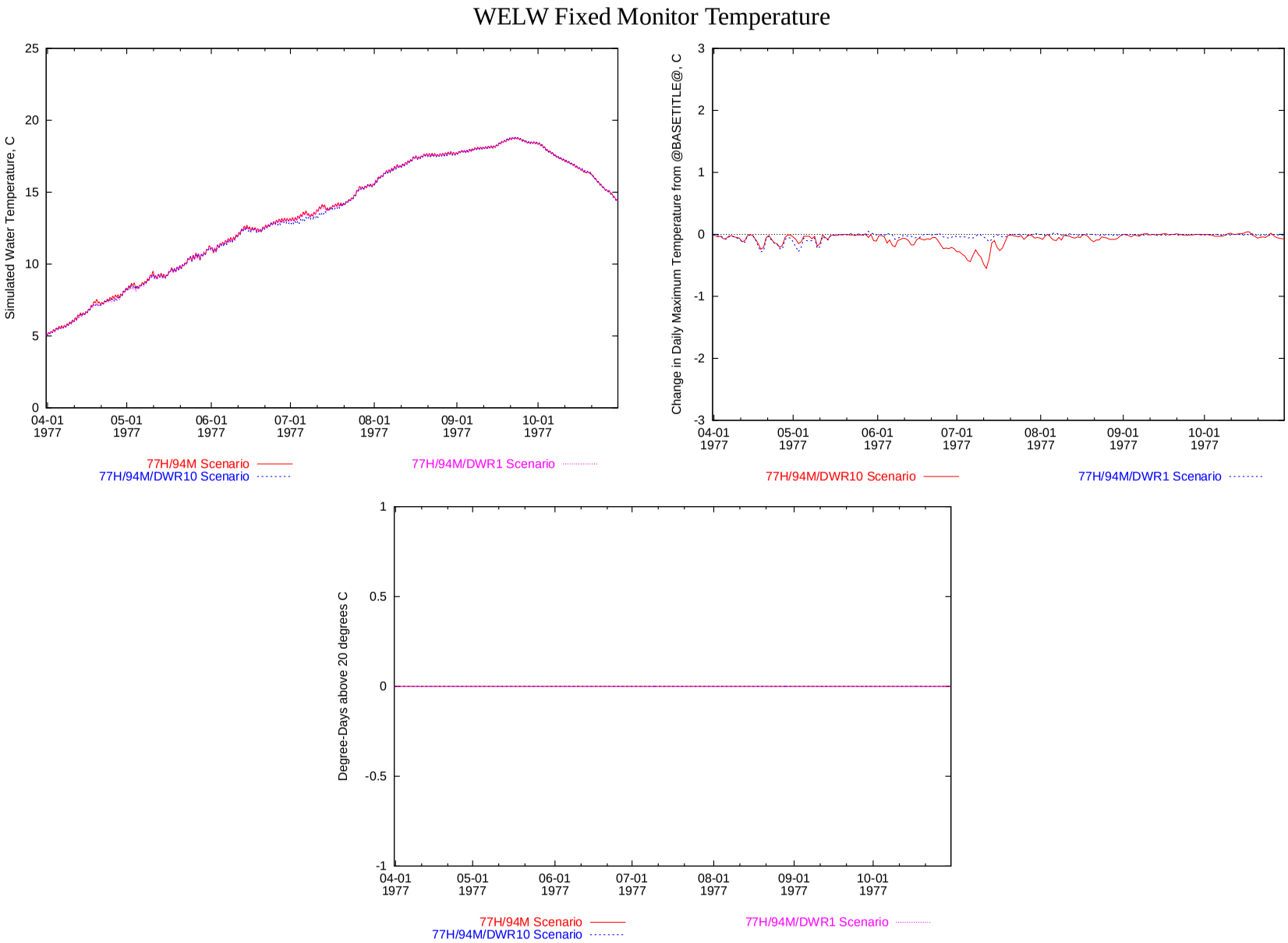

Figure 26: Time series comparison of simulated temperature at the WELW Fixed Monitor.

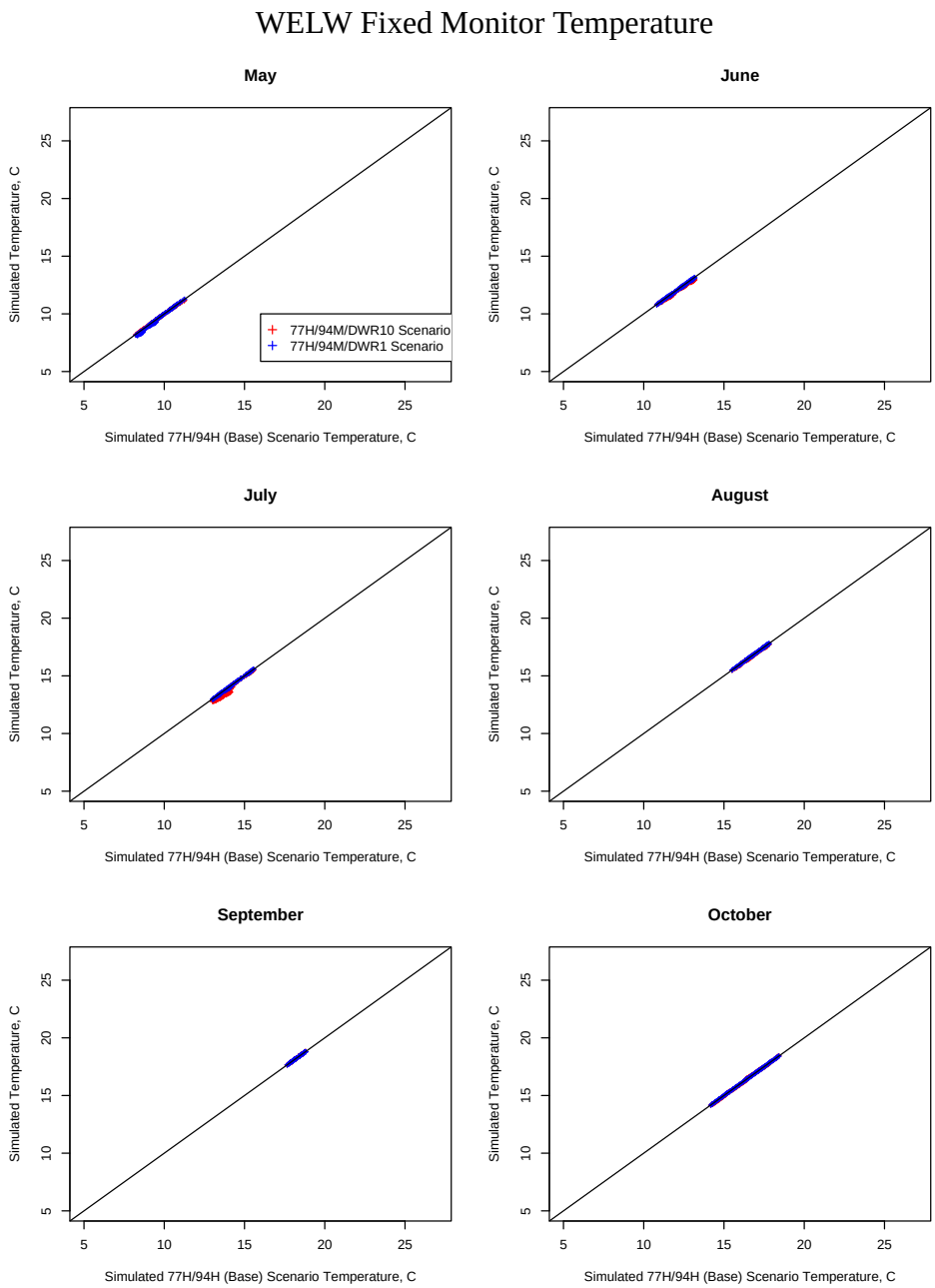

Figure 27: Scatter plot comparison, by month, of simulated temperature at the WELW Fixed Monitor.

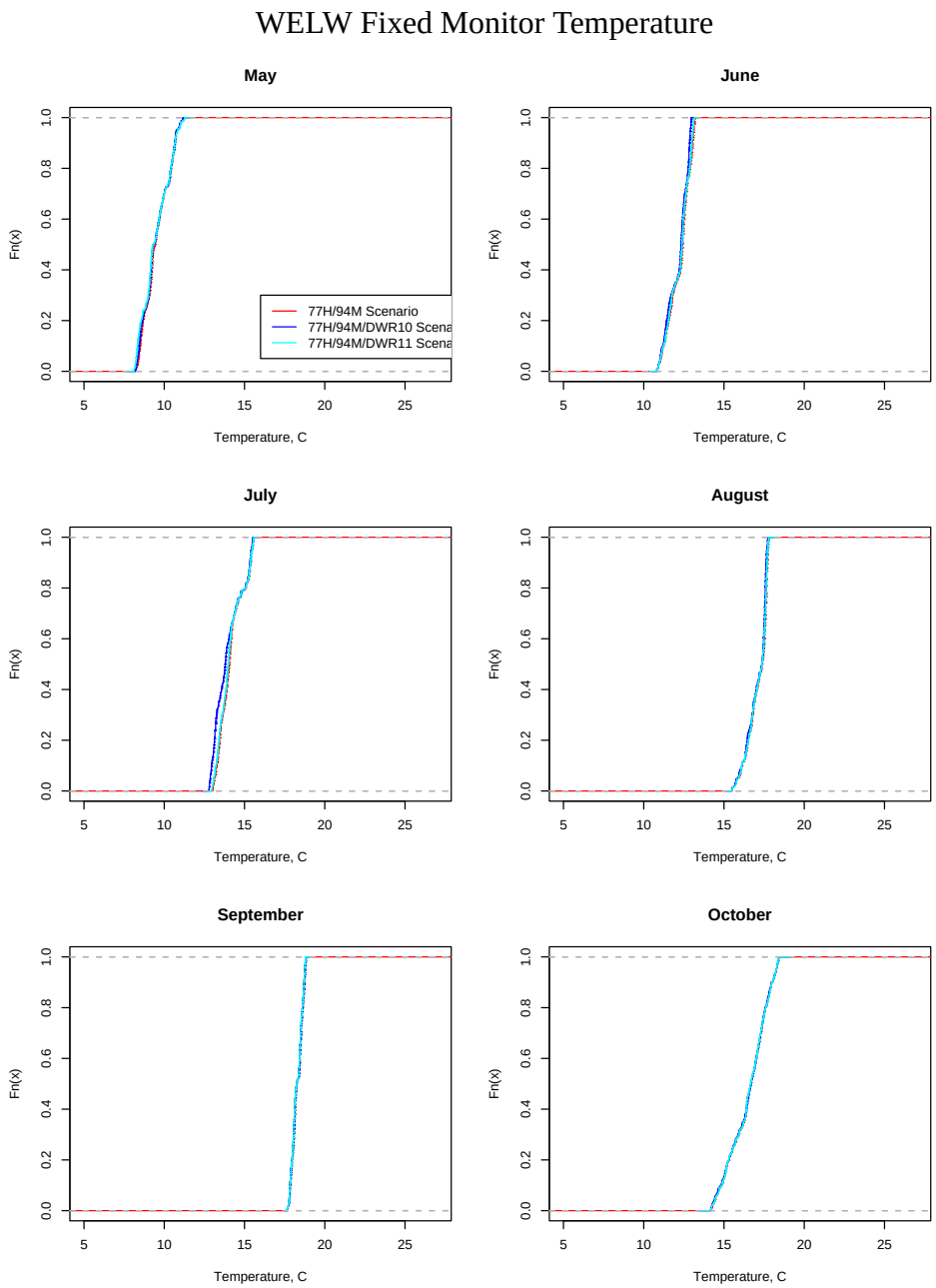

Figure 28: Cumulative frequency distribution (CFD) plot comparison, by month, of simulated temperature at the WELW Fixed Monitor.

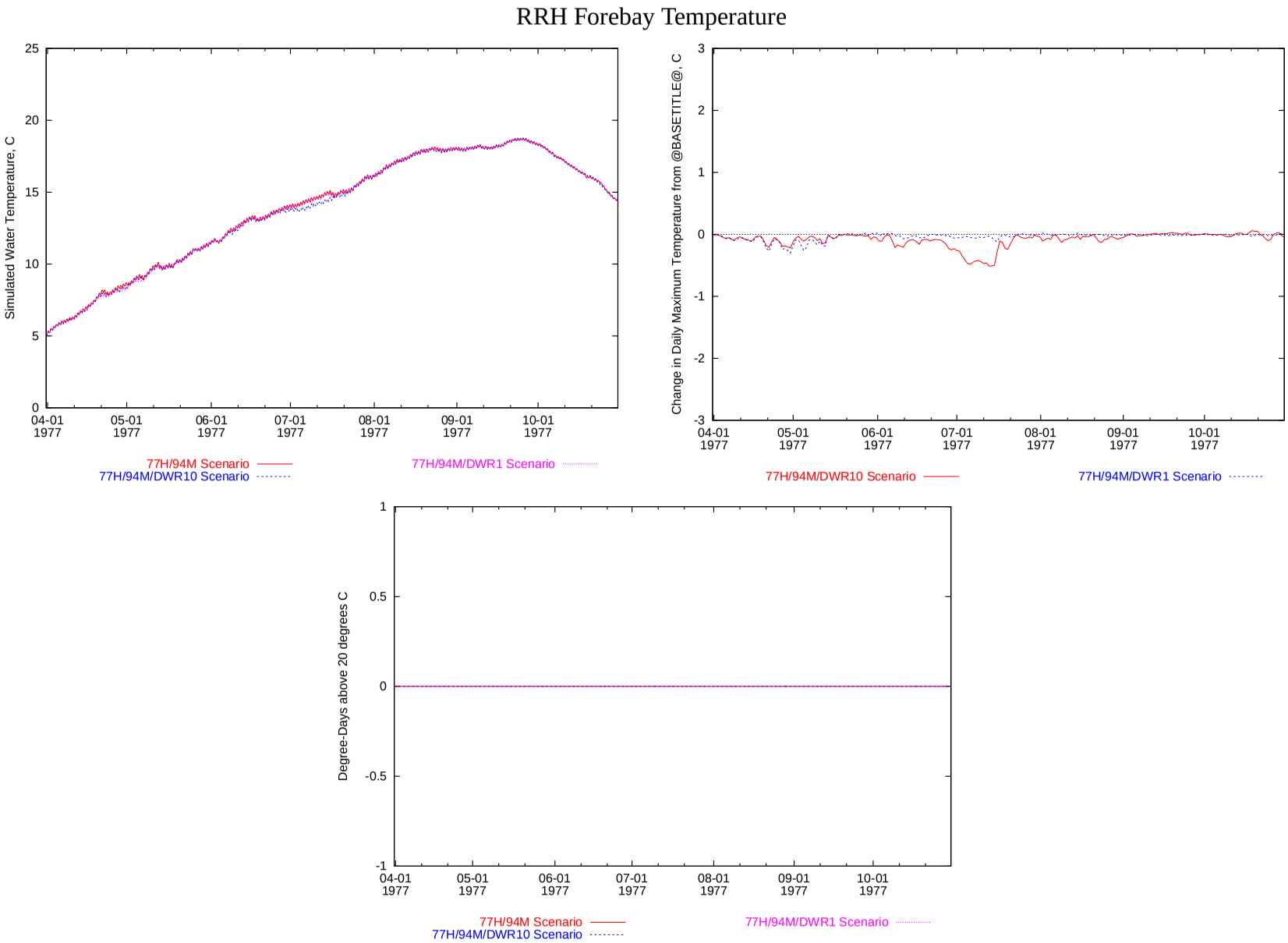

Figure 29: Time series comparison of simulated temperature at the RRH Forebay.

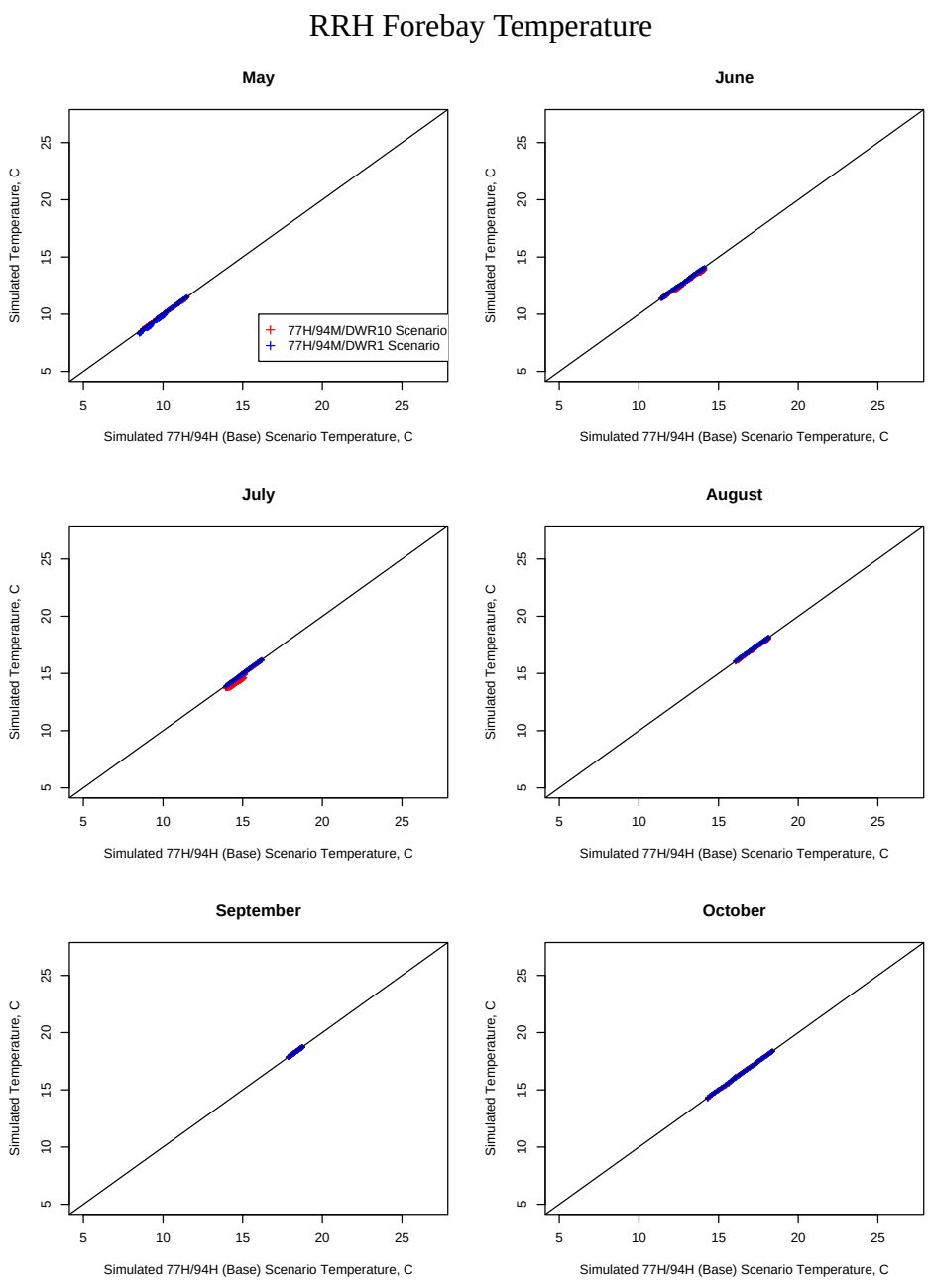

Figure 30: Scatter plot comparison, by month, of simulated temperature at the RRH Forebay.

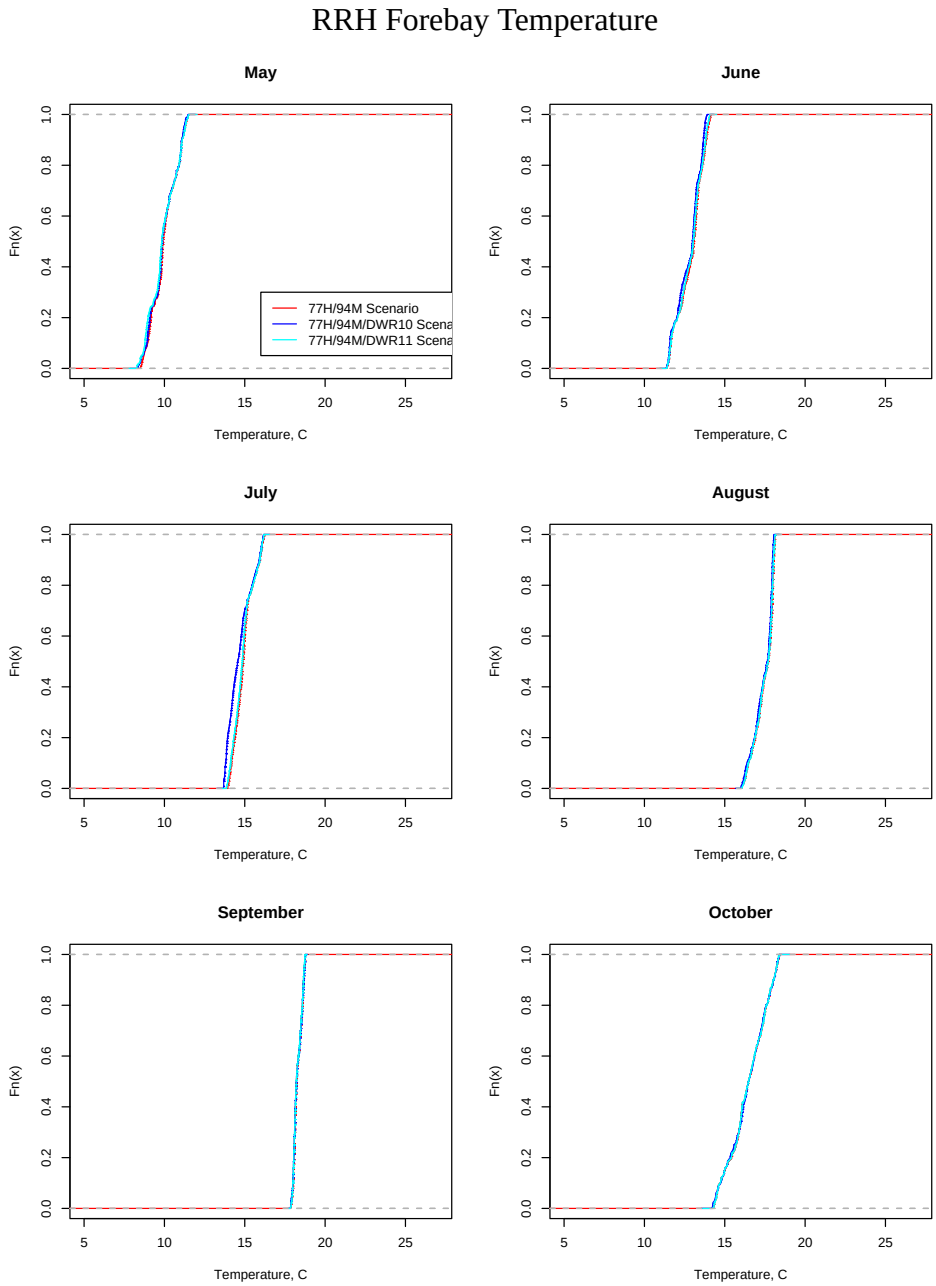

Figure 31: Cumulative frequency distribution (CFD) plot comparison, by month, of simulated temperature at the RRH Forebay.

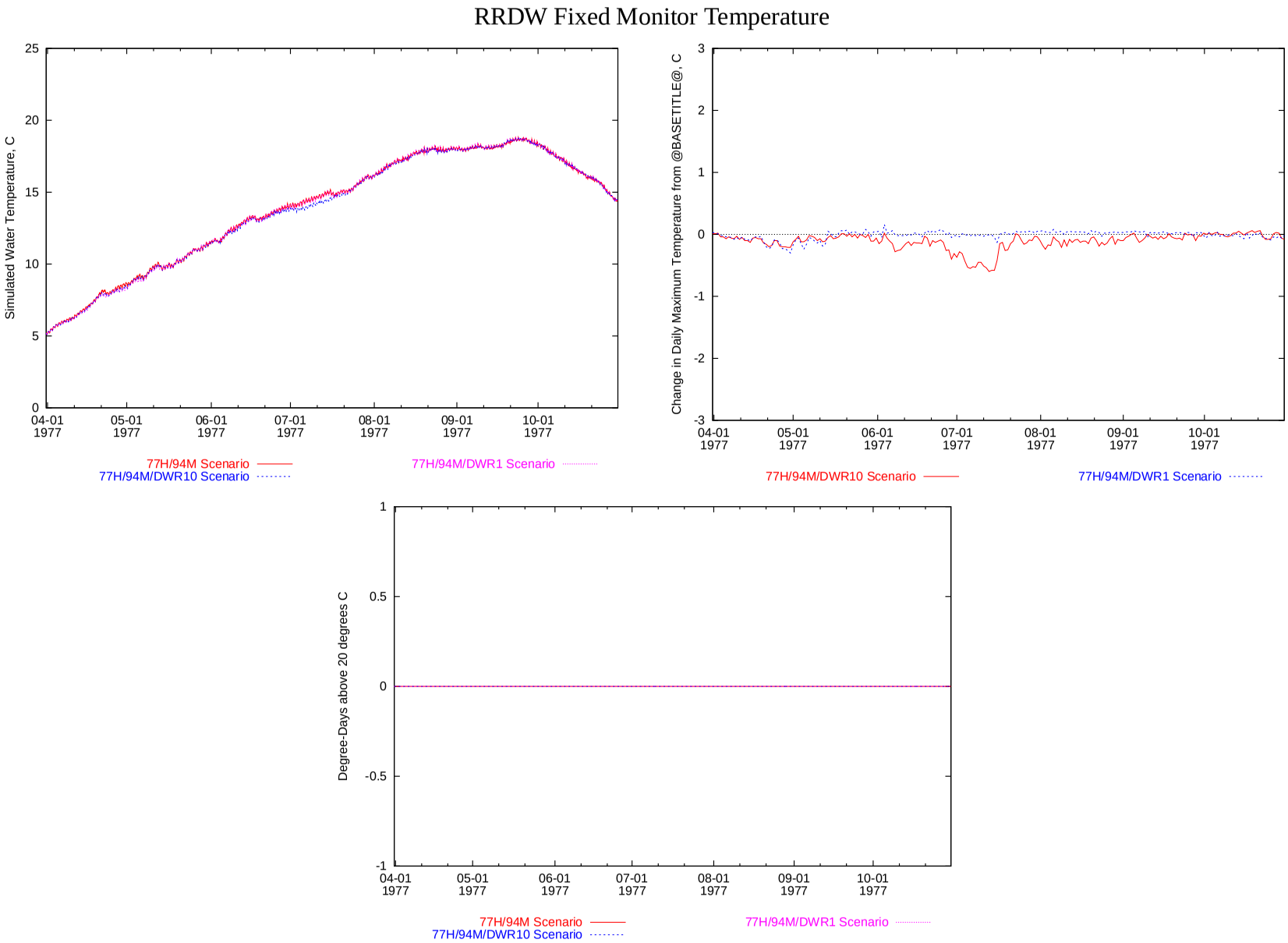

Figure 32: Time series comparison of simulated temperature at the RRDW Fixed Monitor.

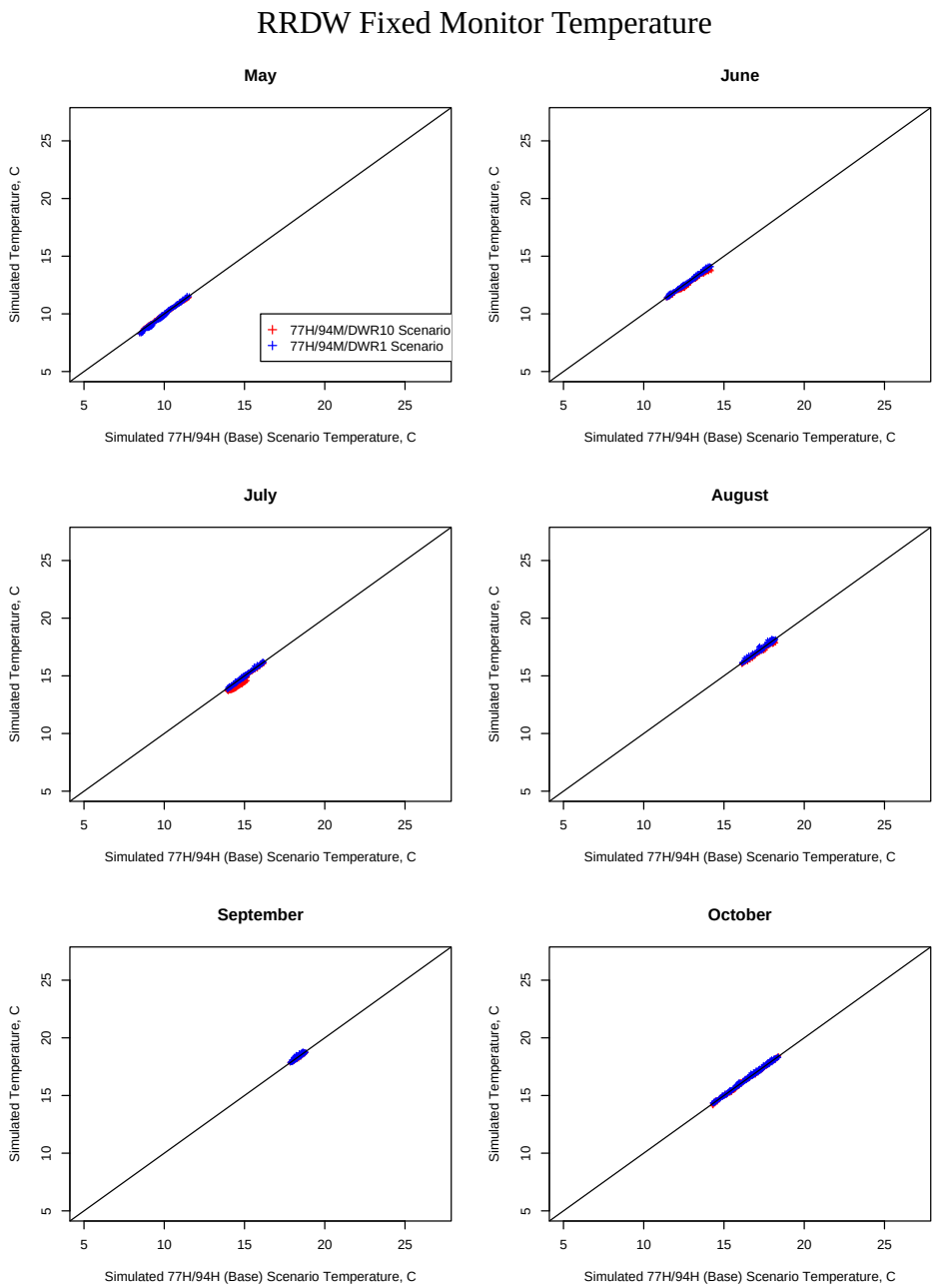

Figure 33: Scatter plot comparison, by month, of simulated temperature at the RRDW Fixed Monitor.

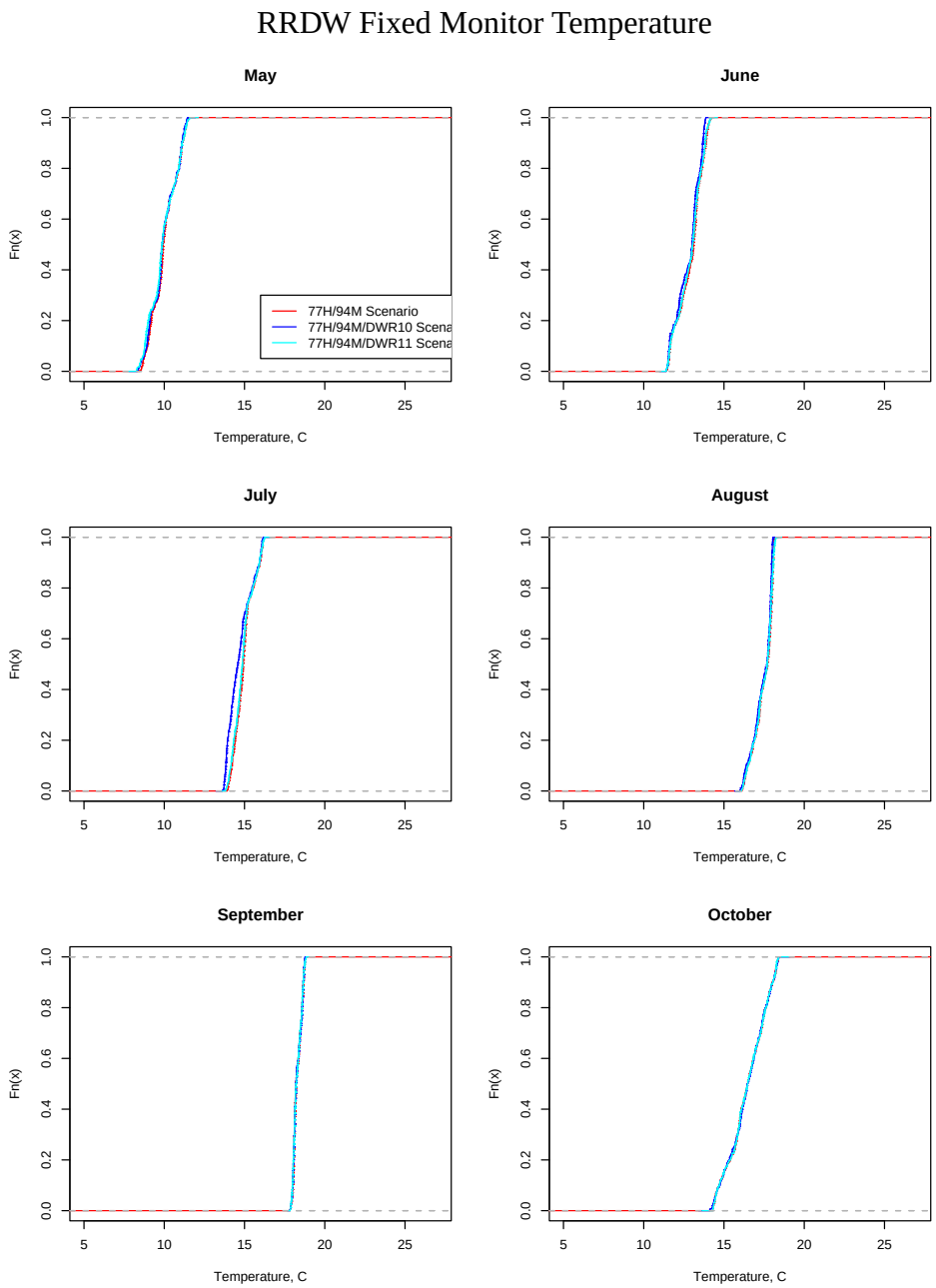

Figure 34: Cumulative frequency distribution (CFD) plot comparison, by month, of simulated temperature at the RRDW Fixed Monitor.

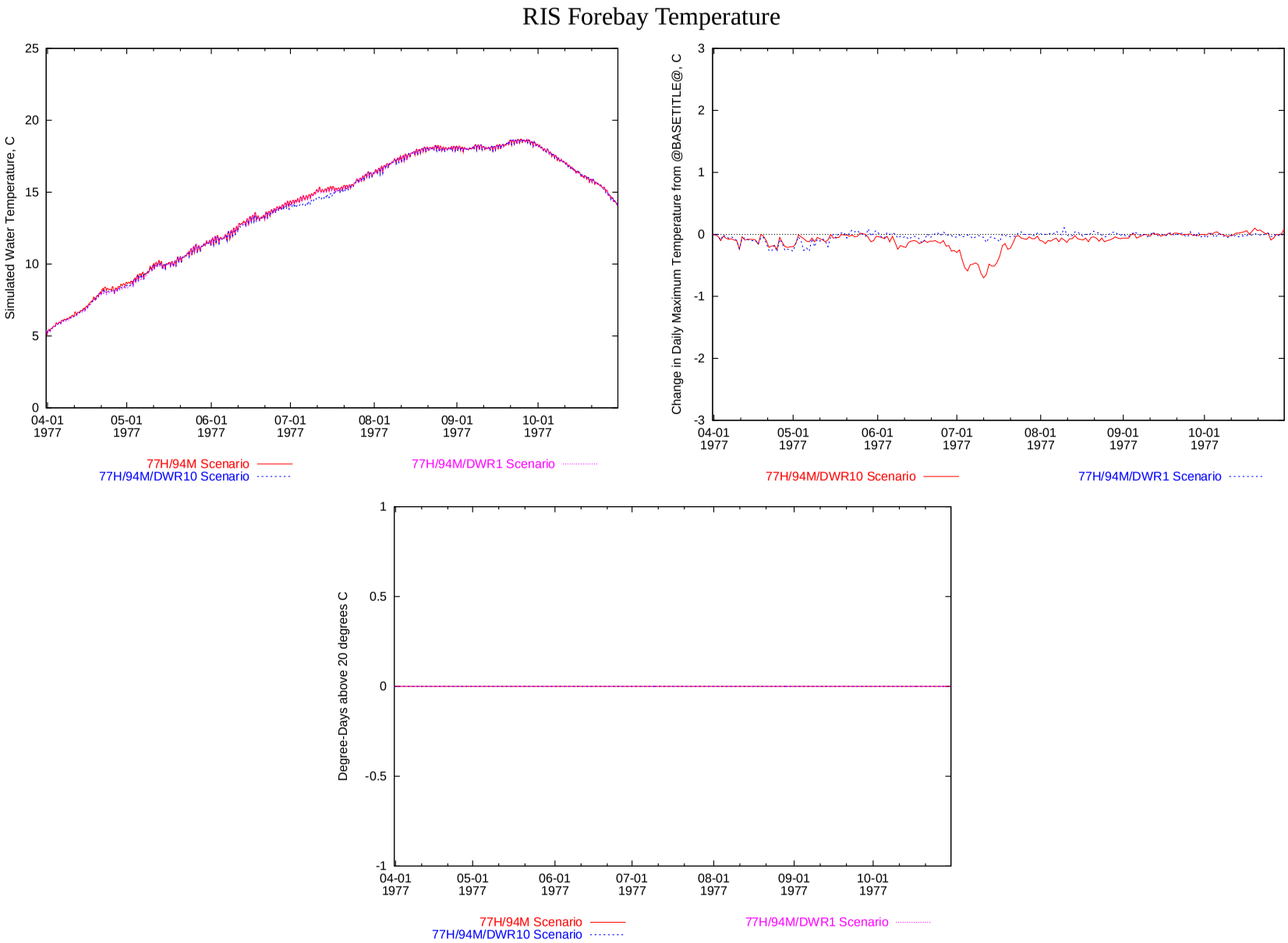

Figure 35: Time series comparison of simulated temperature at the RIS Forebay.

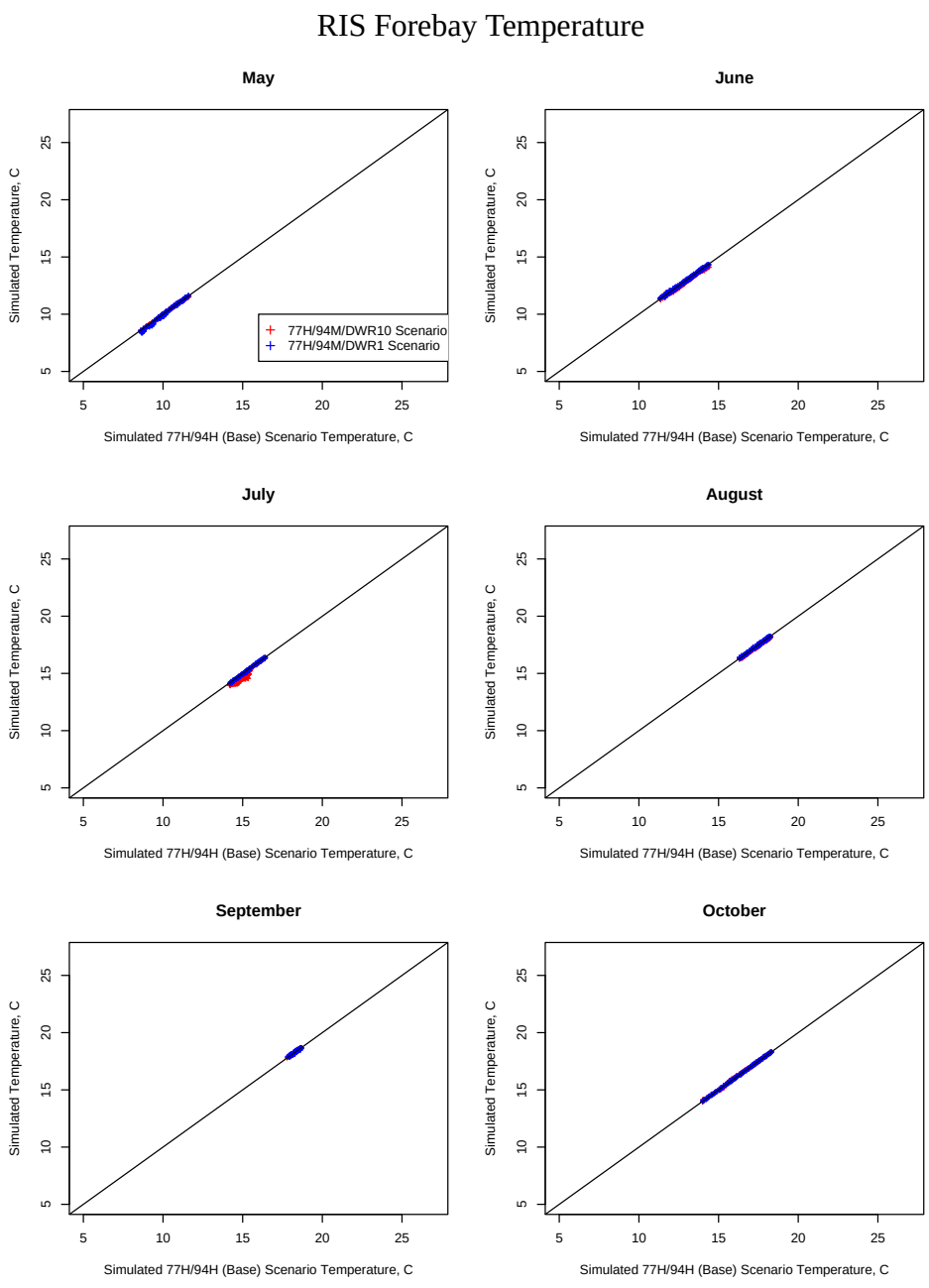

Figure 36: Scatter plot comparison, by month, of simulated temperature at the RIS Forebay.

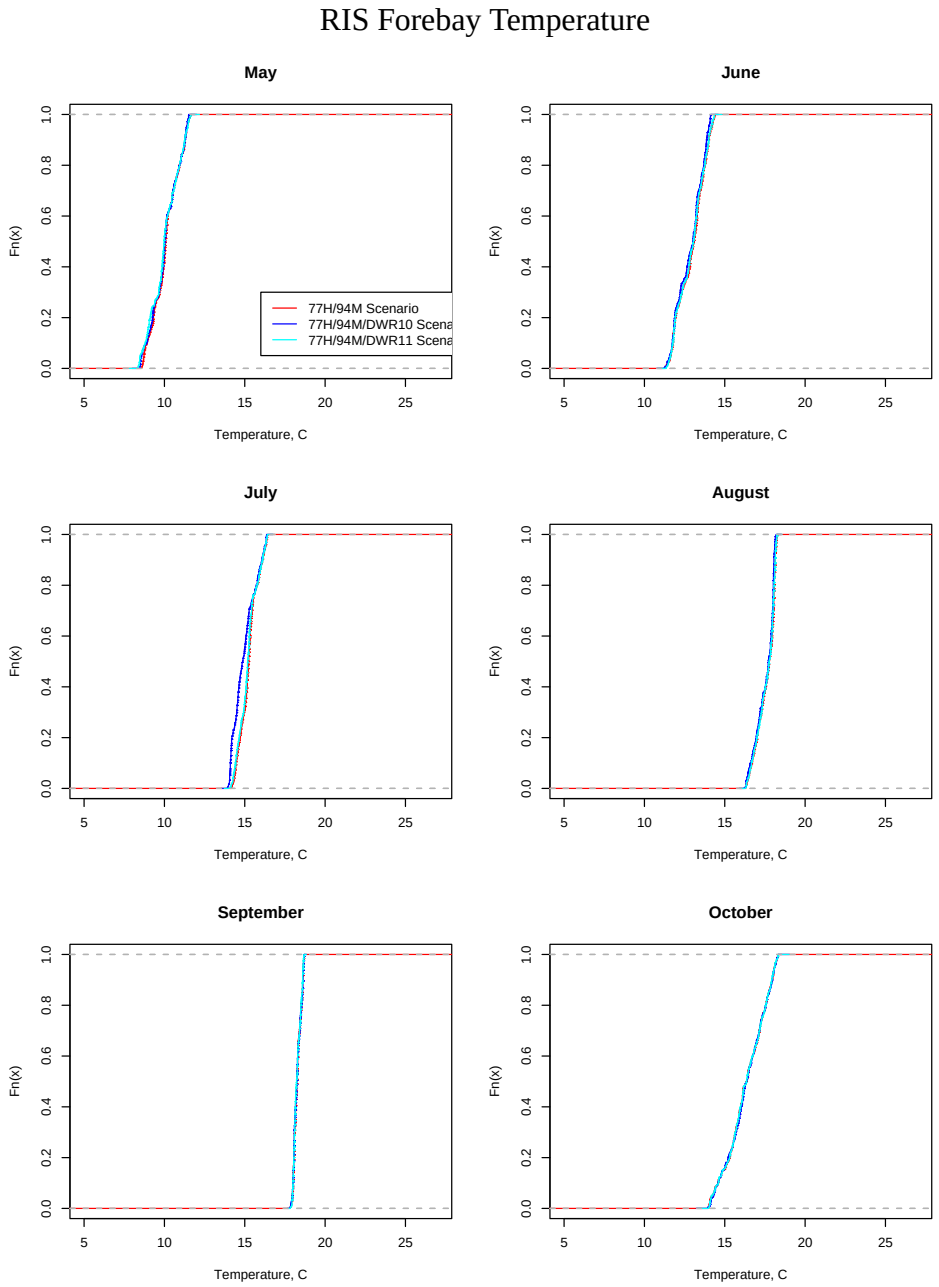

Figure 37: Cumulative frequency distribution (CFD) plot comparison, by month, of simulated temperature at the RIS Forebay.

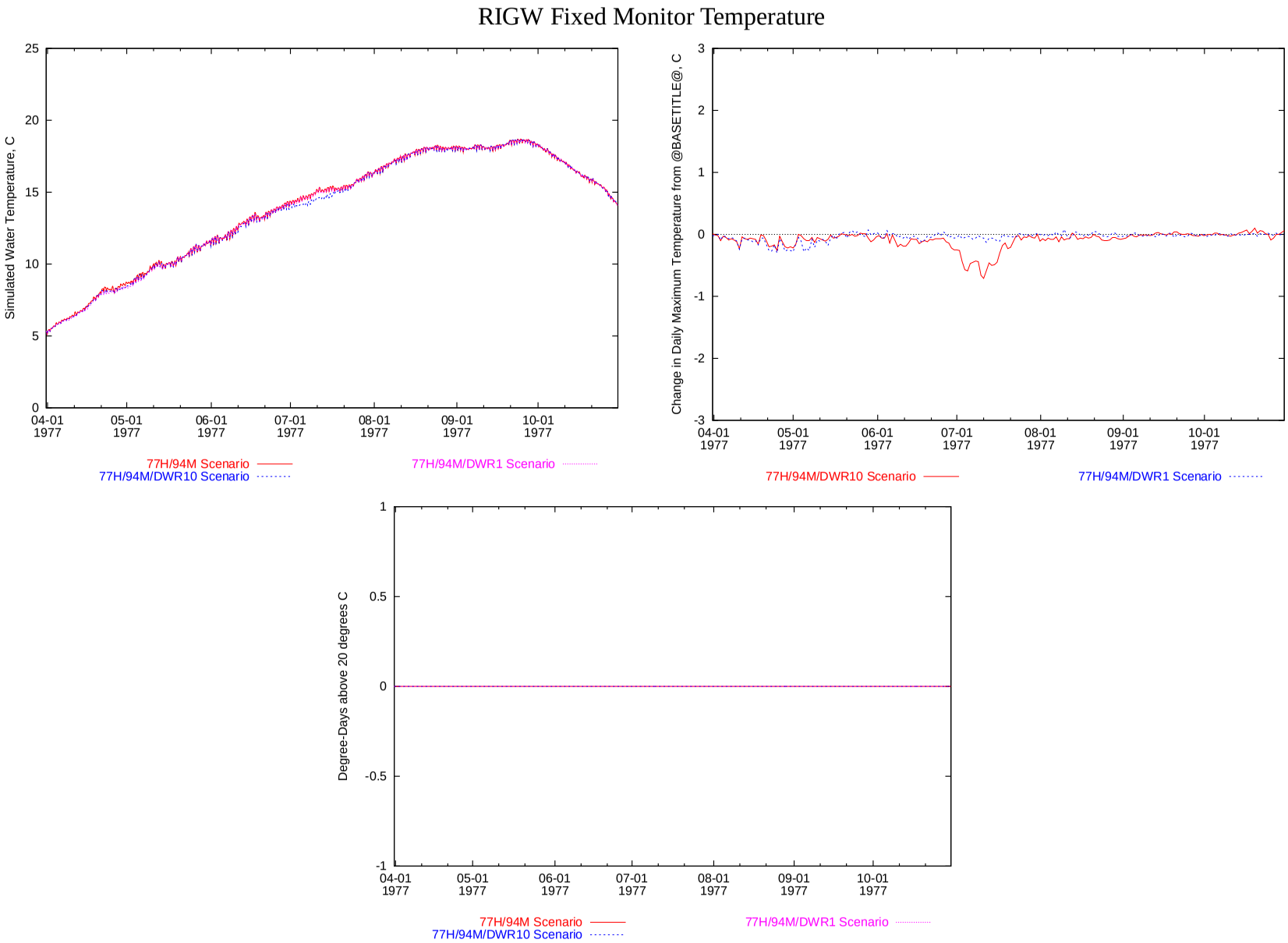

Figure 38: Time series comparison of simulated temperature at the RIGW Fixed Monitor.

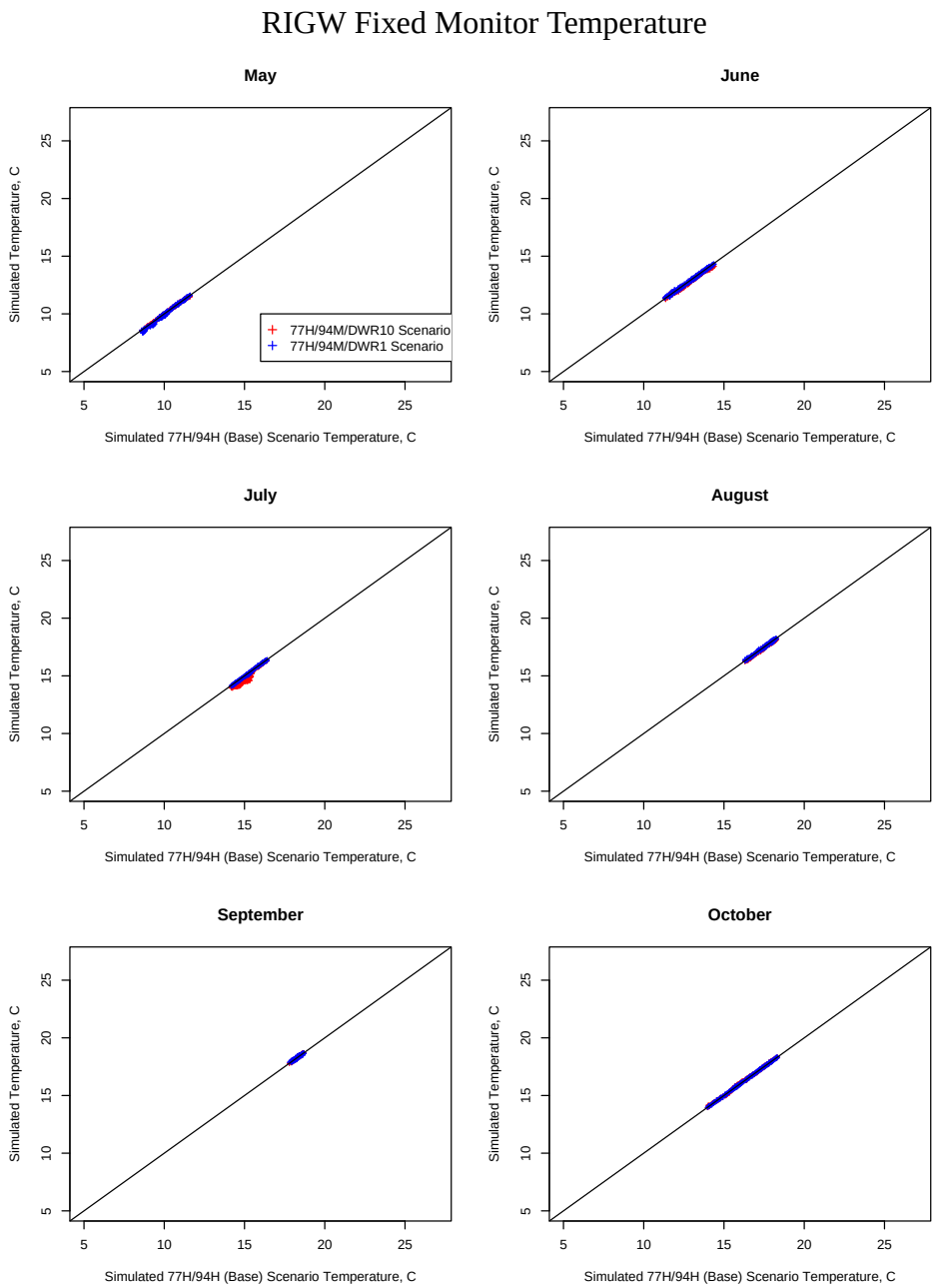

Figure 39: Scatter plot comparison, by month, of simulated temperature at the RIGW Fixed Monitor.

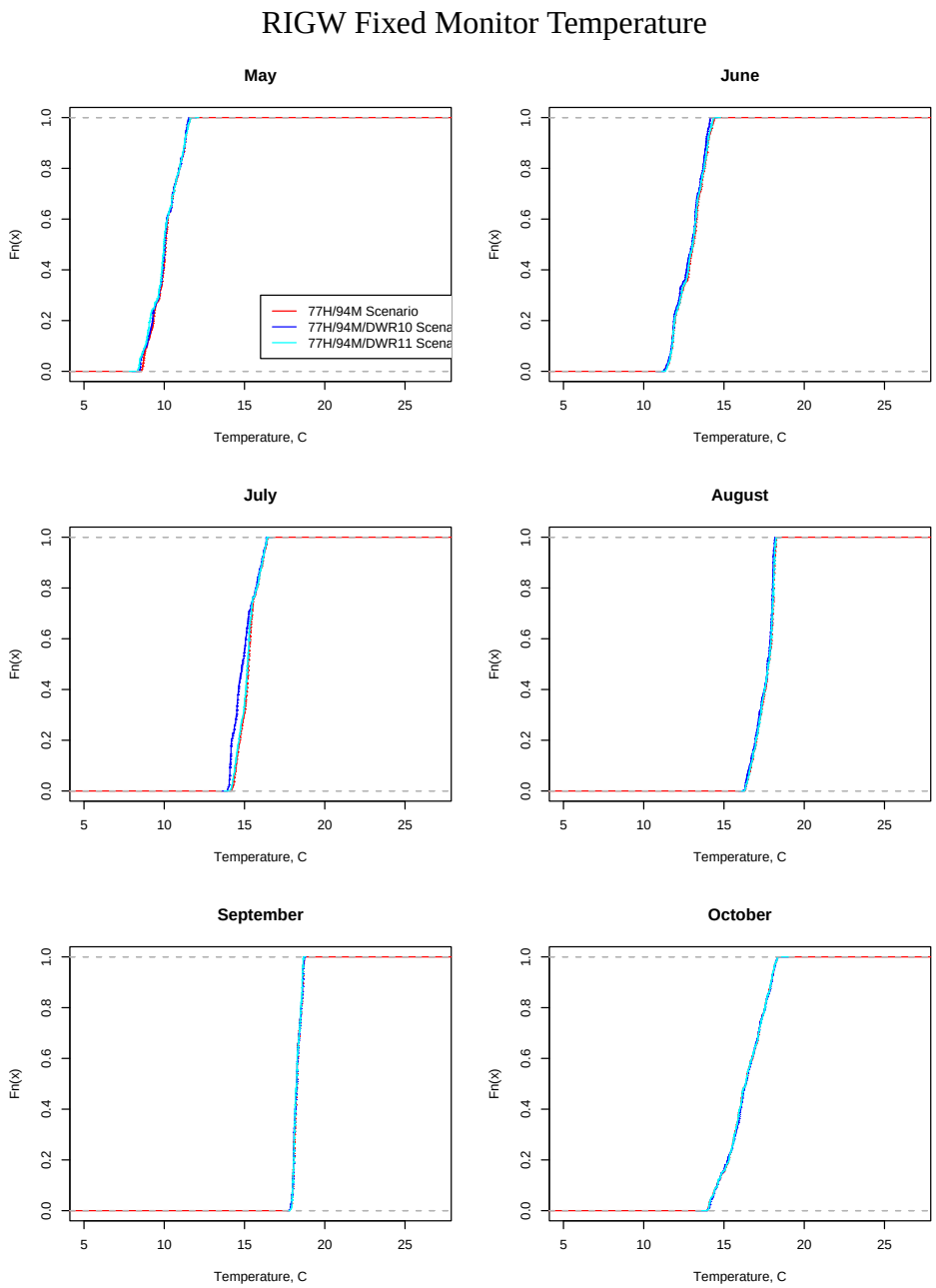

Figure 40: Cumulative frequency distribution (CFD) plot comparison, by month, of simulated temperature at the RIGW Fixed Monitor.

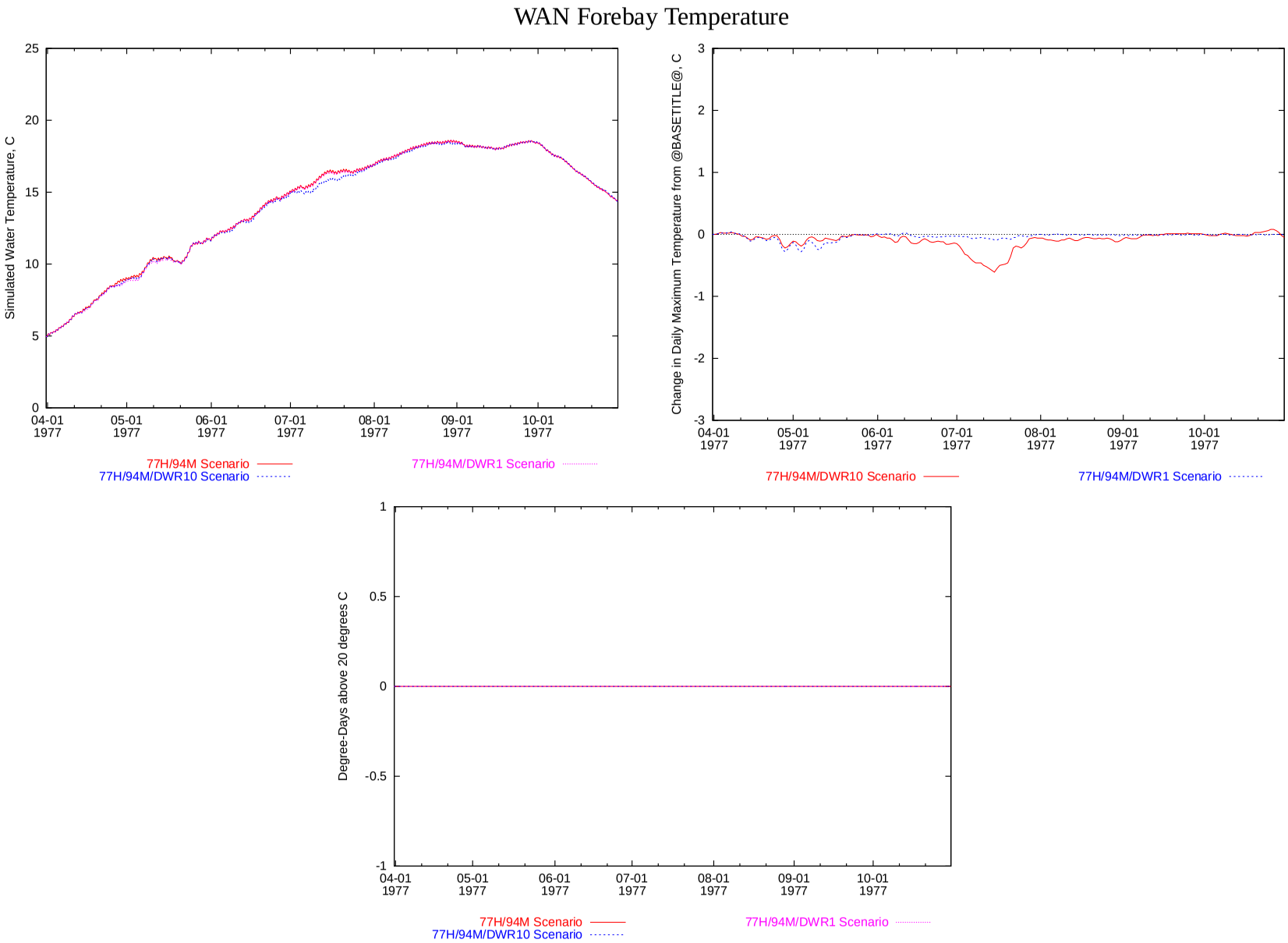

Figure 41: Time series comparison of simulated temperature at the WAN Forebay.

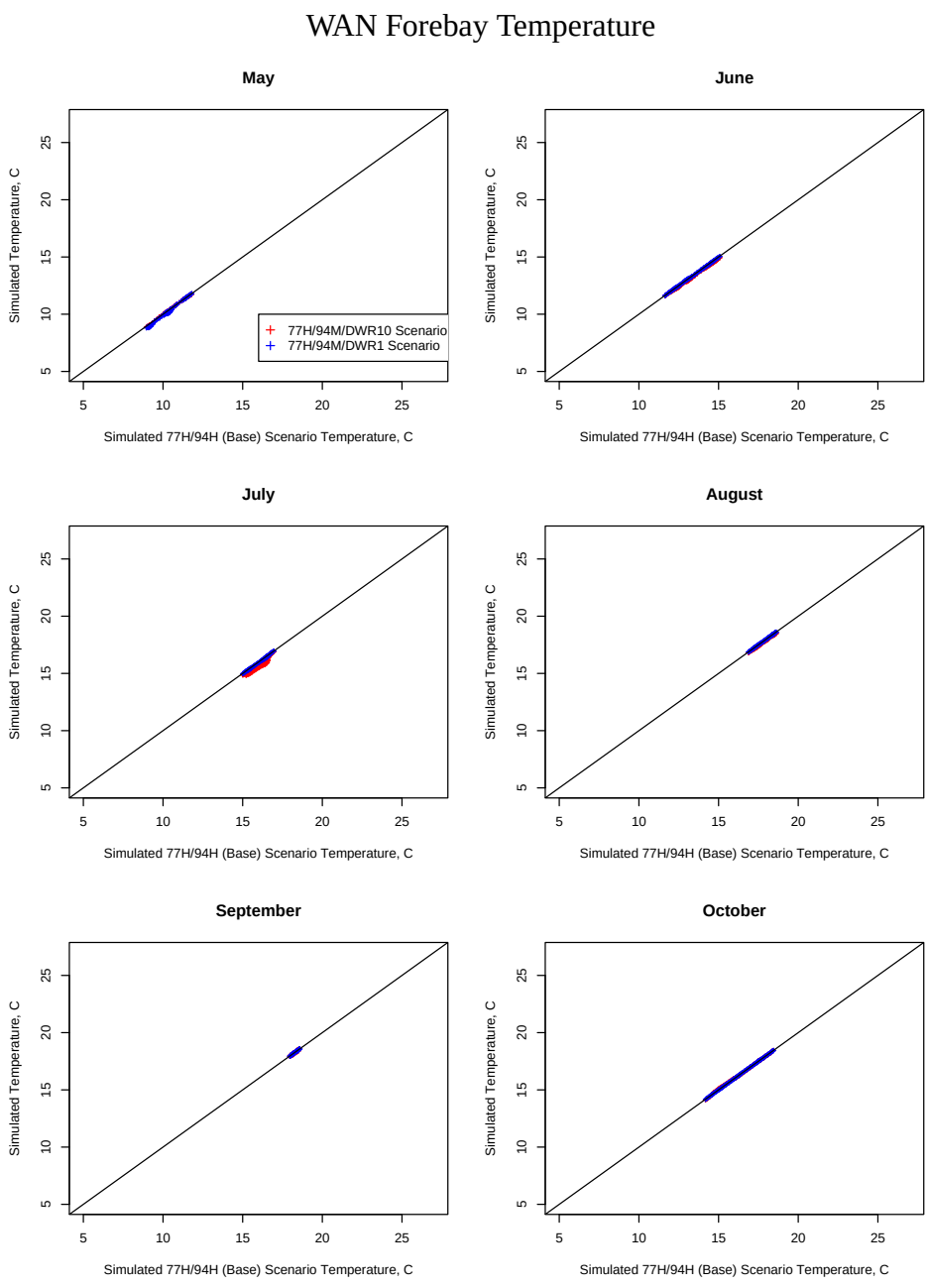

Figure 42: Scatter plot comparison, by month, of simulated temperature at the WAN Forebay.

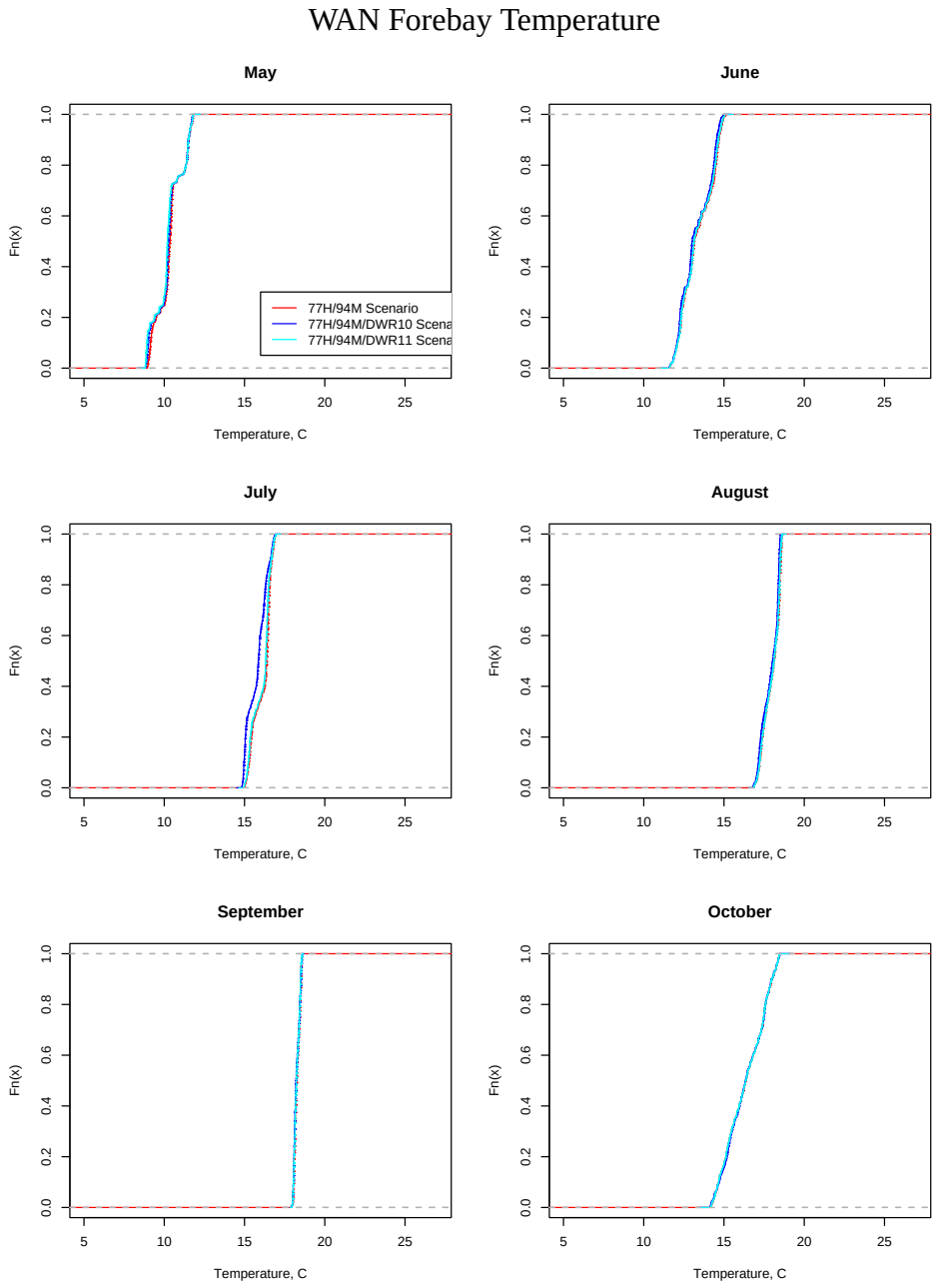

Figure 43: Cumulative frequency distribution (CFD) plot comparison, by month, of simulated temperature at the WAN Forebay.

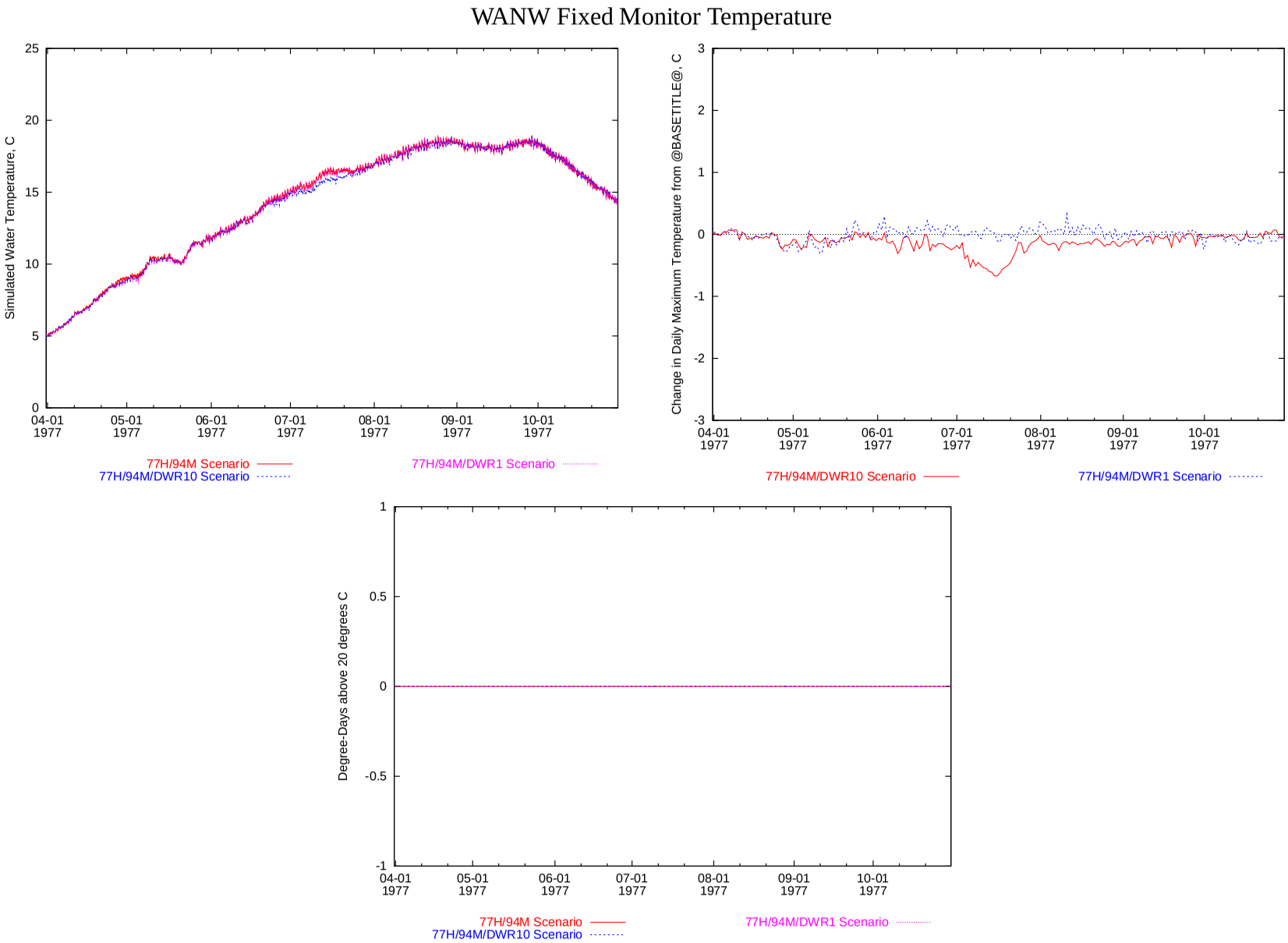

Figure 44: Time series comparison of simulated temperature at the WANW Fixed Monitor.

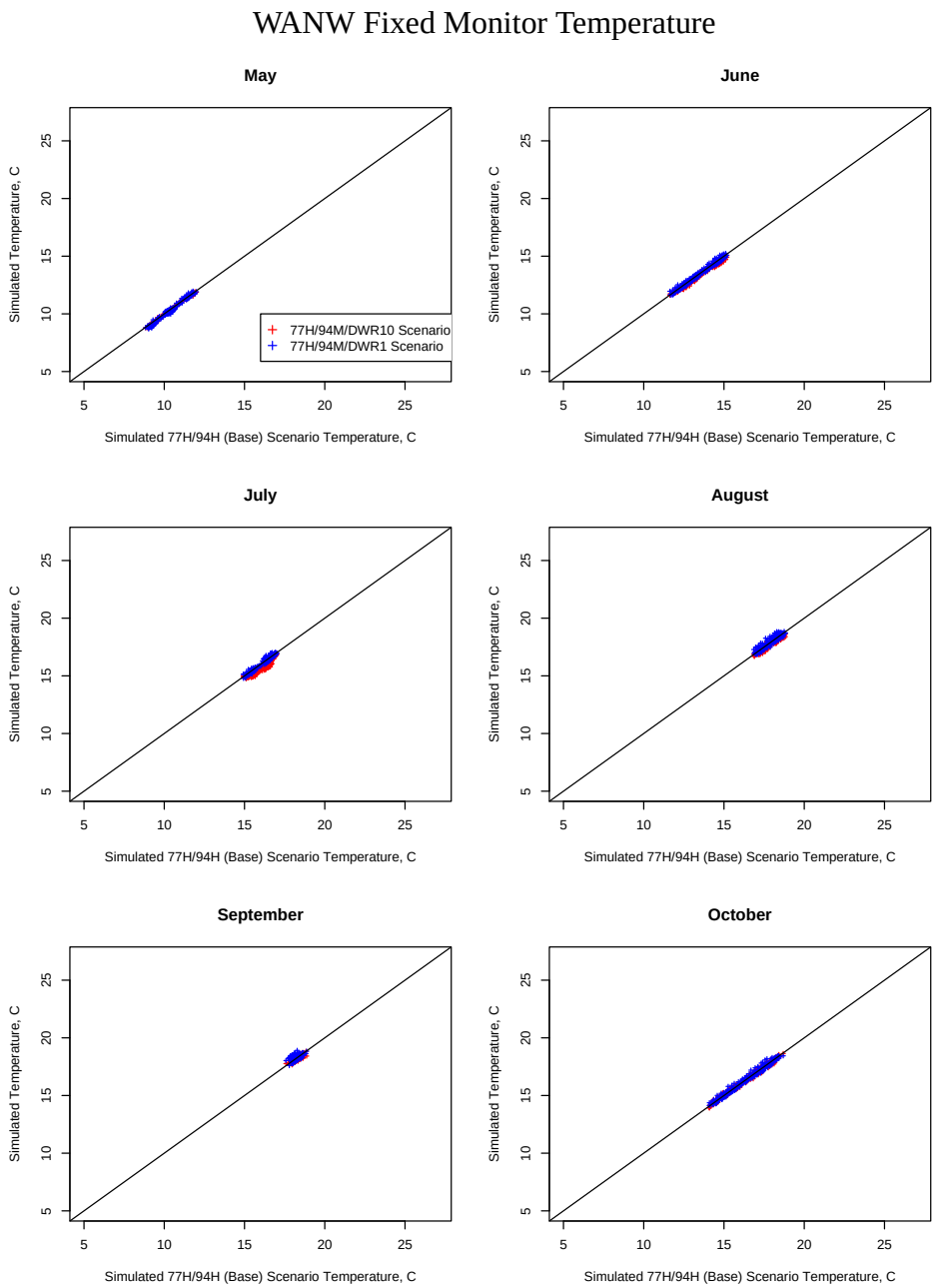

Figure 45: Scatter plot comparison, by month, of simulated temperature at the WANW Fixed Monitor.

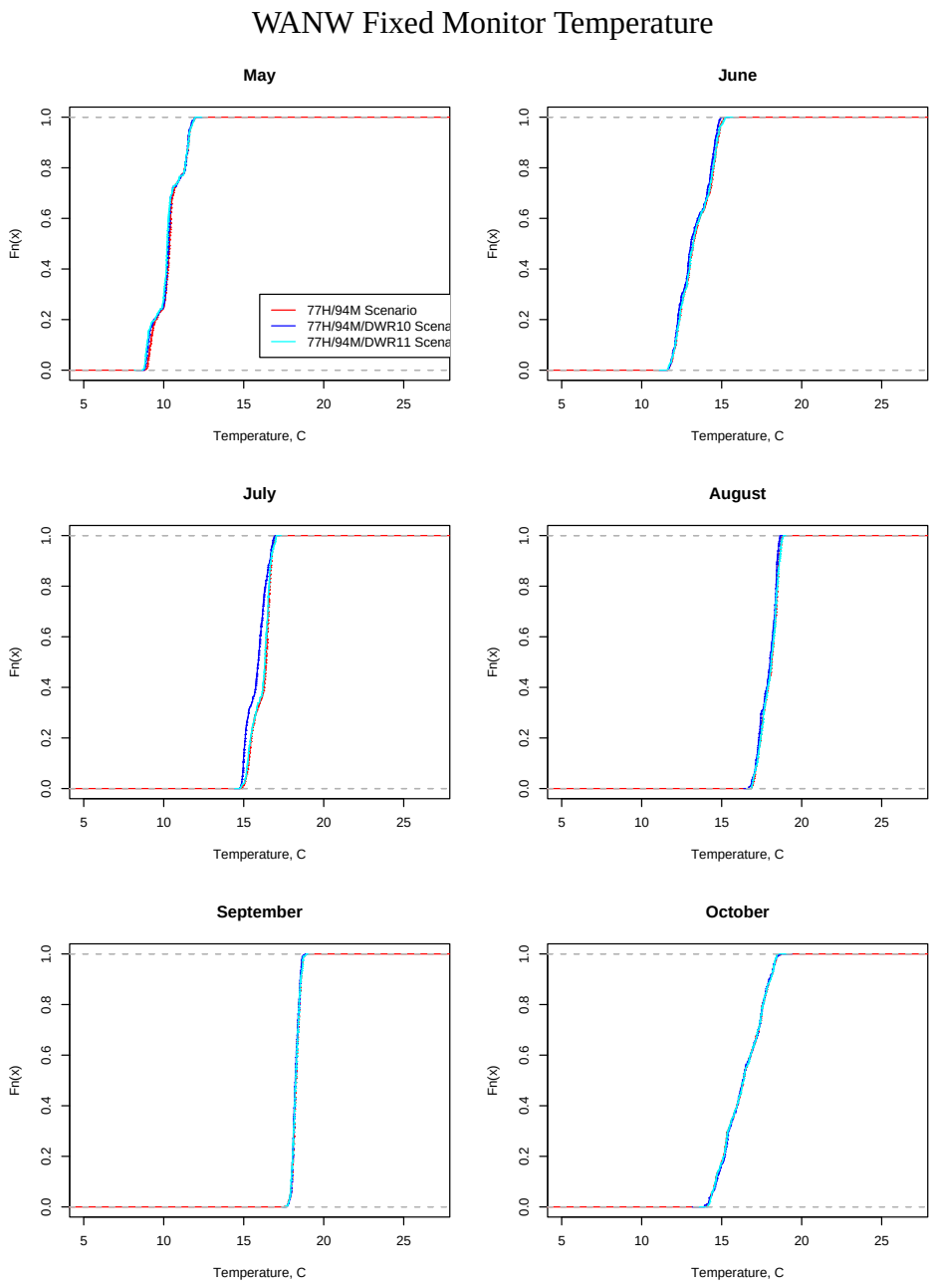

Figure 46: Cumulative frequency distribution (CFD) plot comparison, by month, of simulated temperature at the WANW Fixed Monitor.

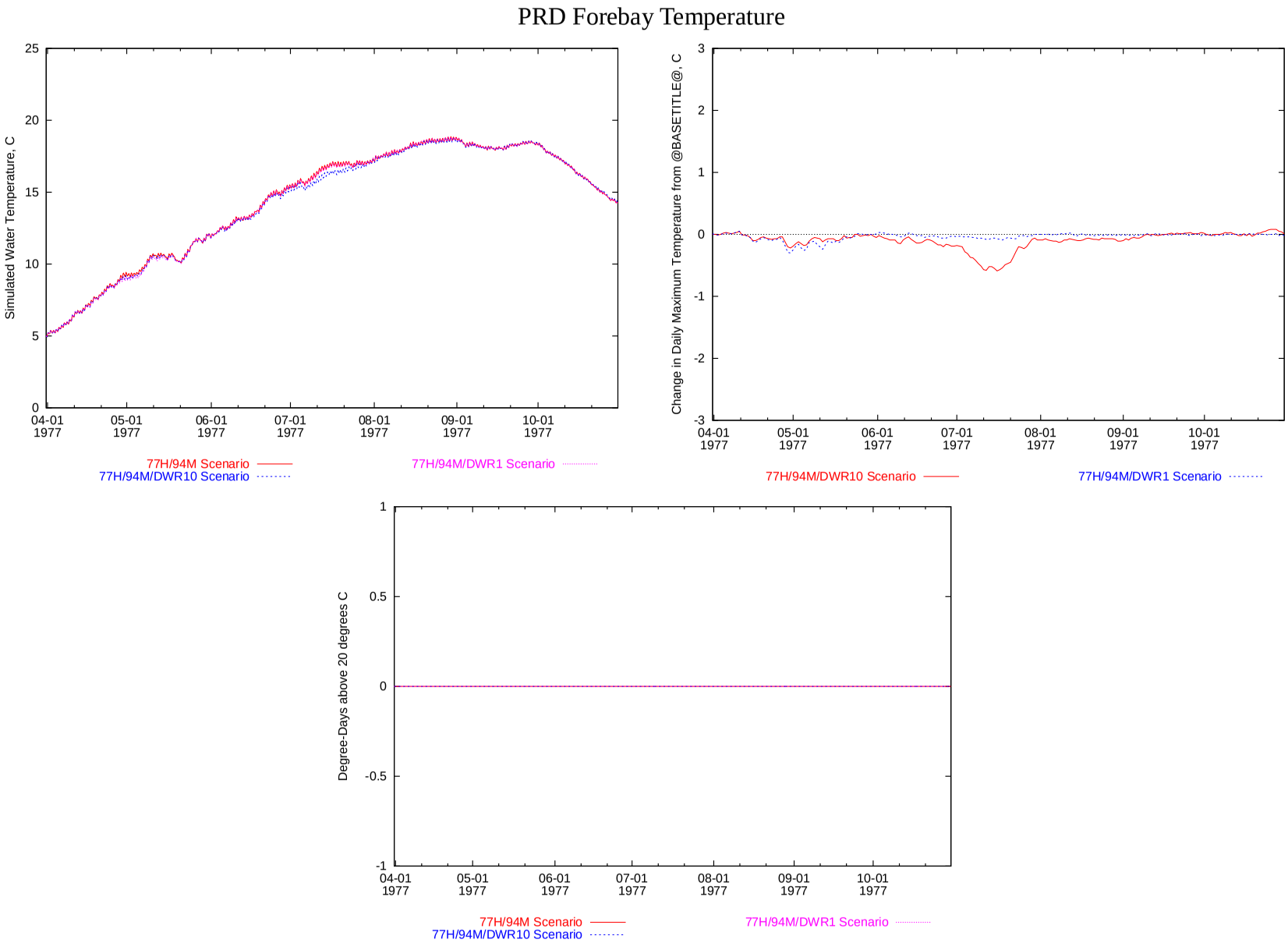

Figure 47: Time series comparison of simulated temperature at the PRD Forebay.

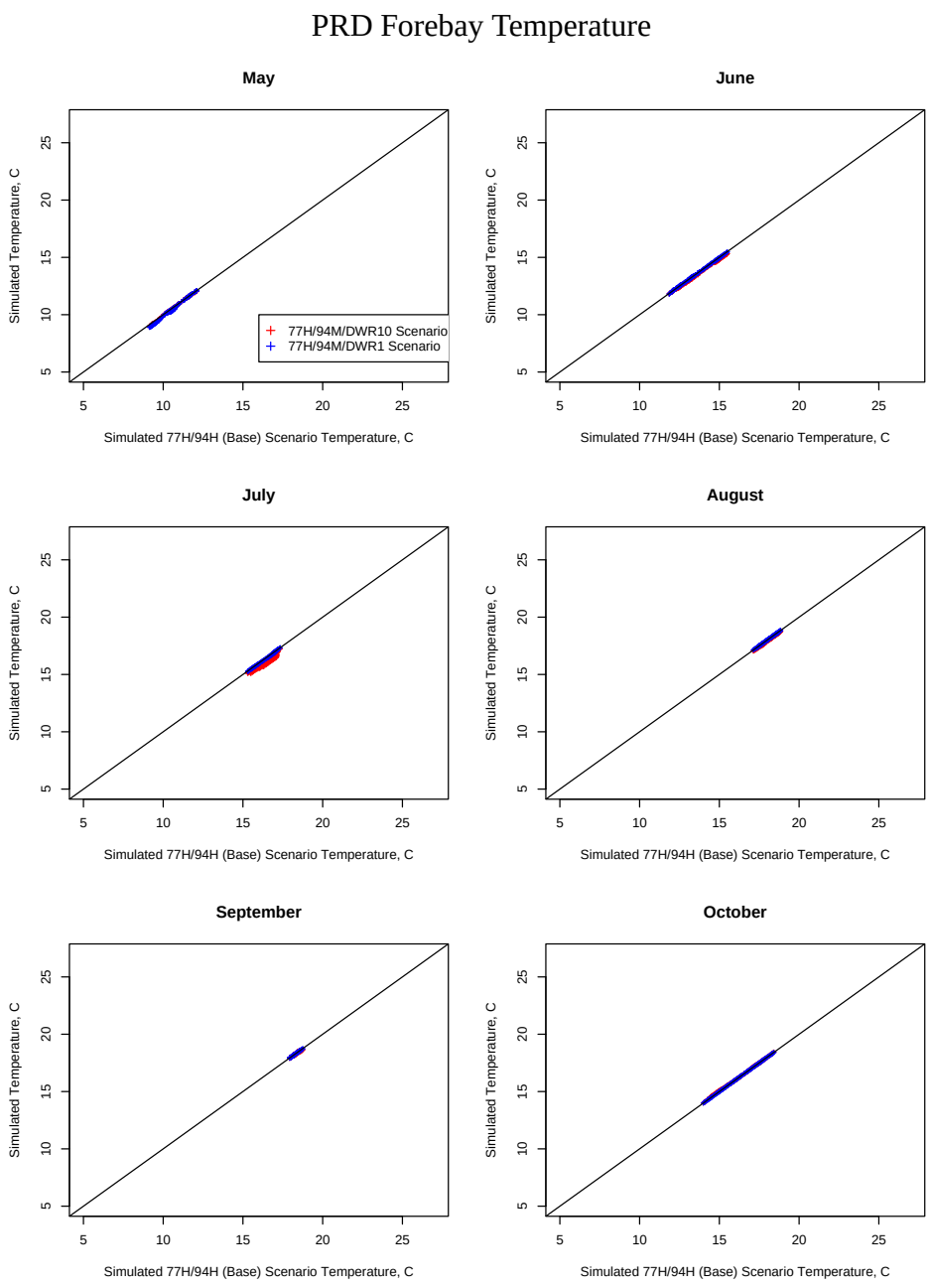

Figure 48: Scatter plot comparison, by month, of simulated temperature at the PRD Forebay.

PRD Forebay Temperature

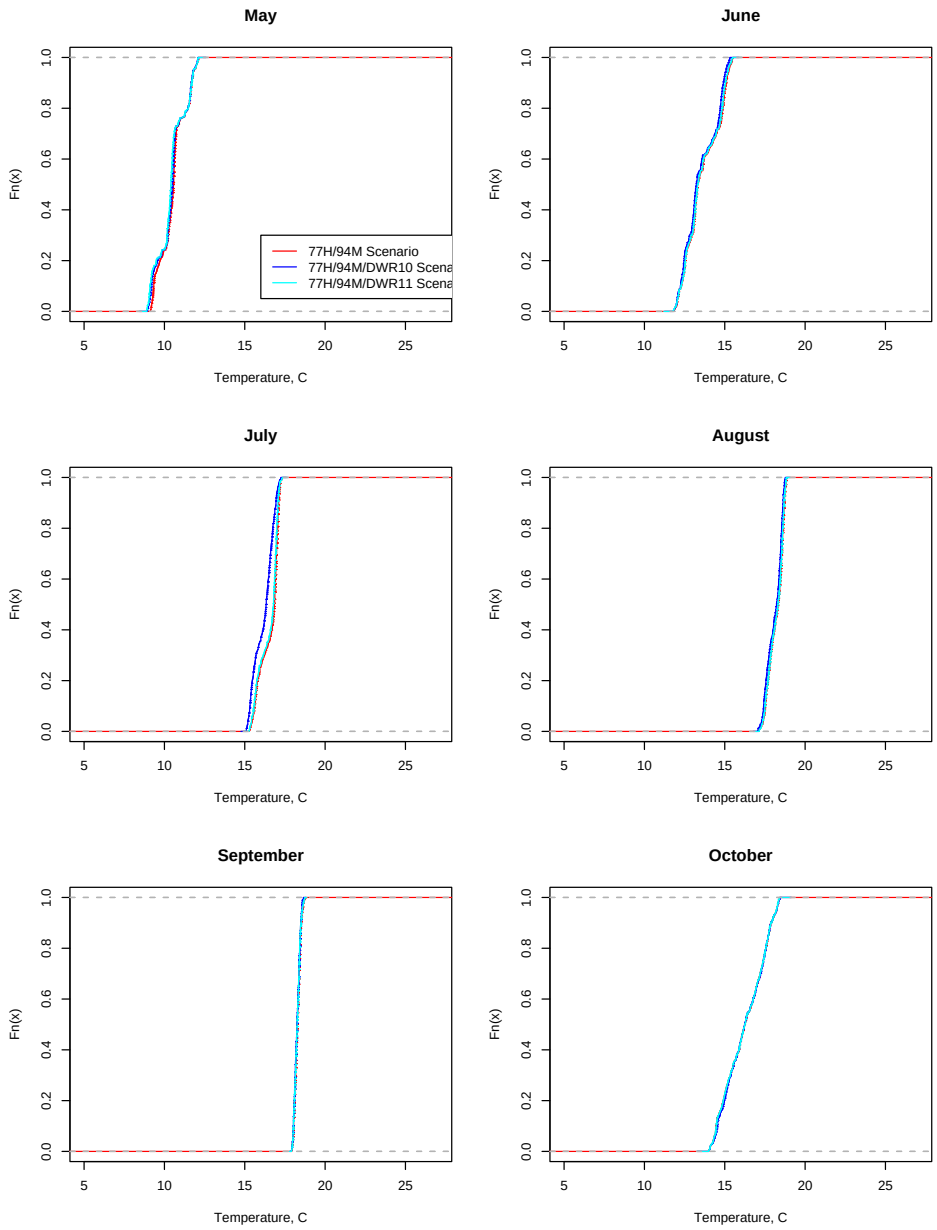

Figure 49: Cumulative frequency distribution (CFD) plot comparison, by month, of simulated temperature at the PRD Forebay.

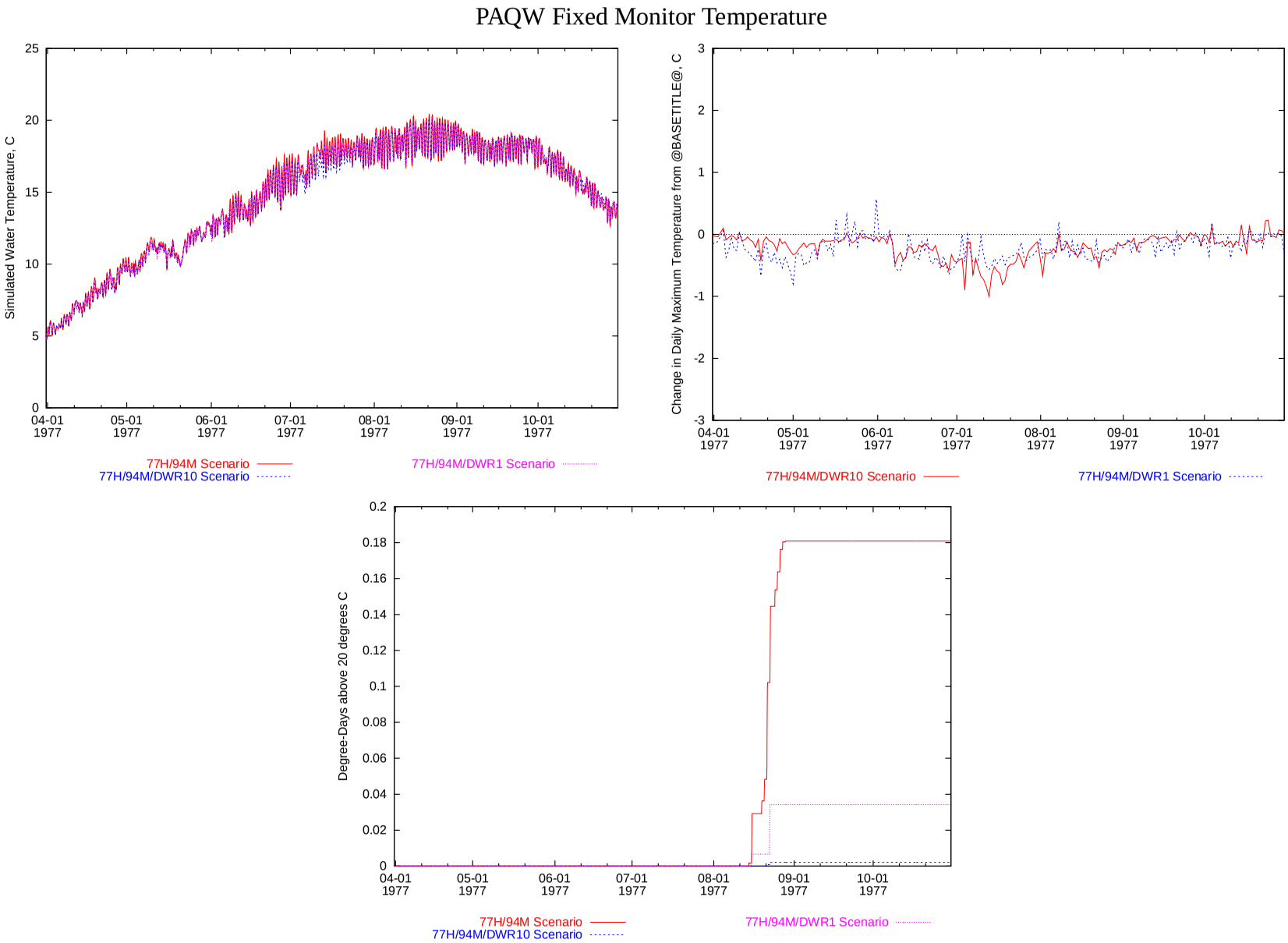

Figure 50: Time series comparison of simulated temperature at the PAQW Fixed Monitor.

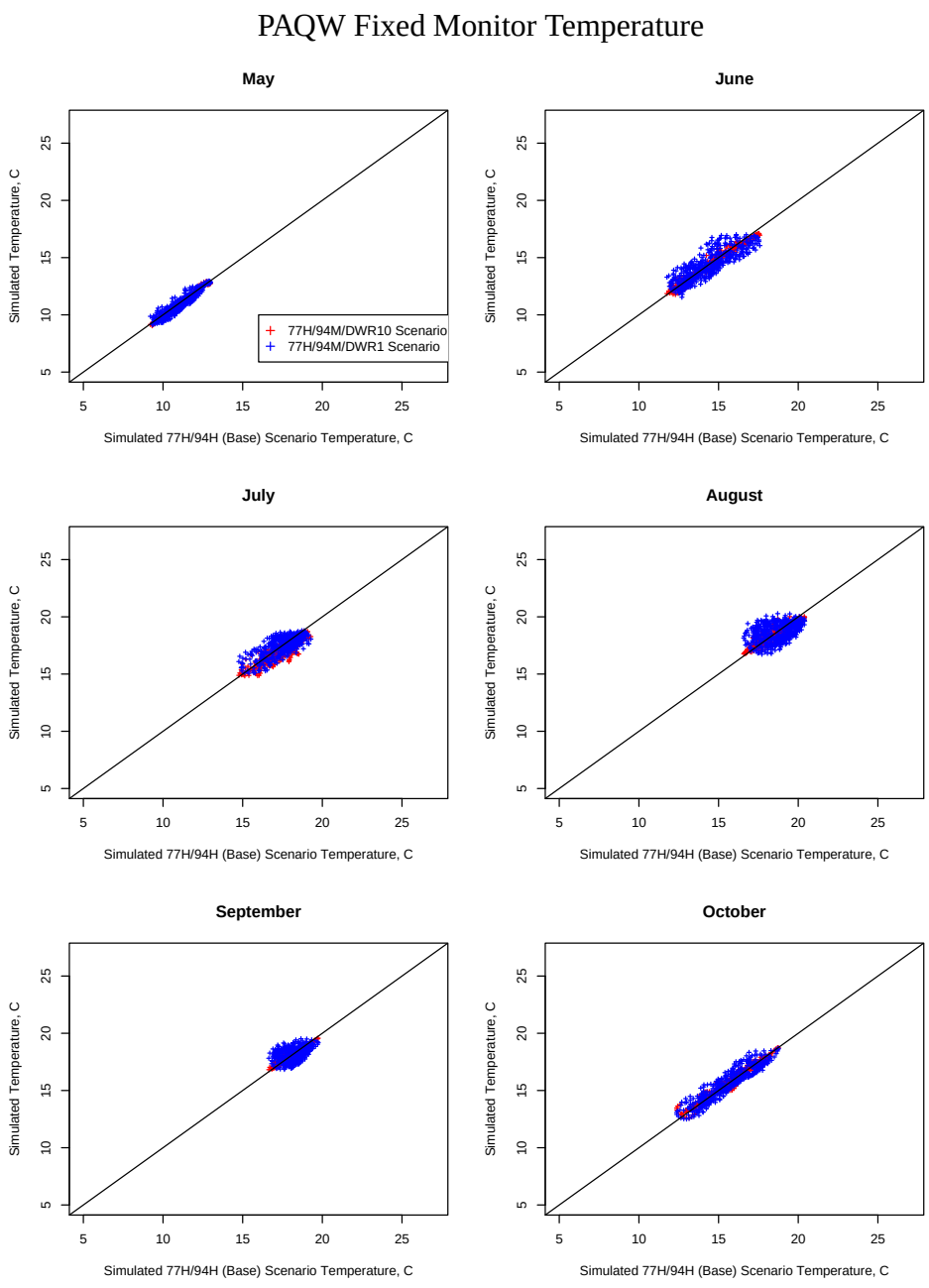

Figure 51: Scatter plot comparison, by month, of simulated temperature at the PAQW Fixed Monitor.

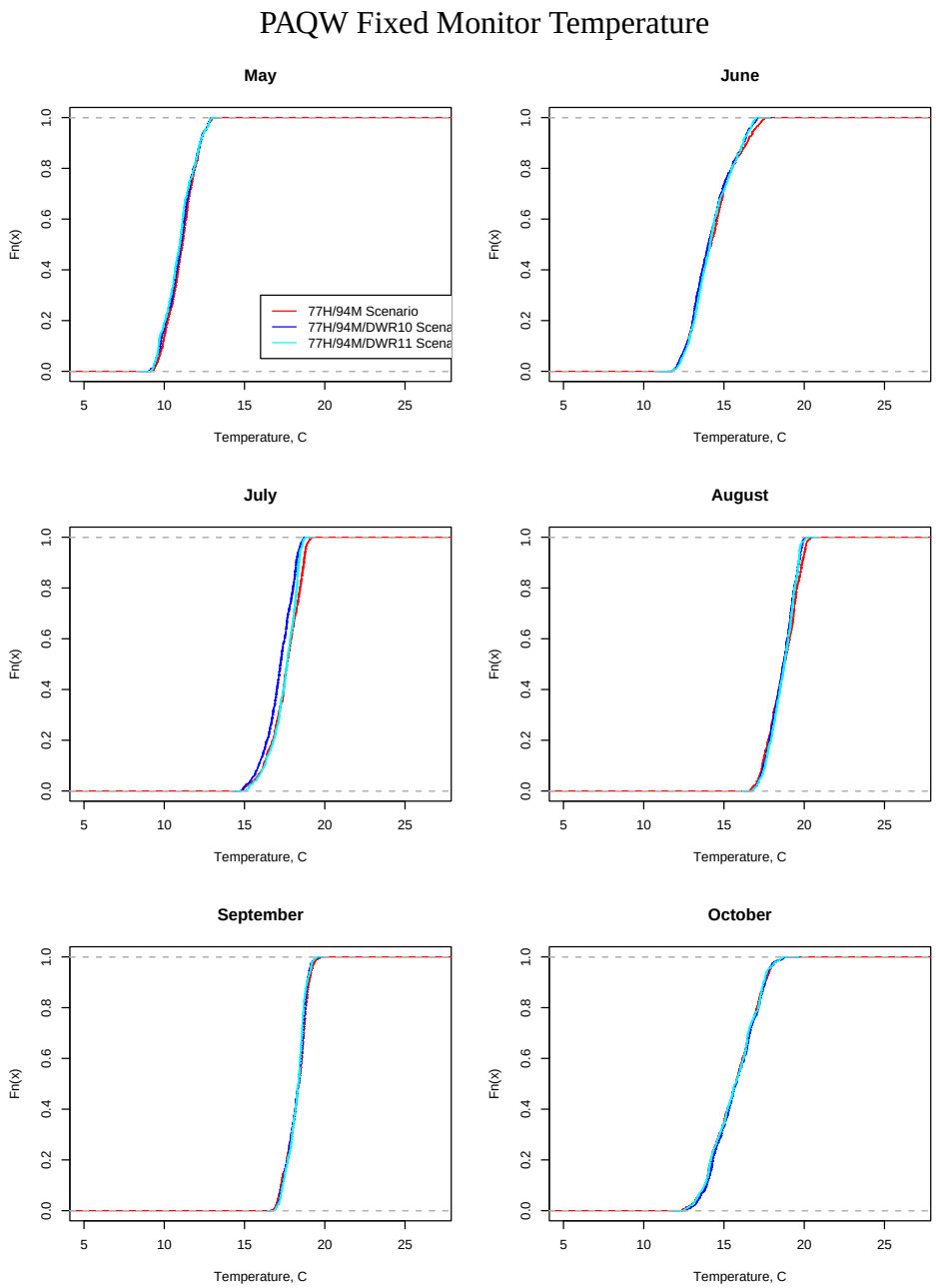

Figure 52: Cumulative frequency distribution (CFD) plot comparison, by month, of simulated temperature at the PAQW Fixed Monitor.

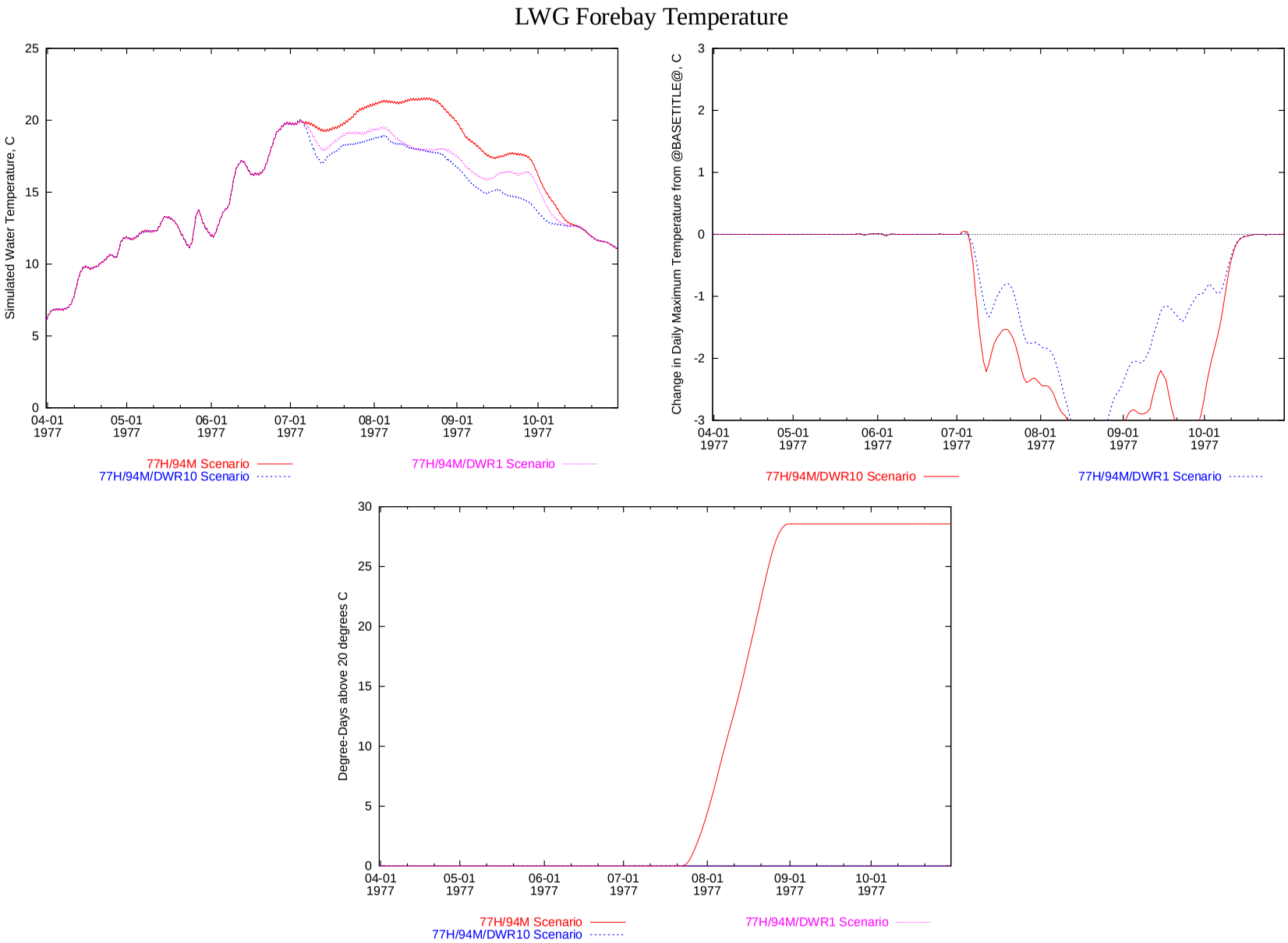

Figure 53: Time series comparison of simulated temperature at the LWG Forebay.

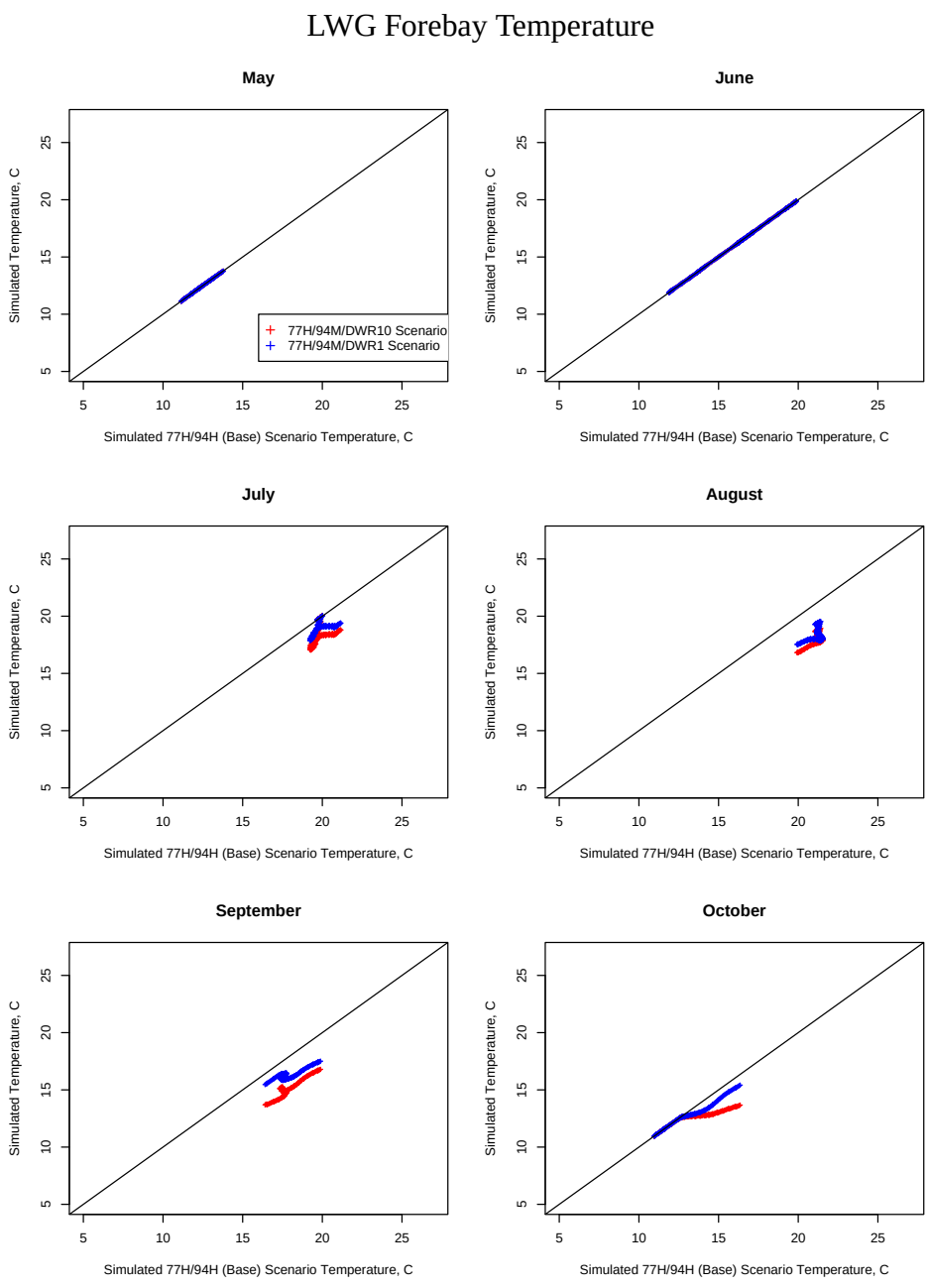

Figure 54: Scatter plot comparison, by month, of simulated temperature at the LWG Forebay.

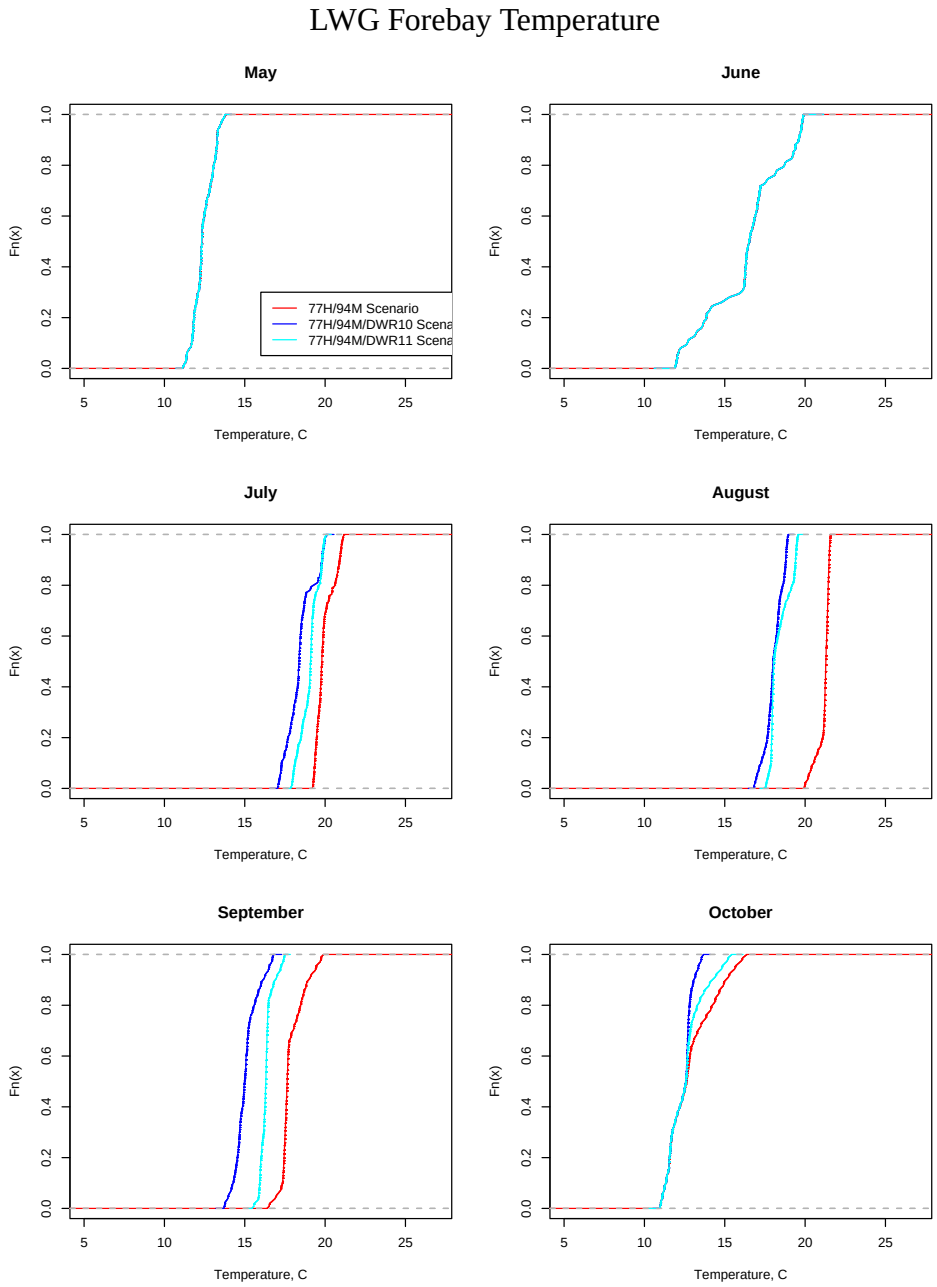

Figure 55: Cumulative frequency distribution (CFD) plot comparison, by month, of simulated temperature at the LWG Forebay.

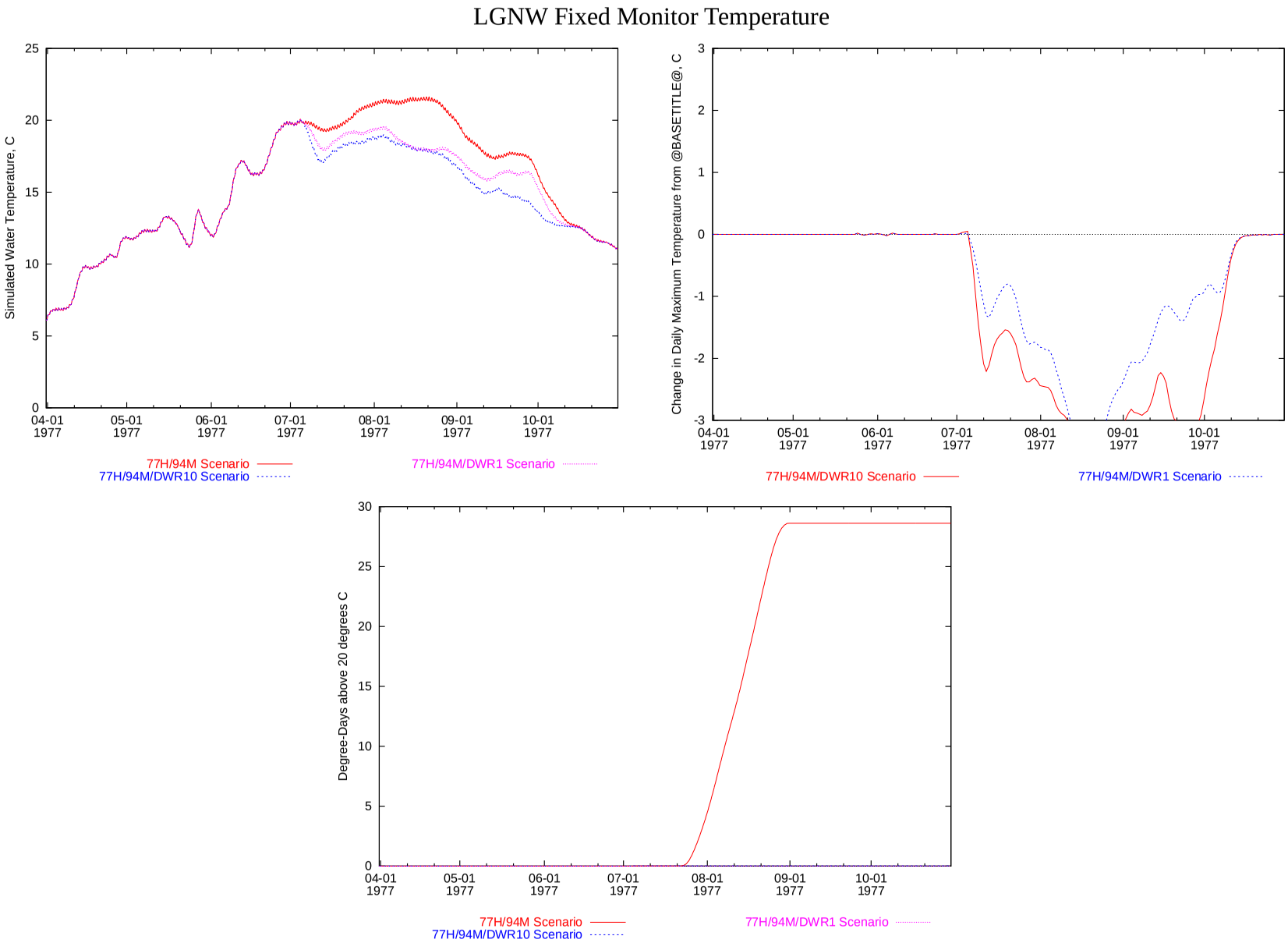

Figure 56: Time series comparison of simulated temperature at the LGNW Fixed Monitor.

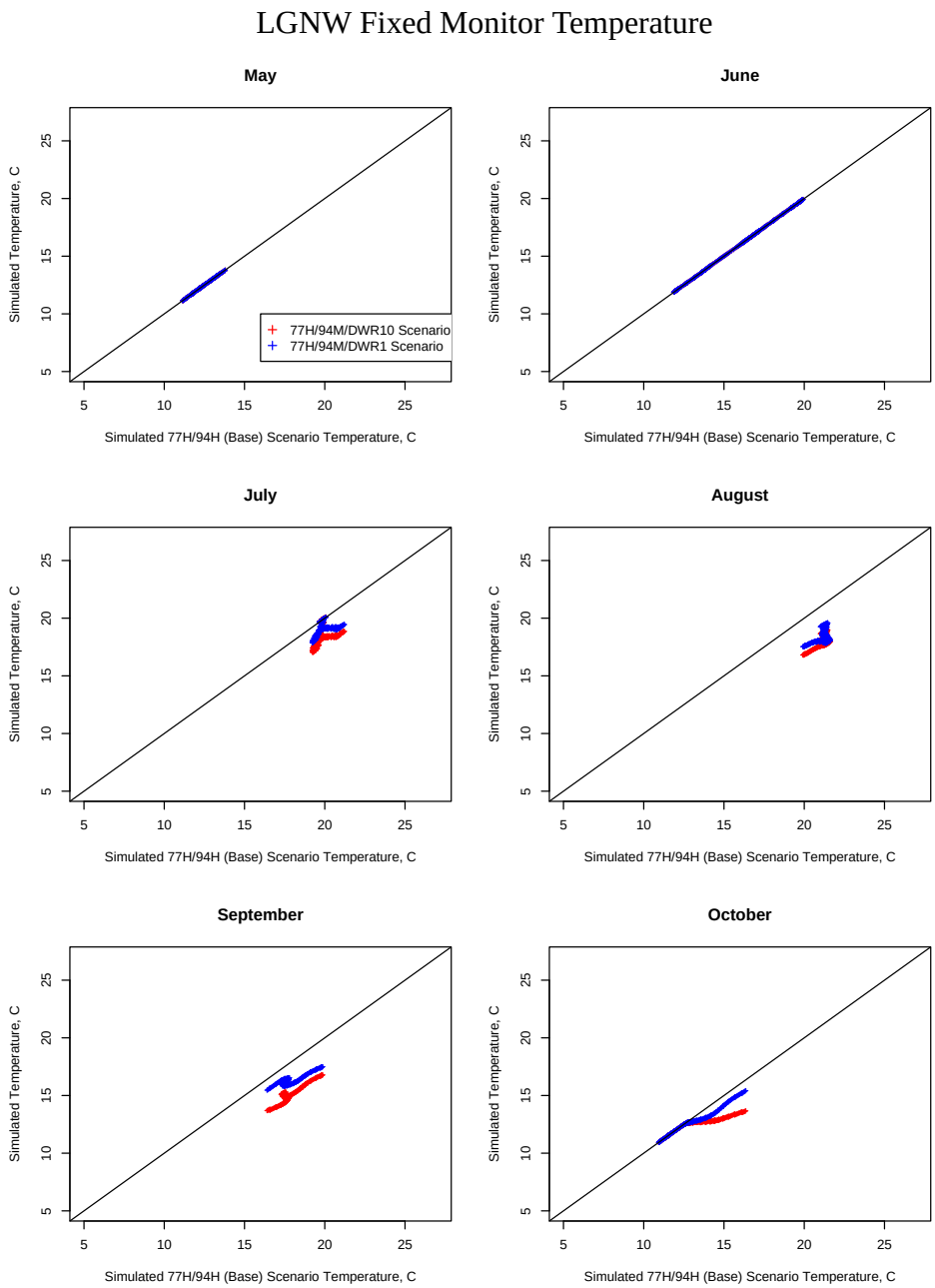

Figure 57: Scatter plot comparison, by month, of simulated temperature at the LGNW Fixed Monitor.

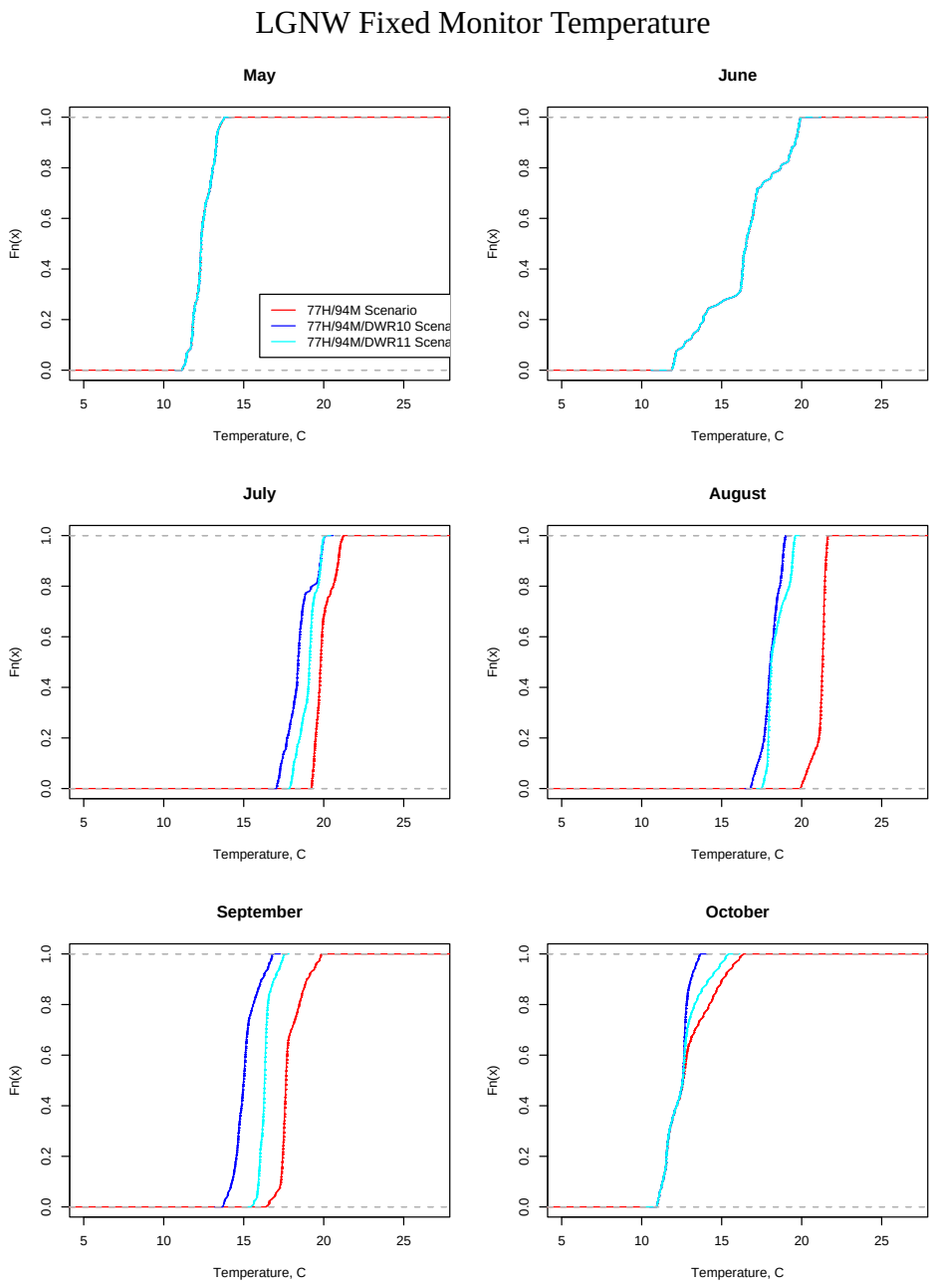

Figure 58: Cumulative frequency distribution (CFD) plot comparison, by month, of simulated temperature at the LGNW Fixed Monitor.

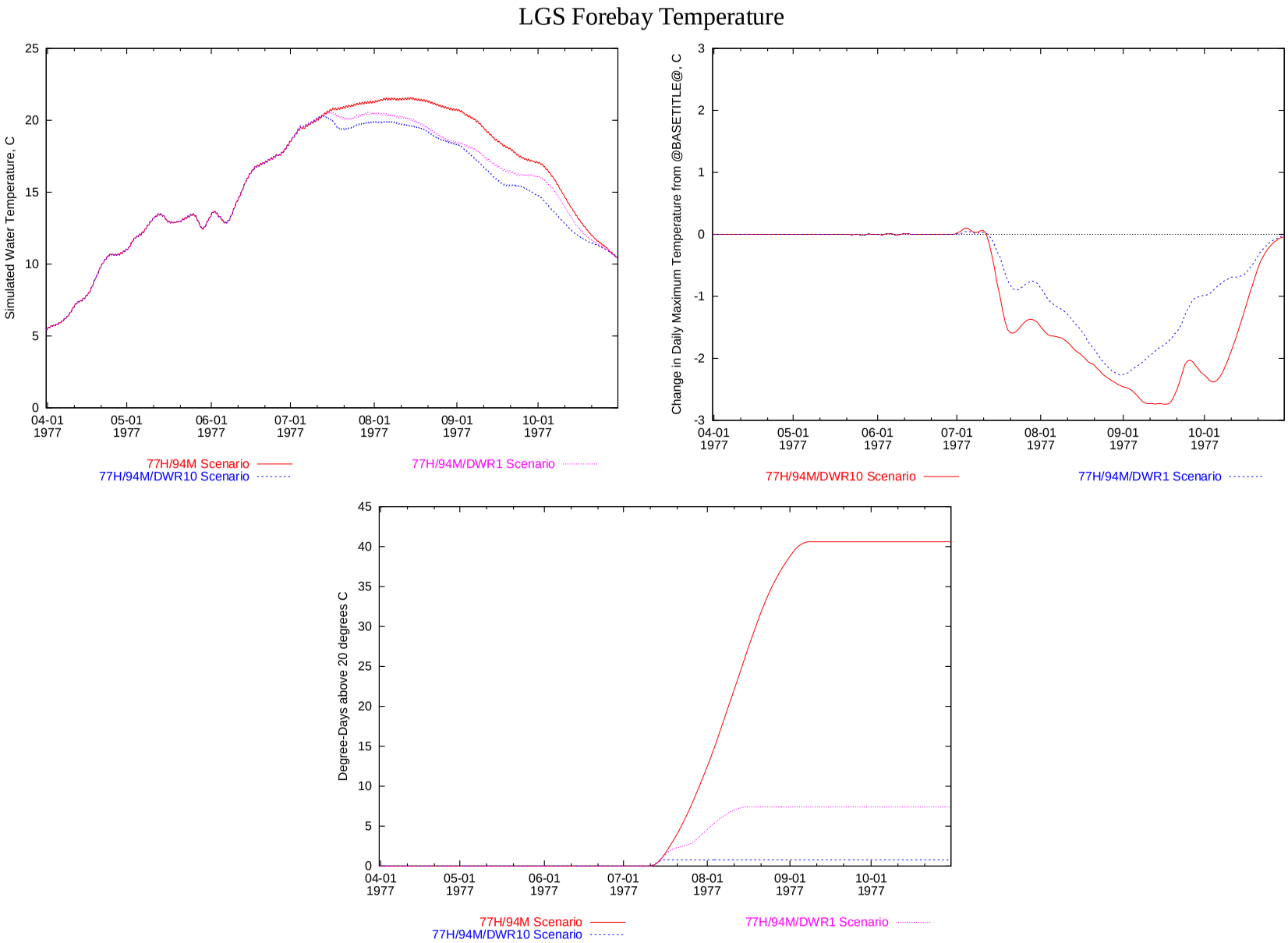

Figure 59: Time series comparison of simulated temperature at the LGS Forebay.

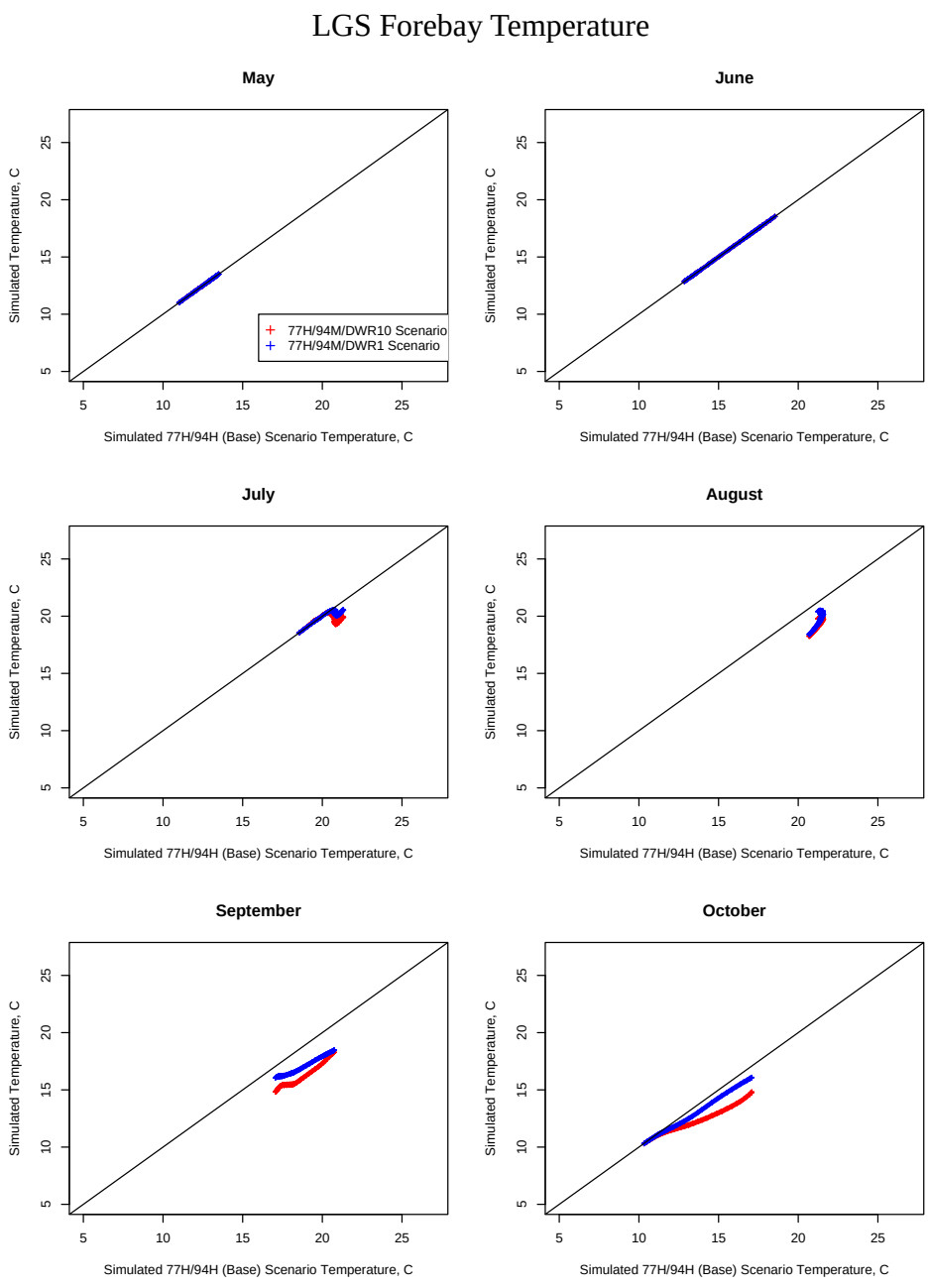

Figure 60: Scatter plot comparison, by month, of simulated temperature at the LGS Forebay.

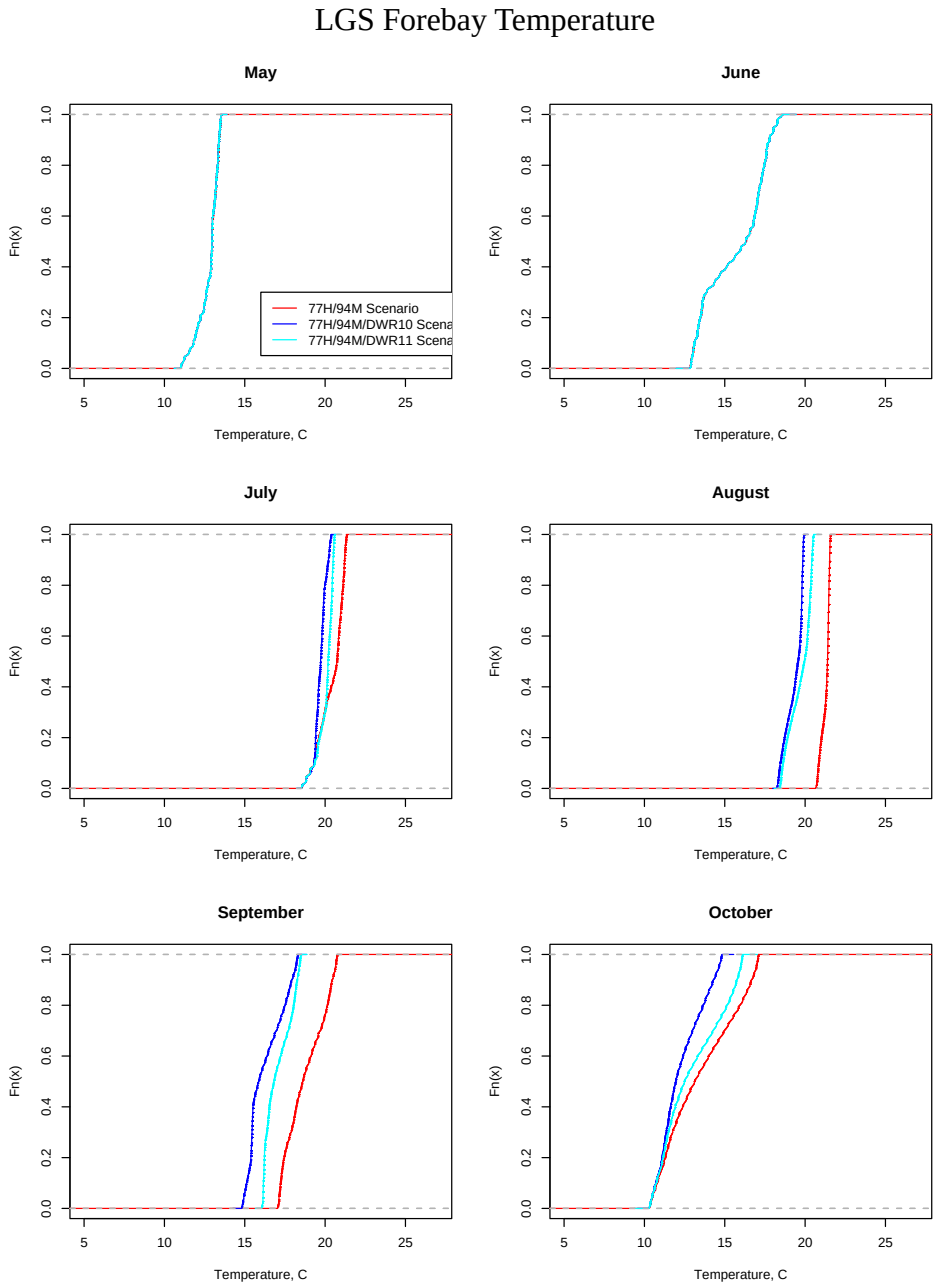

Figure 61: Cumulative frequency distribution (CFD) plot comparison, by month, of simulated temperature at the LGS Forebay.

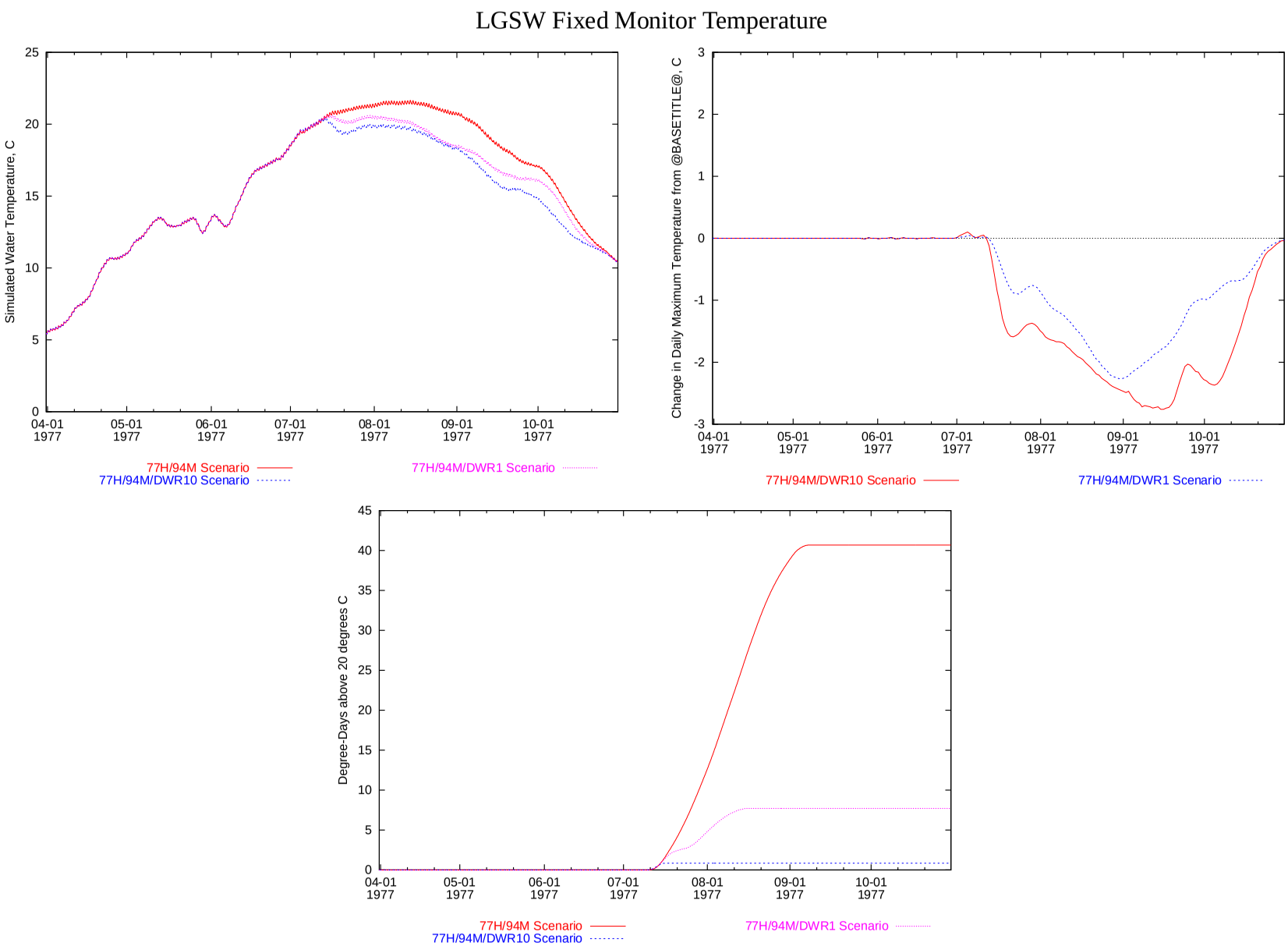

Figure 62: Time series comparison of simulated temperature at the LGSW Fixed Monitor.

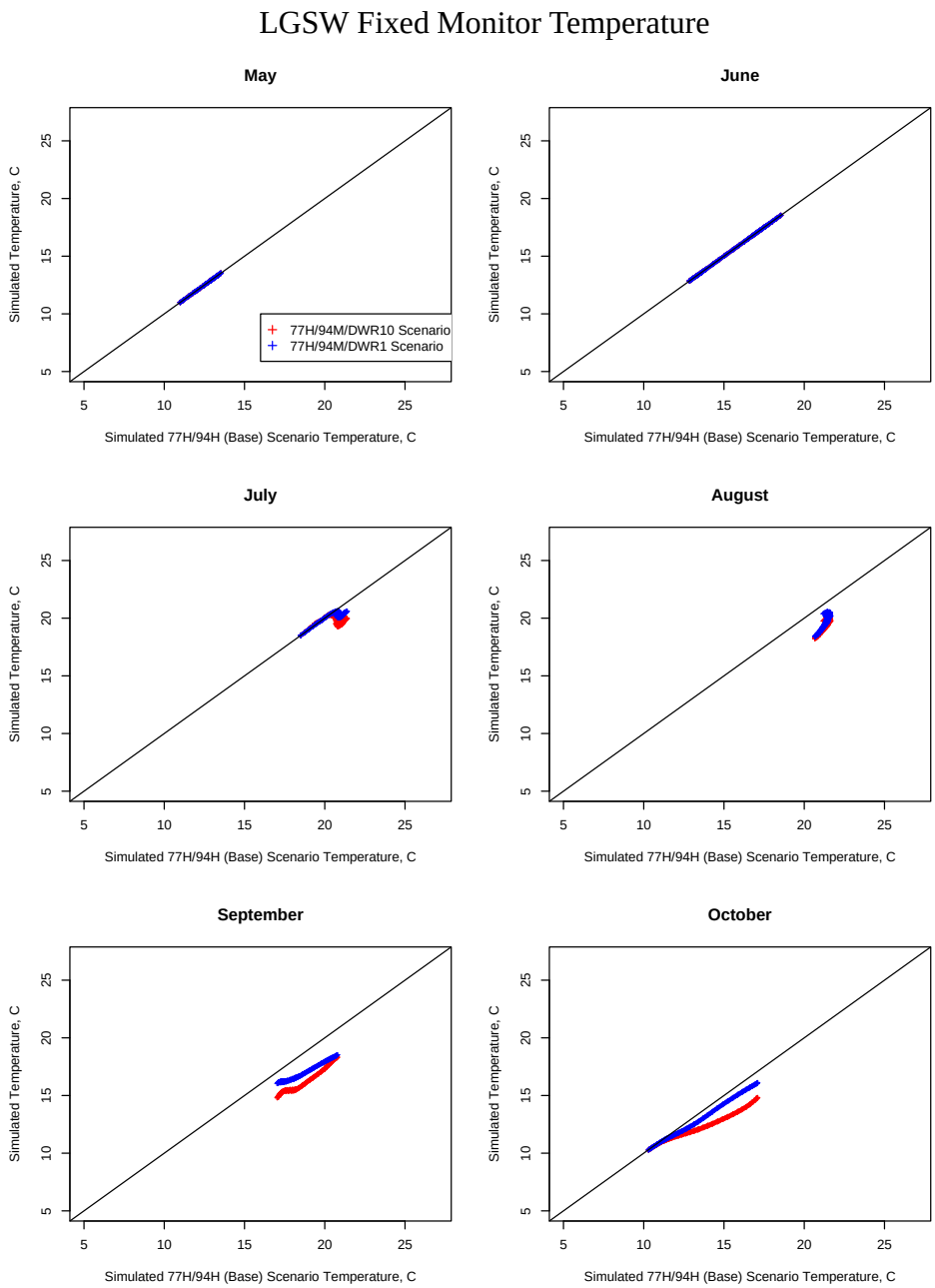

Figure 63: Scatter plot comparison, by month, of simulated temperature at the LGSW Fixed Monitor.

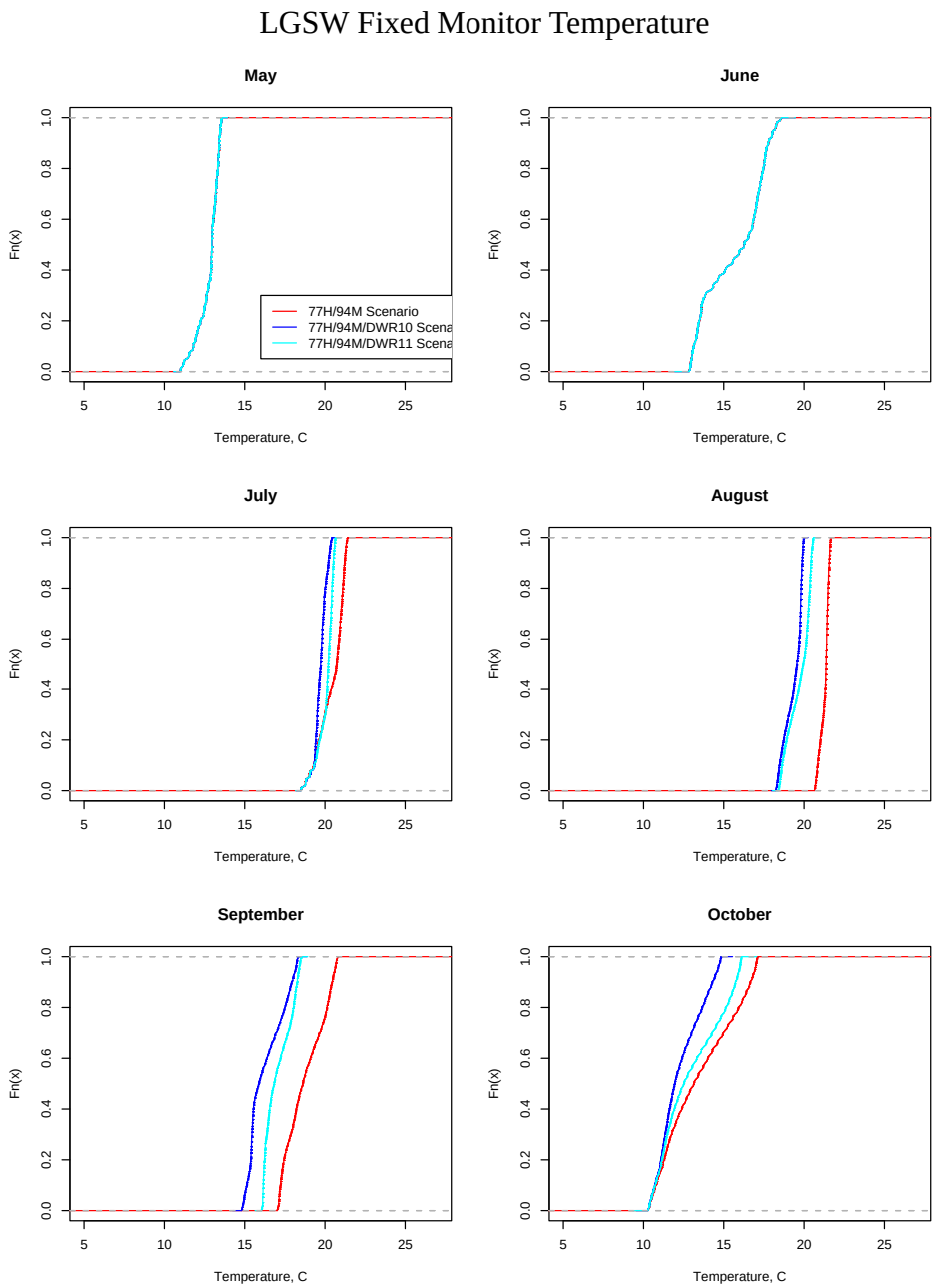

Figure 64: Cumulative frequency distribution (CFD) plot comparison, by month, of simulated temperature at the LGSW Fixed Monitor.

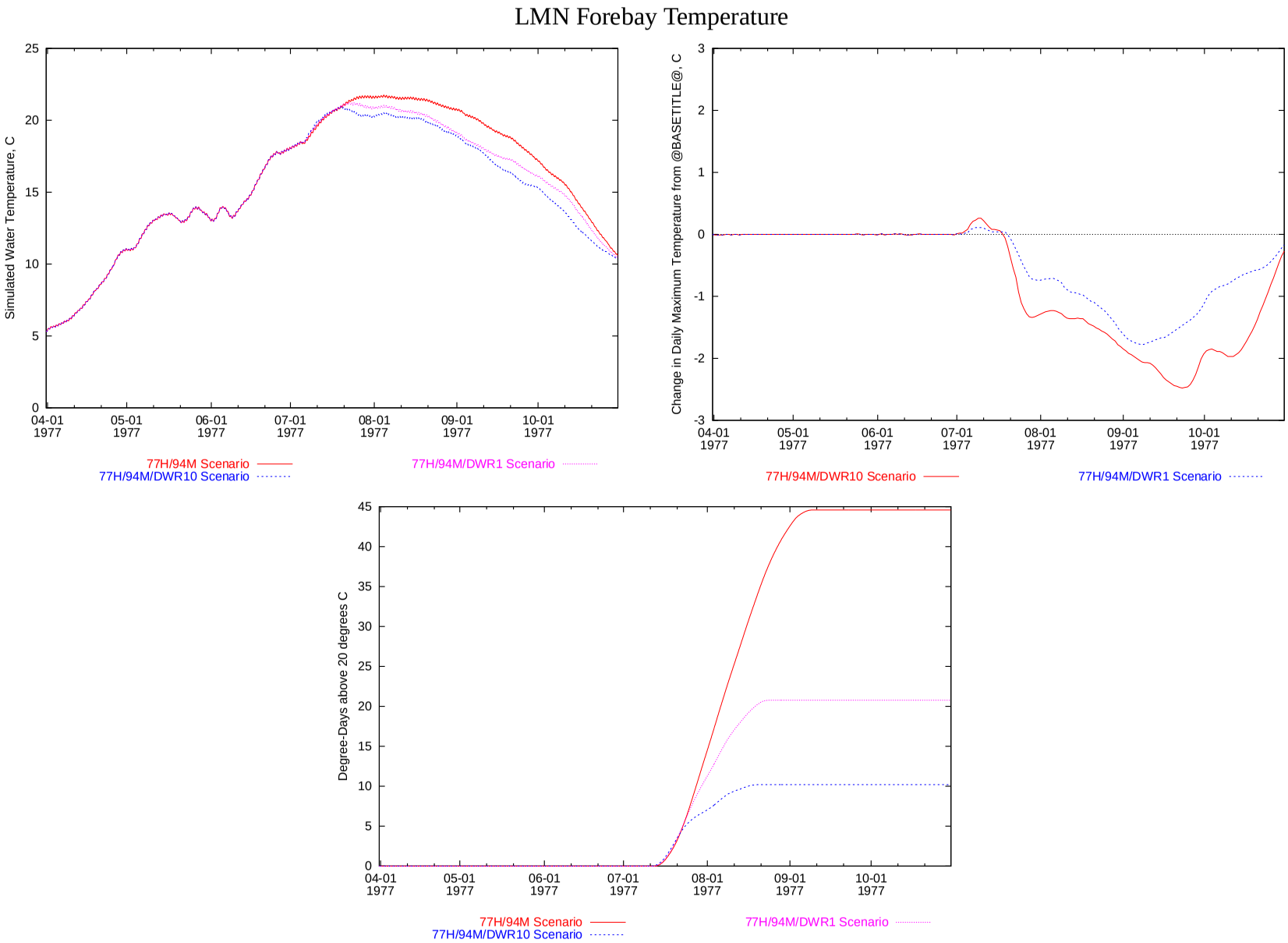

Figure 65: Time series comparison of simulated temperature at the LMN Forebay.

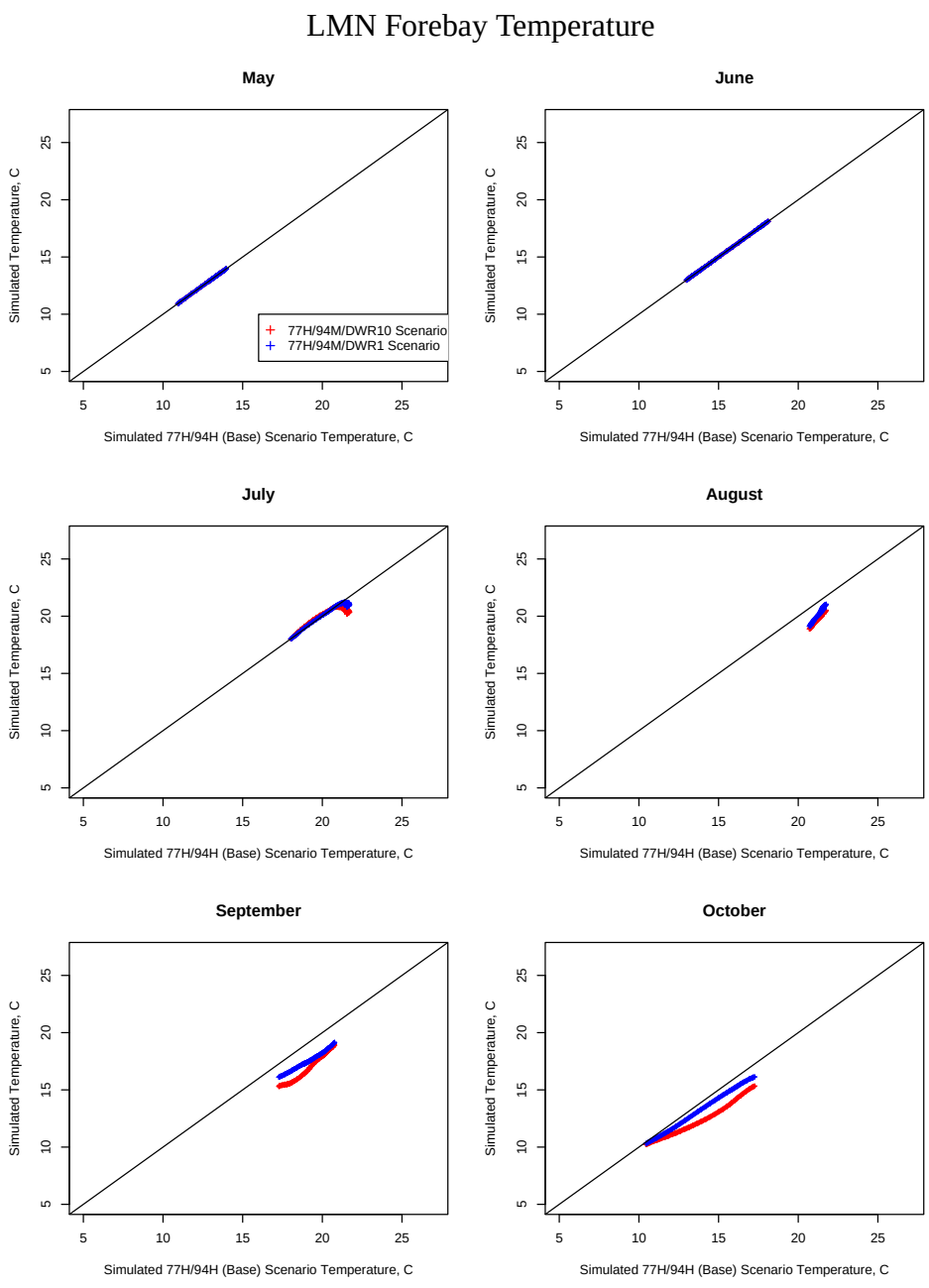

Figure 66: Scatter plot comparison, by month, of simulated temperature at the LMN Forebay.

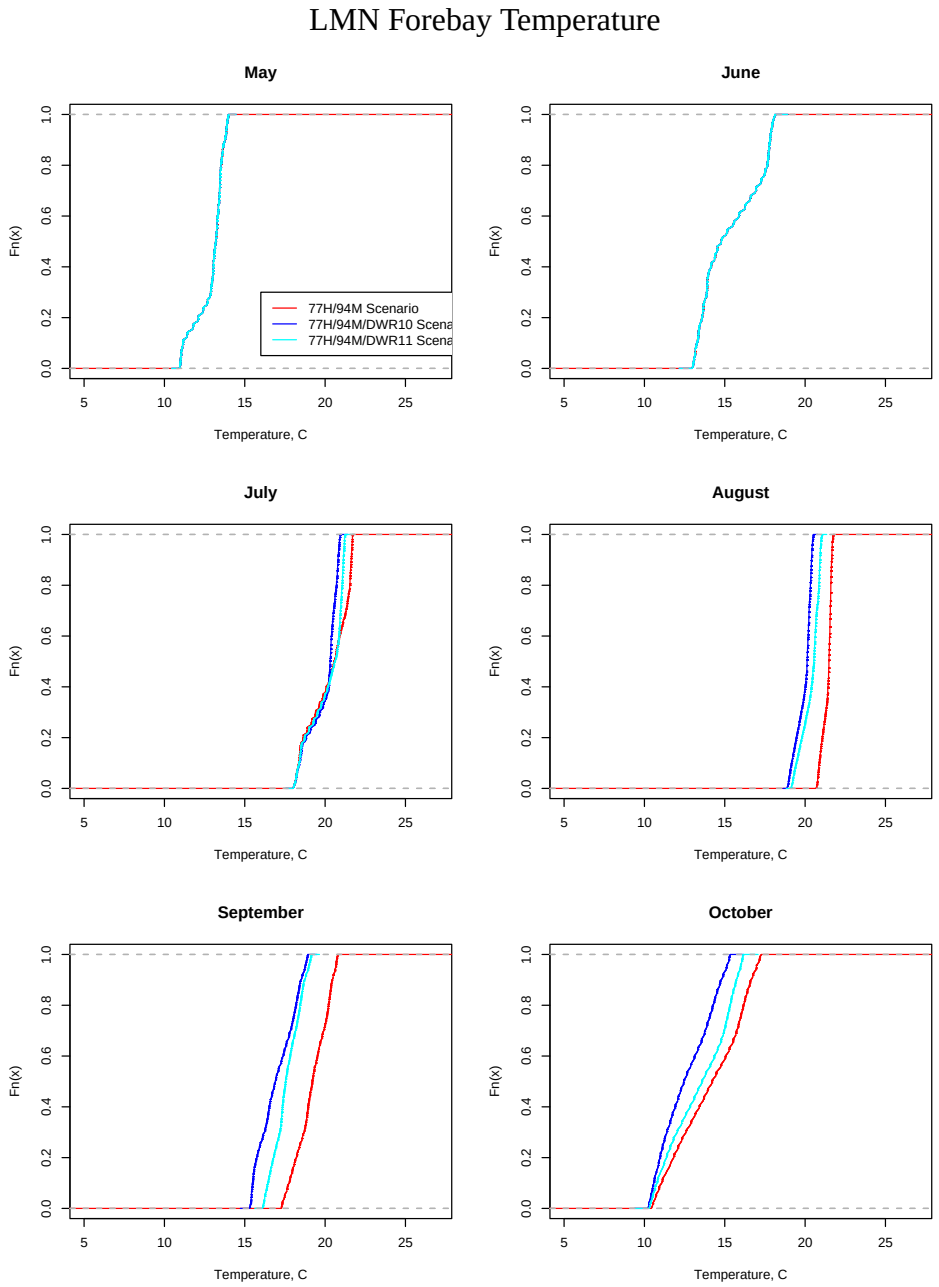

Figure 67: Cumulative frequency distribution (CFD) plot comparison, by month, of simulated temperature at the LMN Forebay.

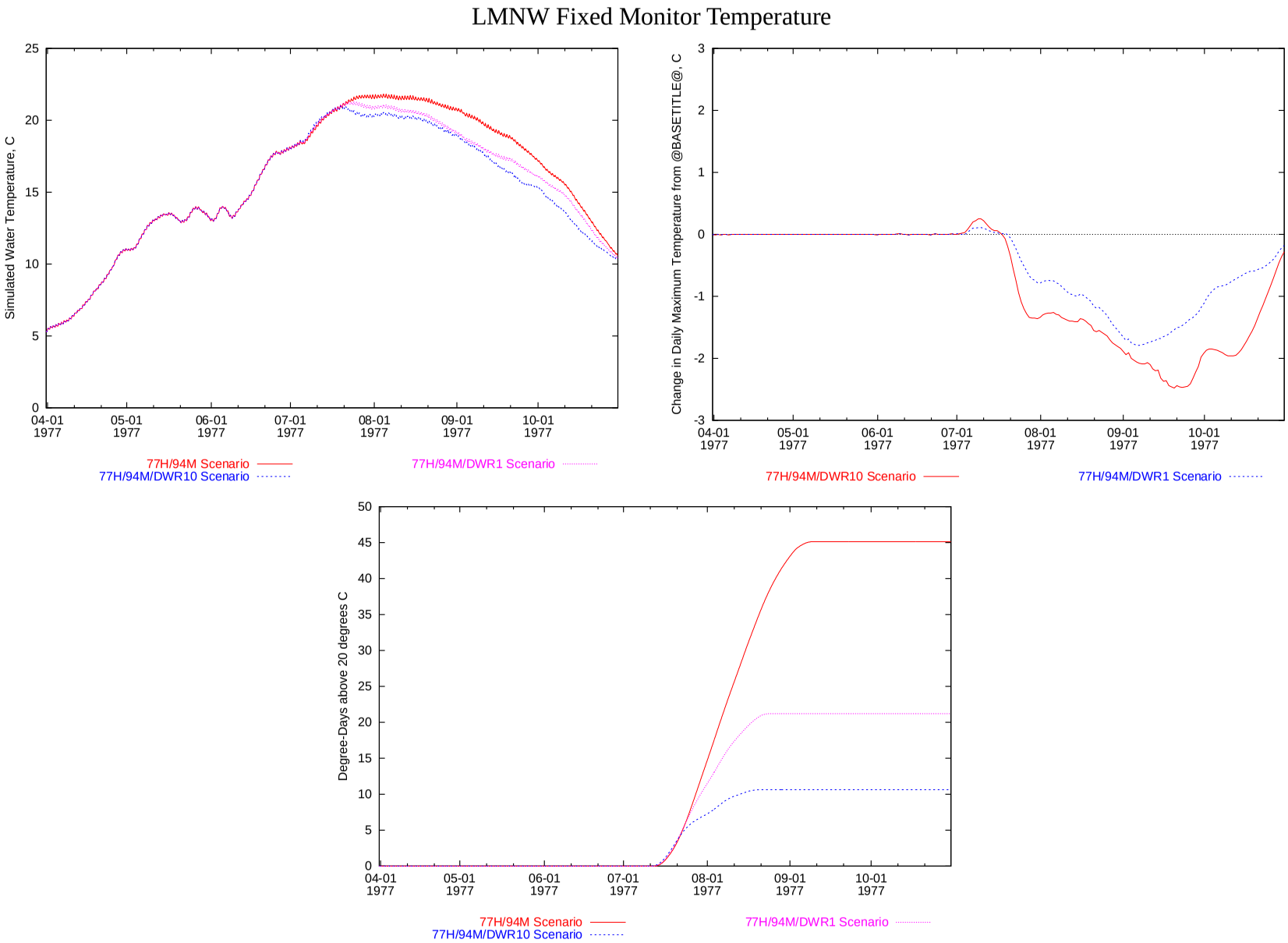

Figure 68: Time series comparison of simulated temperature at the LMNW Fixed Monitor.

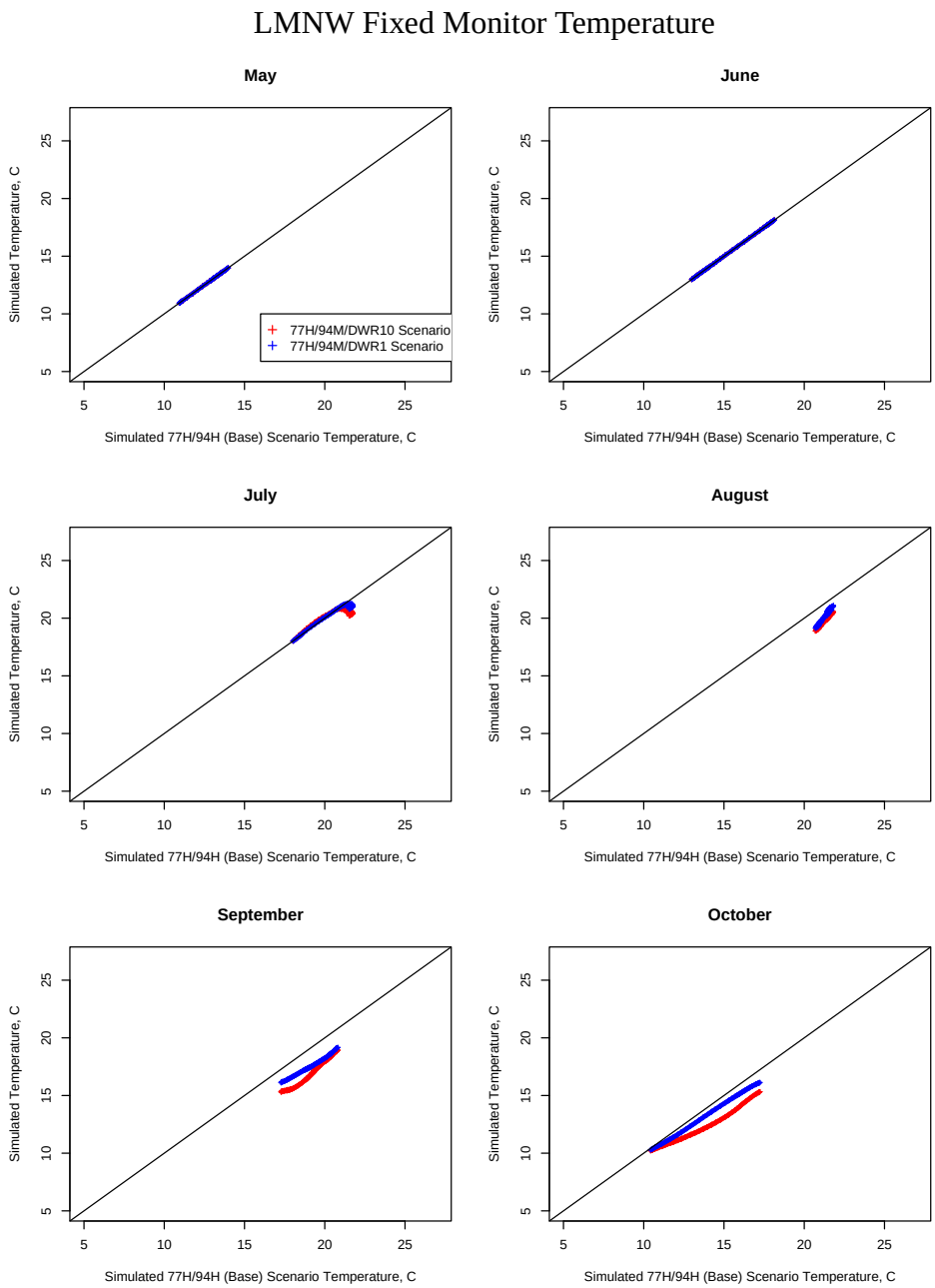

Figure 69: Scatter plot comparison, by month, of simulated temperature at the LMNW Fixed Monitor.

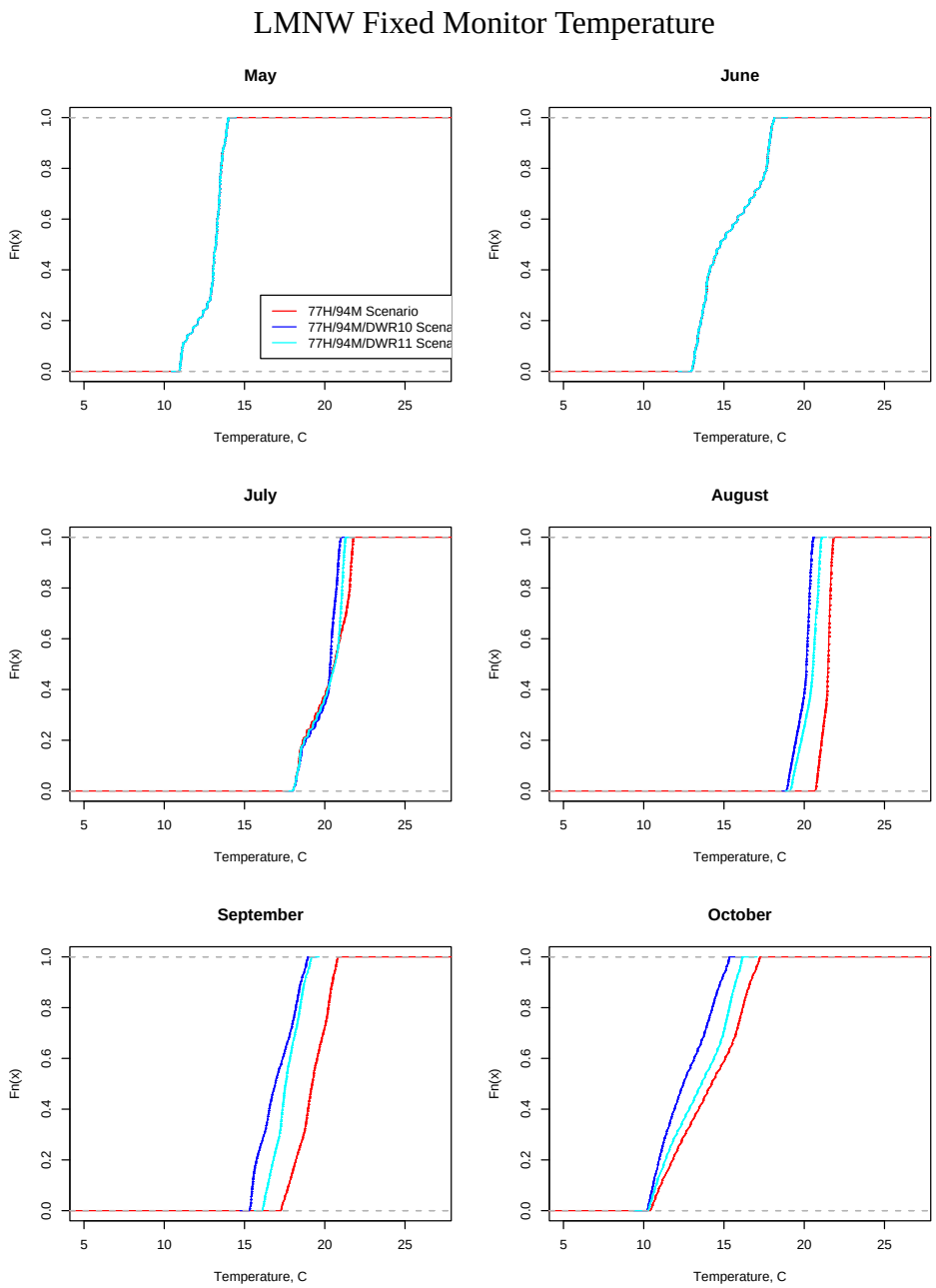

Figure 70: Cumulative frequency distribution (CFD) plot comparison, by month, of simulated temperature at the LMNW Fixed Monitor.

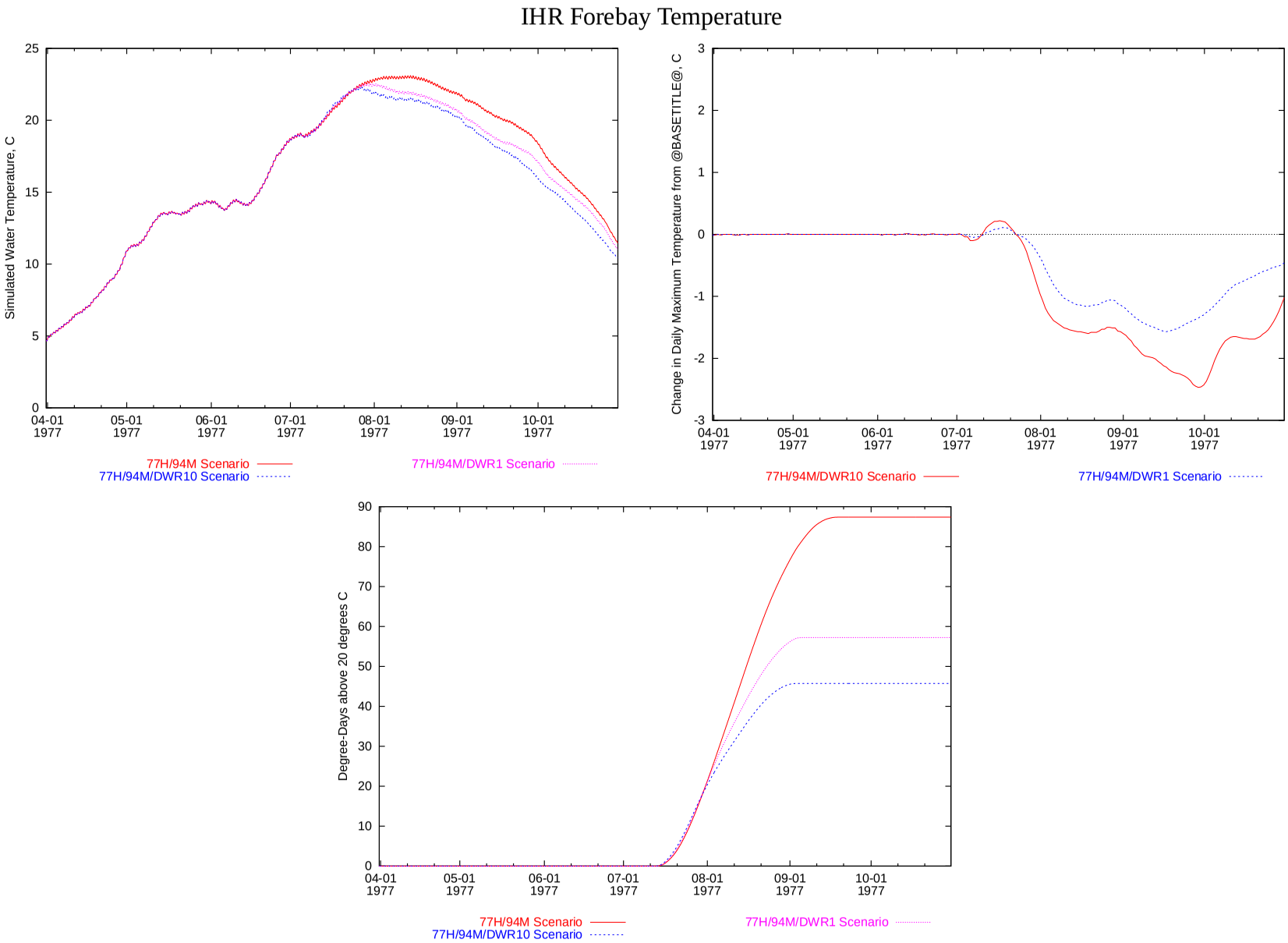

Figure 71: Time series comparison of simulated temperature at the IHR Forebay.

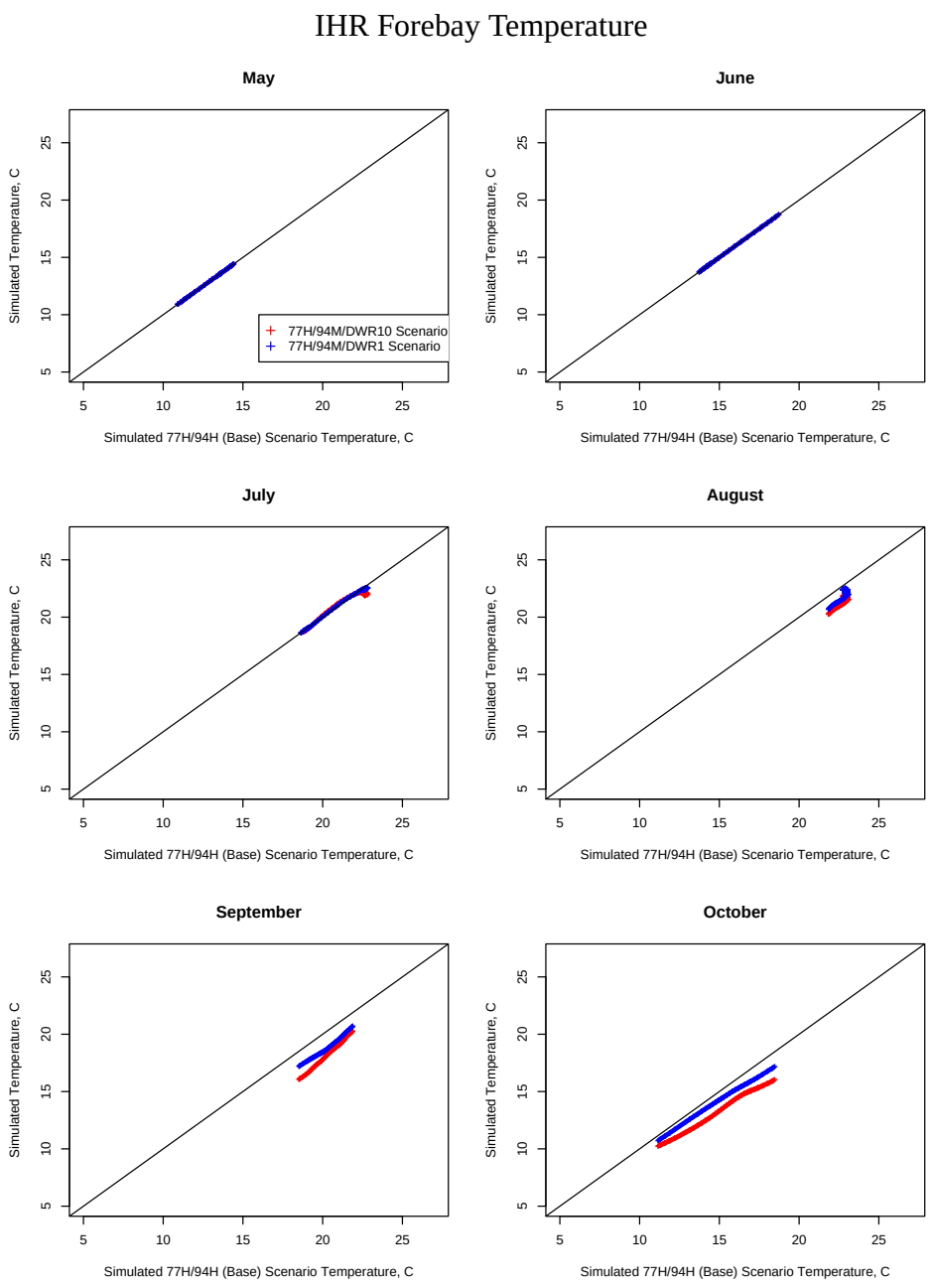

Figure 72: Scatter plot comparison, by month, of simulated temperature at the IHR Forebay.

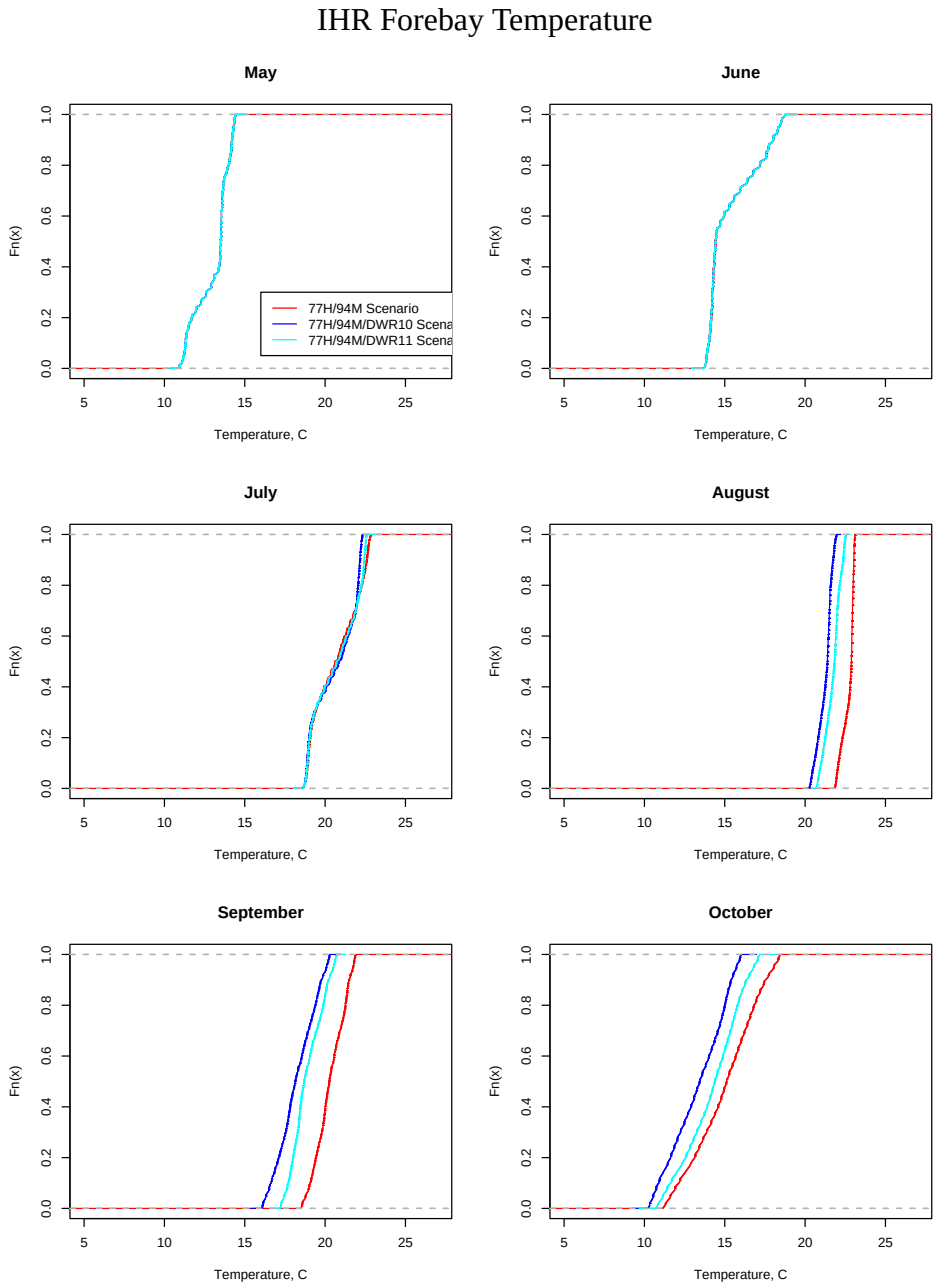

Figure 73: Cumulative frequency distribution (CFD) plot comparison, by month, of simulated temperature at the IHR Forebay.

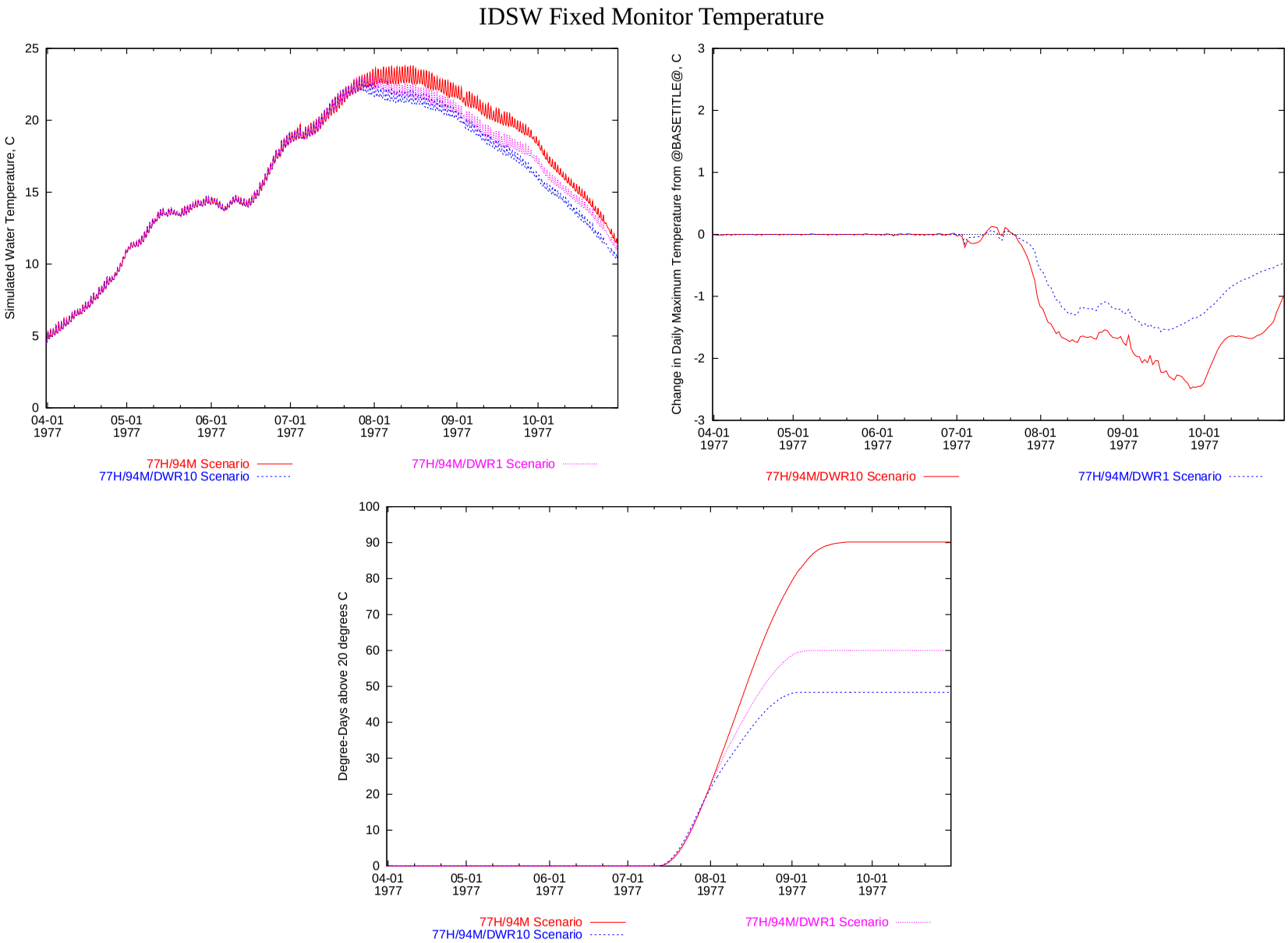

Figure 74: Time series comparison of simulated temperature at the IDSW Fixed Monitor.

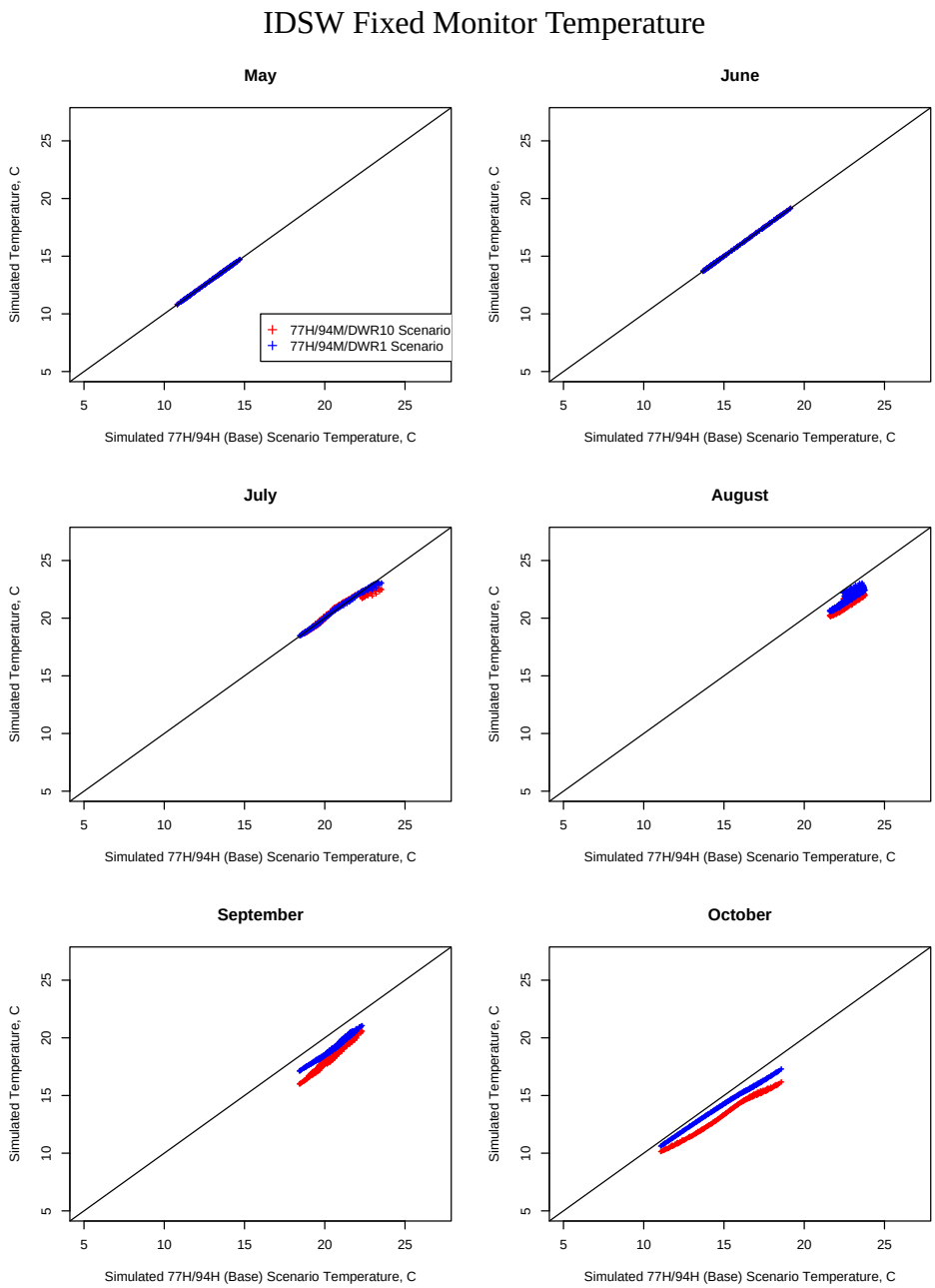

Figure 75: Scatter plot comparison, by month, of simulated temperature at the IDSW Fixed Monitor.

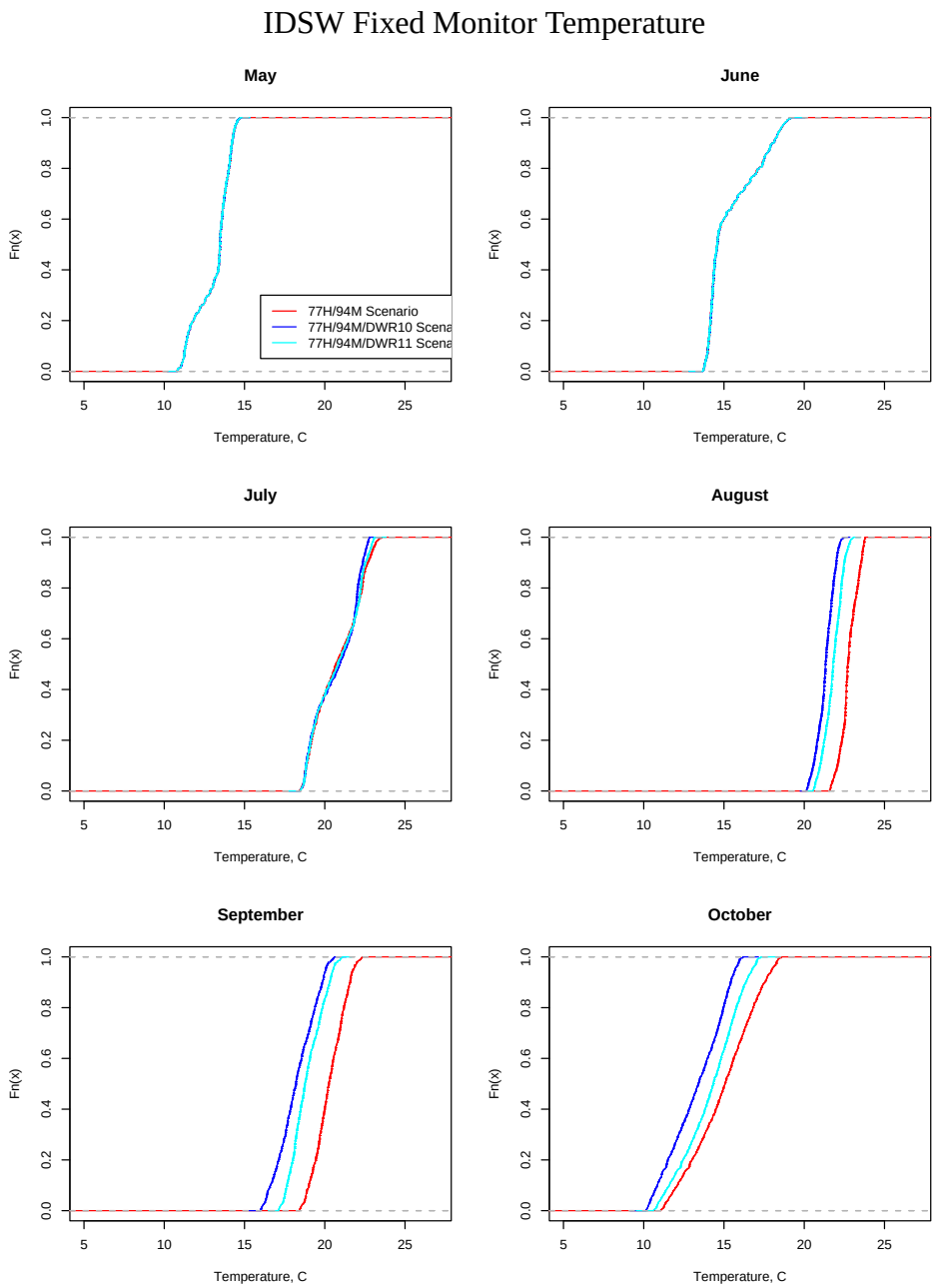

Figure 76: Cumulative frequency distribution (CFD) plot comparison, by month, of simulated temperature at the IDSW Fixed Monitor.

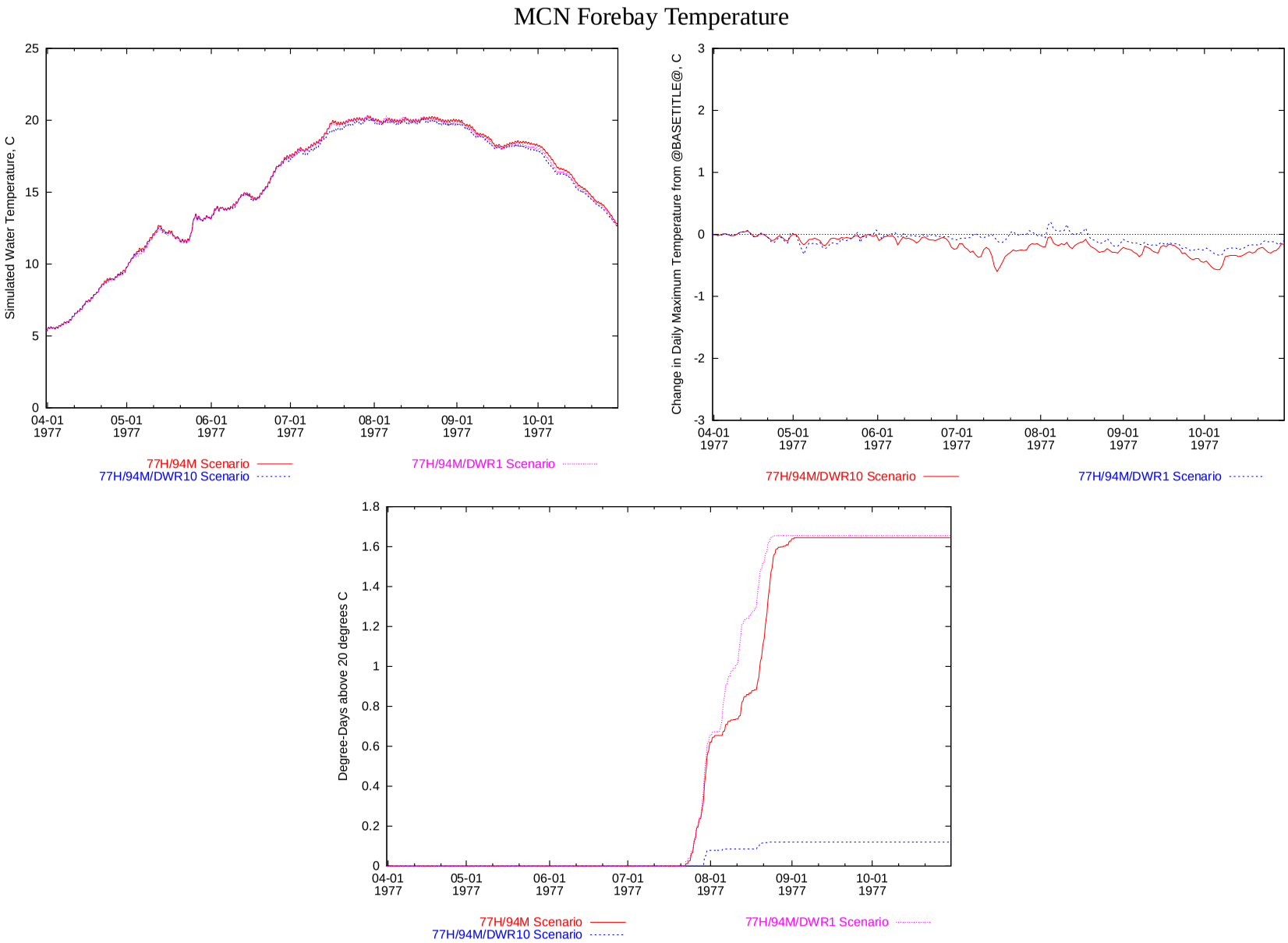

Figure 77: Time series comparison of simulated temperature at the MCN Forebay.

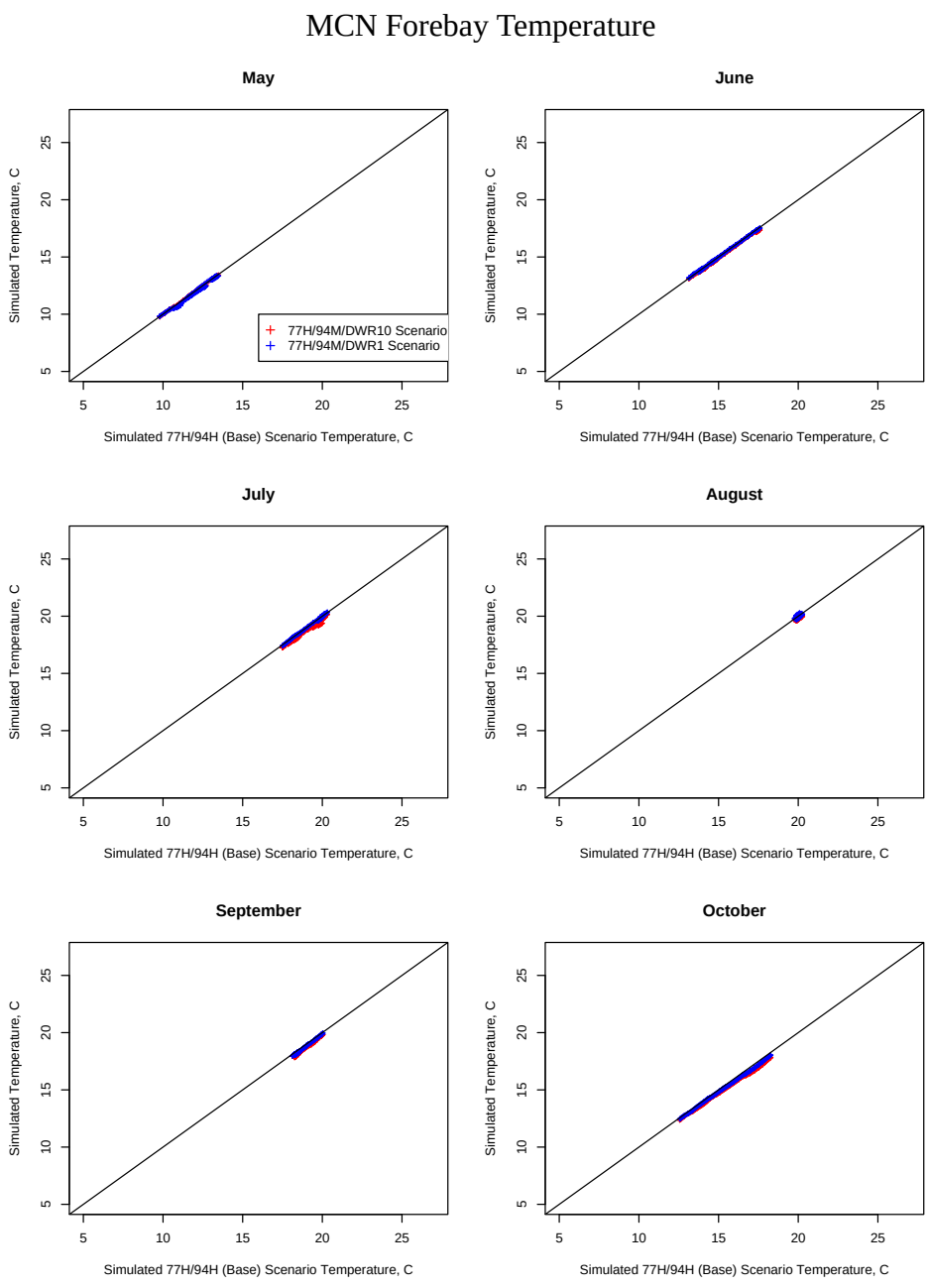

Figure 78: Scatter plot comparison, by month, of simulated temperature at the MCN Forebay.

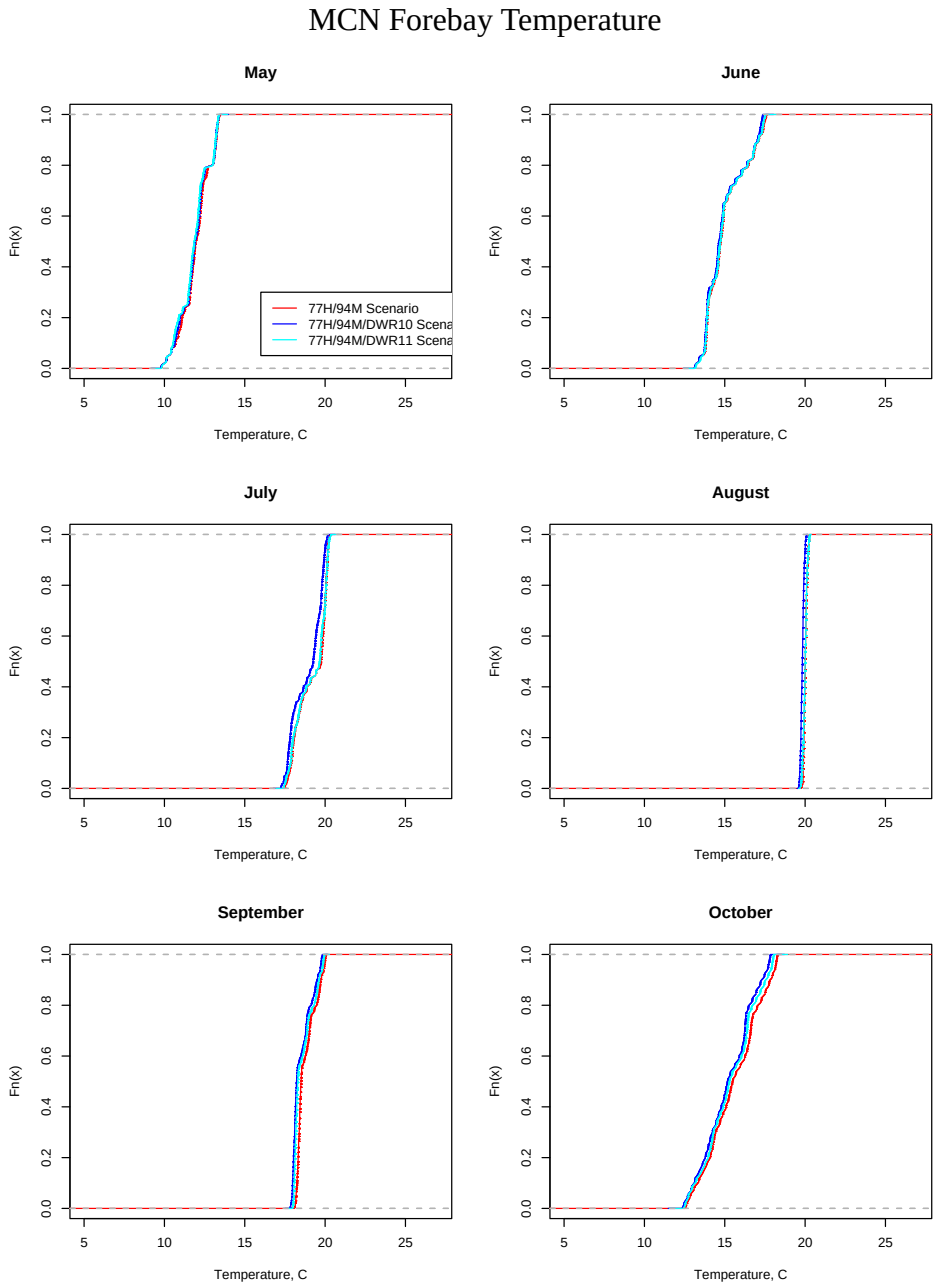

Figure 79: Cumulative frequency distribution (CFD) plot comparison, by month, of simulated temperature at the MCN Forebay.

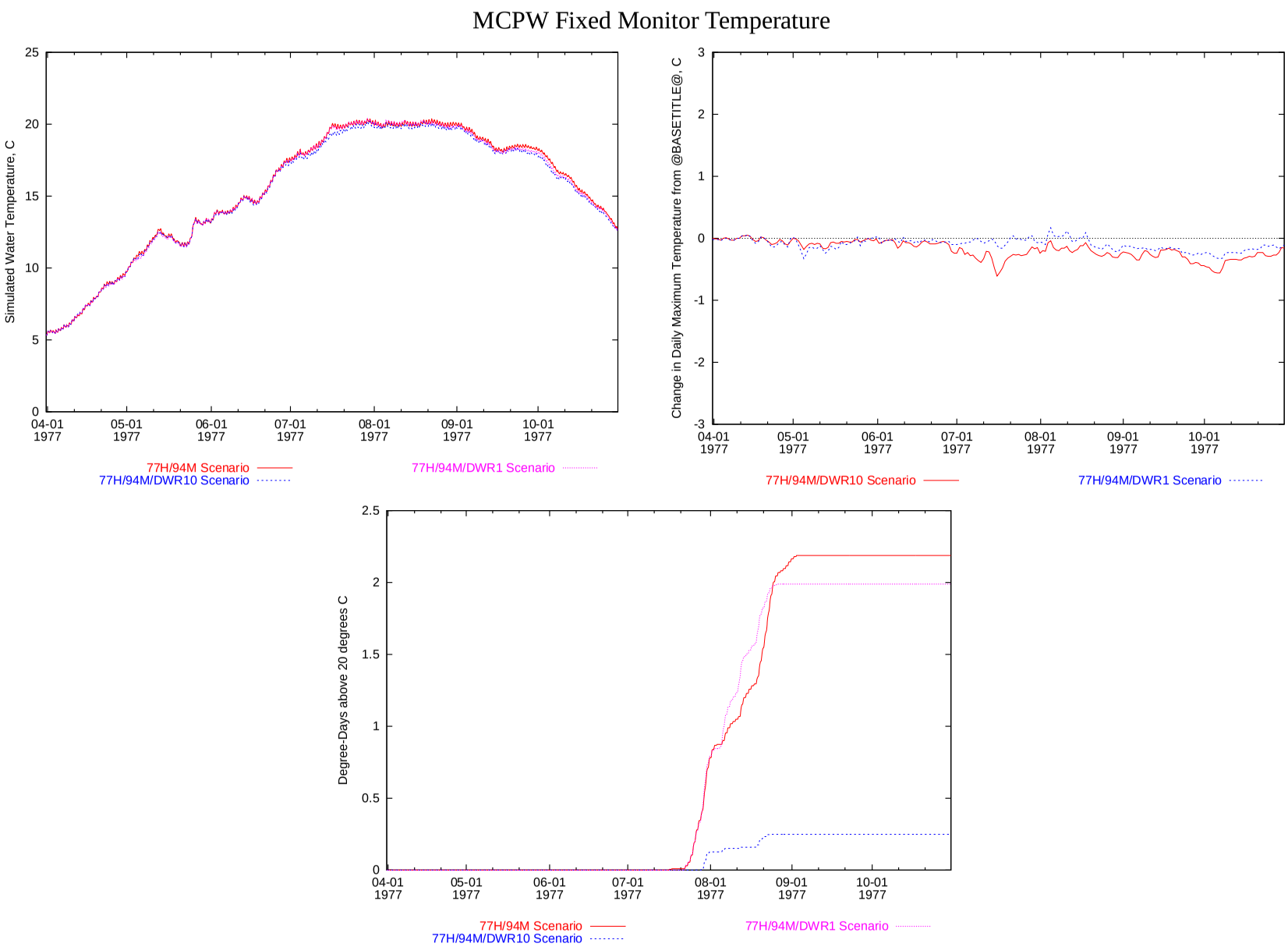

Figure 80: Time series comparison of simulated temperature at the MCPW Fixed Monitor.

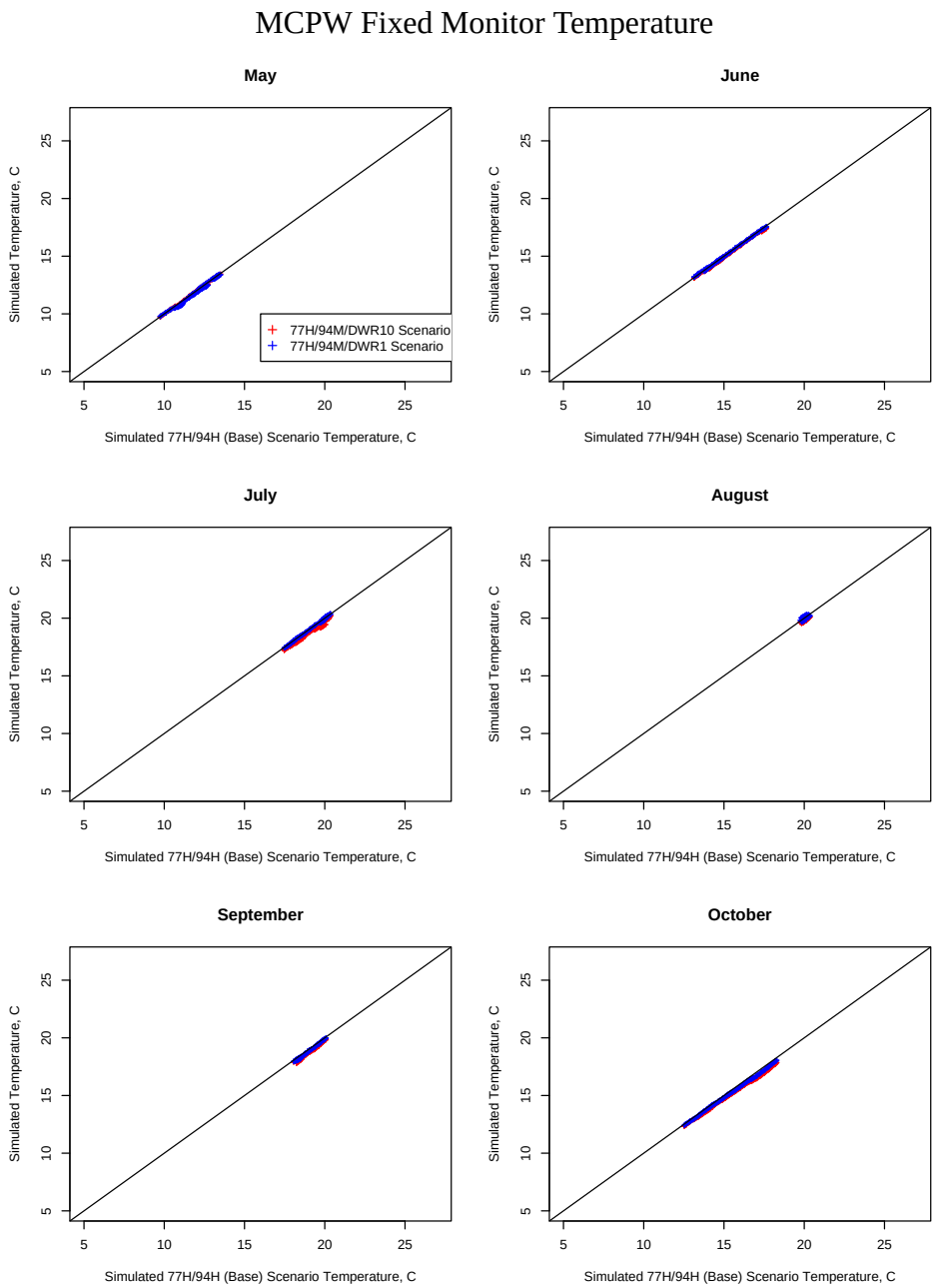

Figure 81: Scatter plot comparison, by month, of simulated temperature at the MCPW Fixed Monitor.

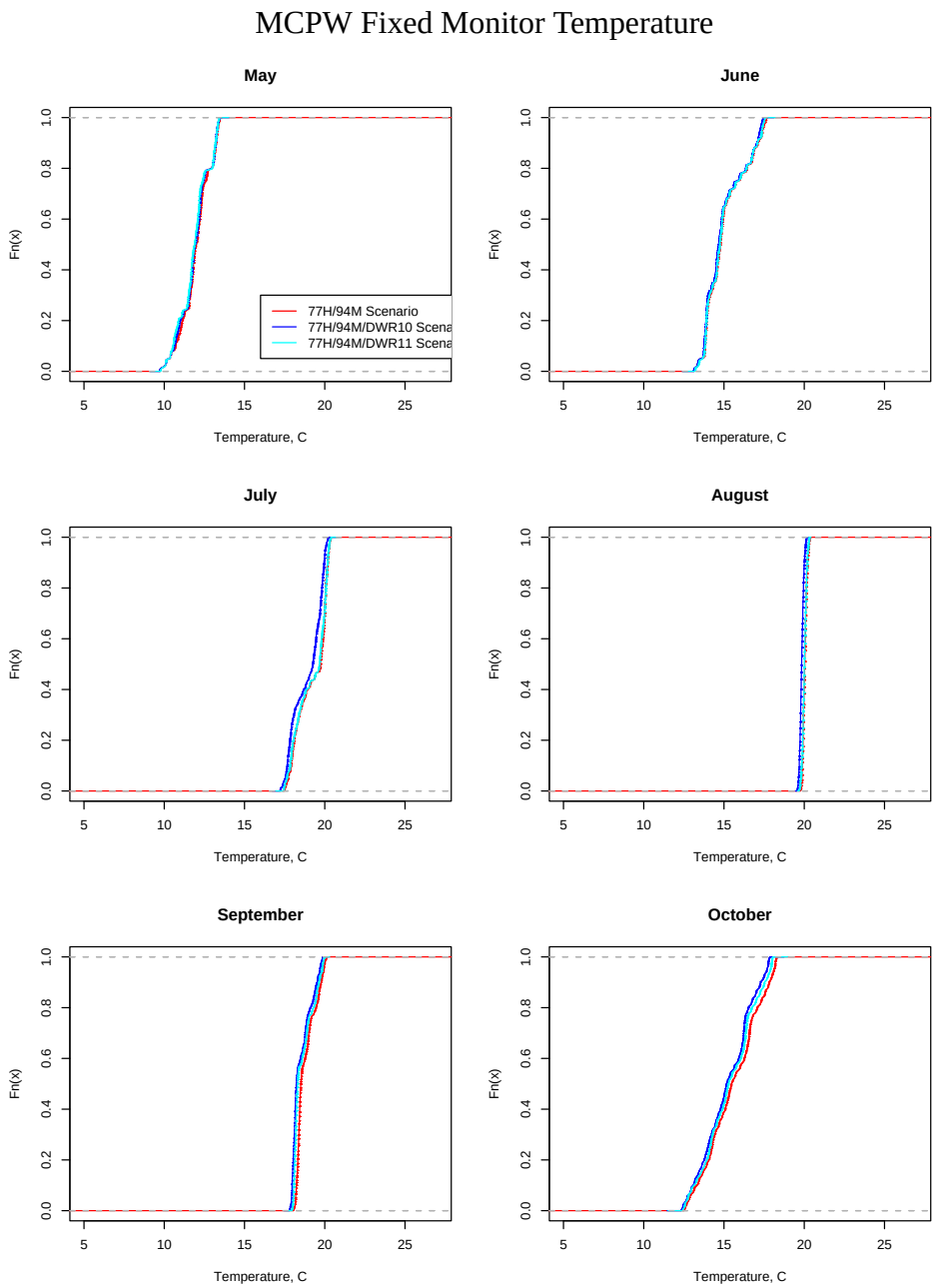

Figure 82: Cumulative frequency distribution (CFD) plot comparison, by month, of simulated temperature at the MCPW Fixed Monitor.

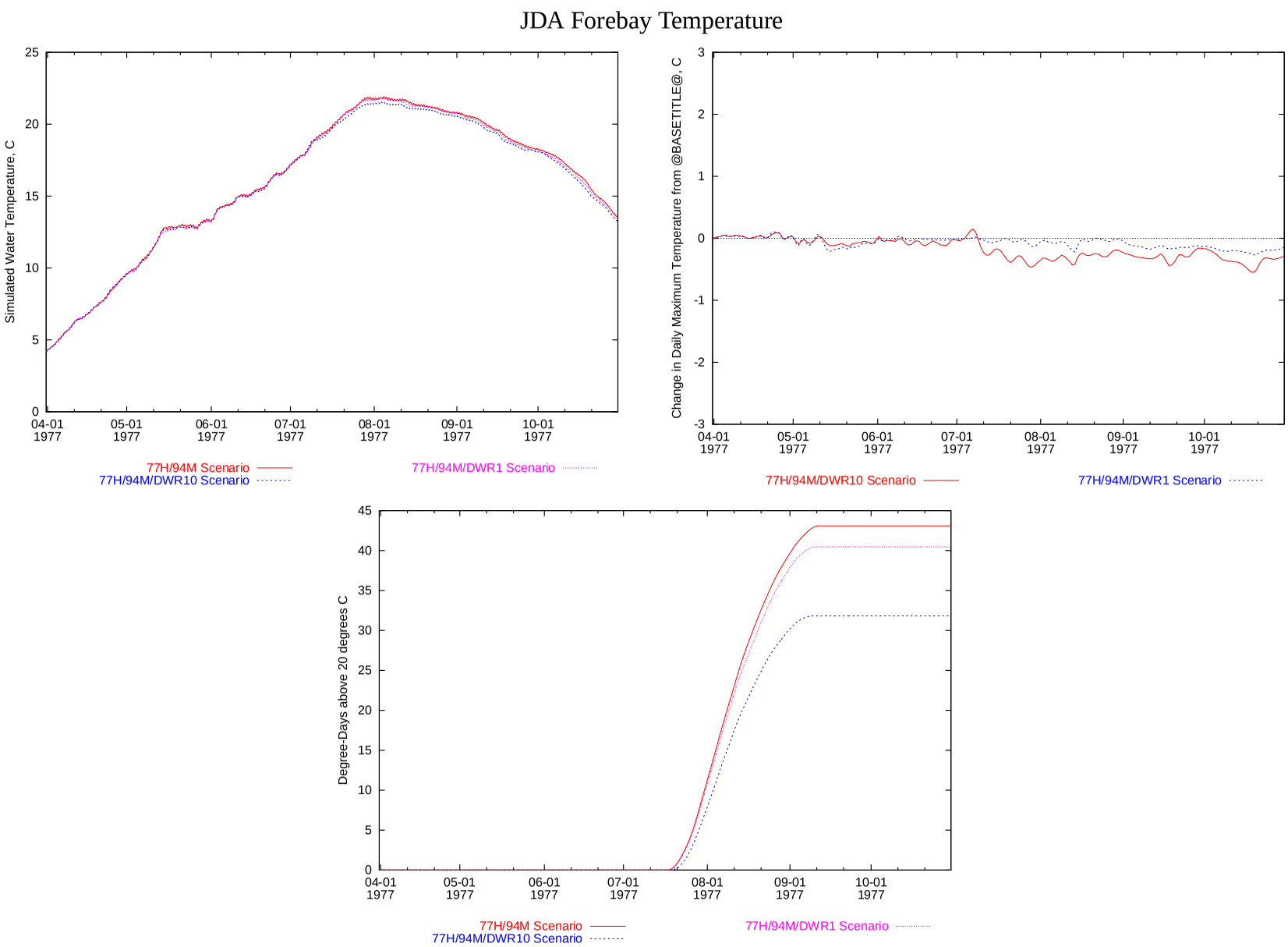

Figure 83: Time series comparison of simulated temperature at the JDA Forebay.

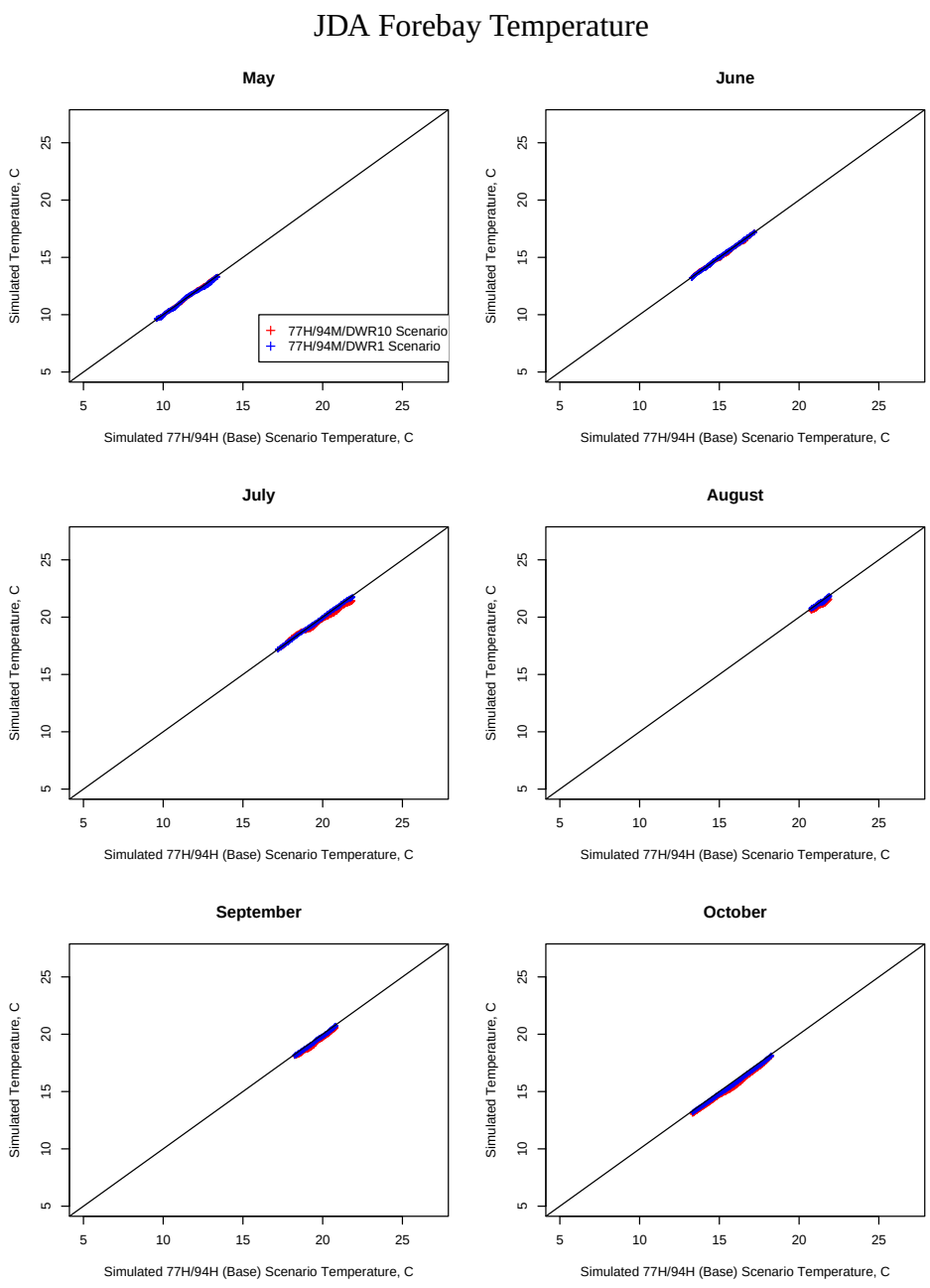

Figure 84: Scatter plot comparison, by month, of simulated temperature at the JDA Forebay.

JDA Forebay Temperature

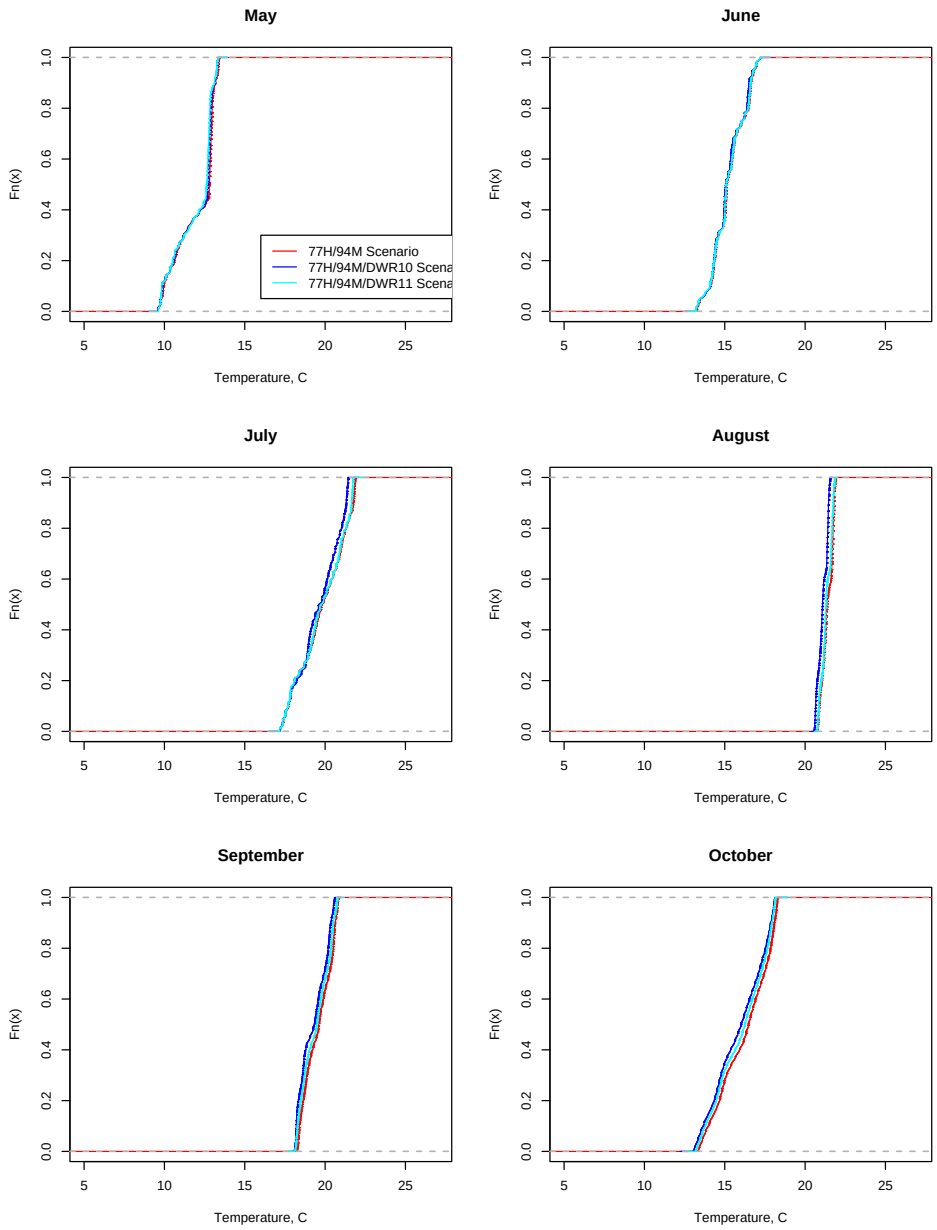

Figure 85: Cumulative frequency distribution (CFD) plot comparison, by month, of simulated temperature at the JDA Forebay.

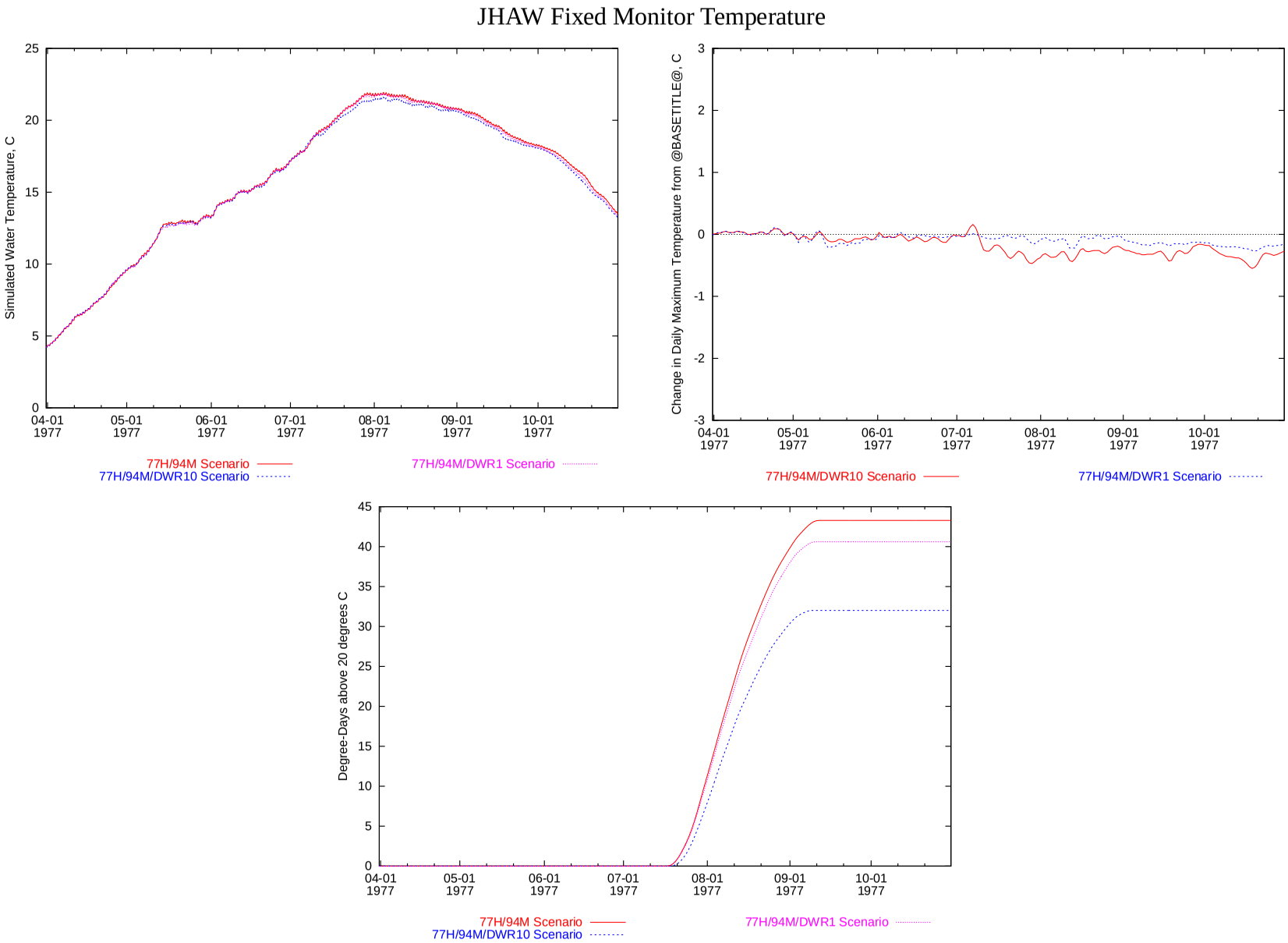

Figure 86: Time series comparison of simulated temperature at the JHAW Fixed Monitor.

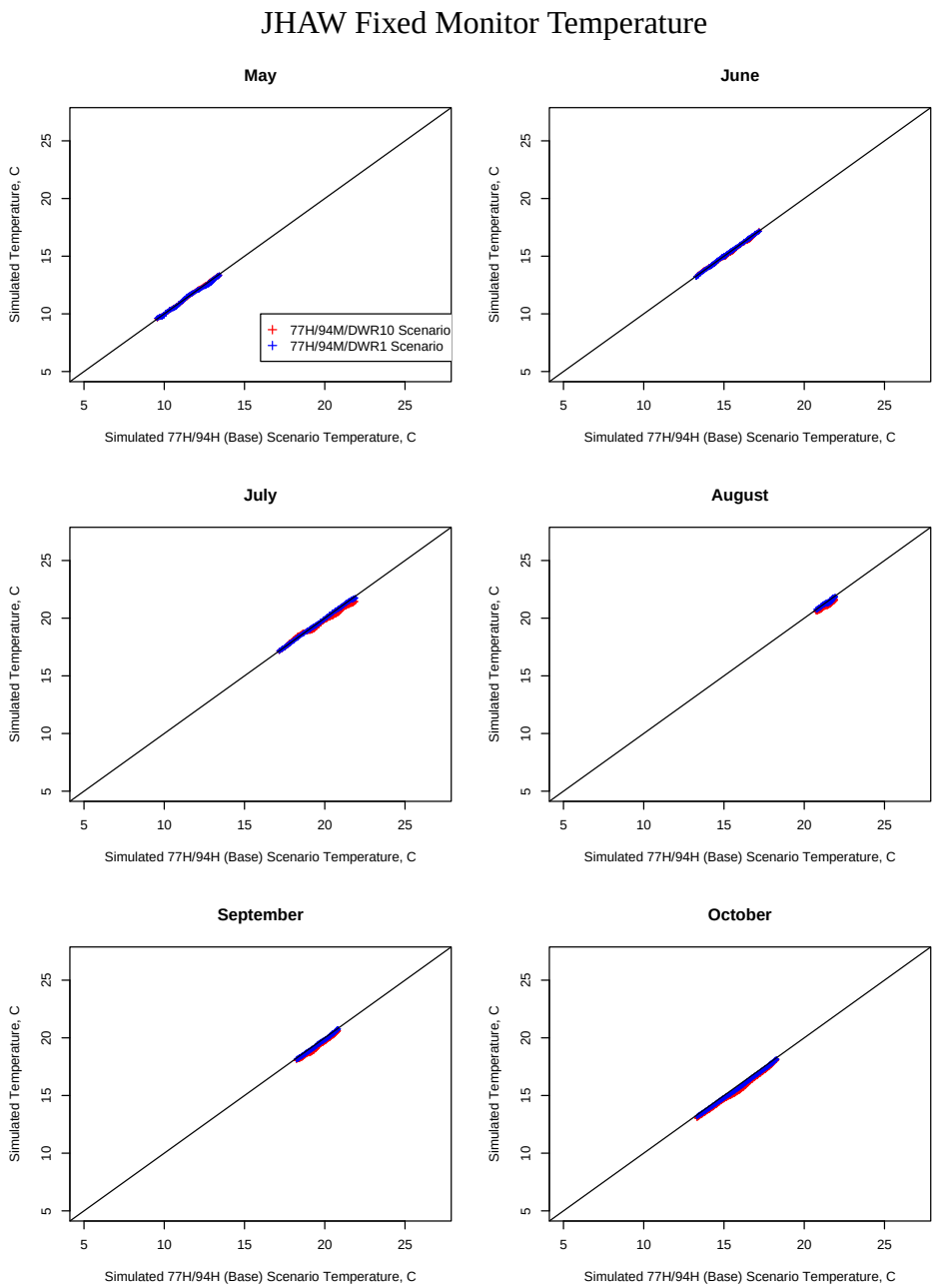

Figure 87: Scatter plot comparison, by month, of simulated temperature at the JHAW Fixed Monitor.

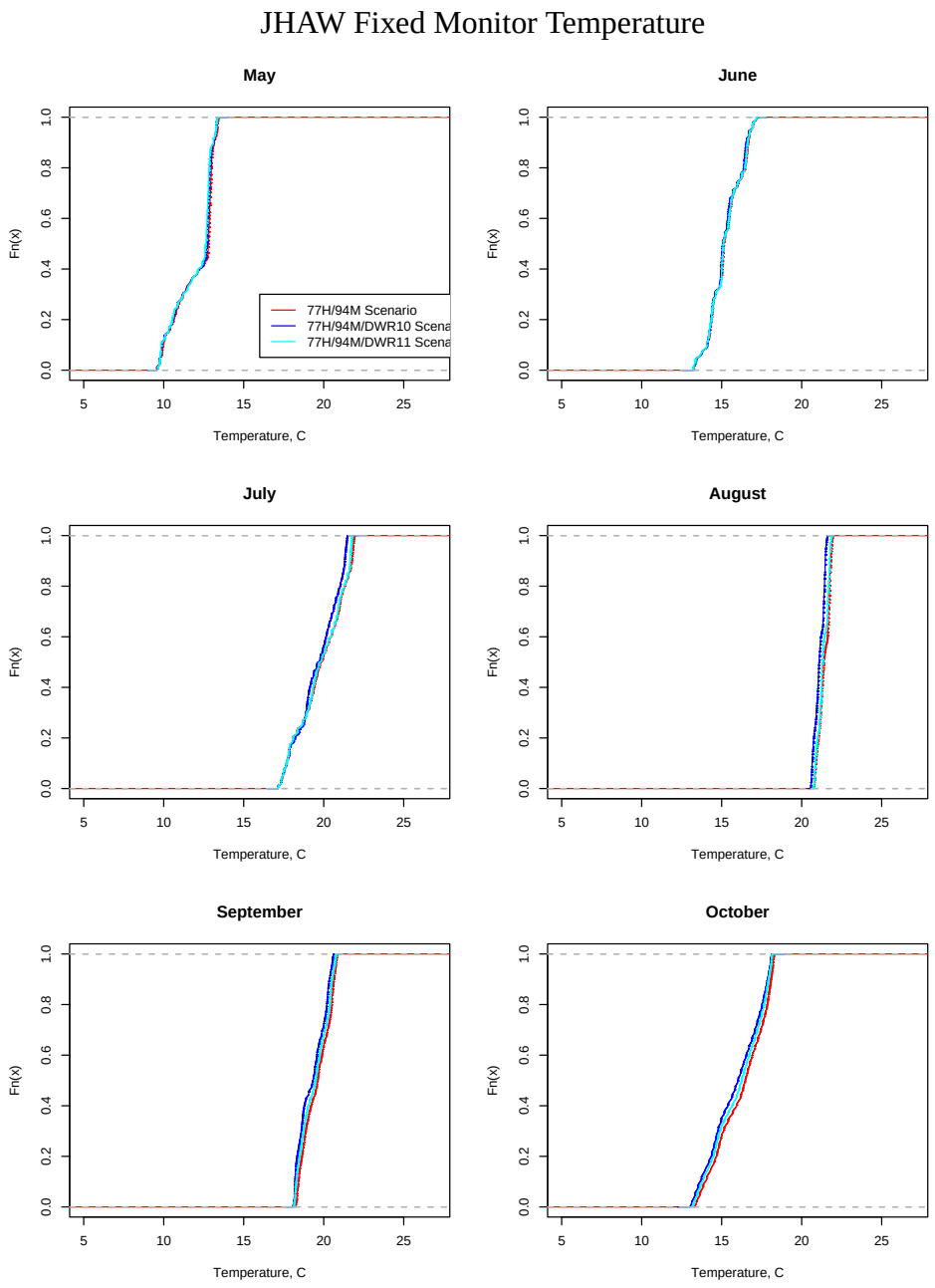

Figure 88: Cumulative frequency distribution (CFD) plot comparison, by month, of simulated temperature at the JHAW Fixed Monitor.

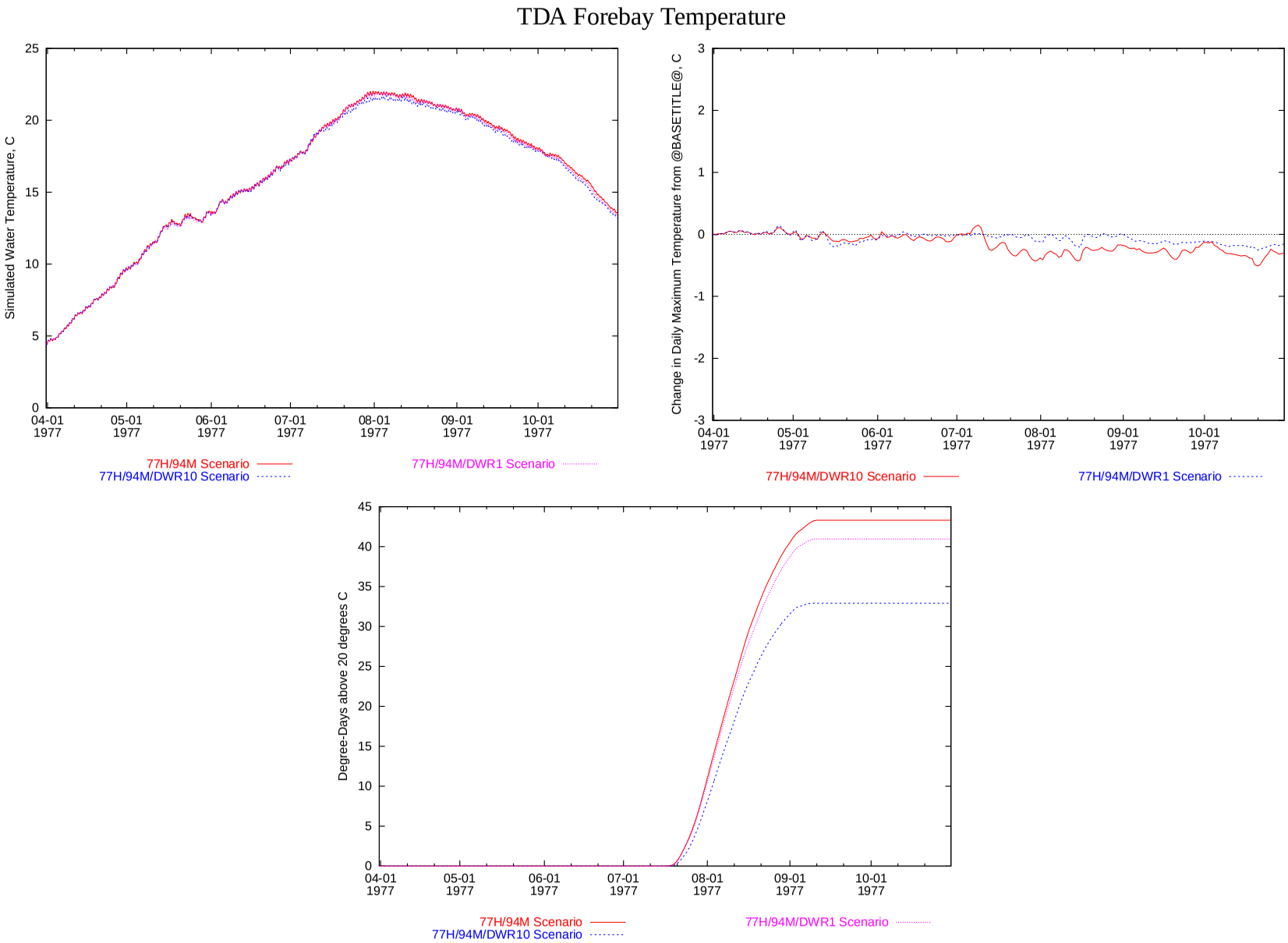

Figure 89: Time series comparison of simulated temperature at the TDA Forebay.

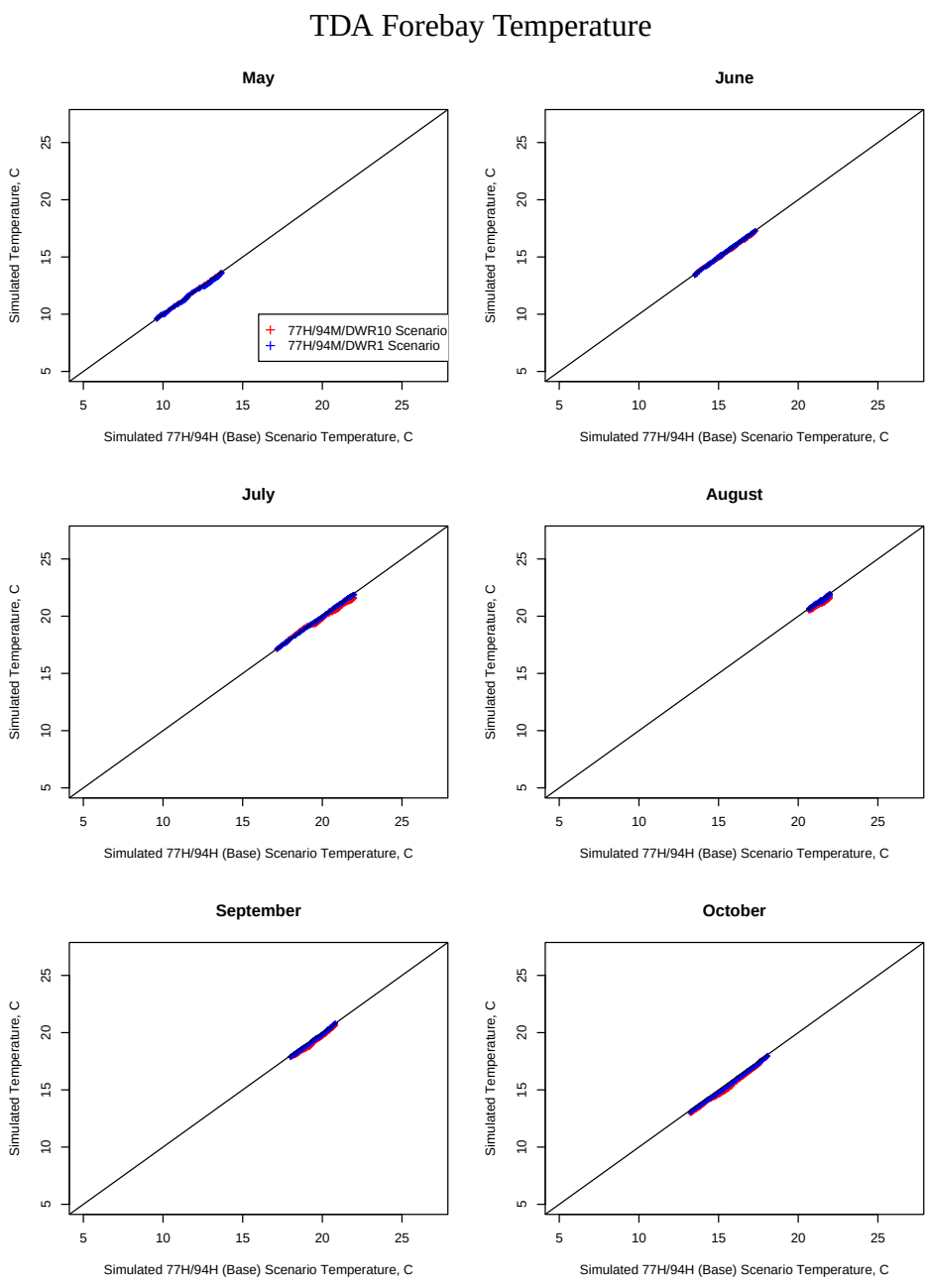

Figure 90: Scatter plot comparison, by month, of simulated temperature at the TDA Forebay.

TDA Forebay Temperature

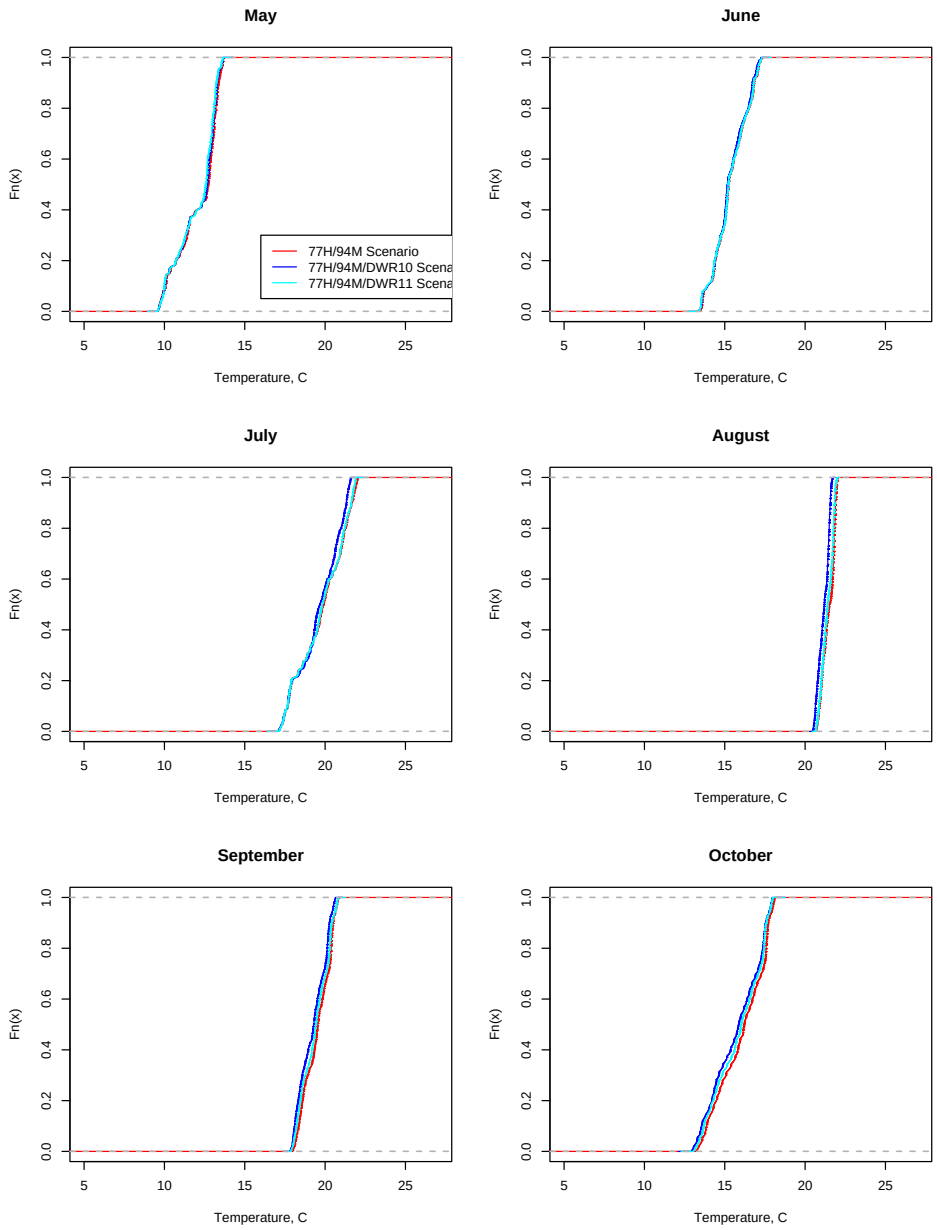

Figure 91: Cumulative frequency distribution (CFD) plot comparison, by month, of simulated temperature at the TDA Forebay.

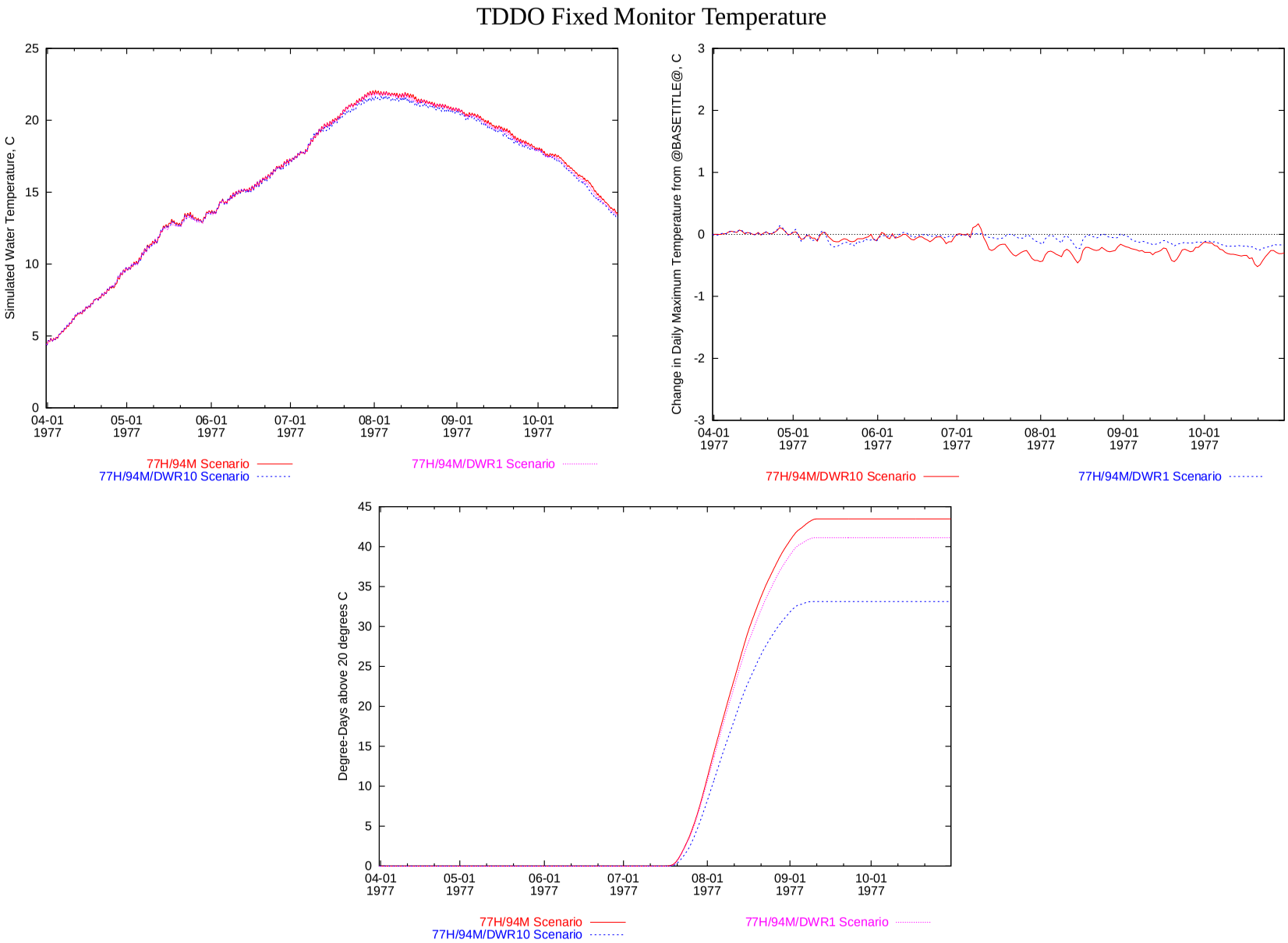

Figure 92: Time series comparison of simulated temperature at the TDDO Fixed Monitor.

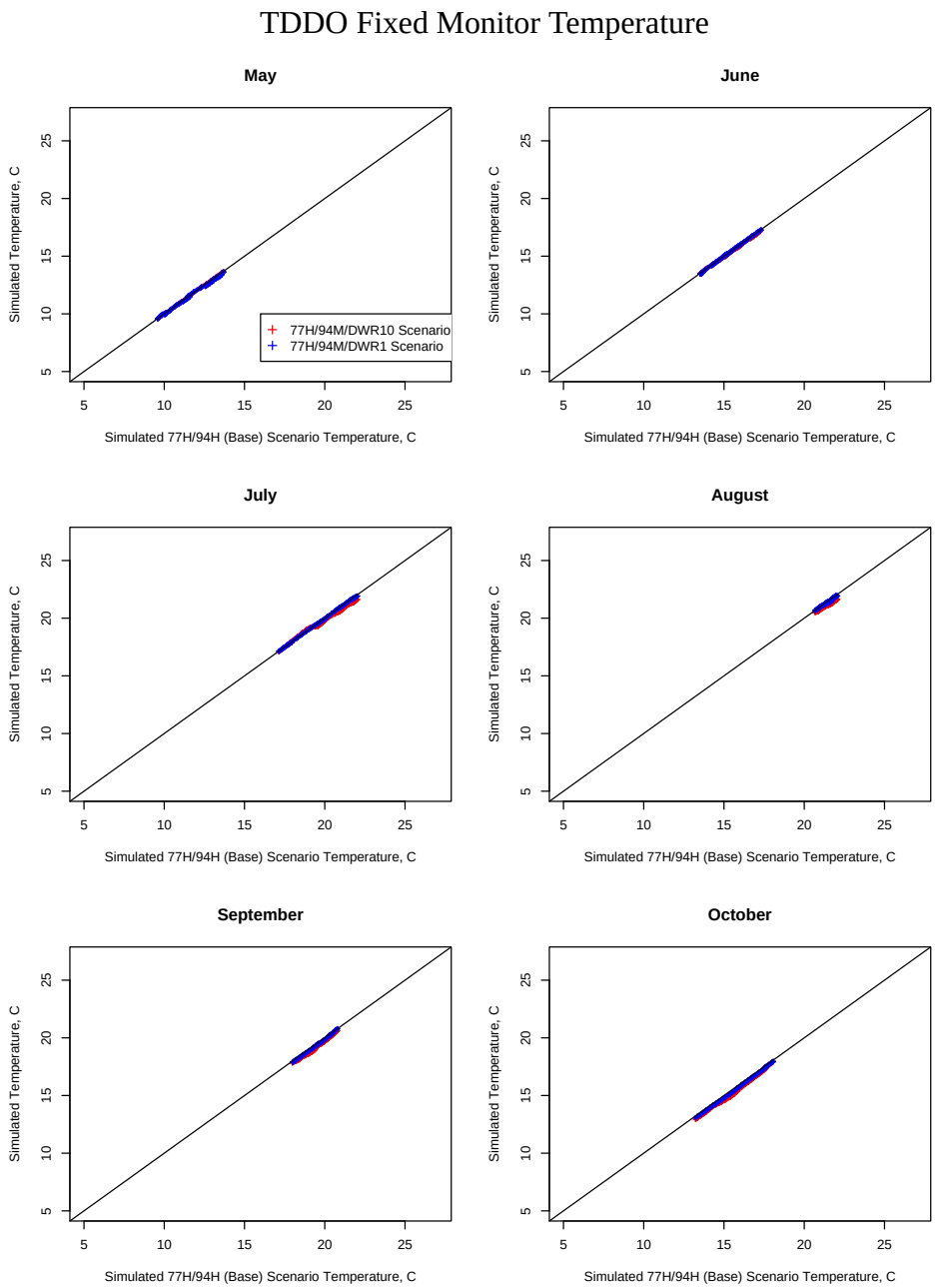

Figure 93: Scatter plot comparison, by month, of simulated temperature at the TDDO Fixed Monitor.

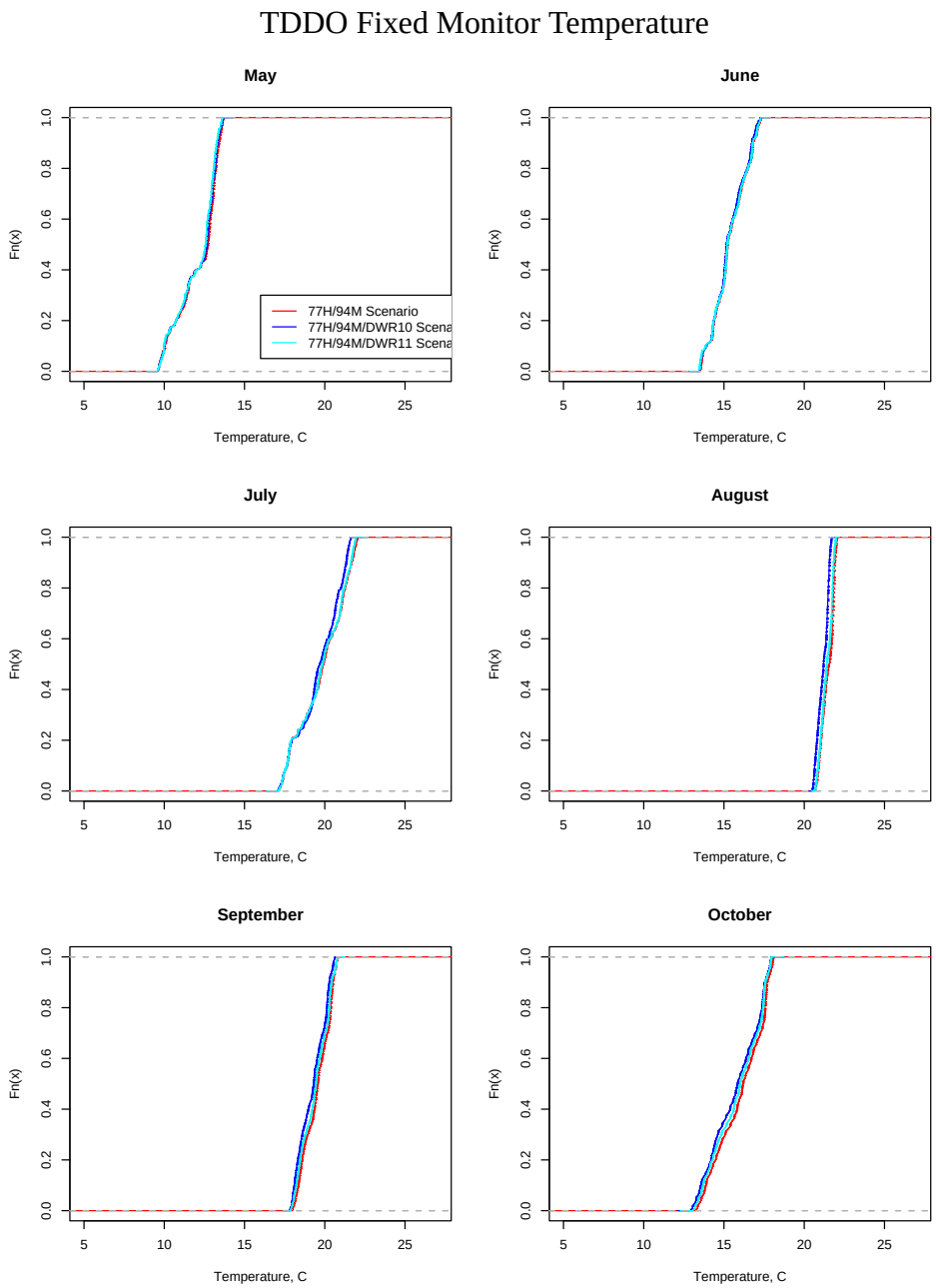

Figure 94: Cumulative frequency distribution (CFD) plot comparison, by month, of simulated temperature at the TDDO Fixed Monitor.

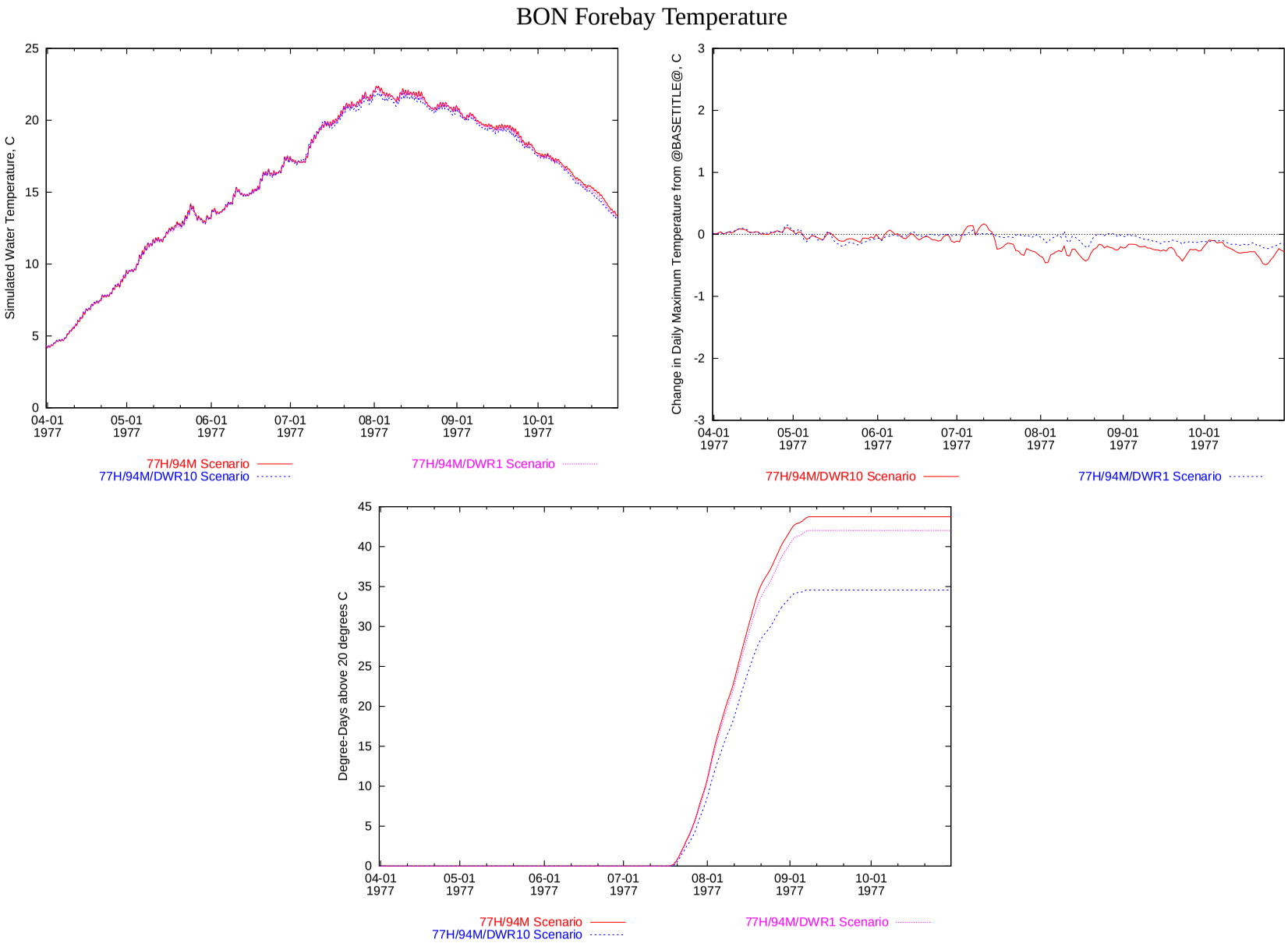

Figure 95: Time series comparison of simulated temperature at the BON Forebay.

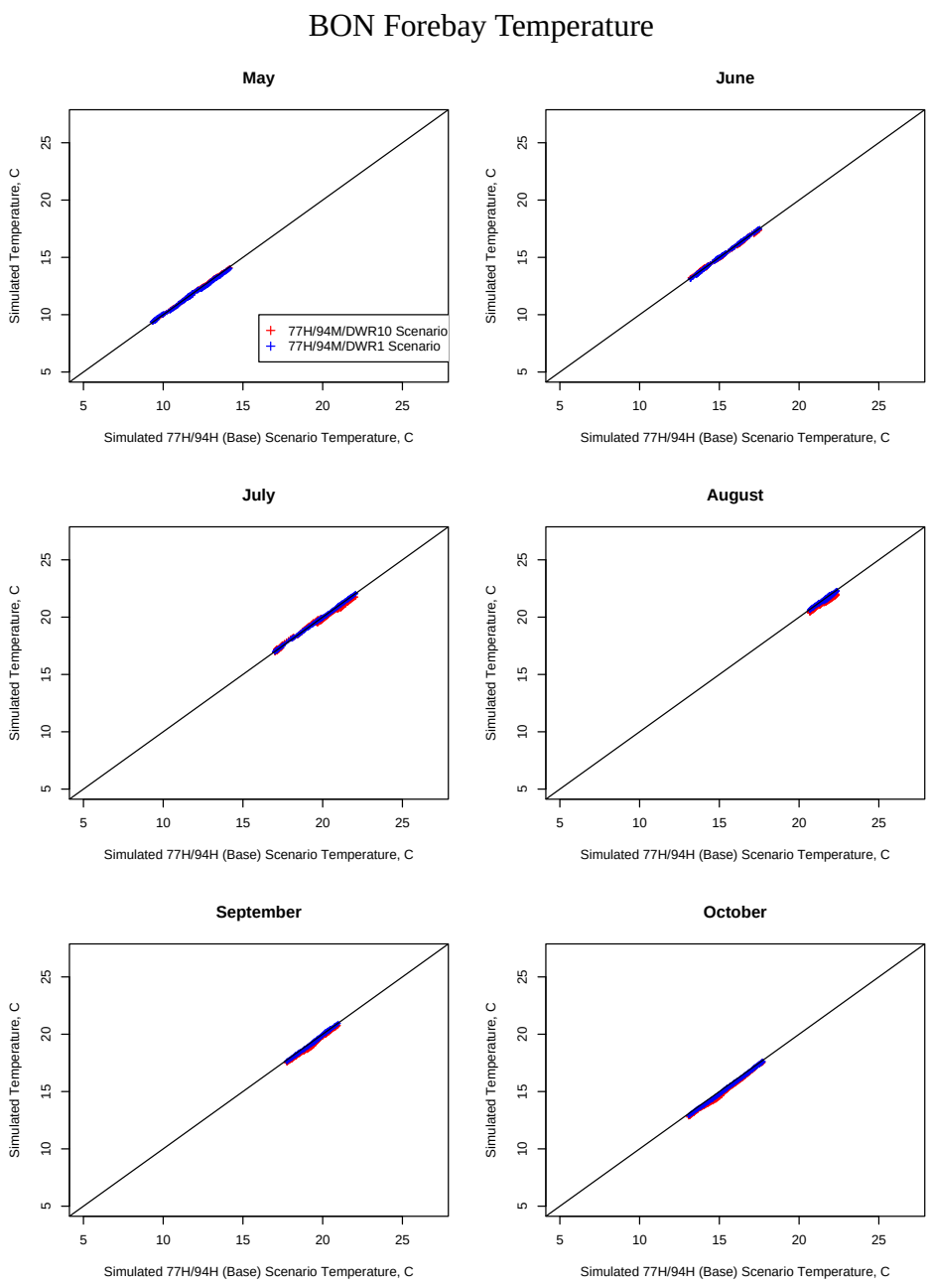

Figure 96: Scatter plot comparison, by month, of simulated temperature at the BON Forebay.

BON Forebay Temperature

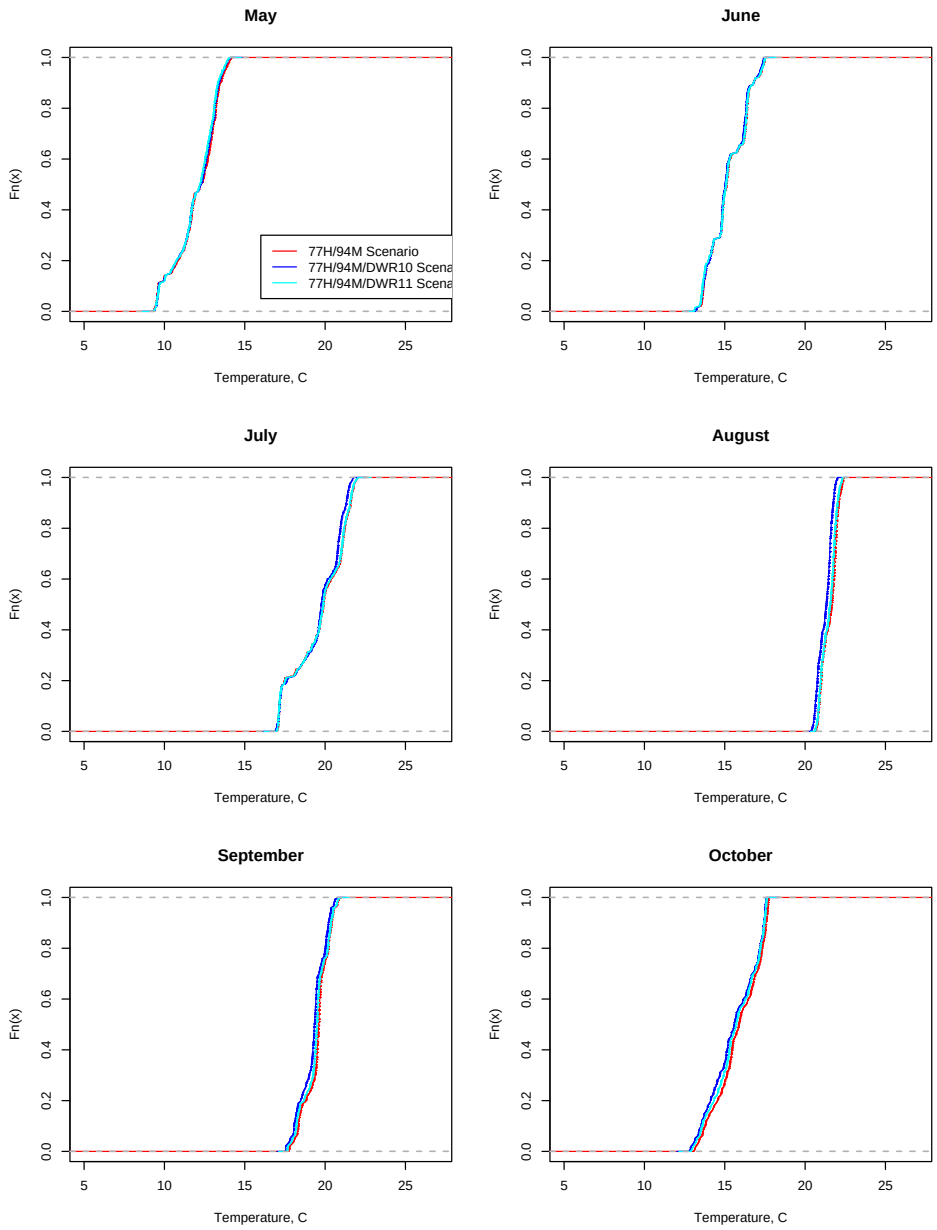

Figure 97: Cumulative frequency distribution (CFD) plot comparison, by month, of simulated temperature at the BON Forebay.

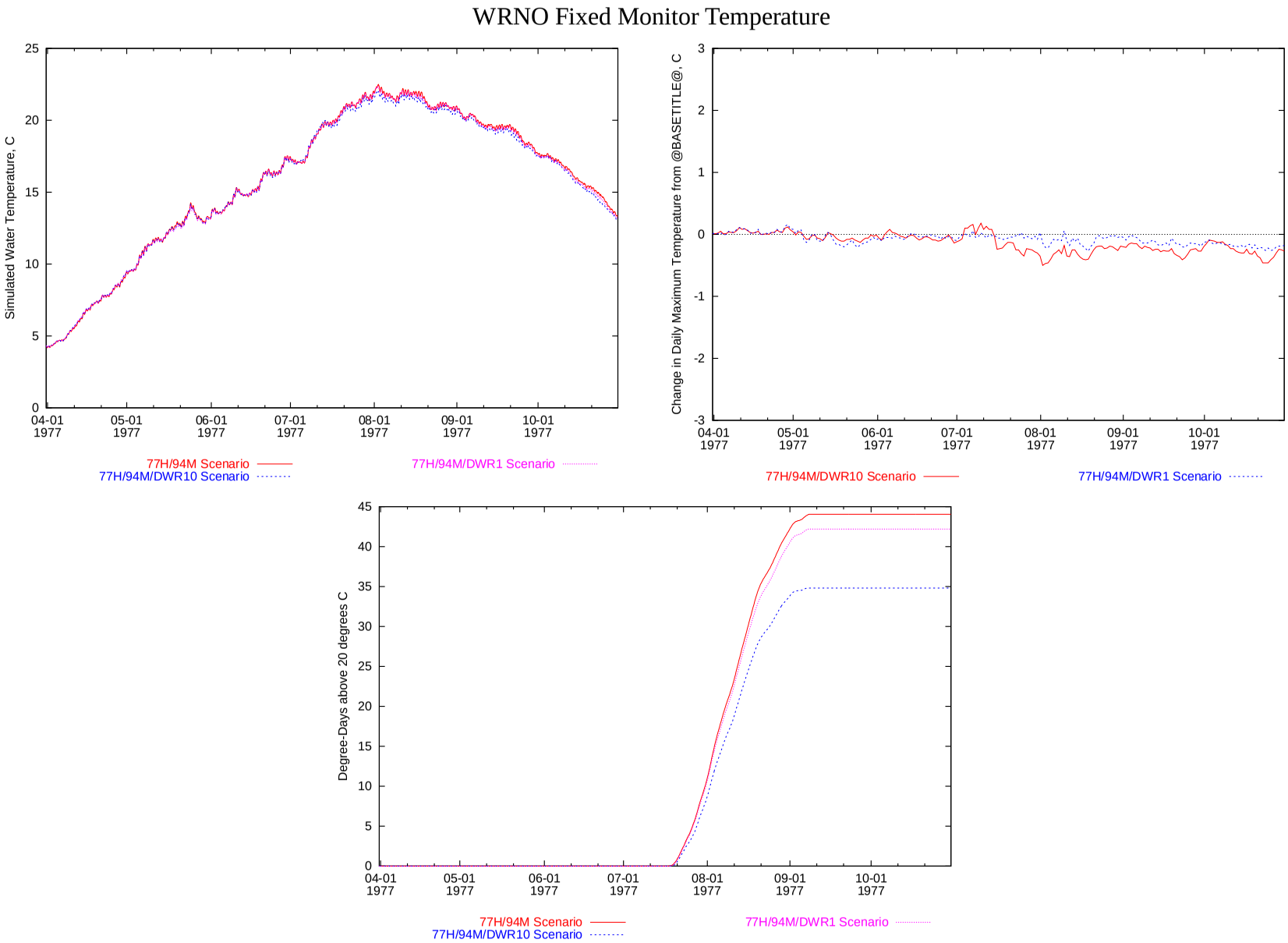

Figure 98: Time series comparison of simulated temperature at the WRNO Fixed Monitor.

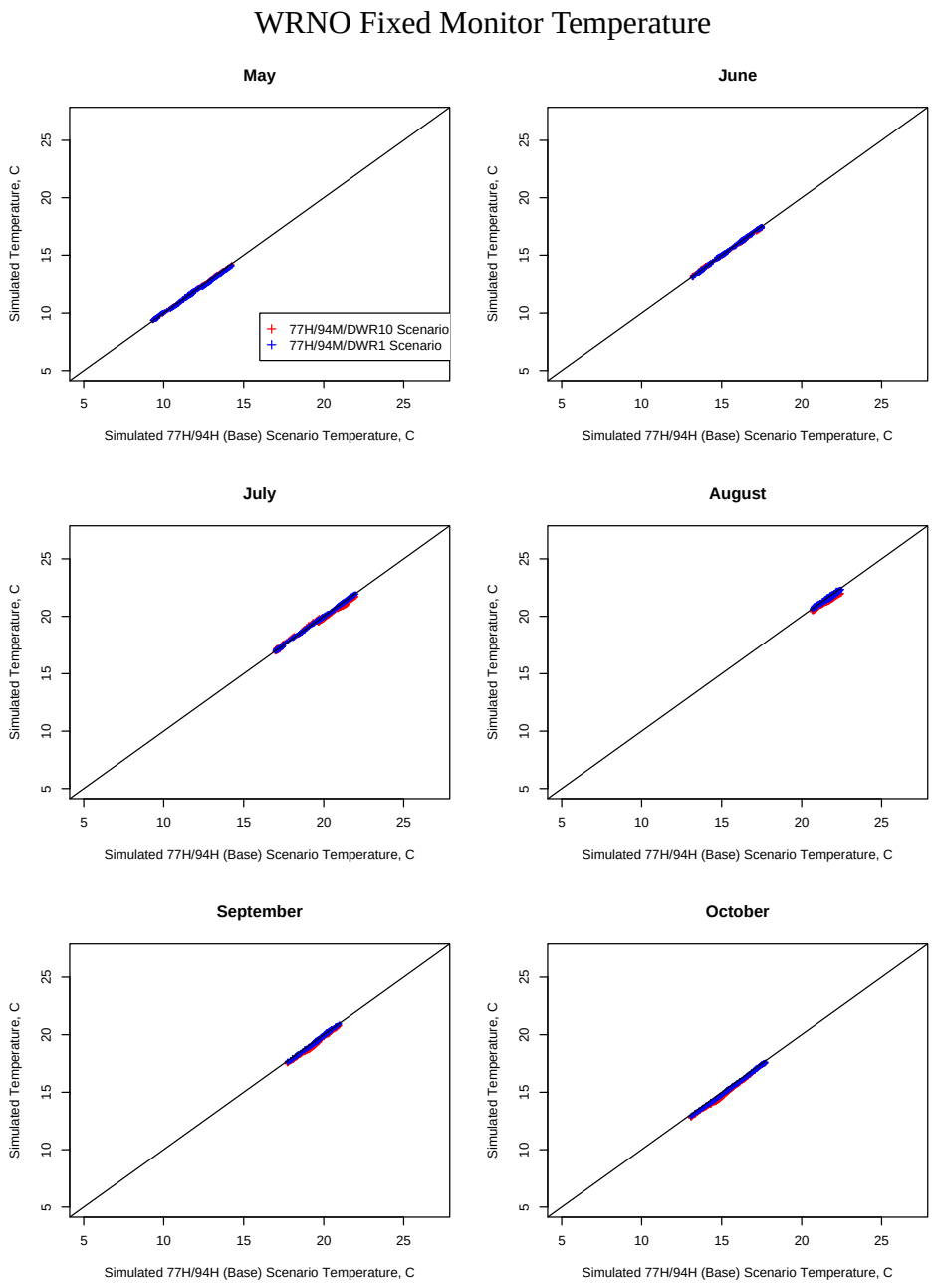

Figure 99: Scatter plot comparison, by month, of simulated temperature at the WRNO Fixed Monitor.

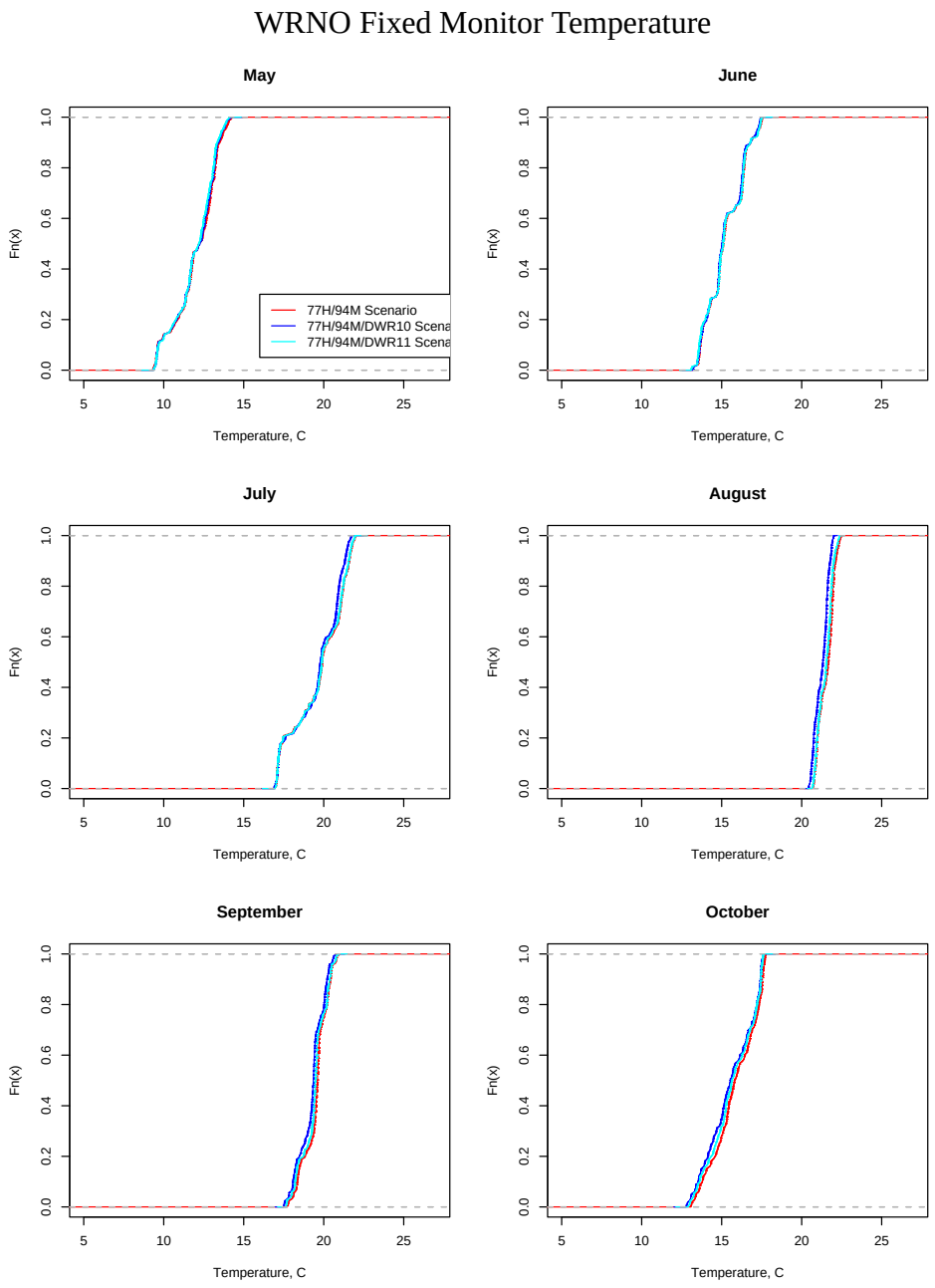

Figure 100: Cumulative frequency distribution (CFD) plot comparison, by month, of simulated temperature at the WRNO Fixed Monitor.

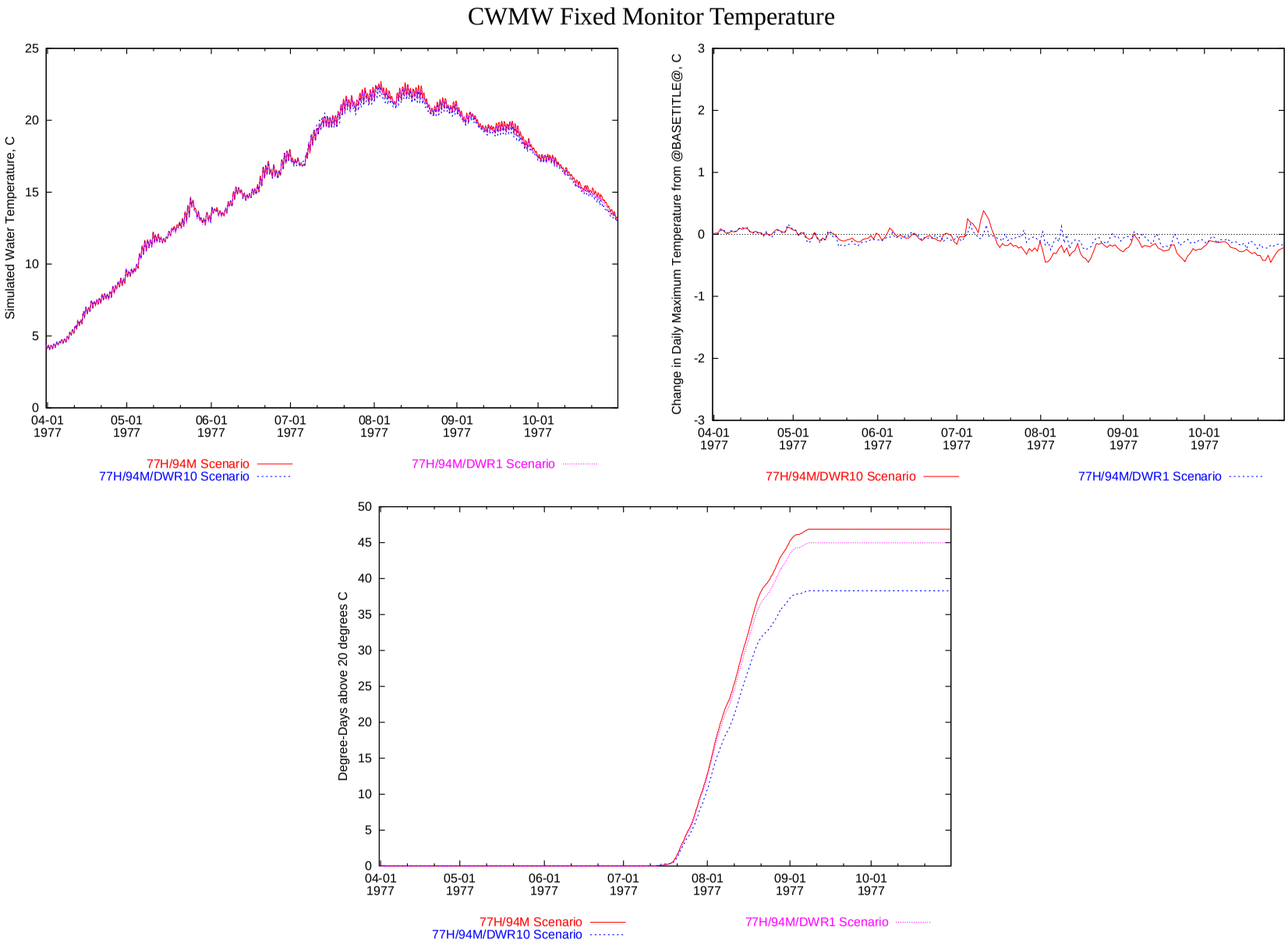

Figure 101: Time series comparison of simulated temperature at the CWMW Fixed Monitor.

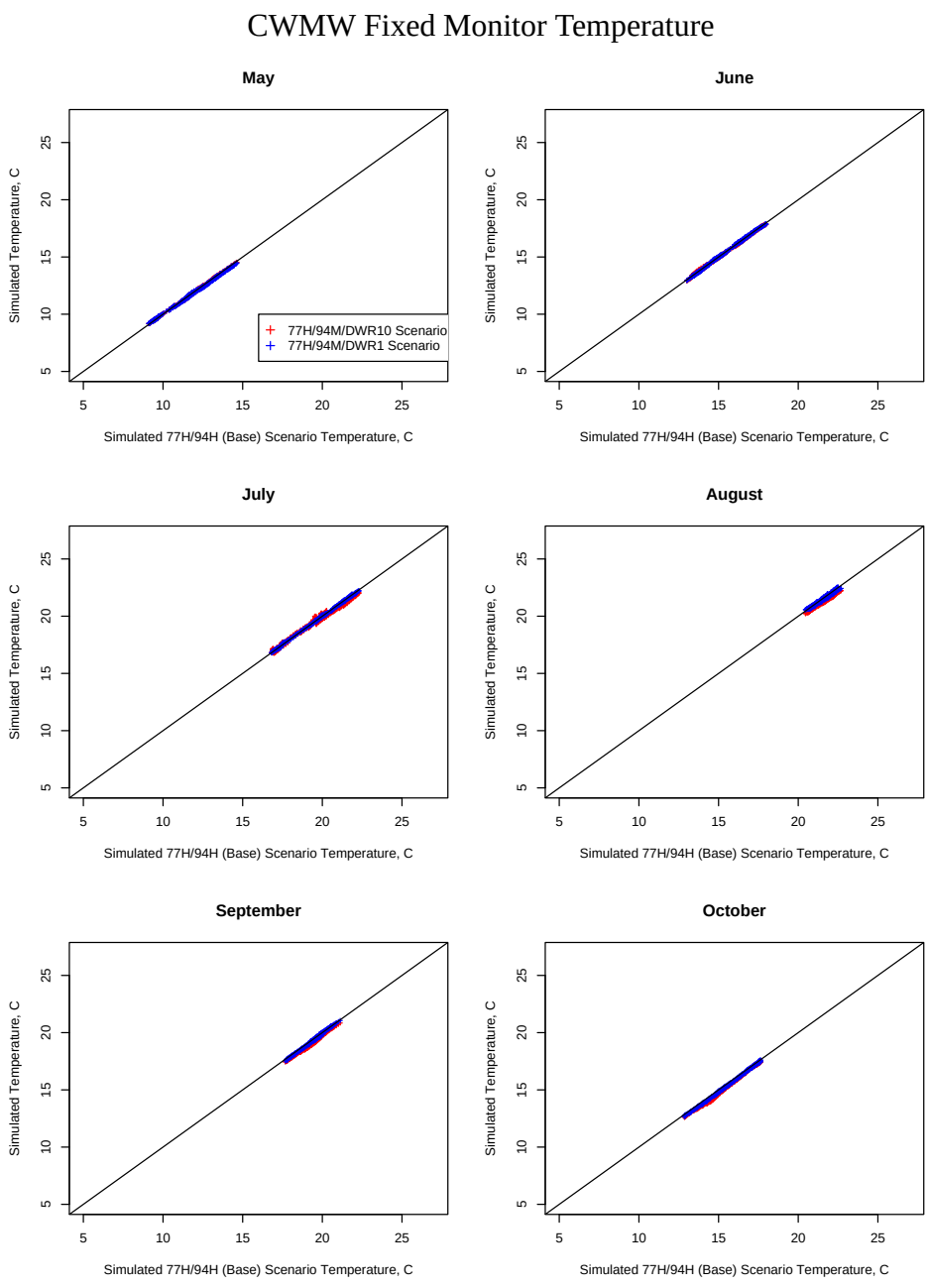

Figure 102: Scatter plot comparison, by month, of simulated temperature at the CWMW Fixed Monitor.

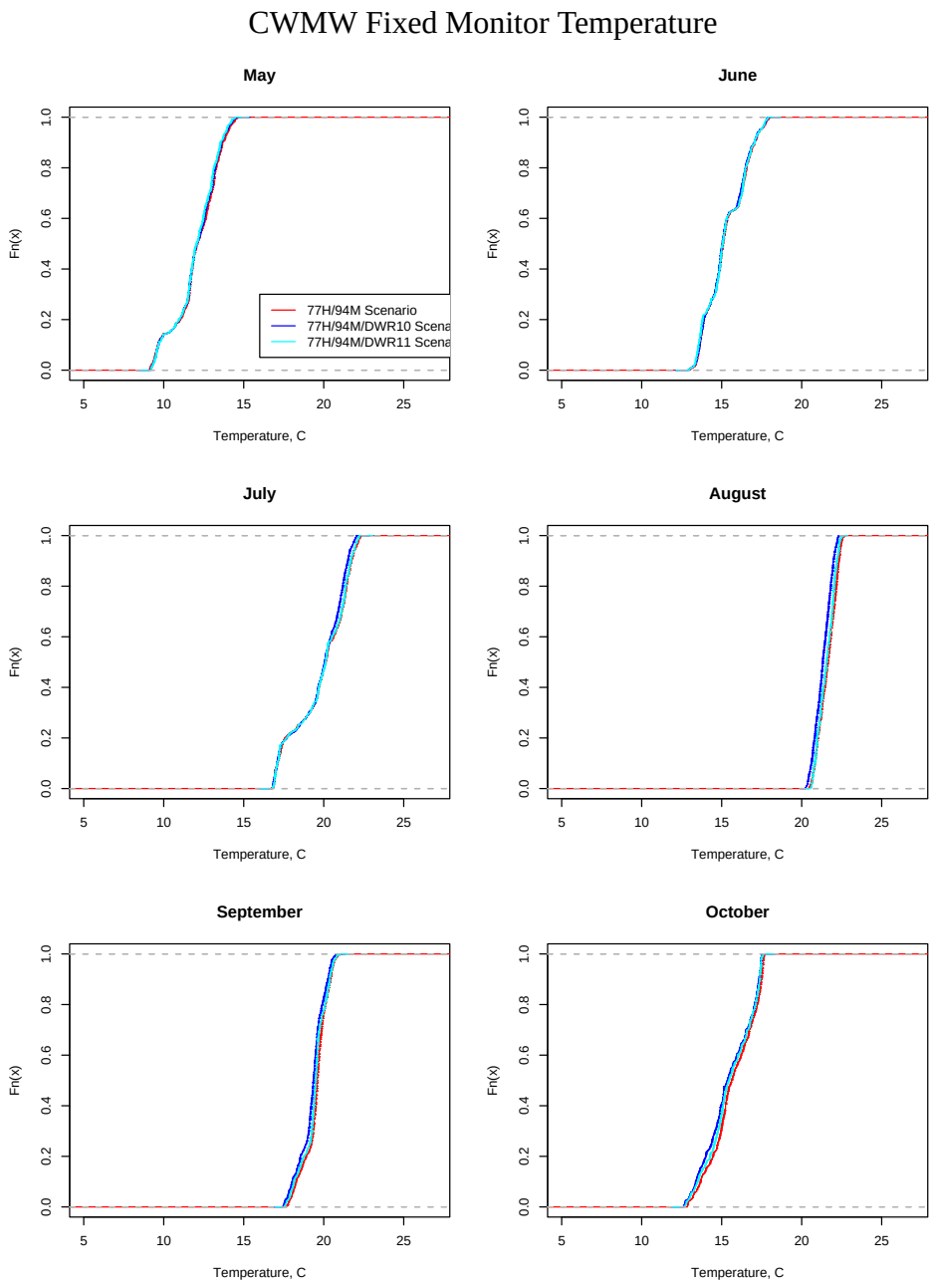

Figure 103: Cumulative frequency distribution (CFD) plot comparison, by month, of simulated temperature at the CWMW Fixed Monitor.

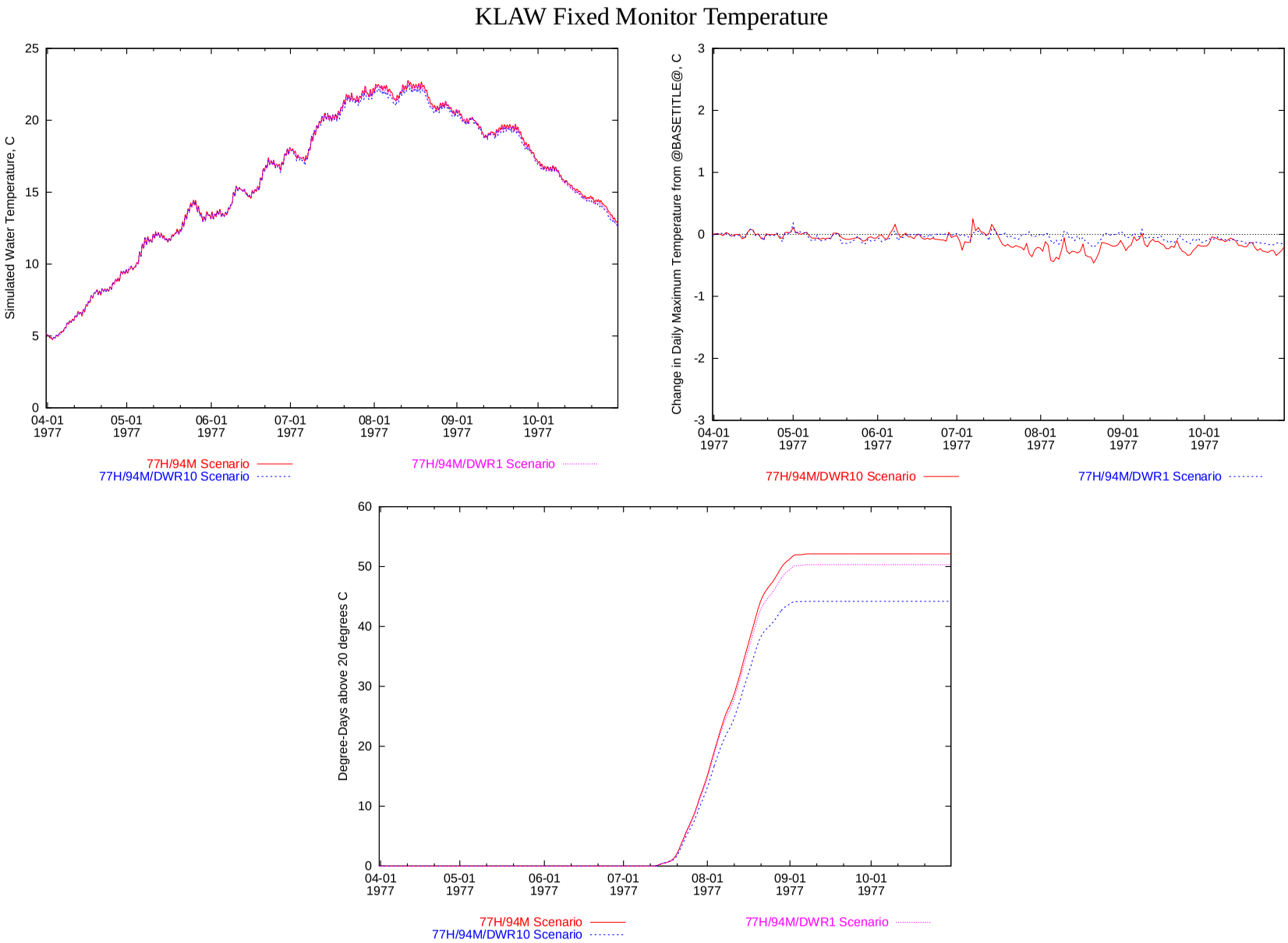

Figure 104: Time series comparison of simulated temperature at the KLAW Fixed Monitor.

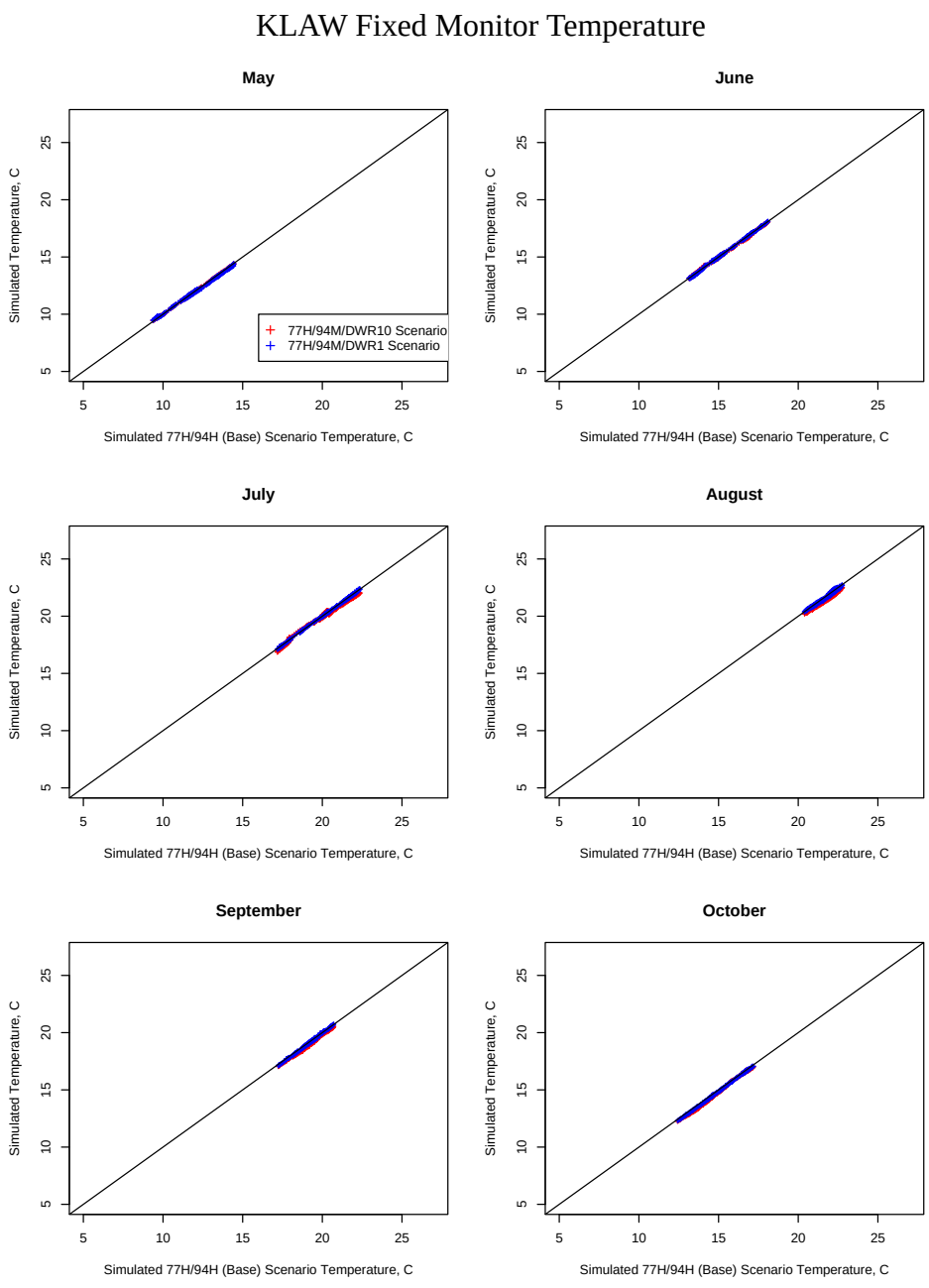

Figure 105: Scatter plot comparison, by month, of simulated temperature at the KLAW Fixed Monitor.

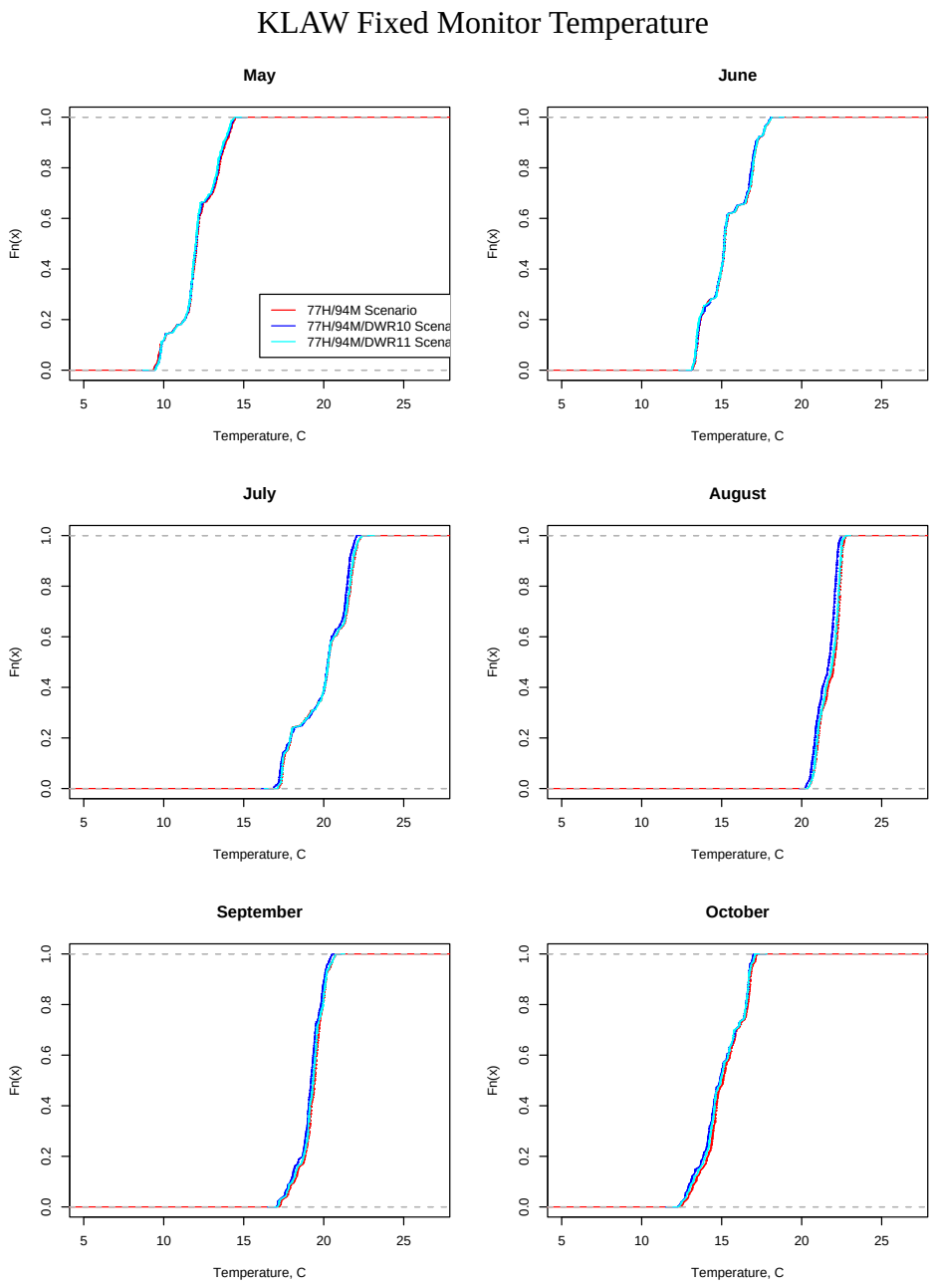

Figure 106: Cumulative frequency distribution (CFD) plot comparison, by month, of simulated temperature at the KLAW Fixed Monitor.

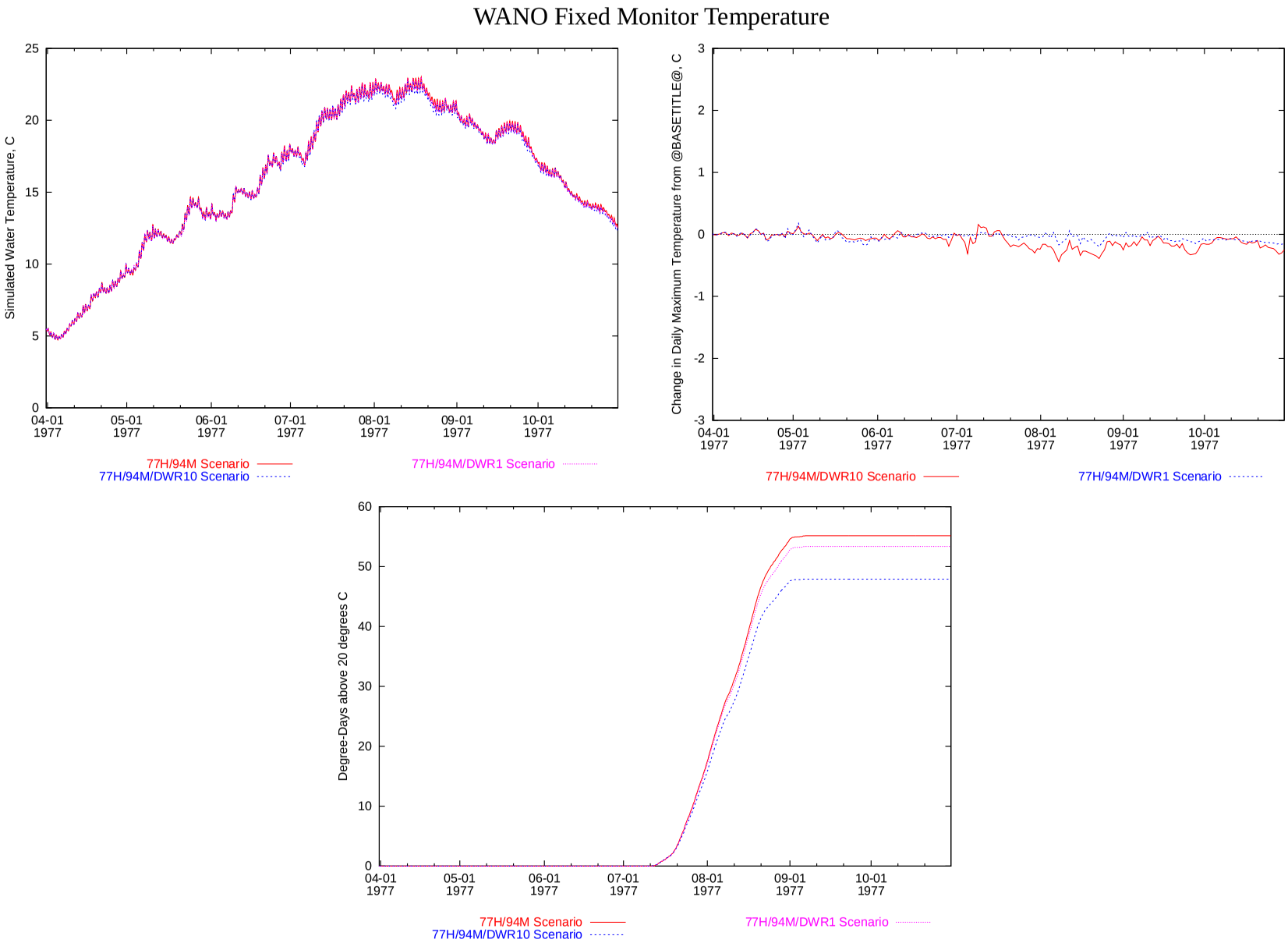

Figure 107: Time series comparison of simulated temperature at the WANO Fixed Monitor.

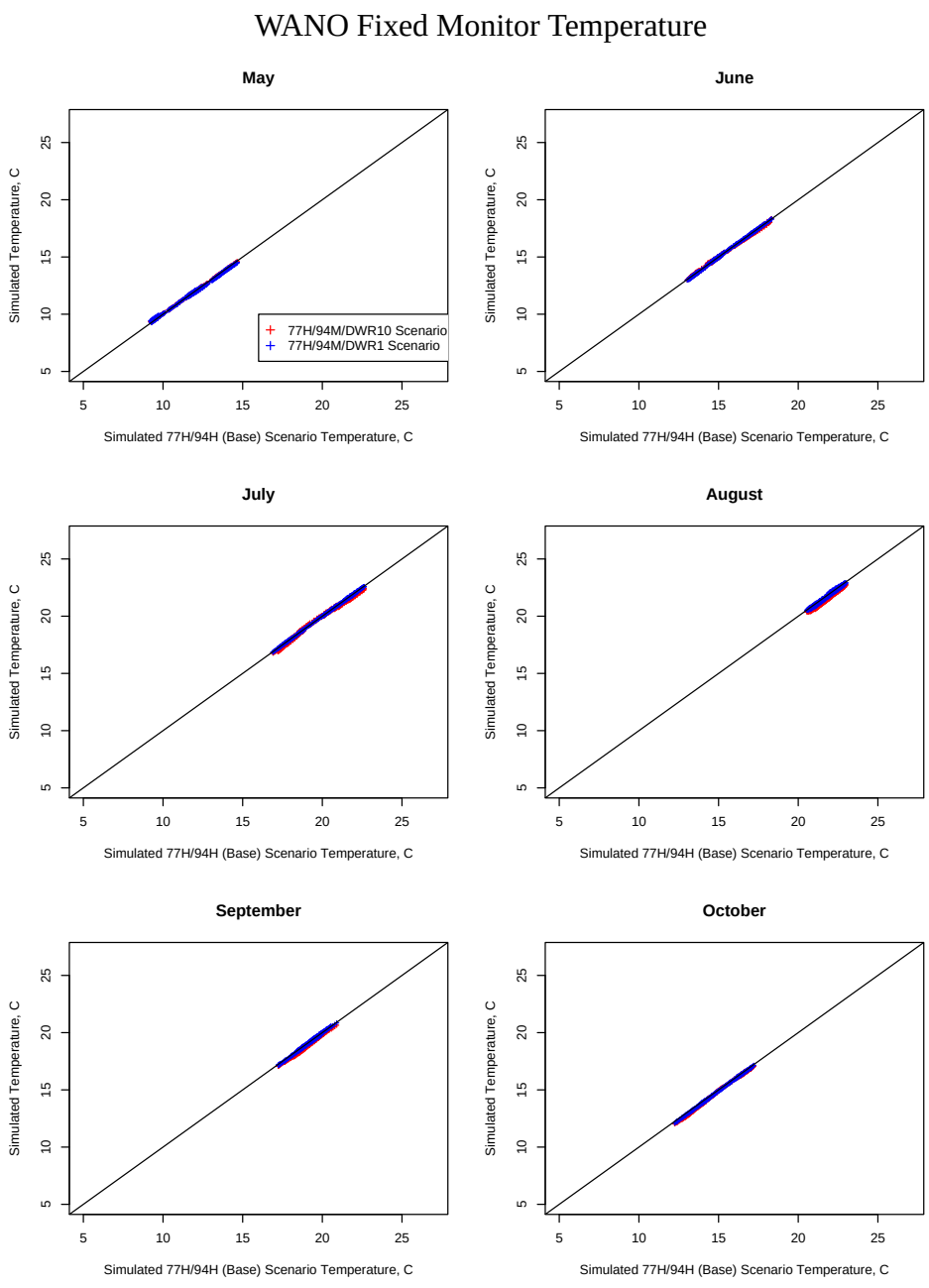

Figure 108: Scatter plot comparison, by month, of simulated temperature at the WANO Fixed Monitor.

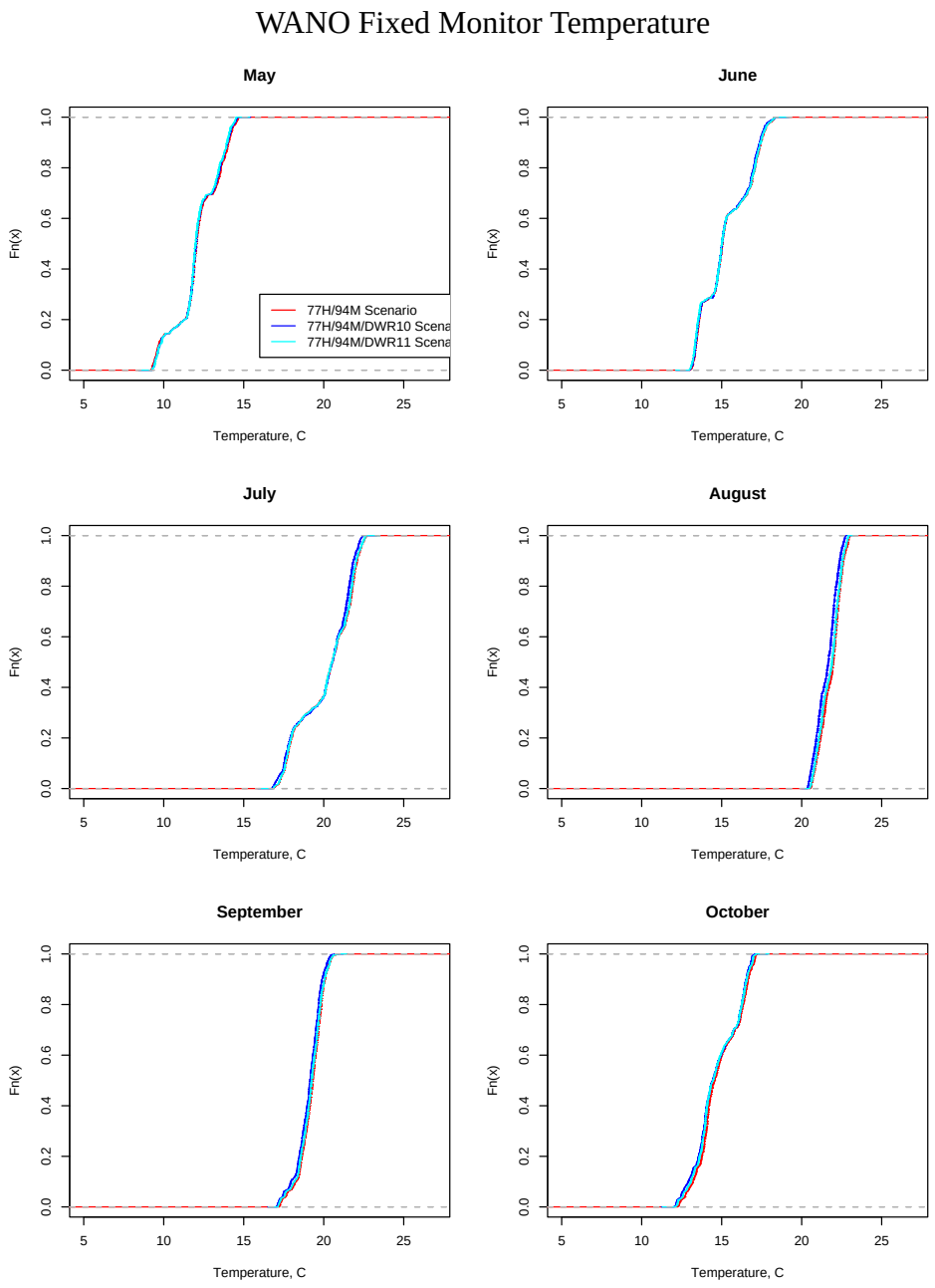

Figure 109: Cumulative frequency distribution (CFD) plot comparison, by month, of simulated temperature at the WANO Fixed Monitor.

6 Scenario Discharge Comparisons

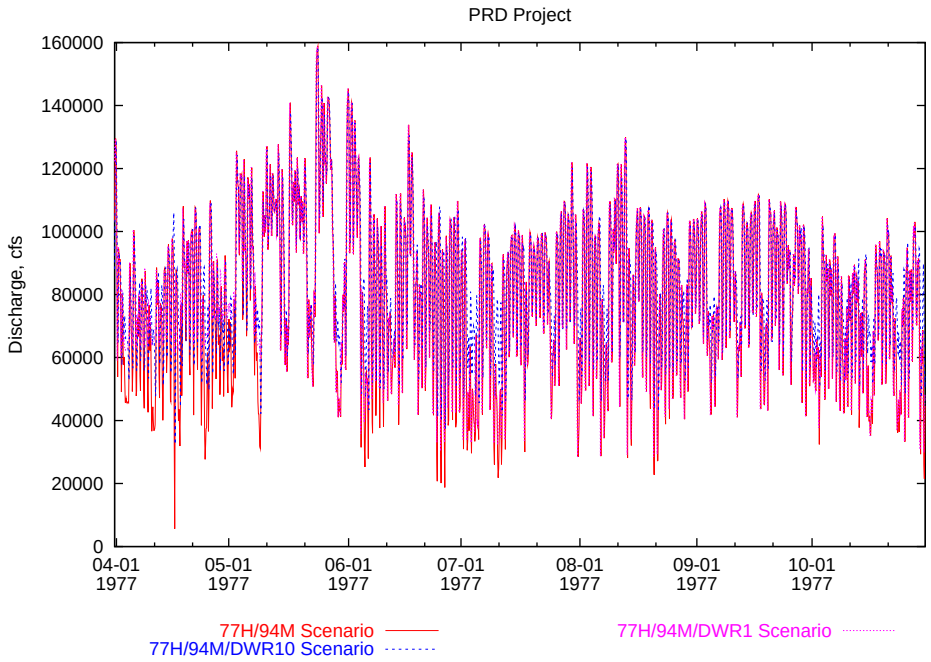

Figure 110: Comparison of simulated discharge at the PRD Project.

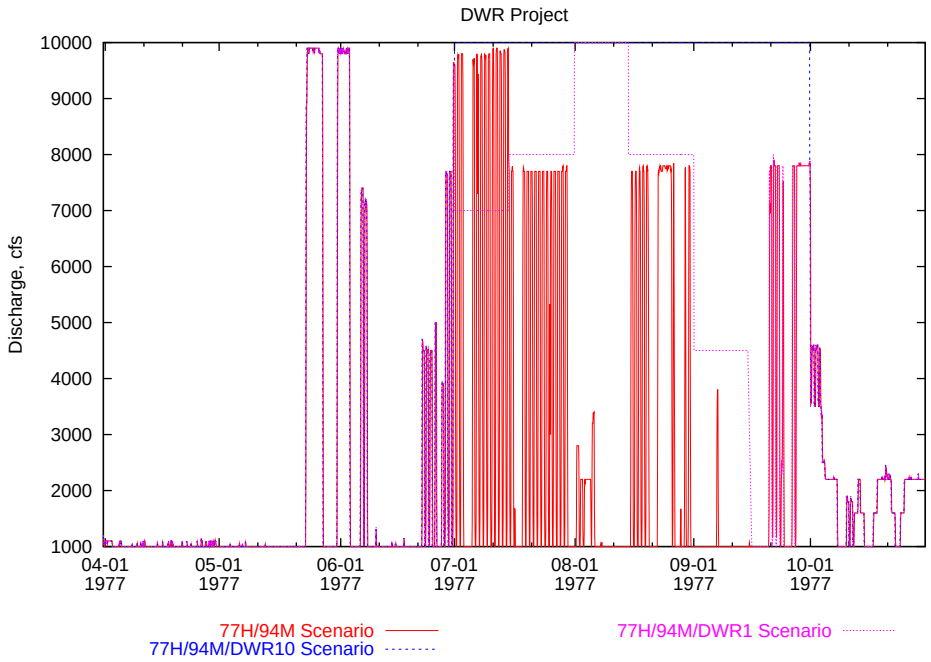

Figure 111: Comparison of simulated discharge at the DWR Project.

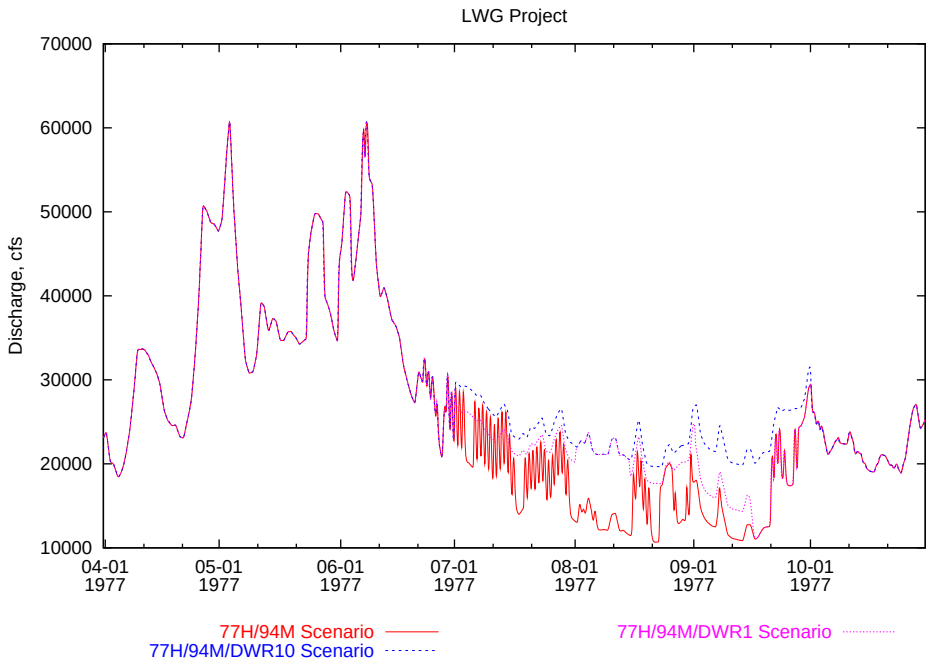

Figure 112: Comparison of simulated discharge at the LWG Project.

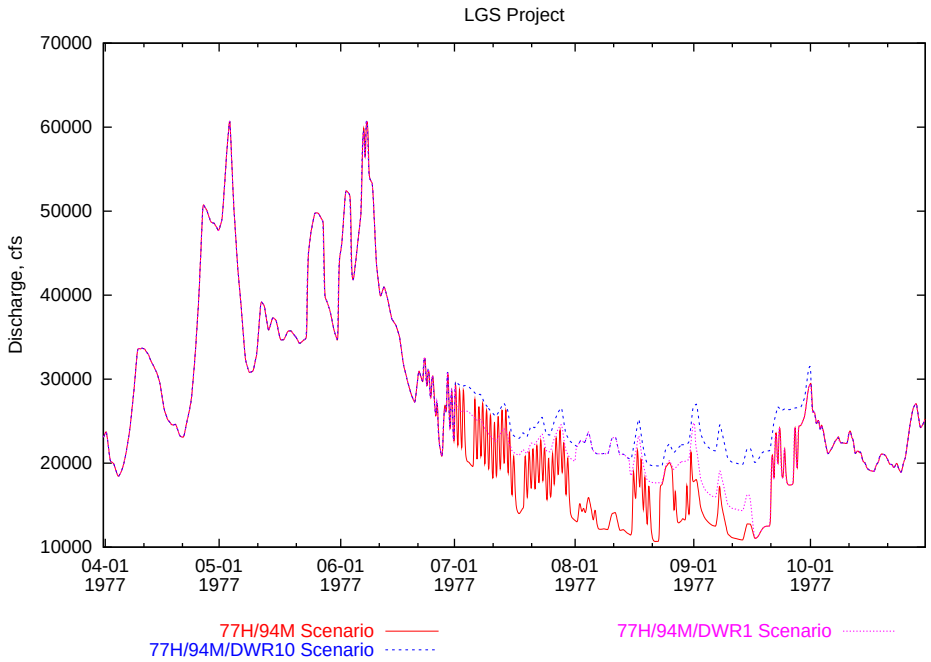

Figure 113: Comparison of simulated discharge at the LGS Project.

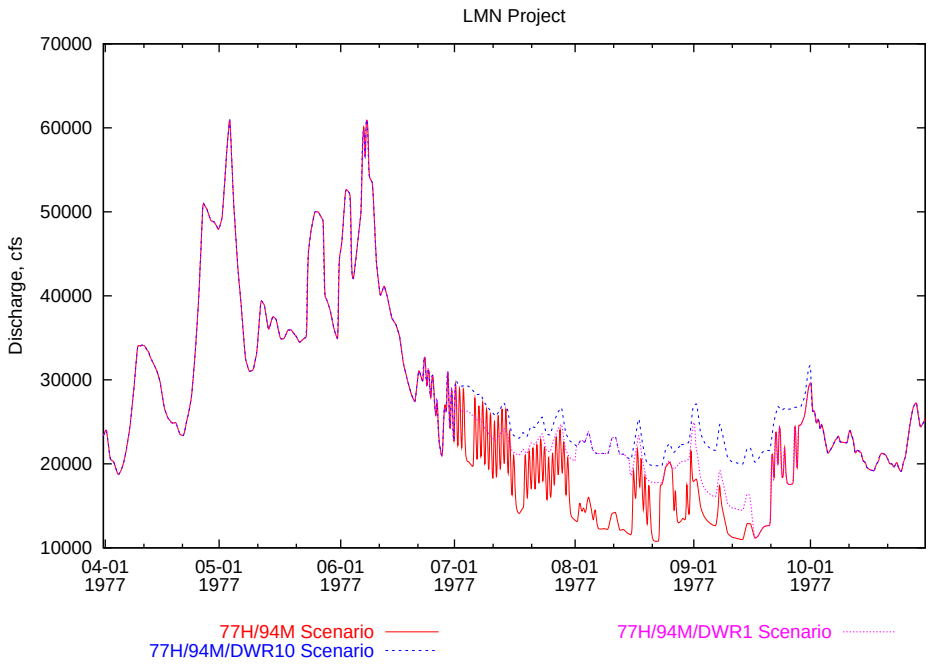

Figure 114: Comparison of simulated discharge at the LMN Project.

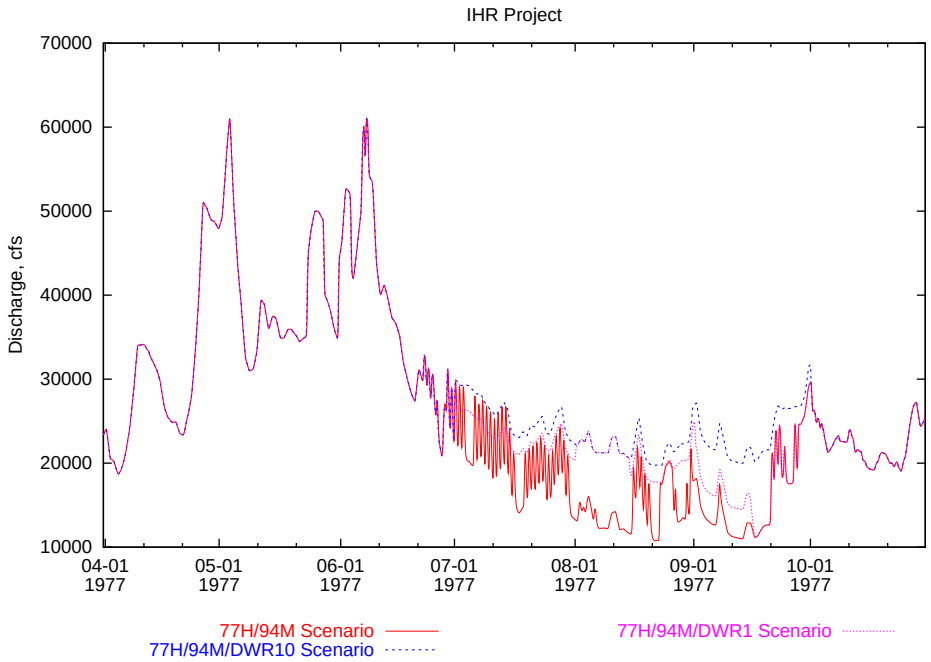

Figure 115: Comparison of simulated discharge at the IHR Project.

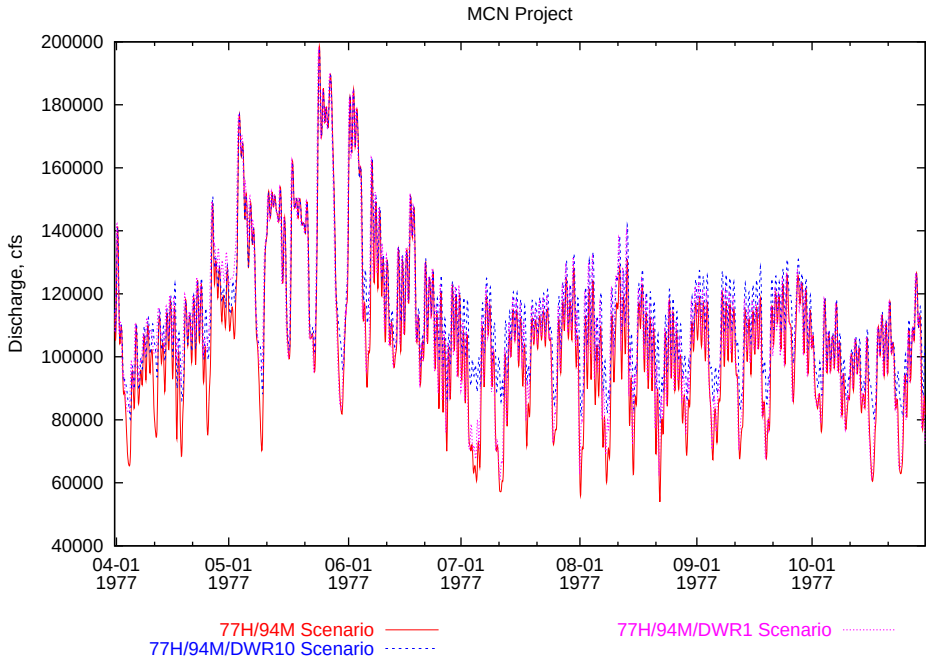

Figure 116: Comparison of simulated discharge at the MCN Project.

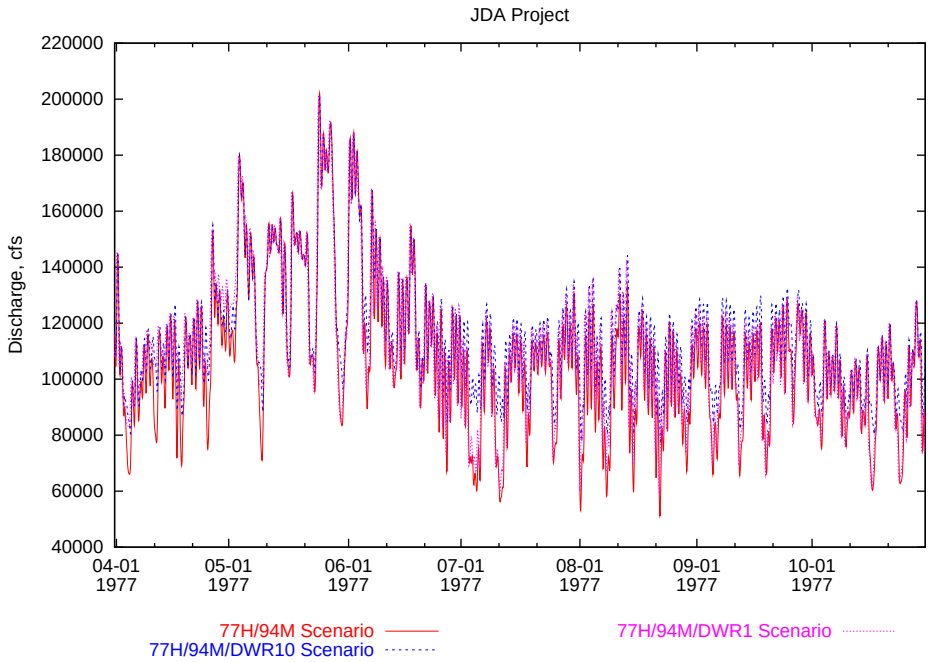

Figure 117: Comparison of simulated discharge at the JDA Project.

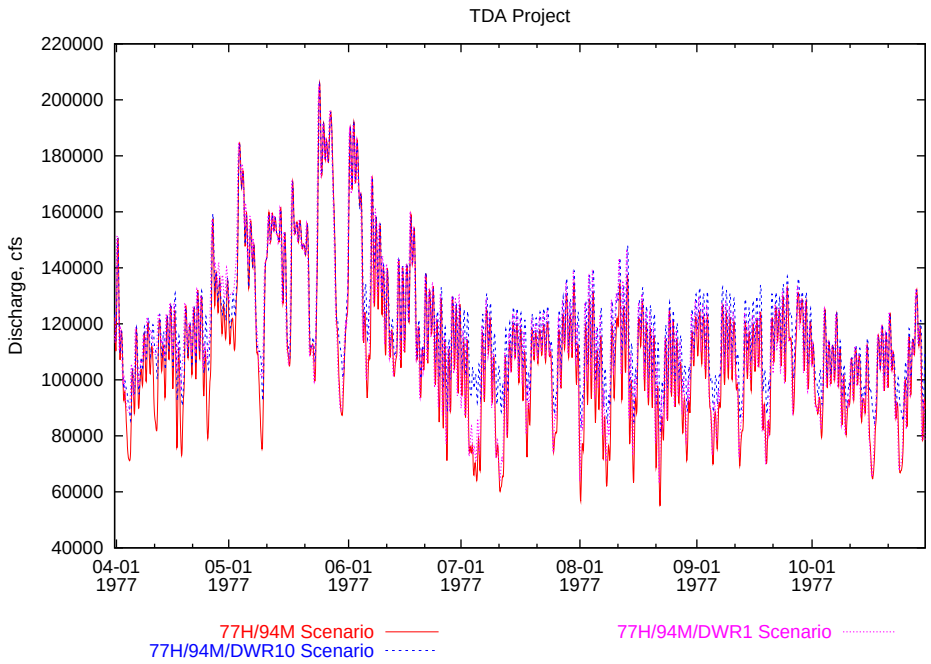

Figure 118: Comparison of simulated discharge at the TDA Project.

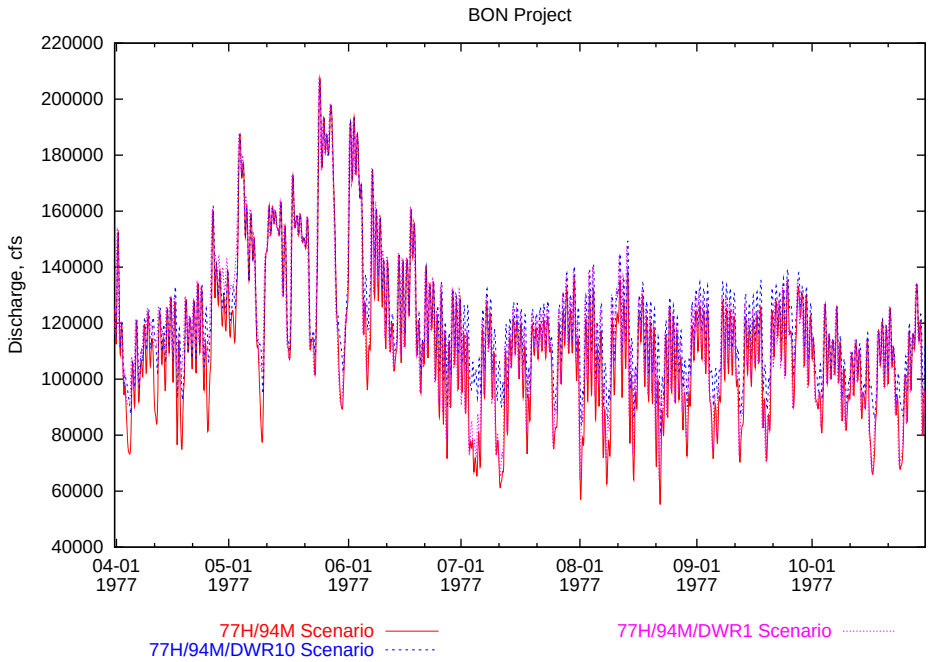

Figure 119: Comparison of simulated discharge at the BON Project.

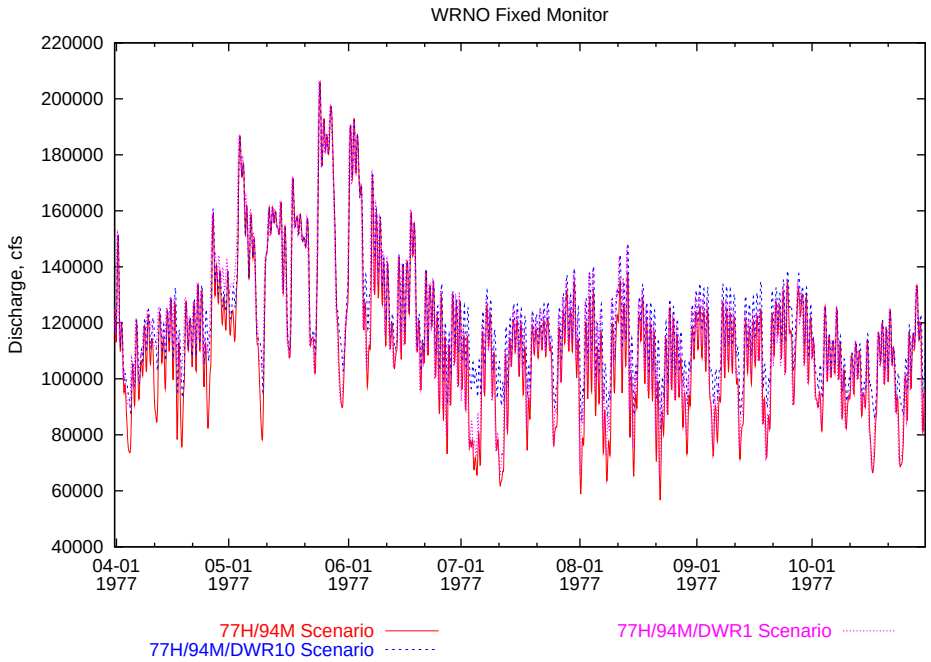

Figure 120: Comparison of simulated discharge at the WRNO Fixed Monitor.

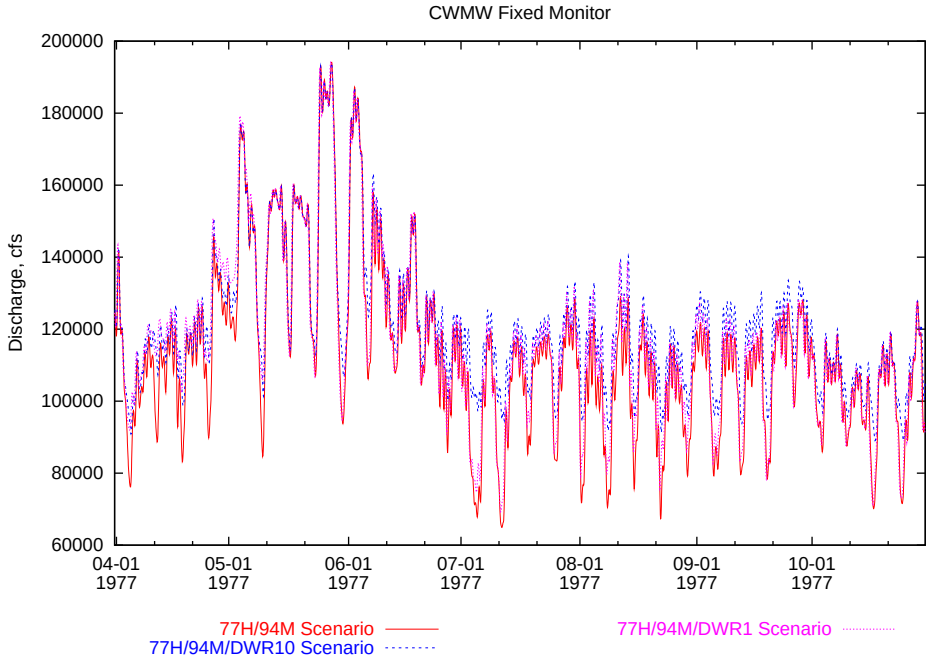

Figure 121: Comparison of simulated discharge at the CWMW Fixed Monitor.

A Estimation of Clearwater Main Stem Temperature

In the 1997 conditions and 77H/94M scenarios, water temperatures for the Clearwater main stem at Orofino and the North Fork Clearwater at Dworshak are assumed to be that observed at the USGS Spaulding gage downstream. This is acceptable since observed flows were used at both of those model boundaries.

In other scenarios, the flows used at the Dworshak model boundary differ from observed, and temperatures are synthetic, so that using the Spaulding temperatures at the Orofino boundary is not acceptable. In these scenarios, a temperature record is estimated for the Clearwater main stem at Orofino using the temperatures from the USGS gage on the North Fork of the Clearwater near Canyon Ranger station (13340600). The Canyon Ranger station was in operation during 1977 and overlaps the Orofino record from 1993 to 1996 (data in hand).

A simple linear regression of daily means at these two station was performed. The results are shown in Figure 122. The developed relation is

$$T_{\text{Orofino}} = 1.1049 T_{\text{Canyon}} + 0.6110$$

The adjusted coefficient of determination (r^2) of this relation is 0.9876 and the standard error is 0.79°C. Clearwater main stem temperatures estimated for 1977 using the above relation are shown in Figure 123.

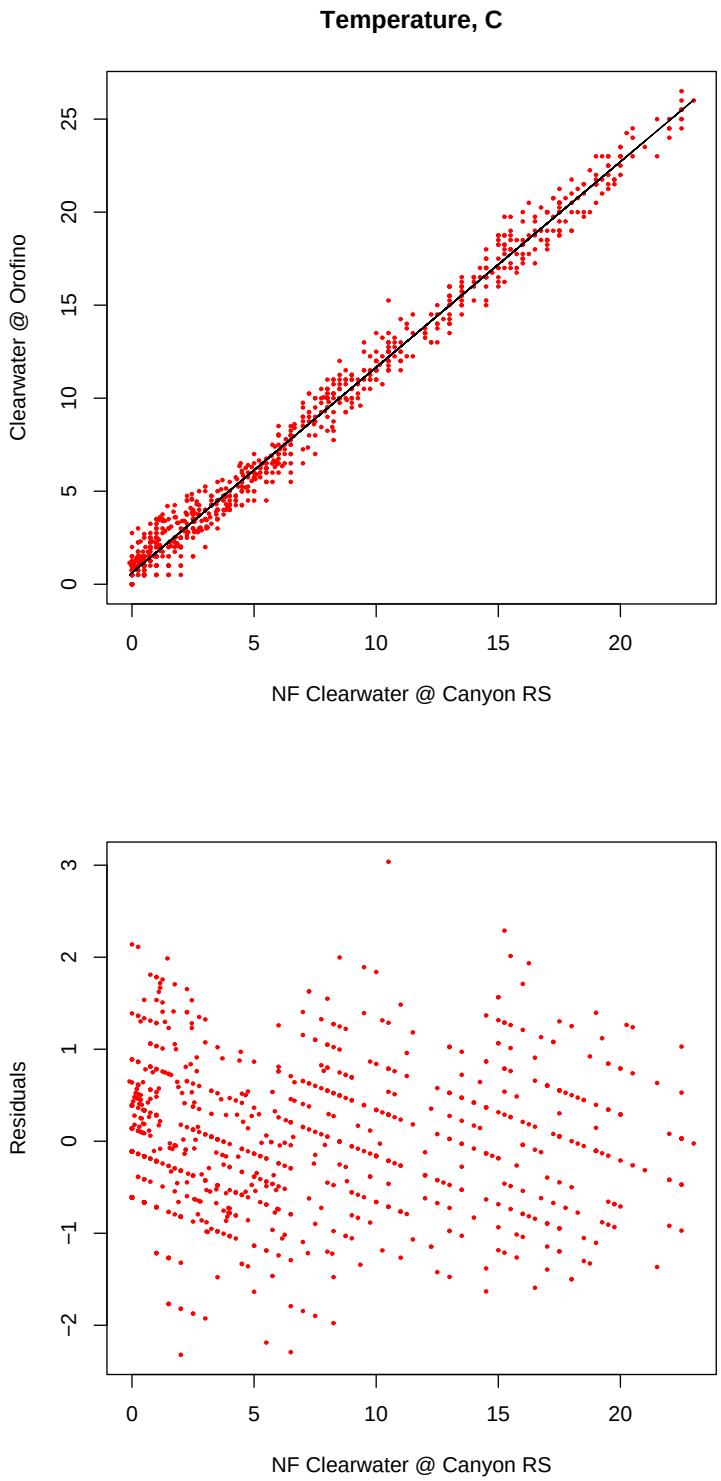

Figure 122: Linear regression estimating Clearwater main stem temperature from North Fork Clearwater temperatures.

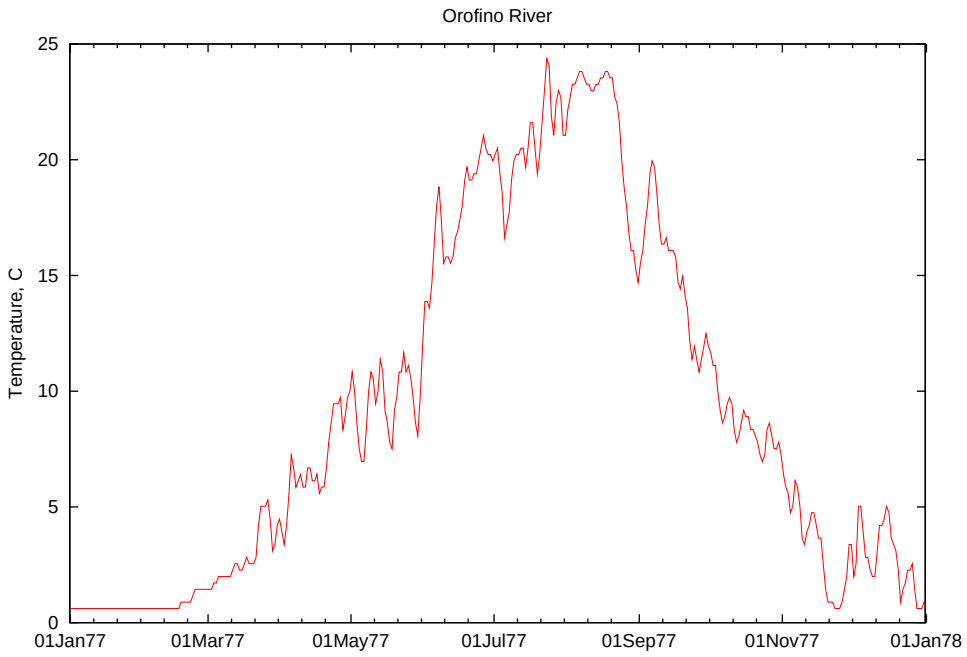

Figure 123: Estimated Clearwater main stem temperatures for 1977.

B Meterological Data

Hanford 1977 Meterology

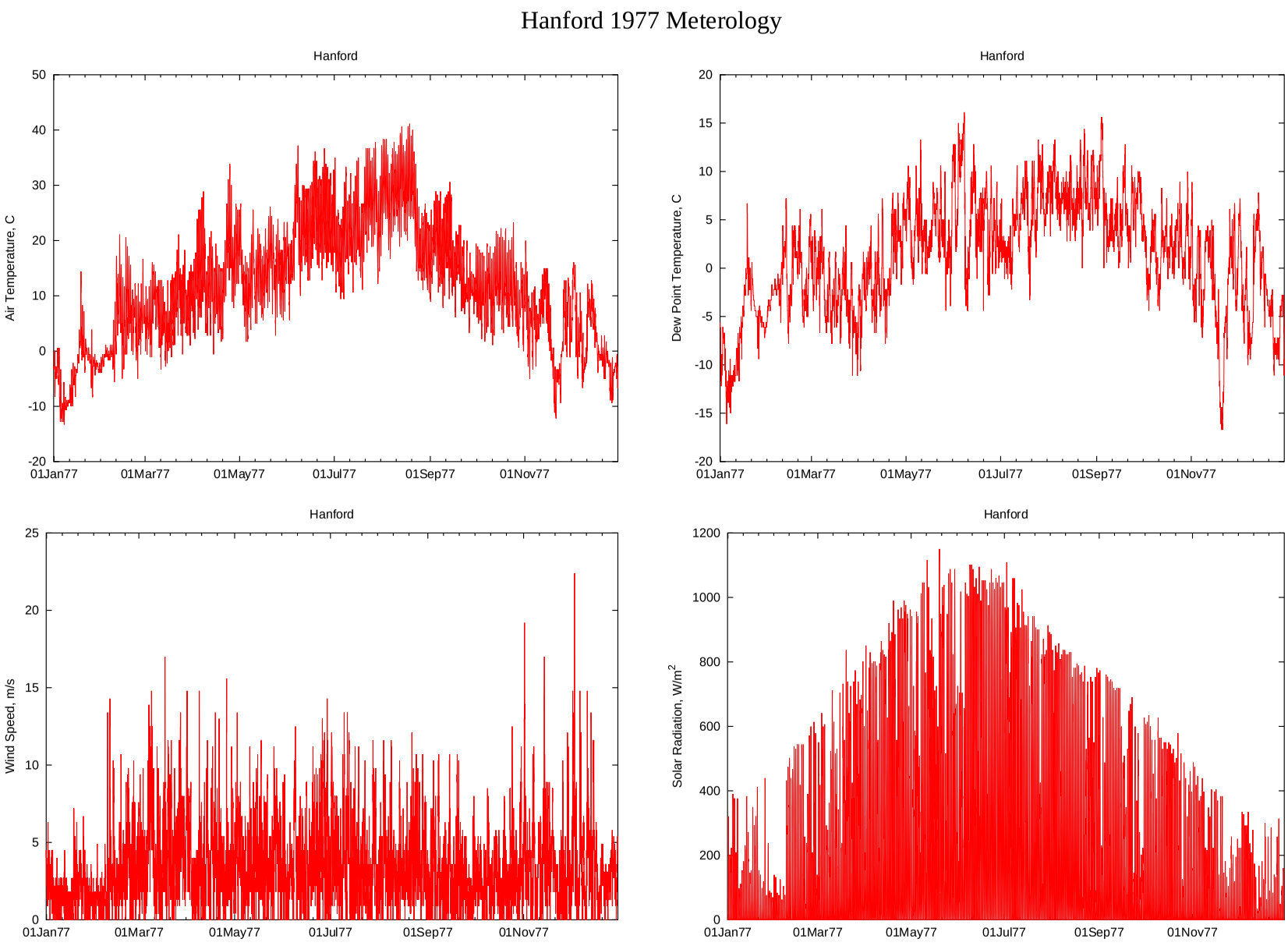

Figure 124: 1977 meterology data at Hanford.

Portland 1977 Meterology

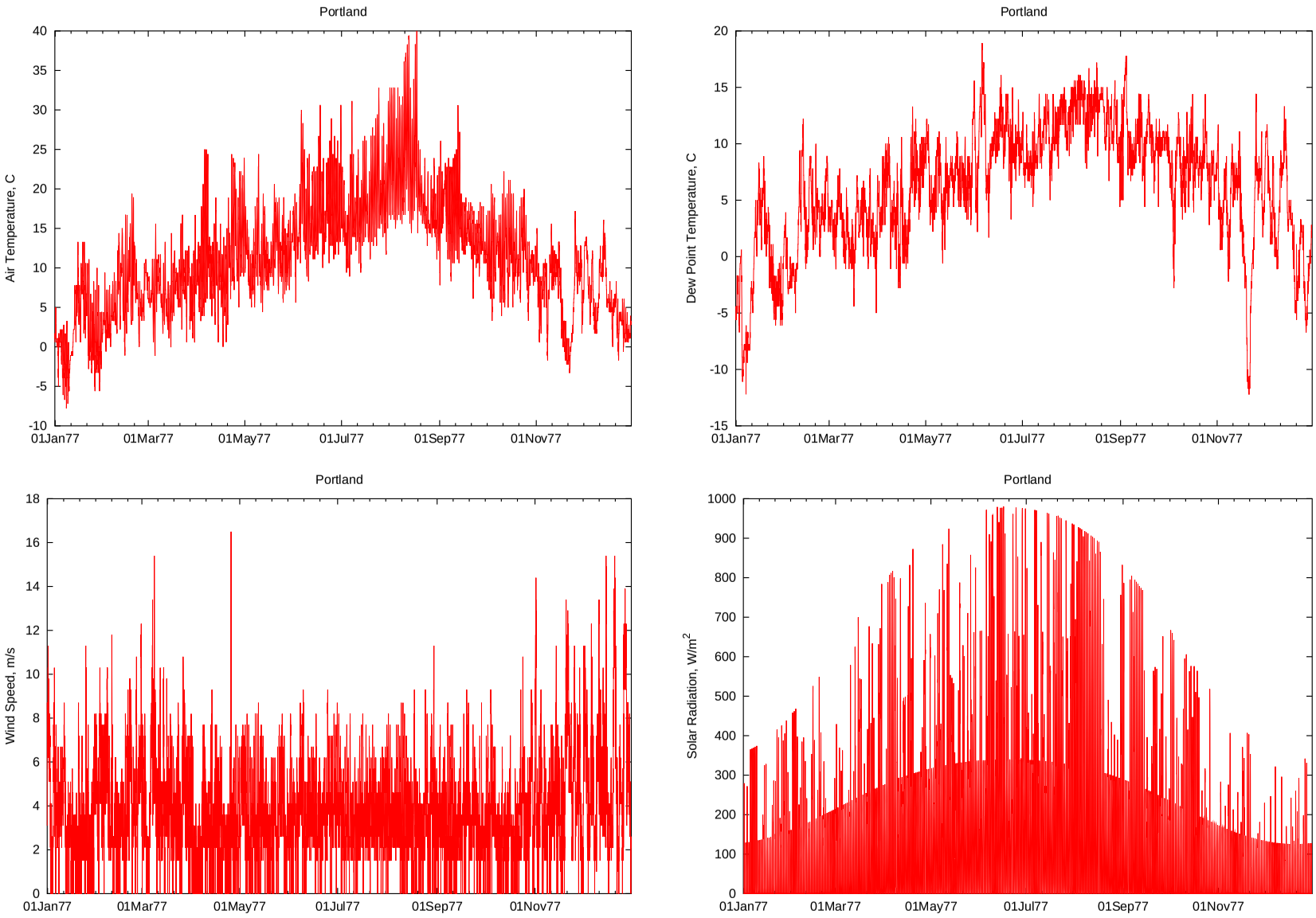

Figure 125: 1977 meterology data at Portland.

Wenatchee 1977 Meterology

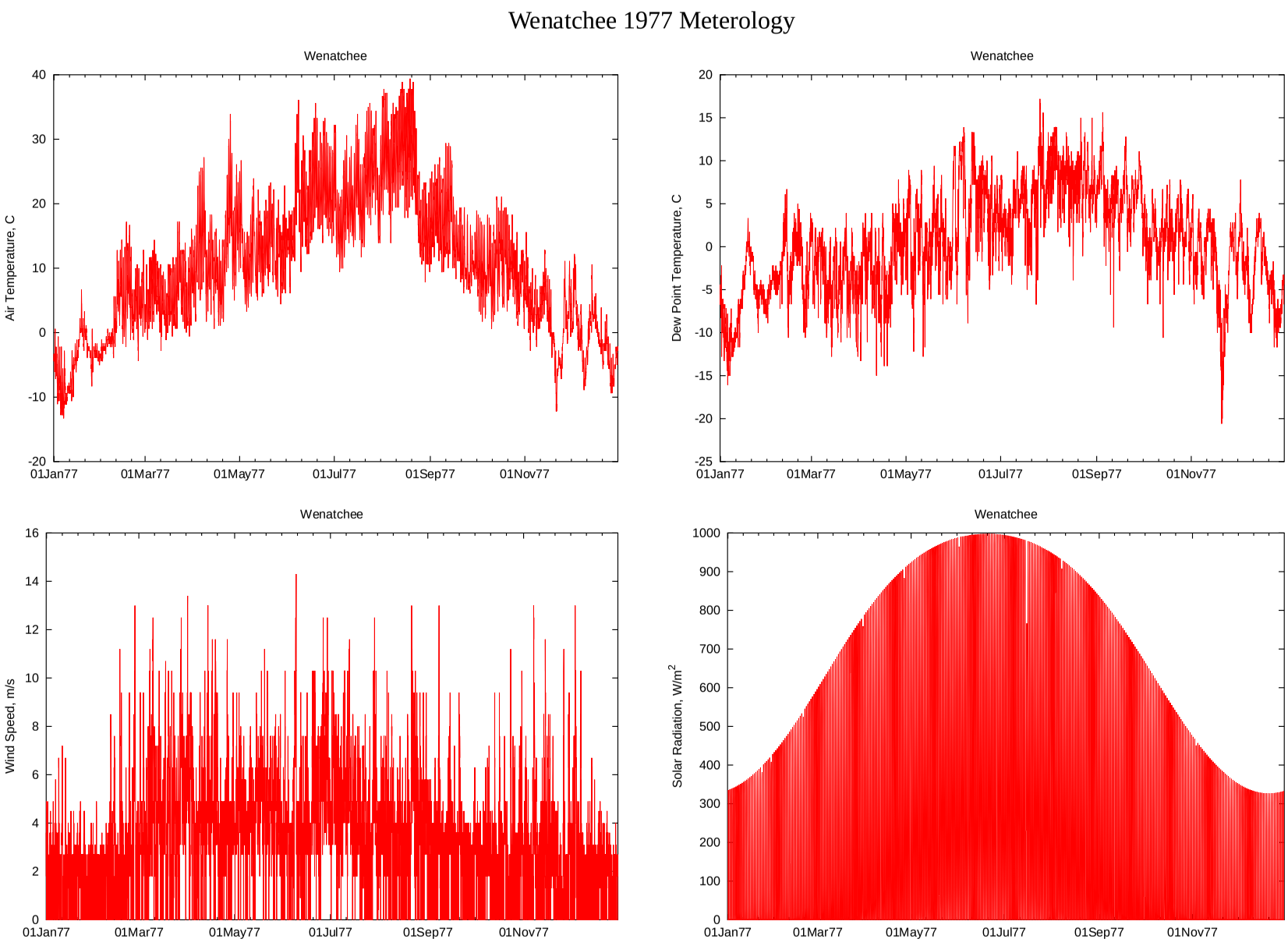

Figure 126: 1977 meterology data at Wenatchee.

Hanford 1994 Meterology

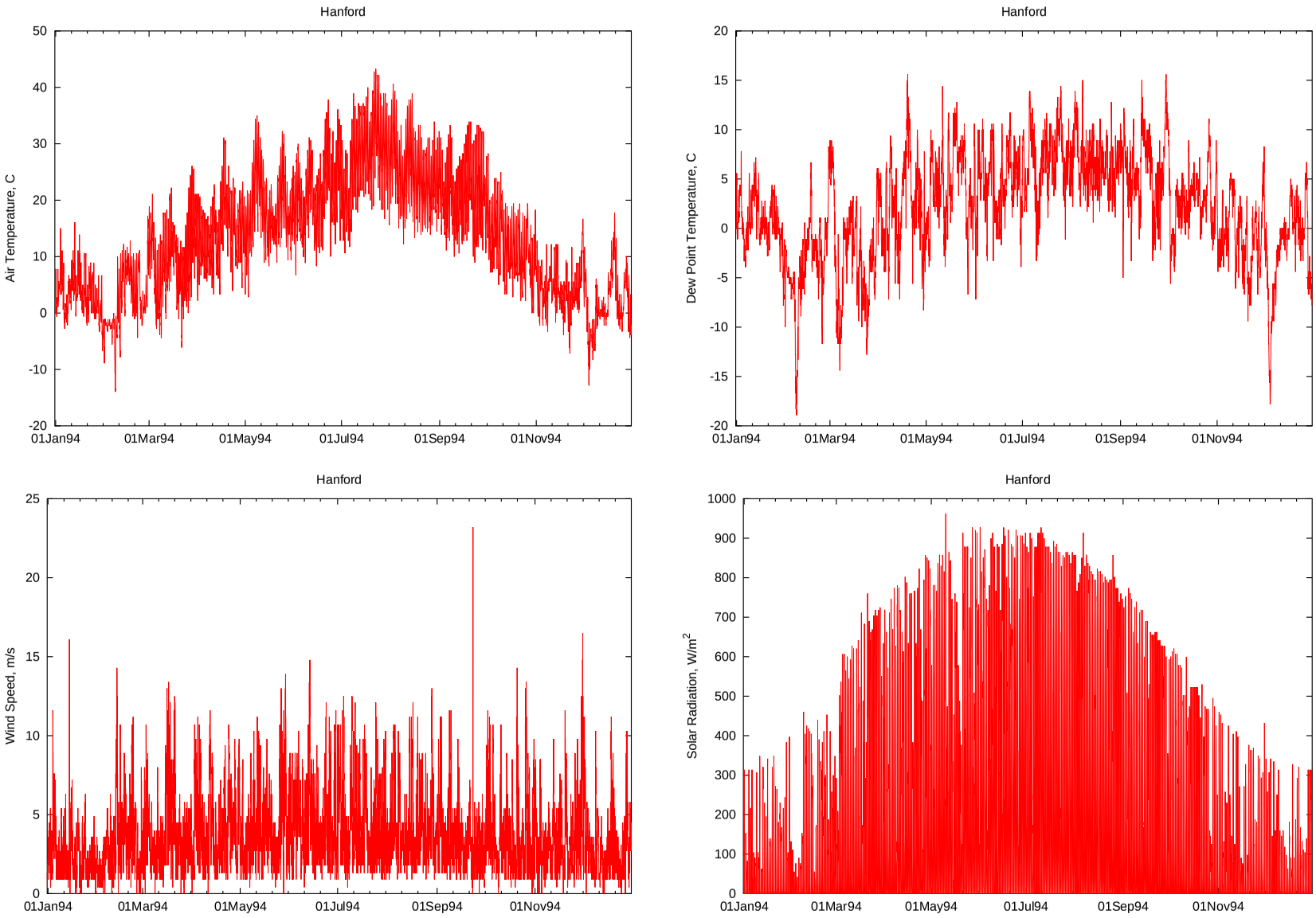

Figure 127: 1994 meterology data at Hanford.

Portland 1994 Meterology

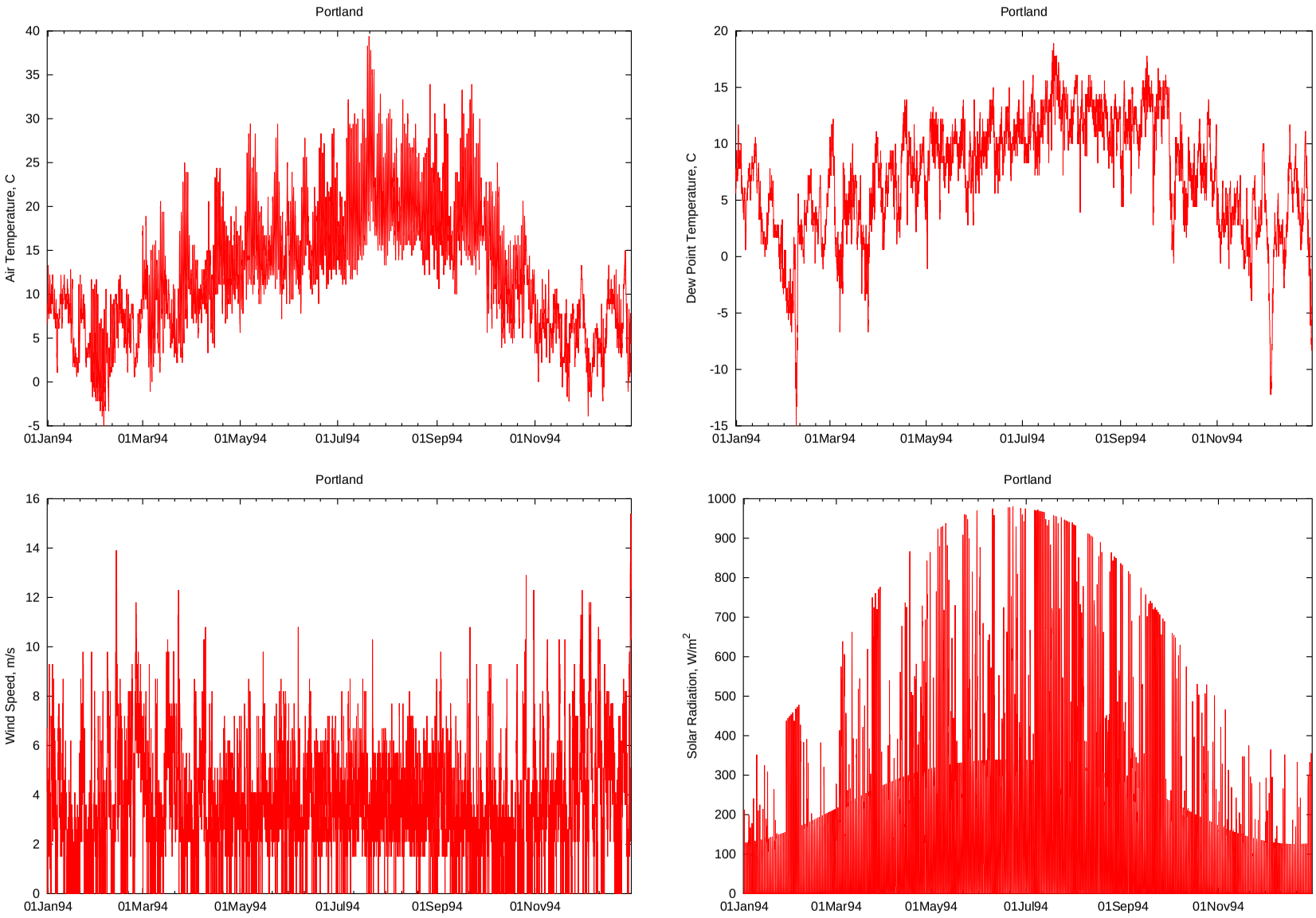

Figure 128: 1994 meterology data at Portland.

Wenatchee 1994 Meterology

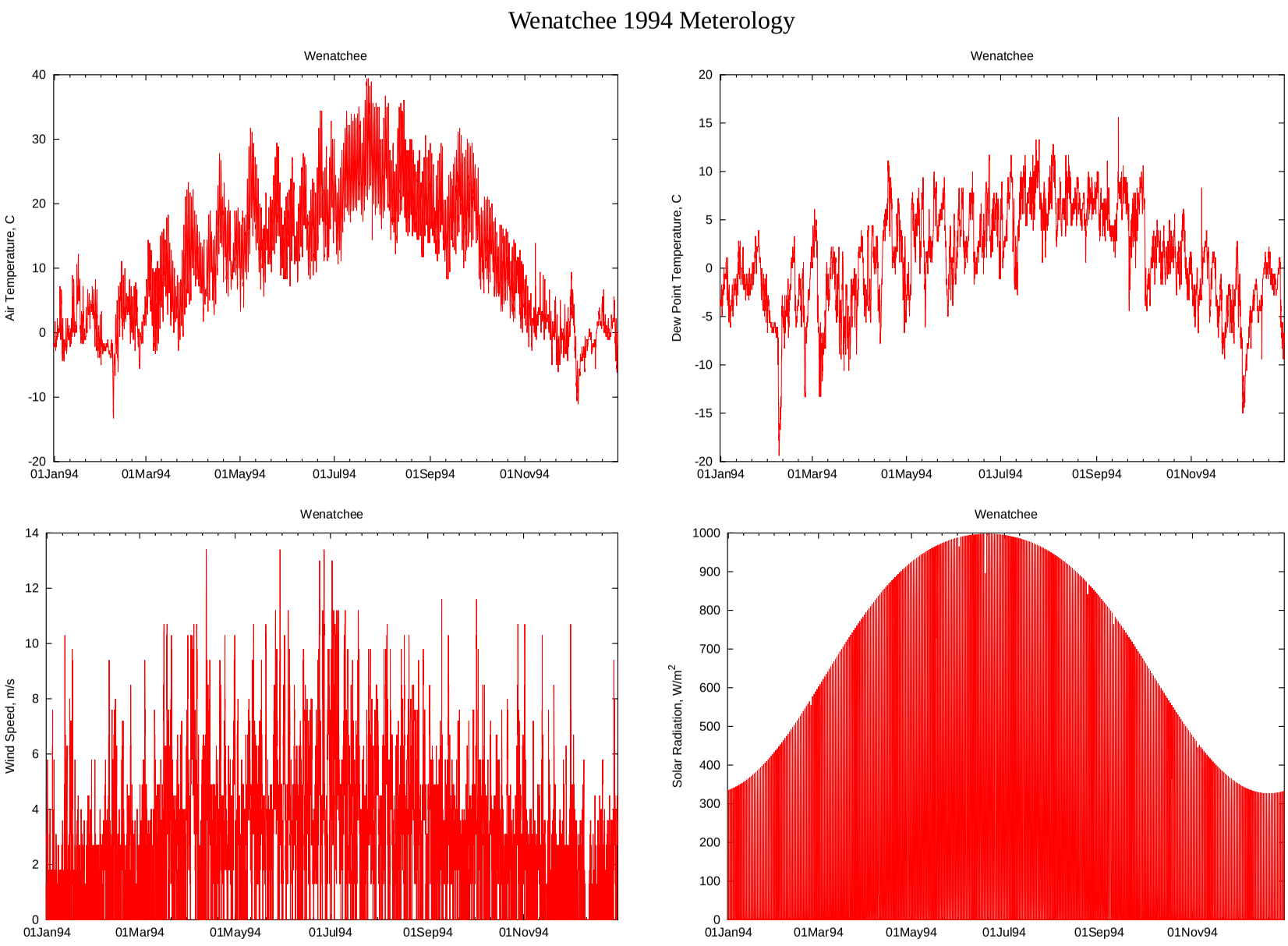

Figure 129: 1994 meterology data at Wenatchee.

C MASS1 Model Schematics

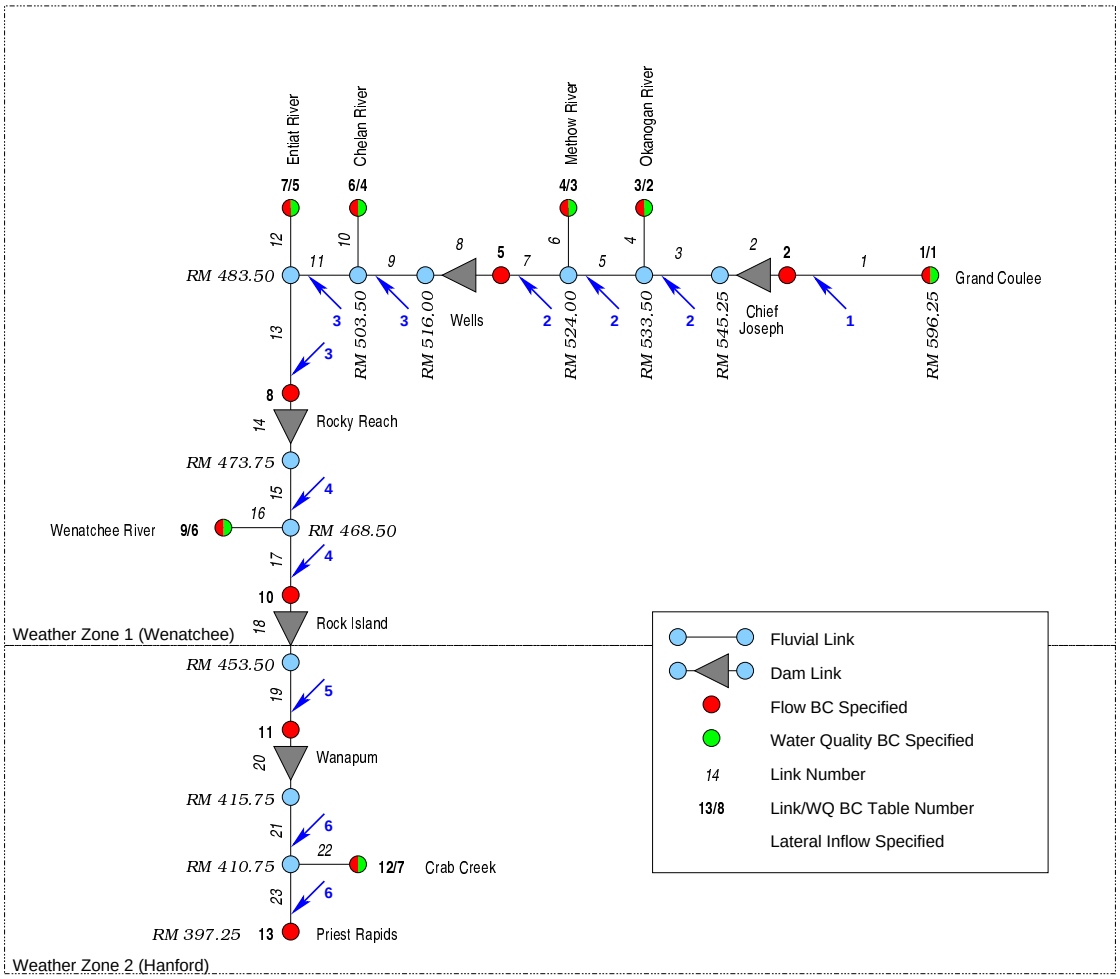

Figure 130: Schematic of MASS1 application to the mid-Columbia.

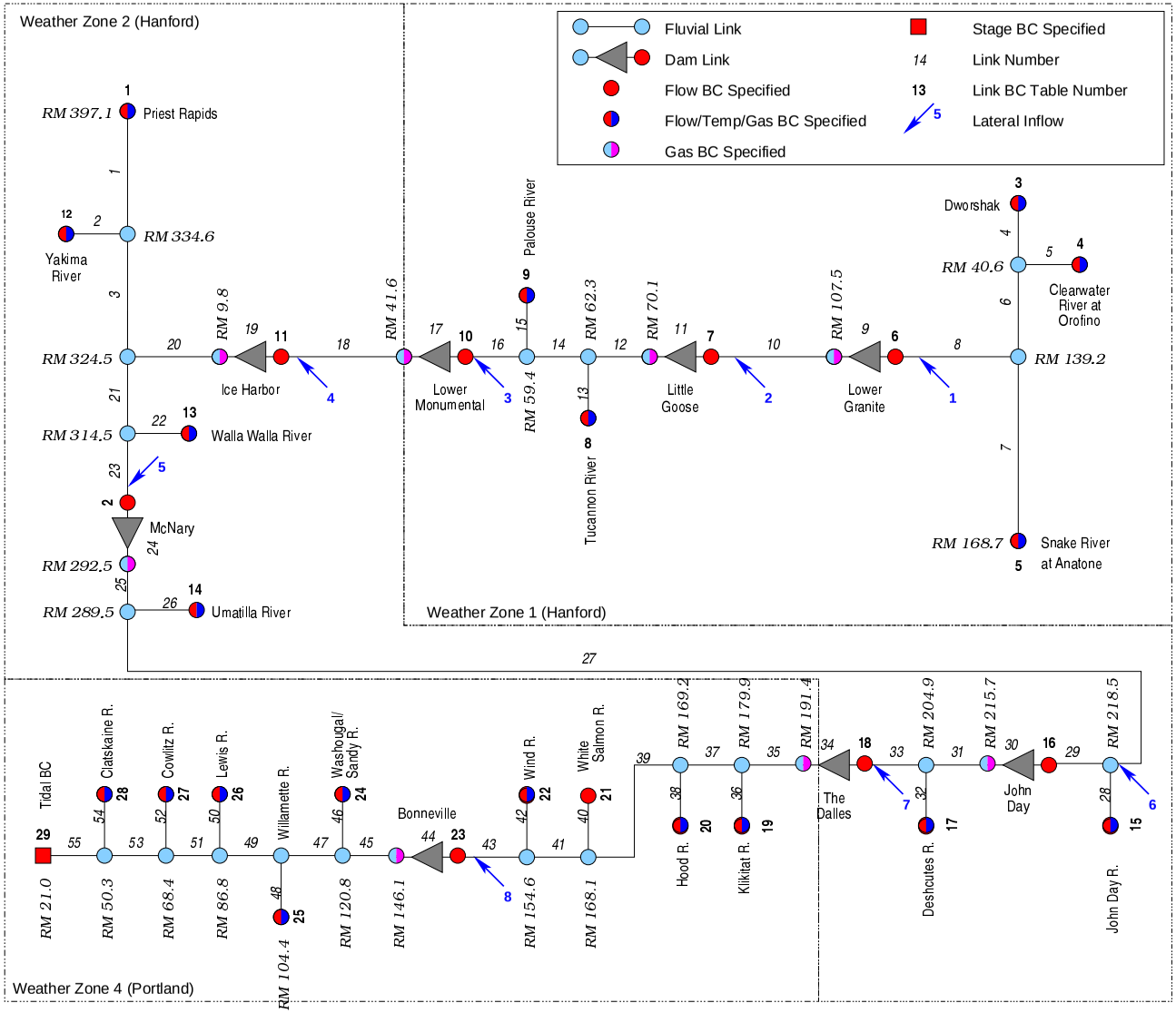

Figure 131: Schematic of MASS1 application to the lower Snake and Columbia Rivers.